Exploring the Influence of Bioactive Glasses on Stem Cell Chondrogenesis for Tissue Engineering

Elena Littmann

Submitted in Accordance with the Requirements for the Degree of Doctor of Philosophy and the Diploma of Imperial College

Imperial College London
Department of Materials

May 2016

Abstract

The development of smart biomaterials which trigger the differentiation of progenitor cells towards a desired lineage continues to pose a challenge for the material science and tissue engineering communities. In order to design such materials, a better understanding of cell-material interactions as well as knowledge of the key physico-chemical parameters responsible for the determination of cell fate are essential. Bioactive glasses are attractive materials for osteochondral repair applications and are known to impact cell behaviour. Characteristically, bioactive glasses modify their local ionic microenvironment by releasing therapeutic ions when introduced in biological fluids. Such bioactive glass extracts have been shown to trigger specific biological responses *in vitro* and *in vivo*.

This thesis explores the influence of key bioactive ion species within bioactive glass dissolution products on the behaviour of human mesenchymal stem cells (hMSCs).

Firstly, the effect of strontium ions within bioactive glass extracts on metabolic processes in hMSCs is studied following a non-biased approach based on a whole genome mRNA microarray. It is demonstrated that such extracts induce an up-regulation of the isoprenoid biosynthesis pathway in hMSCs causing a multifactorial response beyond lineage commitment opening up new avenues of evaluating cell-material interactions.

Secondly, to identify desirable glass compositions for the repair of the osteochondral system, the influence of strontium and/ or magnesium containing bioactive glasses on hMSC chondrogenic differentiation is investigated. Bioactive glass extracts are shown to differentially modify cartilaginous matrix accumulation in hMSC pellets in a composition-dependent manner. Finally, insights into the impact of the hypoxia-mimicking agent cobalt within bioactive glass extracts on hMSC chondrogenic differentiation and (stem) cell behaviour are explored. It is demonstrated that hMSC chondrogenesis in presence of bioactive glass extracts is cobalt dose-dependently reduced.

Collectively, the work described in this thesis has contributed to defining the impact of key ions on hMSC behaviour.

Declaration

I, Elena Littmann, hereby declare that the work presented in this thesis is my own unless otherwise stated. Collaborations are acknowledged in the text. This thesis is a record of the work performed at Imperial College London and at the AO Foundation Davos.

Copyright

The copyright of this thesis rests with the author and is made available under a Creative Commons Attribution Non-Commercial No Derivatives licence. Researchers are free to copy, distribute or transmit the thesis on the condition that they attribute it, that they do not use it for commercial purposes and that they do not alter, transform or build upon it. For any reuse or redistribution, researchers must make clear to others the licence terms of this work.

Acknowledgements

The work described in this thesis would have not been possible without the support of many people to whom I am incredibly grateful. First of all, I would like to thank Prof. Molly Stevens for giving me the opportunity to become part of the Stevens Group. It has been a privilege and pleasure to perform research in such a stimulating and fun environment alongside talented researchers and excellent friends. Molly, thank you so much for your infinite support and guidance throughout my PhD! I would also like to thank my second supervisor Prof. Eduardo Saiz for scientific discussions and mentorship as well as co-ordinating the BioBone project. It has been an absolute pleasure to be part of it.

I have been very fortunate to work alongside excellent scientists, teachers and friends. There are a number of members of the Stevens Group who I would like to especially thank as they have been instrumental for the work presented in this thesis. First and foremost, I would like to thank Dr. Hélène Autefage who has been an incredible teacher and mentor throughout my PhD. Hélène – thank you so, so much for your support, guidance and advice and, of course, for all our discussions, scientific or otherwise. You have been invaluable! Dr. Christine Horejs, Dr. Jean-Philippe St-Pierre, Prof. Lesley Chow, Dr. Joe Steele, Dr. Géraldine Guex and Dr. Jennifer Puetzer deserve thanks for teaching me in the lab and advising me on my experiments. Miss Sabrina Skeete is an organisational wonder – thank you for all the support. Anu Solanki, Carina Almeida, Polina Brangel, Karla Herpoldt and Francesca Tallia made the hard days much easier and the good days even more fun! Thank you for the moral support as well as all the coffee, lunch and dinner breaks. I was lucky to be part of two amazing office families – 2.02 and G0.2A – thank you for such a fantastic (working) environment.

During my second year, I was fortunate to spend six month at the AO Foundation in Davos, Switzerland. I would like to thank everyone at AO Foundation for the warm welcome and making me feel as part of the team. A special thanks to Prof. Mauro Alini and Dr. Marianna Peroglio for receiving me in Davos and supporting my work at AO.

I would like to acknowledge the European Commission funding under the 7th Framework Programme (Marie Curie Initial Training Networks; grant number: 289958, Bioceramics for bone repair) for their generous financial support.

Finally, I would like to thank my parents for their unlimited and invaluable support and encouragement. I couldn't have done it without you! Liebe Mama, lieber Papa, vielen, vielen Dank für Eure grenzenlose Unterstützung. Ich bin euch unendlich dankbar für alles!

Table of Contents

Abstract **3**

Declaration **5**

Acknowledgements **7**

Table of Contents **9**

List of Figures **16**

List of Tables **19**

List of Abbreviations **21**

Literature Review **27**

1.1 Scope of the thesis 28

1.2 Tissue engineering for bone and cartilage repair 30

1.2.1 The need for bone and cartilage repair solutions 31

1.3 The extracellular matrix 32

1.3.1 Bone 32

1.3.1.1 Structural requirements 33

1.3.2 Cartilage 33

1.4 Key cell types of the osteochondral system 35

1.4.1 Osteoblasts 35

1.4.2 Chondrocytes 36

1.4.3 Mesenchymal stem cells 37

1.4.3.1 The use of MSCs for tissue engineering applications 38

1.4.4 Endochondral ossification 40

1.4.4.1 Fracture healing 42

1.5 Biomaterials for bone tissue engineering purposes 43

1.5.1 Calcium phosphate-based ceramics 45

1.5.2 Bioactive glasses 46

1.5.2.1 Structure of bioactive glasses 47

1.5.2.2 The bioactivity of bioactive glasses 47
1.5.2.3 Biological response to bioactive glasses 50
1.6 Bioactive ion species for tissue engineering 50
1.6.1 Cell response to bioactive glass ionic dissolution products *in vitro* 51
1.6.2 Strontium 54
1.6.2.1 Effects of SrR in vitro and in vivo 55
1.6.2.2 Strontium-containing bioactive glasses 56
1.6.3 Cobalt 56
1.6.3.1 Oxygen sensing in cells 58
1.6.3.2 Cobalt's hypoxia-mimicking properties 60
1.6.3.3 The use of cobalt in tissue engineering 61
1.6.3.4 Cobalt-containing bioactive glasses 63
1.6.4 Magnesium and other bioactive ions 64
1.7 Conclusion 66
1.8 Hypothesis and aims of the thesis 67
The Influence of Strontium-containing Bioactive Glasses on the Isoprenoid Pathway in hMSCs 69
2.1 Introduction 70
2.1.1 Gene expression profiling of hMSCs after strontium-containing bioactive glass extract exposure 71
2.1.2 Mevalonate and sterol/steroid biosynthetic pathways 74
2.1.3 Aims and objectives 78
2.2 Materials & Methods 79
2.2.1 Glass synthesis 79
2.2.2 Preparation of bioactive glass-conditioned medium 79
2.2.3 Cell culture 80
2.2.4 Quantitative real time PCR (qPCR) analysis of genes involved in the isoprenoid pathway 81
2.2.5 In-Cell Western analysis 83
2.2.6 Quality analysis of antibodies used for In-Cell Western analysis 84

2.2.6.1 Sodium dodecyl sulphate polyacrylamide gel electrophoresis (SDS-PAGE) 85
2.2.6.2 Electroblotting of proteins to a nitrocellulose membrane 85
2.2.7 Immunofluorescence staining and imaging 86
2.2.7.1 Filipin fluorescence staining of free cholesterol in cultured cells 86
2.2.7.2 Staining of lipid rafts with FITC-conjugated cholera toxin subunit β 86
2.2.7.3 Imaging 87
2.2.8 Statistical analysis 87
2.3 Results 88
2.3.1 Effect of strontium incorporation on bioactive glass ion release 88
2.3.2 Effect of strontium-containing bioactive glass extracts on the isoprenoid pathway on a gene level 89
2.3.3 Effect of strontium-containing bioactive glass extracts on the expression of proteins of the isoprenoid biosynthesis pathway 92
2.3.4 Effect of strontium-containing bioactive glass extracts on membranous cholesterol in hMSCs 94
2.3.5 Effect of strontium-containing bioactive glass extracts on lipid-raft abundance in hMSCs 96
2.3.6 Influence of strontium-containing bioactive glass extracts on the pre-commitment of hMSCs 98
2.4 Discussion 101
2.4.1 Limitations 104
2.5 Conclusion 106
Strontium and Magnesium-containing Bioactive Glasses for Osteochondral Repair ... 107
3.1 Introduction 108
3.1.1 The use of bioactive glasses for cartilage regeneration 108
3.1.2 Mechanisms by which therapeutic ions influence cartilage repair 110
3.1.2.1 The impact of strontium on cartilage repair 111
3.1.2.2 The impact of magnesium on cartilage repair 113
3.1.3 Choice of bioactive glass compositions 115
3.1.4 Aims and objectives 115
3.2 Materials & Methods 117

3.2.1 Glass synthesis 117
3.2.2 Preparation of bioactive glass-conditioned medium 117
3.2.3 Cell culture 118
3.2.4 MTT assay 120
3.2.5 CyQUANT® Direct Cell Proliferation Assay 120
3.2.6 Chondrogenic differentiation of hMSCs 120
3.2.7 Biochemical analysis of hMSC pellets 121
3.2.8 Gene expression analysis of key differentiation markers by qPCR 121
3.2.9 Histology 123
3.2.9.1 Toluidine Blue staining 124
3.2.9.2 Safranin O/ Fast Green staining 124
3.2.10 Immunohistochemistry 125
3.2.11 Fourier transform infrared spectroscopy (FTIR) of hMSC pellet sections 126
3.2.12 Statistical analysis 127
3.3 Results 128
3.3.1 Ionic composition of strontium and/or magnesium-containing BG-conditioned media 128
3.3.2 Metabolic activity and hMSC cell number in presence of BG dissolution products 130
3.3.3 sGAG production of hMSCs in response to BG dissolution products 131
3.3.4 Key chondrogenic marker gene expression in hMSCs during treatment with bioactive glass extracts 133
3.3.5.1 Histology 136
3.3.5.2 Immunohistochemistry (IHC) 137
3.3.5.3 Fourier transform infrared spectroscopy (FTIR) 139
3.3.6 Summary 141
3.4 Discussion 142
3.4.1 Limitations 147
The Influence of Cobalt-containing Bioactive Glasses on hMSC Chondrogenic Differentiation 151
4.1 Introduction 152

4.1.1 The influence of cobalt on hMSC differentiation 155
4.1.2 Aims and objectives 157
4.2 Materials & Methods 158
4.2.1 Glass synthesis 158
4.2.2 Preparation of bioactive glass-conditioned medium 158
4.2.3 Cell culture 159
4.2.3 AlamarBlue® viability assay 160
4.2.6 Chondrogenic differentiation of hMSCs 160
4.2.6.1 Pellet culture 160
4.2.6.2 Culture on poly(ε-caprolactone) (PCL) membranes 161
4.2.7 Biochemical analysis of hMSC-derived tissue in chondrogenic conditions 162
4.2.8 Gene expression analysis of key lineage markers by qPCR 162
4.2.9 Histology 164
4.2.9.1 Toluidine Blue staining 165
4.2.9.2 Safranin O/ Fast Green staining 165
4.2.10 Raman spectroscopy of hMSC pellet sections 165
4.2.10.1 Confocal Raman spectral imaging 166
4.2.10.2 Multivariate data analysis 166
4.2.11 Statistical analysis 166
4.3 Results 167
4.3.1 Ionic composition of CoBG-conditioned DMEM medium 168
4.3.2 hMSC metabolic activity in presence of CoBG dissolution products 169
4.3.3 Downstream effect of CoBG dissolution products on hMSC chondrogenic differentiation 170
4.3.3.1 Accumulation and release of sGAG in hMSC pellet culture model 170
4.3.3.2 Accumulation of sGAG in hMSC-seeded PCL membrane model 172
4.3.3.3 Gene expression of key differentiation markers at early time points of hMSC chondrogenic culture on PCL membranes 175
4.3.4 Cartilage-like tissue formation by hMSC in CoBG-conditioned medium 177

4.3.4.1 Characterisation of extracellular matrix production in hMSC pellet culture by histology 177
4.3.4.2 hMSC chondrogenesis in PCL membrane model 179
4.3.5 Raman spectroscopy mapping of hMSC pellet sections 180
4.4 Discussion 183
4.4.1 Limitations 187
4.5 Conclusion 188
The Influence of Cobalt-containing Bioactive Glasses on hMSC Behaviour 189
5.1 Introduction 190
5.1.1 The influence of cobalt on hMSC behaviour 193
5.1.2 Aims and objectives 196
5.2 Materials & Methods 197
5.2.1 Glass synthesis 197
5.2.2 Preparation of bioactive glass-conditioned medium 197
5.2.3 Cell culture 198
5.2.4 In-Cell Western analysis 198
5.2.4.1 Quality analysis of antibodies used for In-Cell Western analysis 199
5.2.5 Sodium dodecyl sulphate polyacrylamide gel electrophoresis (SDS-PAGE) 200
5.2.6 Electroblotting of proteins to a nitrocellulose membrane 200
5.2.7 MTT assay 201
5.2.8 CyQUANT® Direct Cell Proliferation Assay 201
5.2.9 Filamentous actin staining 202
5.2.10 Colony forming units –fibroblast (CFU-F) assay 202
5.2.11 Migration or scratch assay 203
5.2.12 Statistical analysis 203
5.3 Results 204
5.3.1 Ionic composition of CoBG-conditioned α-MEM medium 204
5.3.2 Stabilisation of HIF-1α by CoBG dissolution products 206
5.3.3 hMSC metabolic activity and proliferation in CoBG conditioned medium 207

5.3.3.1 hMSC metabolic activity in presence of CoBG dissolution products 207
5.3.3.2 hMSC proliferation in presence of CoBG dissolution products 208
5.3.3.3 hMSC morphology in presence of CoBG dissolution products 209
5.3.4 Effect of CoBG extracts on CFU-F forming ability and hMSC migration 211
5.3.4.1 CFU-F formation by hMSCs in presence of CoBG dissolution products 211
5.3.4.2 Migration of hMSCs in presence of CoBG dissolution products 212
5.3.5 Downstream effect of CoBG dissolution products on hMSC cell cycle 214
5.3.6 Summary 215
5.4 Discussion 216
5.4.1 Limitations 222
5.5 Conclusion 223
Conclusions & Future directions 225
References 233
Appendices 273
Appendix A 275
Appendix B 276
Appendix C 277
Appendix D 278
Appendix E 279
Appendix F 281
Appendix G 283
Appendix H 284

List of Figures

1 Literature review

1.1 Cellular organisation and collagen fibre assembly in the different zones of articular cartilage..34

1.2 Process of endochondral bone formation 42

1.3 Regulation of cell behaviour by bioactive glasses 54

1.4 Structure of hypoxia inducible factor-1α (HIF-1α) 59

1.5 Regulation of the HIF-1 pathway 61

2 The Influence of Strontium-containing Bioactive Glasses on the Isoprenoid Pathway in hMSCs

2.1 Overview of BG microarray study design and results 73

2.2 Overview of the isoprenoid pathway and its inhibitors 75

2.3 Influence of sterol/steroid pathway products on cell signalling mechanisms at the plasma membrane. 77

2.4 Human mesenchymal stem cells (hMSC) at passage 5 80

2.5 Antibody characterisation using Western blot analysis 85

2.6 Effect of incorporating strontium into BG on isoprenoid biosynthesis-associated genes 90

2.7 Effect of pamidronate (PAM) and methyl-β-cyclodextrin (MβCD) on isoprenoid pathway-associated genes 92

2.8 Effect of incorporating strontium into BG on protein abundance of isoprenoid pathway-associated enzymes 94

2.9 Effect of incorporating strontium into BG on the membranous cholesterol content in hMSCs . 96

2.10 Effect of incorporating strontium into BG on the lipid raft content in hMSCs 98

2.11 Influence of strontium incorporation into BG on the pre-commitment of hMSCs 100

3 Strontium and Magnesium-containing Bioactive Glasses for Osteochondral Repair

3.1 Primary human mesenchymal stem cells (hMSC) isolated at AO Foundation Davos 119

3.2 Effect of various BG extracts on hMSC metabolic activity and cell number 131

3.3 Effect of various BG extracts on hMSC chondrogenic differentiation 133

3.4 Effect of various bioactive glass extracts on chondrogenic and osteogenic lineage marker gene expression by hMSCs 135

3.5 Effect of various BG extracts on *in vitro* cartilage-like tissue formation assessed by histology 137

3.6 Distribution of type I, II and X collagens in hMSC pellets in presence of various bioactive glass extracts 138

3.7 FTIR analysis of collagen distribution in hMSC pellets after culture in BG-conditioned media 140

3.8 Effect of BG-conditioned media on the mean IR spectra of hMSC pellets 141

4 The Influence of Cobalt-containing Bioactive Glasses on hMSC Chondrogenic Differentiation

4.1 Fibrous PCL membrane immobilised between holders 162

4.2 Effect of CoBG dissolution products on hMSC metabolic activity at early time points 170

4.3 Effect of CoBG dissolution products on sGAG production and release by hMSCs in pellet culture 172

4.4 Effect of CoBG dissolution products on sGAG production by hMSCs seeded on PCL membranes 175

4.5 Effect of CoBG dissolution products on lineage marker gene expression 177

4.6 Effect of CoBG dissolution products on *in vitro* cartilage-like tissue formation by hMSC pellets 178

4.7 Effect of CoBG dissolution products on *in vitro* cartilage-like tissue formation by hMSCs seeded on PCL membranes 180

4.8 Extracellular matrix characterisation of hMSC pellets by Raman spectral analysis 182

5 The Influence of Cobalt-containing Bioactive Glasses on hMSC Behaviour

5.1 Antibody characterisation using Western blot analysis 199

5.2 Effect of CoBG dissolution products on HIF-1α protein abundance 207

5.3 Effect of CoBG extracts on hMSC metabolic activity and cell abundance 209

5.4 Effect of CoBG dissolution products on hMSC morphology 210

5.5 Effect of CoBG extracts on CFU-F formation by hMSCs 211

5.6 Effect of CoBG extracts on hMSC migration and CXCR4 expression 213

5.7 Effect of CoBG dissolution products on protein expression of the cell cycle regulators p21 and p53 215

List of Tables

1 Literature review

1.1 Mechanical properties of cortical and cancellous bone, adapted from Fu *et al.*[13] 33

1.2 HCA layer formation, adapted from Hench, Jones and Rahaman *et al.*[119, 124, 126] 48

2 The Influence of Strontium-containing Bioactive Glasses on the Isoprenoid Pathway in hMSCs

2.1 Glass compositions (mol%) and strontium for calcium substitution (%) 79

2.2 Sequences and cycling conditions of primers used in qPCR 83

2.3 Ion content of strontium-substituted BG-conditioned media measured by inductively coupled plasma optical emission spectroscopy (ICP-OES)..... 88

3 Strontium and Magnesium-containing Bioactive Glasses for Osteochondral Repair

3.1 Glass compositions (mol%) 117

3.2 Details of hMSC donors used for assessment of chondrogenic differentiation in various BG-conditioned media 119

3.3 Primer sequences and cycling conditions.. 123

3.4 Ion content of BG-conditioned DMEM medium 129

3.5 pH values of DMEM and BG-conditioned DMEM medium before and after equilibration 129

4 The Influence of Cobalt-containing Bioactive Glasses on hMSC Chondrogenic Differentiation

4.1 Glass compositions (mol%) 158

4.2 Details of hMSC donors used for assessment of chondrogenic differentiation in CoBG-conditioned media 159

4.3 Primer sequences and cycling conditions 164

4.4 Ion content of CoBG-conditioned DMEM medium 168

4.5 pH values of DMEM and CoBG-conditioned DMEM medium before and after equilibration 169

5 The Influence of Cobalt-containing Bioactive Glasses on hMSC Behaviour

5.1 Glass compositions (mol%) 197

5.2 Ion content of CoBG-conditioned α-MEM medium 205

5.3 pH values of α-MEM and CoBG-conditioned α-MEM medium before and after equilibration ……..205

List of Abbreviations

0%CoBG	Bioactive glass with 0 mol% Co
1%CoBG	Bioactive glass with 1 mol% Co
1.5%CoBG	Bioactive glass with 1.5 mol% Co
2%CoBG	Bioactive glass with 2 mol% Co
A.u.	Arbitrary units
ACI	Autologous chondrocytes implantation
AFM	Atomic force microscopy
ALP	Alkaline phosphatase
ANOVA	Analysis of variance
ARNT	Aryl hydrocarbon receptor nuclear translocator
Asn	Asparagine
bFGF	Basic fibroblast growth factor
BG	Bioactive glass
bHLH	Basic helix-loop-helix
BMP	Bone morphogenetic protein
BP	Bisphosphonate
BSA	Bovine serum albumin
BV	Blood vessels
Ca	Calcium
CaP	Calcium phosphate
CaSR	Calcium sensitive receptor
CBP	Cyclic-AMP responsive element binding (CREB)-binding protein
CFU-F	Colony-forming unit fibroblastic
CG	Collagen-glycosaminoglycan
CM	Chondrogenic medium
Co	Cobalt
COL1A1	Type I collagen gene
COL2A1	Type II collagen gene
COLXA1	Type X collagen gene
Co-MBG	Cobalt-containing 3D mesoporous bioactive glass
Co-TCP	Cobalt-substituted β-tricalcium phosphate

Ct	Threshold cycle
C-TAD	C-terminal transactivator domain
CTX	Carboxy-terminal telopeptides of type II collagen
CTβ	Cholera toxin subunit β
D0	Time of first medium change
DAB	3,3'-diaminobenzidine
Dapi	4',6-diamidino-2-phenylindole
DE	Differentially expressed
DFAT	Dedifferentiated fat cells
DMEM	Dulbecco's Modified Eagle Medium
DMMB	1,9-Dimethyl-methylene blue
DMSO	Dimethylsulphoxide
ECM	Extracellular Matrix
EPO	Erythropoietin
EtOH	Ethanol
F	Female
Farnesyl-PP	Farnesyl pyrophosphate
FBS	Foetal Bovine Serum
FDFT1	Squalene synthase
FDPS	Farnesyl diphosphate synthase
FGF	Fibroblast growth factor
FIH	Factor inhibiting HIF
FPA	Focal plane array
FTIR	Fourier transform infrared spectroscopy
GAG	Glycosaminoglycan
GGPS1	Geranylgeranyl pyrophosphate synthetase 1
GM	Growth medium
HA	Hydroxyapatite
HCA	Carbonate-substituted hydroxyapatite
HEPES	4-(2-hydroxyethyl)-1-piperazineethanesulfonic acid
HIF-1	Hypoxia inducible factor 1
HIF-1α	Hypoxia inducible factor 1α
HIF-1β	Hypoxia inducible factor 1β
HIF-2α	Hypoxia inducible factor 2α
HIF-3α	Hypoxia inducible factor 3α

HMG-CoA	3-Hydroxy 3-methylglutaryl-CoA
HMGCR	HMG-CoA reductase
HMGCS1	HMG-CoA synthase 1
hMSCs	Human mesenchymal stem cells
HRE	Hypoxia responsive elements
ICP-OES	Inductively coupled plasma optical emission spectroscopy
IGFI	Insulin growth factor I
IGFII	Insulin growth factor II
IHC	Immunohistochemistry
KEGG	Kyoto Encyclopedia of Genes and Genomes
M	Male
MACI	Matrix-induced autologous chondrocyte implantation
MCR	Multivariate Curve Resolution
Mg	Magnesium
MMP13	Matrix metalloproteinase 13
MSC	Mesenchymal stem cells
mTOR	Mammalian target of rapamycin
MβCD	Methyl-β-cycoldextrin
ND	Non-detectable
NMDA	N-methyl-D-aspartate receptor
N-TAD	N-terminal transactivator domain
OA	Osteoarthritis
OCT	Optimal cutting temperature
ODDD	Oxygen-dependent degradation domain
OVX	Ovariectomized
P	Phosphorus
PAGE	Polyacrylamide gel electrophoresis
PAM	Pamidronate
PAS	PER-ARNT-SIM
PBS	Phosphate buffered saline
PBSTw	PBS/0.1% Tween (Tw) (v/v)
PCA	Principal Component Analysis
PCL	Poly(ϵ-caprolactone)
PEG	Polyethylenglycol
PFA	Paraformaldehyde

PHD	Prolyl hydroxylase domain containing
PI3K	Phosphatidylinositol 3-kinase
PK	Proteinase-K
PLGA	Poly (lactide-co-glycolide)
POC	Primary ossification centre
Pro	Proline
pVHL	Von Hippel Lindau protein
qPCR	Quantitative real time polymerase chain reaction
RGD	Arginine-glycine-aspartic acid
Rh	Recombinant human
ROS	Reactive oxygen species
RT	Room temperature
RUNX2	Runt related transcription factor 2
SBF	Simulated body fluid
SC4MOL	Methylsterol monooxygenase
SD	Standard deviation
SDF-1	Stromal derived factor 1
SDS	Sodium dodecyl sulphate
sGAG	Sulphated glycosaminoglycans
Si	Silicon
SOC	Secondary ossification centre
SOX9	Sex-determining region Y-box 9
Sr	Strontium
Sr0	Bioactive glass with 0% Sr for Ca substitution
Sr10	Bioactive glass with 10% Sr for Ca substitution
Sr100	Bioactive glass with 100% Sr for Ca substitution
SrR	Strontium ranelate
T0	Time of seeding
TBS	Tris-buffered saline
TEM	Transmission electron microscopy
TGF-β	Transforming Growth Factor β
Tw	Tween
U	Units
UPR	Unfolded protein response
VEGF	Vascular endothelial growth factor

α-MEM	Minimum Essential Medium Eagle alpha modification
β-TCP	β-tricalciumphosphate

CHAPTER 1

Literature Review

1.1 Scope of the thesis

Tissue engineering is an expanding field that aims at regenerating impaired tissues by providing biological substitutes to restore, maintain or enhance tissue and organ function[1-3]. Despite extensive research, (cell-seeded) scaffold systems that mediate functional tissue repair *in vivo* still present a challenge. Substantial advances have been made regarding the requirements for scaffold design, and an extensive body of research is now focussing on the incorporation and/or delivery of bioactive moieties to direct cell behaviour to a desired outcome such as differentiation and extracellular matrix production[4]. Yet, to date little is known about how physico-chemical cues are processed by cells and translated into biological responses. Therefore, a better understanding of the cellular response to (bioactive) materials and the underlying signalling pathways are needed. This thesis is concerned with the influence of key bioactive ion species on the behaviour of human mesenchymal stem cells (hMSC) in the context of a well-established class of biomaterials. Bioactive glasses with different compositions were used to investigate how the delivery of bioactive ions and thus the modification of the ionic environment affect hMSCs. Bioactive glass compositions can be tailored to suit the characteristics and demands of a target tissue and to enhance material-driven cellular responses.

In **Chapter 1** the field of tissue engineering is introduced and the need for sophisticated solutions for bone and cartilage repair is discussed. As an understanding of the characteristics and properties of tissues is essential for the design of suitable tissue-engineered constructs, the bone and cartilage matrix as well as the cell types involved in the formation and maintenance of both tissues are explored. As many tissue engineering approaches involve mesenchymal stem cells and since their behaviour in response to bioactive cues is studied in this thesis, a special focus is given to this cell type. Then biomaterials for bone tissue engineering are reviewed with a particular emphasis on bioactive glasses and their release products. As background to Chapters 2 and 3, the biological response to strontium ions either in form of the drug strontium ranelate or incorporated in bioactive glasses is reviewed. Relating to Chapters 4 and 5, the hypoxia-mimicking agent cobalt is introduced and its biological function as well as its use in biomaterials discussed. Considering the range of topics described in this thesis, a more specific literature review is included at the beginning of each chapter.

Chapter 2 explores the impact of strontium-containing bioactive glass release products on hMSC metabolic processes. It builds on a previously performed whole genome microarray that uncovered unexpected biological responses to strontium-containing bioactive glass dissolution products. It is demonstrated that strontium ions within the bioactive glass dissolution products up-regulate the mevalonate and sterol/steroid biosynthesis pathways. These metabolic changes are shown to translate into an increase in cholesterol and lipid raft content of the cellular plasma membrane indicating a modification of cell signalling processes. This work highlights how simple alteration of a biomaterial

can have profound effects on the biological response. It is hoped that this will guide future tissue engineering scaffold design.

In **Chapter 3** the influence of bioactive glass-derived release products on the chondrogenic differentiation of hMSCs is assessed. In particular, it is focussed on the effect of strontium and magnesium ions. This followed from the findings in Chapter 2, where the introduction of a single bioactive moiety, strontium, led to pronounced changes in cell behaviour. It is demonstrated that bioactive glass release products enhance the metabolic activity of hMSCs, however, there are no significant differences between compositions. Bioactive glass dissolution products are further shown to affect mesenchymal stem cell chondrogenesis in a composition-dependent manner. Chondrogenic differentiation was assessed by quantification of extracellular matrix production and histological as well as immunohistochemical characterisation of *in vitro*-formed tissue. This work represents the first comprehensive study in which the influence of bioactive glass dissolution products derived from different glass compositions on the chondrogenic differentiation of hMSCs is examined. The results give an insight into how ionic environments can differentially affect hMSC differentiation. This knowledge is particularly valuable for the design of osteochondral constructs.

Chapter 4 further explores how bioactive glass dissolution products affect hMSC chondrogenic lineage commitment. Since hypoxia plays a critical role during growth plate development and cartilage formation, bioactive glasses releasing the hypoxia-mimicking agent cobalt are assessed for their potential to support hMSC chondrogenesis. Strikingly, cobalt-containing bioactive glass dissolution products decrease chondrogenic lineage commitment in a cobalt dose-dependent manner evidenced by biochemical and histological analysis. Raman spectral analysis is shown to corroborate these results and further to demonstrate that supplementation of cobalt chloride results in a similar outcome. This reinforces that simple modification of a biomaterial can have a profound effect and need to be carefully evaluated and tested with respect to the biological response.

Chapter 5 builds on the functional outcome described in Chapter 4 and focusses on the impact of cobalt-containing bioactive glass release products on the behaviour of hMSCs. It is shown that the cobalt-containing bioactive glass extracts potently increase the abundance of HIF-1α in hMSCs for at least 48 h and thus successfully mimic hypoxia in the cell. The presence of cobalt had a dose- and exposure time-dependent effect on hMSCs as evaluated by metabolic activity, proliferation, colony-formation and migration assays.

Finally, **Chapter 6** summarises the key findings of the thesis and extents to future work. The research presented in this thesis is then discussed with respect to the wider context of the field aiming at establishing its contribution to tissue engineering.

1.2 Tissue engineering for bone and cartilage repair

In 1993, Langer and Vacanti elegantly defined tissue engineering as

''*an interdisciplinary field of research that applies the principles of engineering and the life sciences towards the development of biological substitutes that restore, maintain, or improve tissue function*"[1].

Tissue engineering is a rapidly evolving field which aims to help the vast clinical need of an ageing population with a more active lifestyle. To date, autografts, tissue transplanted from one part of the body to another, remain the gold standard for the replacement of diseased or damaged tissue. Yet, the established issue of donor site morbidity combined with limited availability of certain tissues necessitate other options. The use of allograft tissue, taken from another individual, is complicated by a possible immune response by the recipient leading to transplant rejection and, on a broader scale, hampered by limited donor tissue supply. Engineered tissue therefore presents an attractive solution with an, in theory, nearly unrestricted availability. Today, the scope of tissue engineering comprises every tissue and organ in the body reflecting the strong clinical demand for novel therapies. For the purpose of this review, a focus is given to the osteochondral system.

Whilst the idea of regenerating and/or replacing impaired tissue dates back as early as 600 BC, the pursued approach has changed considerably. From using parts of the cheek to repair an injured nose to sophisticated (cell-seeded) constructs that offer bioactive cues both soluble and insoluble to aid tissue regeneration. In the next paragraph, a brief overview of the more recent changes in paradigm and philosophy concerning scaffold design will be given. In the 1960s and 1970s implants started to be used routinely in the clinic. Initially, biomedical materials were selected by virtue of their biomedical inertness to avoid an immune response by the body[5]. The focus in the field of biomaterials shifted, however, towards so-called bioactive materials that had the ability to interact with cells and elicited certain cell responses *in vitro* and *in vivo*. The change in paradigm was notably marked by the invention of 45S5 Bioglass® by Professor Larry Hench[6]. Appreciating that artificial implants cannot appropriately replace living tissues, so-called third-generation biomaterials have been developed[5]. These materials are designed to interact with cells to enhance tissue repair while being resorbable, thereby facilitating a replacement by newly formed tissue[5]. Furthermore, they were designed to mimic the properties of the extracellular matrix of the respective tissue. This was accomplished by incorporating bioactive molecules such as growth factors or the integrin binding motif RGD (arginine-glycine-aspartic acid). Hence, today, tissue engineering strategies frequently involve a triad of cells, scaffolds and bioactive moieties[7]. Such cell-seeded scaffolds are then either pre-cultured *in vitro* prior to implantation to allow the deposition of extracellular matrix or directly implanted to the injury site to induce and assist tissue repair *in vivo*.

1.2.1 The need for bone and cartilage repair solutions

Bone has a remarkable regenerative capacity, yet, there is a growing need for functional bone grafts. In the United States, approximately 1.5 million auto- or allo-bone grafts are performed annually with costs likely in excess of $10 billion[8, 9]. This figure is forecasted to double by 2020 due to a variety of factors such as increased life expectancy and changes in lifestyle[10]. Bone grafts are especially needed to fill bigger bone defects and/or support bone repair in the elderly. Osteoporosis related bone defects continue to be a burden for the health system causing annual costs exceeding $17 billion in the United States alone, a number which will likely further increase due to an ageing population[10]. Osteoporosis is characterised by an imbalance in bone turnover with an inappropriately high rate of bone resorption in relation to bone formation[11]. This imbalance causes structural changes in bone leading to reduced bone strength and higher susceptibility to fracture. Autografts remain the gold standard for treatment of bone defects but a shortage of supply and donor site morbidity require the development of engineered scaffolds for bone tissue regeneration[12, 13].

The repair of defects in adult articular cartilage remains a major (clinical) challenge due to the poor intrinsic capacity for self-repair of cartilage[14]. Surgical treatment is currently mainly limited to introducing microfractures to release progenitor cells from the bone marrow into the defect, autologous chondrocytes implantation (ACI) or, more recently, matrix-induced autologous chondrocyte implantation (MACI)[15]. Even minor cartilage lesions may lead to a progressive degeneration of the cartilage layer and subsequently induce osteoarthritic degeneration of the joint[14]. Osteoarthritis (OA) is a degenerative disease of the joint affecting both articular cartilage and the underlying subchondral bone. OA is ranked among the most common musculo-skeletal diseases and is a leading cause of functional impairment in middle-aged subjects. The prevalence of OA increases with age and is thought to affect more than half of the population over 65 years[16]. The aetiology of OA remains incompletely understood but literature agrees that OA is a highly complex, multifactorial disease with an inflammatory component that is initiated by cartilage break-down. OA is most commonly diagnosed in the joints of the hand, hip, knee and foot but can in principle occur in any joint[17]. Pathological changes associated with severe manifestations of OA are loss of joint space, subchondral bone sclerosis and presence of osteophytes (bony outgrowths that form along joint margins)[17]. Currently, there are no satisfying treatment options for OA as drugs have failed so far to induce disease modifying effects. As a last resort, OA patients receive total joint replacement surgery. In 2010 the economic burden associated with total hip and knee replacements in the UK was estimated to be in excess of £800 million while the loss of production associated with OA in the UK in 2002 was £3.2 billion[18]. Therefore, a multidisciplinary approach is likely needed involving the identification of disease-modifying molecules alongside with the development of advanced (cell-seeded) scaffolds to facilitate the repair of defects.

Taken together, there is a growing clinical need for novel, rationally designed (tissue-engineered) constructs for the repair of bone and/or cartilage defects. In this literature review, the extracellular matrix of bone and cartilage will be described followed by an introduction of the key cell types of the osteochondral system. Then, biomaterials for bone tissue engineering will be discussed with a focus on calcium phosphates and bioactive glasses. Finally, the effect of specific bioactive ion species on cell behaviour will be presented with a special emphasis on strontium and cobalt.

1.3 The extracellular matrix

Cells *in vivo* are embedded in a complex network of macromolecules termed the extracellular matrix (ECM). The ECM provides physical and chemical cues to the cells that are substantial for tissue development and maintenance. It is easy to imagine that for the design of successful tissue engineered constructs, a thorough understanding of the ECM is substantial. Ideally, scaffolds used for such applications mimic features of the host tissue ECM. Therefore, the characteristics of bone and cartilage extracellular matrix will be briefly described in the following section.

1.3.1 Bone

The bone matrix is a composite from a materials point of view, comprising organic and inorganic components. The main organic phase of bone is type I collagen that is responsible for the flexibility and elasticity of bone[19]. It is well established that procollagen molecules, triple helical peptide chains, are secreted by the osteoblasts and self-assemble to form a growing collagen fibril. Self-assembly of collagen fibrils creates type I collagen fibres[20]. The triple helical structures of the collagen fibril building units are thought to provide a framework for the growth of the mineral phase[21]. Apart from type I collagen, the organic part of the bone matrix consists of non-collagenous proteins such as sialoproteins and bone gla proteins[22]. The mineral phase of bone is mainly composed of carbonated calcium-deficient apatite (often referred to as carbonated hydroxyapatite), comprising calcium, phosphorous, sodium, magnesium, fluoride and other ions in trace amounts[23, 24]. This inorganic component confers the hardness and stiffness to bone.

Bone mineralisation (calcification) is a continuous process occurring throughout the entire mammalian life. The precise mechanism of how tissues mineralise, however, is still incompletely understood. The common concepts describing biomineralisation involve one or more anionic matrix molecules, among them osteopontin and osteoclacin[25]. These proteins are pivotal for mineral formation and are thought a) to sequester the relevant ions, b) to serve as sites of nucleation and c) to provide a template for growth directing the size, shape and orientation of the crystal[26]. Such non-collagenous matrix proteins are attached to collagen *in vivo* which may imply that both entities act in concert to form

proper hydroxyapatite crystals. To what extent collagen is involved in the nucleation and growth of crystals is still a subject of debate[27].

1.3.1.1 Structural requirements

Ideally, the design of a scaffold aims at recreating the physiological environment found *in vivo*. Therefore, a thorough understanding of the structural characteristics of bone is imperative. Two types of bone are found in the adult human body: cortical and cancellous bone. Whereas cortical or compact bone consists of tightly packed Harvesian systems, cancellous or spongy bone is characterised by a network of trabeculae. Reflecting the differences in structure, the mechanical properties of the two types of bone are remarkably different (Table 1.1).

Table 1.1: Mechanical properties of cortical and cancellous bone, adapted from Fu *et al.*[13].

Property	Cortical bone	Cancellous bone
Compressive strength (MPa)	100 - 150	2 - 12
Flexural strength (MPa)	135 - 193	10 - 20
Tensile strength (MPa)	50 - 151	1 - 5
Young's modulus (GPa)	10 - 20	0.1 - 5

1.3.2 Cartilage

Cartilage in the human body can be classified into elastic, fibro-cartilage, fibro-elastic and hyaline cartilage depending on the composition of the matrix[28]. The type of cartilage covering the end of long bones in the adult is hyaline or articular cartilage. It confers a smooth, low friction gliding surface to the joint and facilitates the transmission of loads during weight-bearing activities. It is a non-vascularised tissue and relies on the diffusion of oxygen and nutrients from the synovial fluid. Native articular cartilage primarily consists of water (75 – 80% wet weight). The majority of its dry weight can be attributed to collagens (50 – 73%) and proteoglycans (15 – 30%)[29]. While type II collagen is the primary collagen component in articular cartilage, also types III, VI, IX and XI can be found[30]. The calcified zone of cartilage also contains type X collagen. Proteoglycans are macromolecules and consist of a core protein connected to one or more side chains of negatively charged glycosaminoglycans (GAG). GAGs are defined as linear, unbranched polysaccharides composed of a repeating disaccharide unit which comprises an amino sugar along with an uronic acid or galactose. The individual members of the GAG family can be grouped into four classes; heparin/ heparan sulphate, chondroitin sulphate/ dermatan sulphate, keratin sulphate and hyaluronan. Except for hyaluronan, all groups are sulphated (sGAG) and are covalently linked to core proteins. Aggrecan is the most abundant proteoglycan in articular cartilage and, by binding to hyaluronan, it forms stable ternary complexes in the extracellular

matrix. Due to the net negative charge of sGAGs such aggregates attract water molecules mediating the formation of hydrated matrices. The swelling of cartilage up to an equilibrium point is regulated by the elasticity of the collagens in the ECM.

Morphologically, articular cartilage can be separated into four zones; superficial, middle, deep and calcified zones (Fig. 1.1). The different zones are characterised by differences in ECM composition and chondrocyte morphology. The superficial zone makes up the first 10 - 20% of the full thickness articular cartilage and contains densely packed, type II collagen fibres which are aligned parallel to the articular surface. The middle zone (40 - 60%) has a higher content of proteoglycans and is characterised by randomly oriented collagen fibres. In the deep zone (30%), collagen fibrils are assembled in a radial fashion and extend into the calcified layer. The proteoglycan content is highest in this zone while the cell density is the lowest. If stained with a basic dye, the deep and calcified zones are separated by the so-called tidemark highlighting the mineralisation front[31]. The calcified cartilage layer builds the interface between the non-mineralised cartilage and bone providing both a mechanical transition and a fixation between the two tissues. Type X collagen is a non-fibrillar, short chain collagen and exclusively localised to the calcified zone of articular cartilage. Type X collagen is only found in the surrounding matrix of hypertrophic chondrocytes and has been linked to endochondral ossification[32]. While the function of type X collagen in endochondral bone formation remains to be fully elucidated, type X collagen is thought to interact with matrix vesicles and appears to play a role in matrix mineralisation.

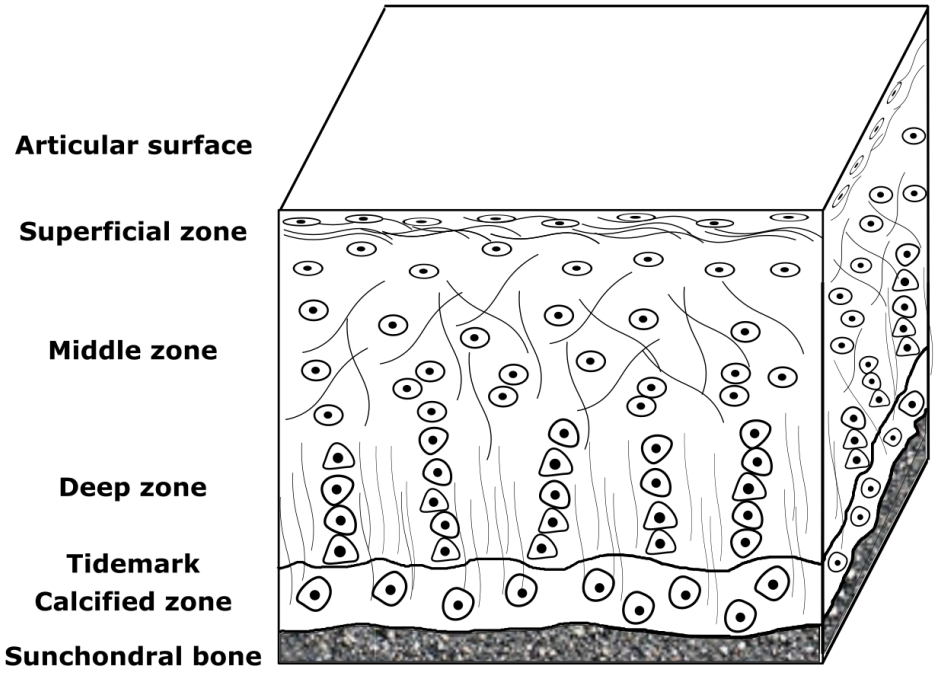


Figure 1.1: Cellular organisation and collagen fibre assembly in the different zones of articular cartilage. A cross-sectional schematic of articular cartilage with the underlying subchondral bone is shown. Adapted from Newman[33].

1.4 Key cell types of the osteochondral system

Whilst the ECM is undoubtedly a decisive parameter in guiding tissue engineering strategies, knowledge of the cell types specific to the tissue and their characteristics is equally important, especially since these cells are responsible for the appropriate ECM production *in vivo*. Therefore, the most relevant cell types for bone and cartilage formation and remodelling will be introduced, namely osteoblasts, chondrocytes and mesenchymal stem cells (MSC). These cell types are useful tools *in vitro* to evaluate the effect of specific materials or cues on cell behaviour, providing information on the possible biological response *in vivo*. In addition, they represent potential sources for cells to be incorporated into scaffolds prior to implantation as a reservoir for tissue formation. Finally, the process leading to ossification during embryonic development will be described as it is crucial for the understanding of the osteochondral system.

1.4.1 Osteoblasts

Osteoblasts are derived from bone marrow MSCs in a multistep differentiation process. For ease of nomenclature, cells committing to the osteogenic lineage can be artificially assigned to the following stages: (1) mesenchymal stem cells, (2) osteoprogenitor cells, (3) pre-osteoblasts and (4) osteoblasts[34]. *In situ*, however, the differentiation of the cells is much better described by a developmental continuum without any distinct classification[34]. Unfortunately, stage-specific developmental markers for osteoblast differentiation are scarce. In general, a progressive up-regulation of master phenotypic markers associated to the osteogenic lineage is interpreted as further commitment to the osteoblast phenotype[35]. For that purpose, runt related transcription factor 2 (RUNX2), osterix, type I collagen, alkaline phosphatase and bone sialoprotein are most frequently used[34].

Mature osteoblasts are responsible for the generation of new bone ECM. Once stimulated, they secrete and deposit the organic component of the bone matrix, termed osteoid. The major component of the osteoid is type I collagen, the most abundant protein in bone, which is essential for bone growth and development. Yet, osteoblasts synthesise and secrete a number of non-collagenous proteins alongside type I collagen that are incorporated in the bone matrix. Among the non-collagenous proteins are osteocalcin, bone sialoprotein, osteopontin and osteonectin[36-38]. As the secretion of osteoid ceases, osteoblasts either become embedded in the bone matrix and differentiate into osteocytes or remain on the surface of the bone and differentiate into lining cells. Once the deposition of osteoid is completed, matrix mineralisation is initiated.

Osteoblast differentiation and the deposition of osteoid are controlled by a plethora of signalling molecules, pathways and direct cell to cell interactions[39]. While the mechanisms of osteogenic differentiation are complex and to date incompletely understood, literature agrees that the transcription factor RUNX2 is the key transcriptional regulator of osteoblast differentiation[40]. In addition, a number of growth factors and hormones are tightly linked to the control of bone formation by regulation of

osteoblast differentiation and activation. The most prominent are: Bone morphogenic proteins (BMPs) and other growth factors, namely fibroblast growth factor (FGF), transforming growth factor beta (TGF-β) and parathyroid hormone[41, 42].

While osteoblasts undisputedly have their merit in assessing the performance of scaffolds for bone tissue engineering purposes *in vitro*, MSCs appear to be the preferred cell type for cell-seeded scaffold approaches[43, 44]. Like all terminally differentiated cells, the proliferative capacity of primary osteoblasts is limited further complicated by a relatively low yield of autologous cells from bone tissue biopsies[44].

1.4.2 Chondrocytes

Chondrocytes are the primary cell type of cartilage and responsible for cartilaginous matrix formation although they only make up 1 - 5% of the volume. Chondrocytes are broadly characterised by their ability to secrete a matrix rich in type II collagen and the proteoglycan aggrecan[45]. Like osteoblasts, they are derived from MSCs in a differentiation process driven by sex-determining region Y-box 9 (SOX9) protein and other transcription factors. Chondrocytes perform a pivotal role in bone formation during embryonic development and bone growth during childhood and adolescence by virtue of the growth plate which is discussed in more detail in 1.4.4[45]. In brief, following chondrogenesis, the chondrocytes either produce matrix to form articular cartilage or undergo proliferation and subsequent terminal differentiation to hypertrophic chondrocytes. The hypertrophic chondrocytes produce a matrix that is eventually resorbed and replaced by bone[31].

Cartilage found in adults is a multi-layered or multi-zonal tissue with a directed orientation and zonal differences in structure and composition. Chondrocytes, the only cellular component of articular cartilage, differ in their morphology and function depending on their zonal localisation which owes to different differentiation stages[31]. In the superficial zone, chondrocytes share properties with MSCs and have a more flattened ellipsoid morphology[46, 47]. Uniquely, chondrocytes of the superficial zone produce lubricin which contributes to a layer of lubricants on the surface of cartilage allowing the efficient movement of joints[31]. In the middle zone, chondrocytes are predominantly spheroid-shaped and the cell density is overall lower. In the deep zone, chondrocytes have an ellipsoid shape and are assembled in columns. Chondrocytes found in the deep zone synthesise relatively the highest amount of the proteoglycan rich matrix while remaining in a resting state. Calcified cartilage represents the interface between the non-mineralised articular cartilage and subchondral bone. Chondrocytes localised to calcified cartilage express markers of the hypertrophic stage of late-chondrocyte differentiation and synthesise a matrix rich in type X collagen as opposed to the type II collagen rich matrix of the superficial and middle zones[48, 49]. Chondrocyte hypertrophy is a regulated process defined by an increase in cell volume, extracellular matrix remodelling and expression of terminal differentiation markers[50, 51]. On a molecular level, hypertrophy is governed by RUNX2 that drives the expression of

terminal differentiation markers, among them most prominently matrix metalloproteinase 13 (MMP13)[52, 53], type X collagen[52], indian hedgehog[54] and vascular endothelial growth factor (VEGF)[55]. While the mechanisms of cartilage calcification are incompletely understood, matrix vesicles released by hypertrophic chondrocytes are thought to initiate mineral formation[56, 57].

When choosing a cell type for tissue engineering purposes both the performance (especially with regards to the extracellular matrix production) and accessibility need to be considered. Intuitively, using the resident cell type of a tissue, in this case chondrocytes, for cartilage repair seems logical. Supporting this notion, articular chondrocytes are the only cell source currently approved for clinical intervention (ACI)[14]. Indeed, the production of cartilaginous ECM produced by primary/ passage 0 articular chondrocytes is unmatched both in terms of synthesis rate and lack of hypertrophy[14]. Yet, considering the low cellularity of cartilage, *in vitro* expansion is necessary to treat bigger lesions and/or prepare cell-seeded scaffolds. Various studies have established that chondrocytes lose their phenotype during *in vitro* expansion, in particular in monolayer culture[58]. This so-called dedifferentiation is characterised by an increase in type I collagen expression while the expression of ECM molecules typical for articular cartilage such as type II collagen and aggrecan is reduced. Tissue produced by such dedifferentiated chondrocytes has fibrocartilage-type characteristics and has inferior mechanical properties that are not fit to repair articular cartilage lesions *in vivo*[58]. Therefore, other cell sources have been evaluated for cartilage tissue engineering, most prominently MSCs.

1.4.3 Mesenchymal stem cells

In their pioneering work, Friendenstein and co-workers first described a small subpopulation of cells found in the bone marrow that adhered to tissue culture plastic and was able to produce colonies from single cells (the colony-forming unit fibroblastic, CFU-Fs)[59]. Furthermore, *in vivo* transplantation of cells originated from a single colony led to the generation of a variety of skeletal tissues (bone, cartilage, adipose and fibrous tissue)[60, 61]. Initially such cells were referred to as “stromal” or “osteogenic” stem cells until, in 1991, Caplan coined the term “mesenchymal stem cell” (MSC) which gained widespread popularity[62]. In their seminal work, Pittenger *et al.* demonstrated the tri-lineage (osteogenic, adipogenic and chondrogenic) differentiation potential of MSCs *in vitro* further highlighting their value for tissue repair applications[63]. While the initial studies on MSCs were exclusively focused on MSCs isolated from the bone marrow, today the term MSCs encompasses cells isolated from nearly every connective tissue including adipose tissue, synovium and dental pulp[61]. Yet, whether MSCs isolated from other tissues share all characteristics with bone-marrow isolated MSCs is being questioned[14, 43]. For the purpose of this thesis, it will be specified if MSCs were not isolated from the bone marrow. In 2006, the International Society of Cellular Therapy proposed a minimum set of three criteria to define MSCs[64]. MSCs must be plastic-adhered and demonstrate tri-lineage differentiation potential (osteoblasts, adipocytes and chrondocytes) *in vitro*. As an antigen exclusively linked to MSCs has not been identified

so far, cells are classified as MSCs by the extracellular marker expression of CD105, CD73 and CD90 and the absence of CD45, CD34, CD14 or CD11b, CD79 or CD19.

In summary, MSCs are a group of non-hematopoietic, multipotent and clonogenic cells with the potential of self-renewal residing in the bone marrow or other connective tissues[65]. While the ability of MSCs to give rise to osteoblasts, adipocytes and chondrocytes is one of their key characteristics, the potential to differentiate into other mesoderm-type cells including skeletal or smooth muscle cells remains a subject of debate[61, 66]. Even more controversially discussed is the commitment to non-mesodermal lineages such as the differentiation into neuronal cells or hepatocytes[65, 67, 68]. Indeed, the term "mesenchymal stem cell" continues to be questioned and has been described as inappropriate by some as evidence for the multilineage differentiation potential beyond the skeletal system of single MSCs *in vivo* is lacking[61]. In this context, alternative terms including "skeletal stem cells" or "mesenchymal stromal cells" have been proposed[61].

1.4.3.1 The use of MSCs for tissue engineering applications

Due to their relative ease of isolation and expansion as well as their capacity to contribute to the regeneration of mesenchymal tissues including bone and cartilage, MSCs have received considerable attention in the field of skeletal tissue engineering[63, 69]. In addition, the use of MSCs does not bear any of the ethical constraints associated with embryonic stem cells. Therefore, an extensive amount of research has been dedicated to the directed *in vitro* osteogenic and chondrogenic differentiation of MSCs for the fabrication of engineered bone tissue-like structures, as reviewed by Abdallah and Khassem[70] and Arvidson *et al*.[69]. To that end, a vast amount of (3D) culture systems, soluble factors as well as scaffold structures and surface modifications have been explored to identify "optimal" conditions for tissue repair. Yet, MSCs are not only interesting for tissue engineering *in vitro* or *in vivo* but they are also a powerful tool to study the response of primary stem cells to a potential scaffold or implant.

Beyond their obvious value for bone/cartilage regeneration, more recently, the immunomodulatory and anti-inflammatory properties of MSCs have been recognised[71, 72]. MSCs are now known to produce a plethora of soluble bioactive factors thereby influencing their cellular environment and especially the immune system. This ability may ultimately have a bigger impact on their clinical use and commercial value than the originally pursued multilineage differentiation potential[73]. Yet, the immunomodulatory properties of MSCs are beyond the scope of this work. Upon bone injury, MSCs are thought to be recruited to the damaged site as part of the physiological healing process[74]. A number of growth factors have been identified to play crucial roles in the differentiation and lineage commitment of MSCs. For the purpose of this literature review, emphasis will be given to the processes underlying MSC differentiation towards osteoblast and chondrocyte lineages only. RUNX2/Cbfa is considered as the master regulatory transcription factor responsible for early osteogenic differentiation and skeletal development[75]. RUNX2 controls the commitment to the osteoblast lineage

from multipotent mesenchymal cells, promoting the multistep developmental process that eventually leads to the osteoblast phenotype. Highlighting the importance of RUNX2 in osteoblast development, it has been shown that RUNX2-deficient (RUNX2 -/-) mice are devoid of osteoblasts resulting in a lack of bone formation[76]. RUNX2 controls osteoblast differentiation by binding to the promoters of several genes known to be predominantly expressed in mature osteoblast, including type I collagen, osteonectin, osteocalcin and osteopontin. Furthermore RUNX2 is responsible for the induction of alkaline phosphatase (ALP) expression[75, 77-79].

Differentiation of MSCs into chondrocytes is thought to be directed by the transcription factor SOX9 and its downstream cofactors SOX5 and SOX6[80]. Highlighting the importance of SOX9 for chondrogenesis, knock out MSCs (SOX9 -/-) have lost the potential to differentiate into chondrocytes[81]. In *in vivo* experiments using mouse embryos, SOX9 inactivation in limb MSCs after mesenchymal condensation revealed that the transcription factor was also pivotal for later stages of cell commitment to the chondrogenic lineage and, together with SOX5 and SOX6, chondrocyte proliferation and extracellular matrix production[82]. Type II collagen is only one of the essential cartilage extracellular matrix components whose gene expression is regulated by SOX9. For a review on the role of SOX9 in chondrogenesis, please refer to Akiyama[80]. Considering the drawbacks associated with the use of chondrocytes for cartilage tissue engineering, MSCs have received considerable attention as an attractive alternative cell source. One of the main advantages of MSCs is their capacity to be readily expanded *in vitro* prior to chondrogenic differentiation. *In vitro*, chondrogenesis is usually induced by a high density (pellet) culture that aims at recapitulating MSC condensation during embryonic development and the use of chondrogenic factors such as TGF-β and dexamethasone[83]. Yet, chondrogenic differentiation of MSCs using the traditional protocols is flawed as MSCs tend to differentiate further along the endochondral route giving rise to MSC-derived chondrocytes that express hypertrophic markers such as type I and type X collagens as well as MMP13 warranting further optimisation of the differentiation techniques[84].

To date no single protocol or a combination of factors have been identified or agreed upon as the ideal route for osteogenic or chondrogenic differentiation of MSCs; yet, there is mounting evidence that the 3D structure of scaffolds, extracellular matrix proteins such as integrins and soluble factors like growth factors all play a crucial role in the event of differentiation that need to be considered[85]. In view of the *in vivo* physiological situation it is not surprising that no single agent has the power to drive differentiation but rather a combination and interplay of several factors is required. Overall, since their discovery in the 1970s, MSCs have attracted considerable attention by the tissue engineering and regenerative medicine communities due to their unique properties. The fact that nearly 600 clinical trials using MSCs are listed on clinicaltrials.gov is testament to the therapeutic value of this cell type for cell therapy and tissue regeneration applications.

1.4.4 Endochondral ossification

During embryonic development, bone formation occurs via two distinct processes; a) intramembranous ossification which describes the direct differentiation of MSCs to osteoblasts or b) endochondral ossification, involving the formation of a cartilage template and its replacement by bone. Independent of the mechanism, bone development is initiated by the migration of MSCs to the site of future skeletogenesis[34]. The interaction of the MSCs with the extracellular matrix and surrounding epithelial cells allow the aggregation of MSCs (MSC condensation) and a subsequent commitment to the chondrogenic or osteogenic lineage[34]. Flat bones such as the skull develop through intramembranous ossification. In this process, MSCs commit to the osteogenic lineage by differentiating first into osteoprogenitor cells and then further into osteoblasts[86]. The endochondral ossification process is responsible for the formation of the majority of bones in the body including all long bones[87]. Here, mesenchymal condensation results in a cartilaginous template that is later replaced by bone (Fig. 1.2). Thus, endochondral ossification is characterised by a complex cascade of events resulting in the formation of mineralised bone tissue on a cartilage scaffold[88].

Initially, condensed MSCs differentiate into chondrocytes, the main cell type of cartilage[45]. A growing cartilage layer is formed via chondrocyte proliferation and deposition of a cartilaginous ECM rich in type II collagen and proteoglycans. MSCs located in the periphery of the cartilage template differentiate into osteoblasts and begin to deposit a mineralised matrix eventually forming the bone collar. Simultaneously, a subset of the chondrocytes in the centre of the template adopts a hypertrophic phenotype characterised by the secretion of type X collagen, MMP13 and VEGF. Blood vessel formation into the calcified cartilage layer is initiated by VEGF and MMP13 secretion. MMP13 activity mediates the degradation of collagen fibrils and aggrecan creating space for blood vessel invasion[88]. Along with the growing capillaries, chondroclasts and osteoclasts are recruited that break down the calcified cartilaginous matrix. Blood vessels further facilitate the influx of haematopoietic cells that will later form the bone marrow as well as osteoblasts progenitor cells that deposit a type I collagen rich matrix giving rise to the primary ossification centre (POC)[89]. Secondary ossification centres arise at the ends of the of the cartilage template where the events of the primary ossification centre are recapitulated. To allow bone growth, a layer of cartilage between the primary and the secondary ossification centre (SOC) of the long bones of the limb remains. In this layer termed growth plate the developmental processes of bone formation are recapitulated. The growth plate disappears in humans once adolescence is terminated and hyaline articular cartilage exclusively remains localised to each end of the bone[45].

Once bone is formed, it is a dynamic tissue that is continuously being built, broken down and rebuilt in a process called bone remodelling. The dynamic nature of bone requires balanced actions of osteoblasts (bone forming cells) and osteoclasts (bone resorbing cells). Bone remodelling is a process that occurs continuously throughout life. The “bone remodelling cycle” is a multistage process consisting of activation, resorption, reversal, and formation phases[90]. Bone tissue is broken down and

absorbed by multinucleated cells termed osteoclasts that are exclusively found in bone. The mineralised bone matrix is efficiently resorbed by these cells leaving so-called resorption pits in the surface of the bone. Unlike osteoblasts, osteoclasts are derived from hematopoietic stem cells and share precursors with macrophages[90]. Following resorption, osteoblasts are recruited to the resorption pit and are activated to refill the resorbed lacunae with bone matrix[90]. Osteoblast recruitment and activation is thought to be mediated by osteoclast derived factors[90]. When the actions of osteoclasts and osteoblasts fail to be coordinated, diseases such as osteoporosis arise.

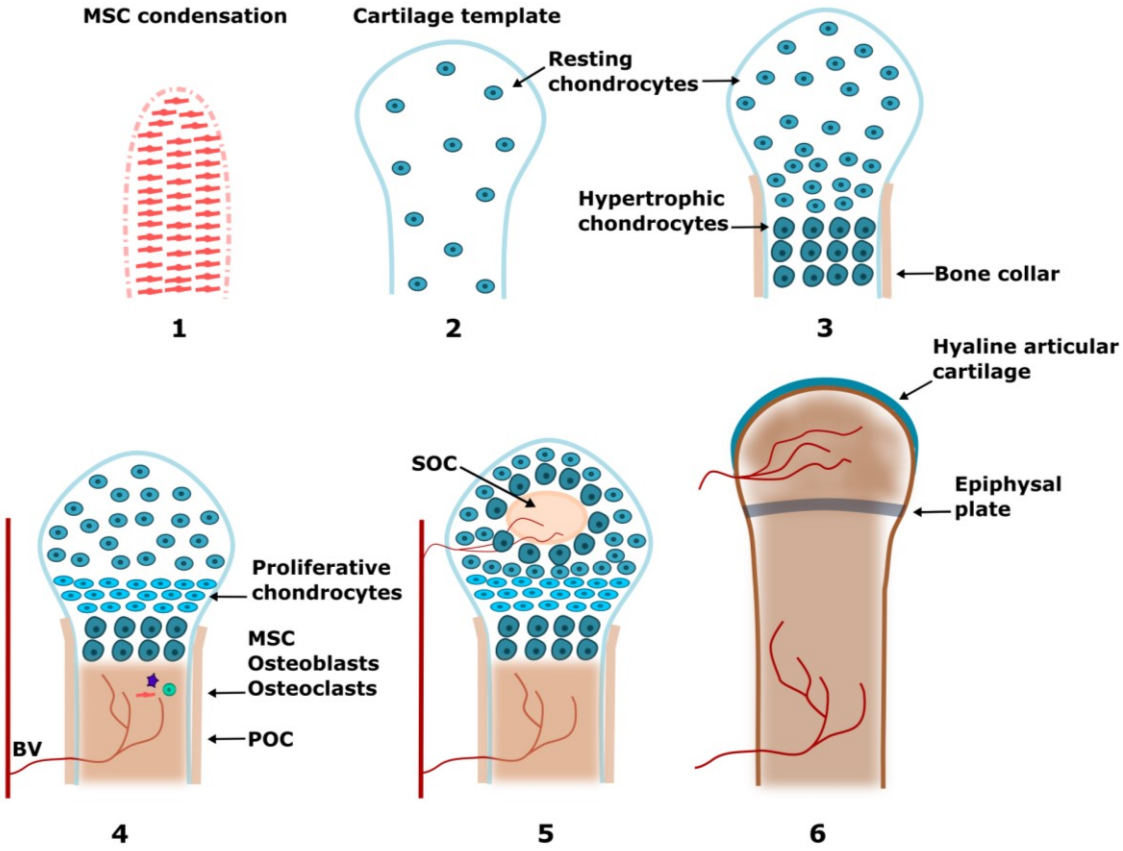


Figure 1.2: Process of endochondral bone formation. 1) Initially, mesenchymal stem cells (MSC) condense and 2) differentiate into chondrocytes to form the cartilage template of endochondral bones. 3) Cells in the periphery differentiate directly into osteoblasts and form the bone collar while chondrocytes in the centre become hypertrophic. 4) The hypertrophic chondrocytes initiate mineralisation and undergo apoptosis. Blood vessels invade the central region and allow the influx of MSCs, osteoblasts and osteoclasts initiating the formation of the primary ossification centre (POC). The osteoclasts break down the calcified cartilage matrix while the osteoblasts secrete bone matrix. The developing bone grows through chondrocyte proliferation. 5) Secondary ossification centres (SOC) arise in the epiphyses. 6) A layer of resting chondrocytes remains between the POC and the SOC termed the epiphyseal growth plate to allow bone growth until adolescence is terminated. At the end of the long bones a stable layer of hyaline articular cartilage persists. BV = blood vessels. Adapted from Kronenberg and Thompson *et al.*[45, 91].

1.4.4.1 Fracture healing

The mechanisms underlying fracture healing are complex and remain incompletely understood[8]. In general, bone is a tissue with great self-regenerative properties that can heal without the formation of fibrous scar tissue under optimal conditions. If certain conditions are met, including close proximity of fracture ends and mechanical stability, bone repair occurs in a relatively simple process termed primary fracture healing. In primary fracture healing the ends of the fracture either, if in direct contact, re-connect in a mechanism reminiscent of bone remodelling or, if a small gap remains, via the deposition

of intramembranous bone. The newly deposited bone is then remodelled by osteoclasts to re-establish the Haversian system of mature bone. If the optimal conditions for fracture healing are not met, a multi-stage process called secondary fracture healing is initiated. Secondary fracture healing can broadly be described in three stages: inflammation, callus formation and remodelling. Here, bone formation has characteristics reminiscent of both intramembranous bone formation and endochondral ossification. After the formation of a hematoma, the subsequent acute inflammation phase initiates the defect repair by creating an appropriate cytokine and growth factor environment and by recruiting osteoprogenitor cells and MSCs. In a complex series of events that follows, MSC either differentiate into osteoblasts (periosteum) or to chondrocytes (central region). The chondrocytes in the central areas secrete cartilaginous matrix thereby producing a cartilage scaffold. In a process resembling the events during growth plate development, the chondrocytes become hypertrophic and initiate the calcification of the cartilaginous matrix before undergoing apoptosis. The cartilage matrix is removed by osteoclasts while osteoblasts start to deposit a type I collagen rich matrix. In the final stage of secondary fracture healing, the newly deposited bone is remodelled to restore the Haversian system.

1.5 Biomaterials for bone tissue engineering purposes

With the advancement of the field of tissue engineering, the level of complexity and sophistication of biomaterials and scaffold systems increased considerably. Numerous biomaterials in combination with a variety of fabrication techniques have been explored for the design of scaffolds. While a plethora of differing approaches is being pursued, there is general agreement on key scaffold requirements. The principal aim of a scaffold is to support cell invasion, proliferation, differentiation and eventually the formation of native-like tissue, in addition to offering mechanical stabilisation throughout the regenerative process. Beyond that, a scaffold can have specific features or display special cues to enhance its biological activity with the ultimate goal of instructing the *in vivo* environment to form new tissue. Generally, properties such as biocompatibility, biodegradability, mechanical properties, scaffold architecture and manufacturing technology need to be considered for scaffold design and influence as well as depend on the choice of biomaterial[2].

From here onwards, the focus will be on scaffolds for bone tissue engineering. Reviewing the literature, it is well established that a number of architectural characteristics, including porosity, pore size and interconnectivity are essential for the development of scaffolds that support tissue repair. Pore size and porosity need to allow for cell migration, proliferation, blood vessel invasion as well as mass transport, e.g. of nutrients and waste. Pore diameters in the range of 200 µm to 900 µm have been reported as the optimal pore size for bone repair applications[44, 92]. A more recent study has reinforced the importance of carefully tailoring the pore size of scaffolds[93]. The number of MC3T3-E1 cells seeded in a 3D collagen-glycosaminoglycan scaffold and cultured for up to 7 days was significantly higher

when the mean pore size was 325 μM compared to scaffolds with pore sizes of 85 μM to 190 μM[93]. Murphy *et al.* argued that the bigger pores allowed a better cell infiltration and reduced cell aggregation along the edges of the scaffolds. Furthermore, a high pore-interconnectivity is desirable. Yet, from a mechanical viewpoint, a high porosity along with high mechanical strength poses a great challenge[94]. Apart from the macroporosity, the microstructure, also referred to as microporosity, affects the bone regeneration efficiency of materials[95]. In essence, studies have shown that higher microporosity of calcium phosphate based ceramics correlates with increased bone formation[96, 97]. A porosity of <10 μm appears to be desirable. More recently, the importance of the nanotopography of materials has been highlighted[98]. For example, it has been demonstrated that surface properties on a nano-scale can positively affect the differentiation of MSCs towards the osteogenic lineage[99].

Four classes of synthetic bone grafts can be identified based on their chemical composition: metals such as magnesium alloys, ceramics such as calcium phosphates and bioactive glasses, polymers and composites thereof[95]. Not only can the choice of material determine the performance of the bone substitute but also its architectural properties on a macro-, micro- and nano-scale. It is widely agreed that the ideal characteristics of a scaffold comprise: (1) a 3D network of interconnected pores that allow cell migration and cell growth as well as mass transport of nutrients and waste, (2) a biocompatible material that degrades in a controlled manner to match cell/ tissue growth, (3) surface modifications on the micro- and nano-scale to mediate cell attachment, proliferation and differentiation, as well as (4) adequate mechanical properties to match those of the tissues at the site of implantation[100]. An extensive amount of research has been dedicated to the development of scaffolds that tick all boxes; however, to date no single material can satisfy all requirements. While scaffold-free systems for the regeneration of bone, cartilage and osteochondral lesions have been evaluated, load bearing defects cannot be appropriately treated with cells alone. In this section, (1) calcium phosphate-based ceramics and (2) bioactive glasses will be introduced as scaffold materials. The use of synthetic and natural polymers for the fabrication of scaffolds for bone and especially osteochondral tissue engineering is subject of intensive research but is beyond the scope of this literature review. To date, there is no tissue-engineered construct for bone tissue regeneration with full approval for clinical use available. Meanwhile, a few bone grafts (engineered scaffolds/ biomaterials) have received regulatory approval and are starting to be used in the clinic such as Infuse® Bone Graft (Medtronic Sofamor Danek), a bovine type I collagen sponge soaked in recombinant human (rh)BMP2 used for fusion of spinal cage, Osigraft (Stryker), bovine type I collagen with rhBMP7 applied to long bone non-unions and Vitoss Bone Graft Substitute (Stryker), a bone void filler consisting of a porous foam comprising β-tricalcium phosphate (β-TCP), bovine type I collagen and bioactive glass. As a cautionary note, there is mounting evidence that Infuse® Bone Grafts cause a number of adverse effects such as ectopic bone formation warranting the evaluation of the delivery of growth factors for bone repair[101].

When evaluating the performance of scaffolds/biomaterials for bone regeneration *in vitro* and *in vivo*, a number of terms should be defined:

(1) Osteogenic: describes the intrinsic capacity to stimulate bone healing by the presence of cells, typically MSCs or osteoprogenitors[102].
(2) Osteoinductive: describes the potential to recruit MSCs and stimulate these cells to commit to the osteogenic lineage. Osteoinductive materials stimulate bone growth in ectopic sites, e.g. muscle[103, 104].
(3) Osteoconductive: is the ability of a material to induce bone formation along the sides of the implant.
(4) Osteoproductive: is the ability of a material to induce bone formation by cells away from the implant-bone interface[105].
(5) Bioactivity in the context of biomaterials has been defined by Hench *et al.*: "A bioactive material is one that elicits a specific biological response at the interface of the material which results in the formation of a bond between the tissues and the material"[6]. This definition alludes to the hydroxyapatite-like layer that is formed on the surface of some biomaterials, i.e. bioactive glasses and other (bioactive) ceramics. More recently bioactivity has also been used to describe the capacity to elicit or modulate biological activity in general[106].

1.5.1 Calcium phosphate-based ceramics

The success of calcium phosphate-based ceramics (CaP) for bone tissue engineering stems from their similarity in composition to the inorganic component of bone[107]. With respect to osteoinductive properties, CaP-based ceramics are the most extensively studied materials. CaPs with flat surfaces are generally understood to lack the ability to induce *de novo* bone formation (in nonosseus sites)[108]. Whether CaPs are osteoinductive appears to depend on a range of factors such as topography, geometry, composition, macropore size, and percent porosity of the CaP[107].

The most frequently used building blocks for CaP based ceramics are β-TCP and hydroxyapatite (HA) that are both considered to be osteogenic materials. Both ceramics show bioactivity *in vitro* and *in vivo*, albeit to different extents, and have found application in the clinic[109]. The observation that CaP based ceramics induce bone formation is attributed to their ability to precipitate a biological carbonated apatite layer on their surface[95]. The precipitation of the bone-like apatite layer is initiated by calcium and phosphate ions released by CaP based materials. β-TCP and HA differ in respect to their degradation rate and mechanical strength. β-TCP is more bioactive owing to higher dissolution rates compared to HA but the mechanical strength of sintered HA tends to be superior to β-TCP. Studies have shown that the rapid dissolution of β-TCP can trigger unfavourable immunologic reactions *in vivo*[109]. Dense stoichiometric HA particles on the other hand poorly perform *in vivo* in terms of bioactivity[109]. The solubility and hence bioactivity of HA can be improved by

modifying surface topography and particle size or by preparation of substituted HA[110, 111]. More recently, biphasic calcium-based ceramics composed of HA and β-TCP have been developed[112]. Biphasic materials with tuneable β-TCP/HA ratios may solve the shortcomings of their individual components. The clinical application of CaPs is currently limited to non-load bearing defects due to the inherent brittleness and low flexural/tensile strength of ceramics[113]. However, different fabrication techniques such as freeze casting have been explored to overcome this limitation[94]. Another approach is the reinforcement of CaPs with fibres which has been shown to improve strength and toughness[114]. Based on their strong osteoinductive capacity, CaP ceramics are widely used as coatings of bioinert metals for bone tissue engineering purposes[115]. Furthermore, they are frequently incorporated in composite scaffolds together with synthetic or natural polymers as reviewed elsewhere[116].

1.5.2 Bioactive glasses

Another group of biomaterials that falls within the class of ceramics and is frequently used for tissue engineering applications are bioactive glasses. In 1969 Professor Larry Hench developed the first bioactive glass termed 45S5 which was later marketed as Bioglass®[117]. The 45S5 bioactive glass (in this thesis referred to as 45S5 BG) is composed of 46.1 mol%, SiO_2, 26.9 mol% CaO, 24.4 mol% Na_2O, 2.6 mol% P_2O_5. It has not only the ability to form a hydroxyapatite (HA) layer *in vitro* in solutions lacking calcium or phosphate ions but also the ability to bind to bone *in vivo*[118]. Indeed, 45S5 BG was the first documented synthetic material to chemically bond with bone. Remarkably, the strength of the bond between 45S5 BG and bone was stronger than that of bone itself. Since 1985, 45S5 BG has been used for bone repair purposes in more than one million orthopaedic operations[119]. Initially, monoliths of 45S5 BG were used as middle ear implants (Douek-MED™) and later as tooth root implants (Endosseous Ridge Maintenance Implant (ERMI®)). A drawback of these 45S5 BG cones was that they either needed to be custom shaped for each patient or were offered in set sizes, hindering commercial success and clinical use even though the implants performed well in trials. In contrast, bioactive glasses in particulate form have gained some commercial success in non-load bearing applications. Generally, such bioactive glass granules tend to be mixed with blood to obtain a putty-like consistency before being pressed into the defect by the surgeon. The first commercial particulate 45S5 BG product was PerioGlas® which was marketed for periodontal disease-linked jaw defects in 1993 and is now sold in 35 countries[119]. Soon after, a 45S5 BG particulate product for orthopaedic defect repair was released under the name NovaBone (Nova-Bone Products LLC), which was later modified by the addition of a polyethylene glycol and glycerine binder to obtain a putty (NovaBone Putty). The first bioactive glass particulate product not based on the 45S5 BG composition is BonAlive® ((S53P4) 53.8 mol% SiO_2, 21.8 mol% CaO, 22.7 mol% Na_2O, 1.7 mol% P_2O_5) (BonAlive Biomaterials, Turku, Finland)[120]. BonAlive® is used for treatment of bone defects and was approved for the European market in 2006. Possibly the biggest commercial success of bioactive glass is its

incorporation in toothpaste for hypersensitive teeth (NovaMin Technology, FL; now owned by GlaxoSmithKline, UK). NovaMin is a very fine powder of 45S5 BG that is now sold as component of toothpaste for hypersensitive teeth in more than 20 countries.

1.5.2.1 Structure of bioactive glasses

Glasses can be defined as amorphous solids without a long-range atomic order[107, 121]. Furthermore, all glasses show a region of glass transformation behaviour. This glass transition range is specified as the temperature region in which a system transforms from a supercooled liquid to a solid glass[107, 121]. Oxide glasses are commonly either produced via a melt quench route or by a sol-gel process. The melt-quench route was used to prepare all bioactive glasses used in the experiments presented in this thesis. In the melt quench route, precursor materials are melted in precious metal or ceramic crucibles at high temperatures between 1,200°C and 1,500°C. The melt is then rapidly quenched. If the cooling is sufficiently rapid, no crystallisation will occur and a glass will form. The fabrication of bioactive glass via the sol-gel route relies on the assembly of silica nanoparticles at room temperature[122]. Typically, sol-gel-derived bioactive glasses have fewer components than melt-derived glasses and a higher silica content. Furthermore, sol-gel-derived glasses are characterised by an inherent nanotopography resulting in relatively high surface areas and dissolution rates[119].

In the early 1930s the random network theory was introduced by Zachariasen to explain the properties of glasses[123]. In essence, he defined three different structural components of glasses. The network formers build the backbone of glasses and can form glasses in absence of other components. The most common network formers are silica (SiO_2), phosphorous pentoxide (P_2O_5) and boron trioxide (B_2O_3)[107]. All bioactive glasses used in the experiments presented in this thesis are based on silica. The SiO_4 tetrahedron is the basic building block of silica-based glasses and forms a continuous 3D network[121]. Neighbouring SiO_4 tetrahedra are connected through Si-O-Si bonds also known as bridging oxygen atoms. Bioactive glasses are special in that they classically have a lower silicon content than conventional glasses leading to a more open silicon network. Network modifiers, as their name indicates, modify the glass structure by breaking bridging oxygen bonds thereby reducing the degree of network connectivity of the SiO_4 tetrahedra[107]. The incorporation of network modifiers causes a reduction in glass transition temperature (T_g) and an increase in degradability. Typical network modifiers are alkali or alkaline-earth metals. A number of alkali and alkaline-earth metals are frequently incorporated in bioactive glasses such as sodium, potassium, calcium and strontium. Additional network modifiers are zinc, copper and silver. The third category of structural components in a glass was termed network intermediates. Intermediate ions such as magnesium can either function as network formers or as modifiers whilst not being able to form a glass network on their own.

1.5.2.2 The bioactivity of bioactive glasses

Bioactive glasses have a higher amount of network modifiers than conventional glass which is key to their bioactivity. When exposed to aqueous solutions such as body fluids network modifiers exchange

with H^+ ions in solution. Chemical reactions at the surface of the glass eventually result in the formation of an apatite layer on the surface of the bioactive glass. The bioactivity of bioactive glasses was initially attributed to this apatite layer; however, it is now well recognised that the ion release products themselves have biological functions and can interact with cells. Yet, the observed strong bonding of 45S5 BG to bone *in vivo* owes undoubtedly to the carbonate-substituted hydroxyapatite (HCA) layer that forms on the surface of bioactive glass following dissolution[124]. The mechanism of HCA layer formation has been extensively studied and described by Hench and colleagues[125]. Essentially, five reaction stages have been proposed that lead to the formation of the HCA layer in body fluid *in vivo* or in simulated body fluid (SBF) *in vitro* (Table 1.2):

Table 1.2: HCA layer formation, adapted from Jones, Hench and Rahaman *et al.*[119, 124, 126].

Stage	Reaction
1	Rapid ion exchange reactions between the glass network modifiers (Na^+ and Ca^{2+}) with H^+ (or H_3O^+) ions from the solution, leading to hydrolysis of the silica groups and the creation of silanol (Si–OH) groups on the glass surface: e.g. $Si\text{-}O\text{-}Na^+ + H^+ + OH^- \rightarrow Si\text{-}OH^+ + Na^+(aq) + OH^-$ The pH of the solution increases due to the consumption of H^+. The change in pH can be quite pronounced and is relatively fast as it occurs during the first minutes to hours of immersion in an aqueous buffer[107].
2	The increase in pH leads to the breakdown of Si-O-Si bonds and the dissolution of silica, in the form of silicic acid, $Si(OH)_4$, into the solution, and the formation of Si–OH (silanol) groups on the glass surface: $Si\text{-}O\text{-}Si + H_2O \rightarrow Si\text{-}OH + OH\text{-}Si$
3	Condensation and repolymerisation of an amorphous SiO_2-rich layer on the surface of the glass depleted in alkali and alkaline-earth cations.
4	Further dissolution of the glass, coupled with migration of Ca^{2+} and $(PO_4)^{3-}$ ions to the surface through the SiO_2-rich layer, forming a film rich in amorphous $CaO\text{-}P_2O_5$ on top of the silica-rich layer.
5	As the glass continues to degrade, OH^- and CO_3^{2-} from the solution are incorporated into the CaP rich film which then crystallises as an HCA layer.

The above outlined mechanisms hold true for bioactive glasses in general, yet the kinetics of the dissolution process and of HCA layer formation depend on the respective glass composition[119]. Apart from network connectivity, it has been shown that the nature of the network modifiers can alter glass solubility and degradation rates. Wallace *et al.* demonstrated that the systematic substitution of calcium oxide by sodium oxide led to an increase in the rate of ion exchange (solubility)[127]. This phenomenon

was explained by a lower packing density caused by a lower field strength of sodium ions and subsequent weaker ionic cross-links. Similarly, the replacement of calcium by strontium on a molar basis was demonstrated to increase glass solubility[128]. Here, the bigger ion radius of strontium resulted in a lower packing density of the glass.

Since the HCA layer shares similarity with apatite, the mineral constituent of bone, it is thought to be responsible for the tight binding to bone tissue[126]. The exact biological mechanisms promoting the strong bonding of the HCA layer to bone; however, remain incompletely understood. Once the HCA layer has formed, proteins such as growth factors and collagens are believed to absorb to the HCA layer, thus promoting the attachment, proliferation as well as differentiation of osteoprogenitor cells and finally the production of ECM by them[5]. The mineralisation of the deposited ECM to a nanocrystalline mineral at the surface of the bioactive glass/ HCA layer is thus thought to underlie the firm boding to bone[129].

Apart from their bone bonding properties, 45S5 BG implants have been recognised to promote new bone formation along the implant surface as well as away from the bone/ implant interface. These characteristics are being referred to as osteconductive and osteoproductive, respectively[105, 124]. The discovery of 45S5 BG with its striking osteogenic properties has spurred the development of bioactive glasses and doped systems for tissue engineering. Since 1969, numerous bioactive glasses varying in their compositions and fabrication techniques have been evaluated; however, 45S5 BG still excels with respect to its biological properties[119]. A limitation of 45S5 BG and bioactive glasses in general is the difficulty to process them into porous 3D scaffolds. To fabricate bioactive glass scaffolds, bioactive glass particles are commonly reheated (sintered) in order to be shaped into a desired form. Yet, if enough energy is supplied, the atoms of the glass network can rearrange into a crystalline structure[121]. Highly bioactive glasses such as 45S5 BG are more prone to crystallisation and thus have a smaller sintering window. Devitrification of 45S5 BG reduces the bioactivity and delays the formation of a HCA layer[130]. Bioactive glasses such as 13-93 (54.6 mol% SiO_2, 22.1 mol% CaO, 6.0 mol% Na_2O, 7.9 mol% K_2O, 7.7 mol% MgO, 1.7 mol% P_2O_5) have been developed and have a bigger sintering window than 45S5 BG which was achieved by modifying the glass composition. There are a number of different techniques available to fabricate melt-derived bioactive glass scaffolds including the use of sacrificial polymer templates; however, all require sintering as final step[107, 119]. Due to the difficulties that are encountered when sintering glass particles into a dense network, 3D porous scaffolds are frequently limited by their low strength[131]. Furthermore, much like for CaPs, a general limitation of bioactive glasses is their inherent brittleness. Of note, it has been shown that with tailored architectures, mechanical properties of porous 3D bioactive glass scaffolds can be improved[107]. Undoubtedly, the way a glass is fabricated will dictate glass properties and thus will naturally have a considerable influence on cell-material interactions. Yet for the purpose of this literature review, fabrication techniques will not be addressed. Due to their osteogenic properties, bioactive glasses have been used for the fabrication of polymer/ bioactive glass or hydrogel/ bioactive glass composites and coatings for metal implants.

1.5.2.3 Biological response to bioactive glasses

A large body of evidence suggests that bioactive glasses are osteoproductive *in vivo*. Hence, new bone is not only formed along the axis of the implant, a characteristic which is termed osteoconductive, but also away from the implant which has been termed osteoproductive by Wilson[105]. Furthermore, bioactive glass granules have been shown to enhance osteogenic differentiation of MSCs *in vivo*[132]. The assessment of bioactive glasses *in vitro* and *in vivo* has been traditionally focussed on bone and osteogenic cells. Thus, a number of studies have investigated the influence of bioactive glasses on pre-osteoblastic cell lines[133, 134], primary osteoblasts[135-137], foetal osteoblasts[138] and bone marrow stromal cells[139]. In essence, it has been shown that 45S5 BG and other glass compositions have the ability to promote osteoblast proliferation and differentiation by enhancing the expression of key phenotypic markers such as RUNX2, type I collagen and osteocalcin[137, 140, 141]. For example, it was demonstrated that a sol-gel bioactive glass of the composition 60 mol% SiO_2, 36 mol% CaO, 4 mol% P_2O_5 supported nodule formation and mineralisation by primary human osteoblasts[135]. Similarly, primary osteoblasts seeded on melt-derived 45S5 BG discs showed a higher rate of proliferation and increased osteogenic marker gene expression compared to control[137]. Likewise, although not as extensively studied, bioactive glasses have an effect on MSCs. It has been shown that the presence of silica-based bioactive glass powders (both sol-gel and melt-derived) increased the differentiation of rat bone marrow cells into ALP positive cells after three weeks of culture[142]. Furthermore, an increased production of mineralised nodules has been observed[142].

Considering the nature of bioactive glasses and the release of ions that occurs during their degradation, it appears to be extremely important to analyse the influence of these ionic products on the surrounding tissue.

1.6 Bioactive ion species for tissue engineering

Historically, inert (bio)materials were considered preferable for the fabrication of implants to circumvent foreign body reactions[5]. In contrast, current efforts in the field of (bone) tissue engineering are focused on the development of complex (3D) scaffolds that are designed to interact with the host tissue and, ideally, support its regeneration[4]. In addition to the biomaterial, (micro)porosity, pore size and surface topography of a scaffold, supplementation with bioactive molecules has a significant impact on MSCs and cells of the osteogenic lineage in terms of viability, proliferation, differentiation and matrix production *in vitro*, as well as on bone formation *in vivo*[143]. Introduction of bioactive molecules to the defect site can be achieved by two different strategies: bioactive molecules can be immobilised on the surface of the scaffold by chemical or physical interactions, or the scaffold itself is used as a carrier system, releasing soluble bioactive molecules to influence the biological response[144]. The latter method is frequently used for the delivery of growth factors or DNA plasmids. The delivery of these

molecules and their controlled release is highly complex and is beyond the scope of this literature review. Apart from proteins or peptides, ions, such as Sr^{2+}, Mg^{2+}, Zn^{2+}, Ca^{2+}, PO_4^{3-} are involved in biological processes and have the ability to trigger various cell responses, depending on the nature of the ion(s) and their concentration. Due to their low price, availability and bioactivity, incorporation of biologically active ions within bone substitutes appears thus as an attractive way of modifying cell/materials interactions.

To this end, scaffolds that feature bioactive moieties have been developed. The local release of bioactive moieties from a graft is a great advantage as the therapeutic agents are delivered to the site of desired tissue repair whilst minimising systemic effects. In this context, bioactive glasses present attractive carrier systems for the delivery of therapeutic ions. By modifying the glass network and composition, the release rates of key ions can, in theory, be adjusted and ideally be optimised. A further advantage of bioactive glasses is that they allow the continued release of bioactive ions and thus a sustained therapeutic effect throughout the degradation process.

Crystalline ceramics such as CaP-based materials have similarly been doped with certain bioactive ion species (e.g. Sr) to enhance their bioactivity and/or mechanical properties; however, this is beyond this literature review[145].

In Chapter 2 and Chapter 3, the question was pursued of how incorporation of strontium within the structure of bioactive glasses would affect the human MSC (hMSC) response. In the following two chapters (Chapter 4 and Chapter 5), the influence of cobalt-containing bioactive glasses on hMSC behaviour was assessed. The next sections are thus focussing on the current knowledge we have regarding the cell response to bioactive glasses and their ionic dissolution products with a particular emphasis on the bioactive ions strontium and cobalt.

1.6.1 Cell response to bioactive glass ionic dissolution products *in vitro*

The bioactivity of bioactive glasses is thought to be mediated by two independent mechanisms, (1) direct cell-scaffold surface interactions and (2) effects of ionic dissolution products on MSCs and cells of the osteogenic lineage (Fig. 1.3). For the purpose of this thesis, the impact of bioactive glass dissolution products on the cell response will be discussed in detail. In the literature different experimental set ups have been described to study the influence of bioactive glass ionic dissolution products on cells *in vitro*; a) cells are cultured in presence of bioactive glass particles, b) a bioactive glass disc is immersed in the culture medium of cells that are grown on tissue culture plastic or c) medium containing ionic glass extracts but no particles (in this work termed bioactive glass-conditioned medium) is prepared prior to the addition to cells. The benefit of the first and second approach is a dynamic release of ions from the particles or disc that mimics the conditions *in vivo* after graft implantation. Yet, as the ion release is not steady it is difficult to link cellular behaviour to a certain ionic environment. The first culture method has the disadvantage that a subset of cells is in direct contact

with the glass particles which may bias the overall result. Moreover, a comparable ion release between replicates and independent experiments is difficult to assure as the ion release from particles might differ. Comparing the first and the second experimental set up, the latter is preferable if the influence of the ion release products alone is the focus of the study. The third approach similarly avoids direct material-cell interactions while additionally ensuring a constant and comparable medium composition. This system facilitates the comparison of different glass compositions especially when the impact of (the concentration of) certain key ions is concerned. While the stable ionic composition of the concentration is an advantage it comes with the disadvantage that this approach is unlikely reminiscent of conditions cells encounter *in vivo* after graft implantation.

To properly dissect the effect of ionic dissolution products of bioactive glasses as opposed to direct cell-material interactions, bioactive glass-conditioned medium, containing the ionic dissolution products of the glasses, need to be tested on cells. For a comprehensive review on the biological response to ionic dissolution products from bioactive glasses please refer to Hoppe *et al.*[146]. Xynos and colleagues were the first to document the effect of 45S5 BG-conditioned medium on human osteoblasts[147]. Osteoblast proliferation was increased after 4 days of culture in 45S5 BG-conditioned medium compared to medium only suggesting that the ionic dissolution products of 45S5 BG acted as mitogens and thus provided an adequate stimulus for cell proliferation. The mitogenic activity was partly attributed to the up-regulation of insulin growth factor II expression (IGF-II) as well as the increased availability of unbound IGF II protein in the medium[147]. Xynos and colleagues went on to further dissect the influence of 45S5 BG-conditioned medium on gene expression by performing a cDNA microarray analysis. Gene expression profiling of human osteoblasts treated with 45S5 BG-conditioned medium for 48 h revealed a greater than two-fold up-regulation of 60 genes compared to control indicating a profound effect of the ionic dissolution products on the cells[148]. The most significantly up-regulated genes were associated with signal transduction, growth and cell-cycle regulation[148]. Underscoring the pioneering work by Xynos *et al*. bioactive glass-conditioned medium using 45S5 BG but also other compositions, was shown to modify gene expression in human foetal osteoblasts[149, 150] and human primary osteoblasts[151]. In particular, the influence of bioactive glass derived ionic products on genes involved in bone growth and development was studied and found to be up-regulated. Notably, ionic extracts increased the expression of alkaline phosphatase, osteonectin and bone sialoprotein in the absence of osteogenic supplements in human foetal osteoblasts[150]. Similarly, several studies have demonstrated a pro-angiogenic effect of bioactive glasses and their ionic dissolution products *in vitro* using fibroblasts and endothelial cells. For a review discussing the *in vitro* and *in vivo* angiogenic effects of bioactive glasses, please refer to Gorustovich *et al.*[152]. A recent study suggested an increase in mineral formation and the production of osteocalcin and type I collagen by adipose tissue-derived hMSCs in bioactive glass-conditioned osteogenic medium compared to control[153]. Bioactive ions alone in absence of osteogenic factors did not enhance osteogenic lineage commitment of the adipose-tissue derived hMSCs even though gene expression of osteogenic markers

appeared to be up-regulated after 14 days of culture. The authors argued that this effect might have been caused by very low levels of phosphorous in the osteogenic factor-free medium. In contrast, Reilly *et al*. did not observe a consistent effect of 45S5 BG dissolution products on hMSC osteogenic differentiation[154]. Yet, the same group demonstrated that ALP activity of murine MSCs was enhanced in presence of 45S5 BG dissolution products[139]. In both studies, the effect of the dissolution products seemed to some degree donor dependent. Regarding the mode of action of bioactive dissolution products, the bioactive ions are thought to activate intracellular signalling mechanisms (Fig. 1.3). Notably, there is evidence that the presence of bioactive glass ionic dissolution products in the medium changes the intracellular levels of ions. The calcium content in osteoblasts cultured in 45S5 BG particle-containing medium was found to be increased while the concentration of a range of ions was increased in a study using a different bioactive glass composition[155, 156].

To enhance and tailor the bioactivity of biomaterials for specific (tissue engineering) applications, various key metallic ions have been incorporated in bioactive glasses and other ceramics. The optimisation of stimulatory effects on osteogenesis and angiogenesis as well as the introduction of antibacterial properties have been most widely pursued. To that end, cobalt, copper, magnesium, silver, strontium and other key biologically active ions were used to dope bioactive glasses. For the purpose of this literature review, the ion species strontium, cobalt and magnesium will be discussed in more detail.

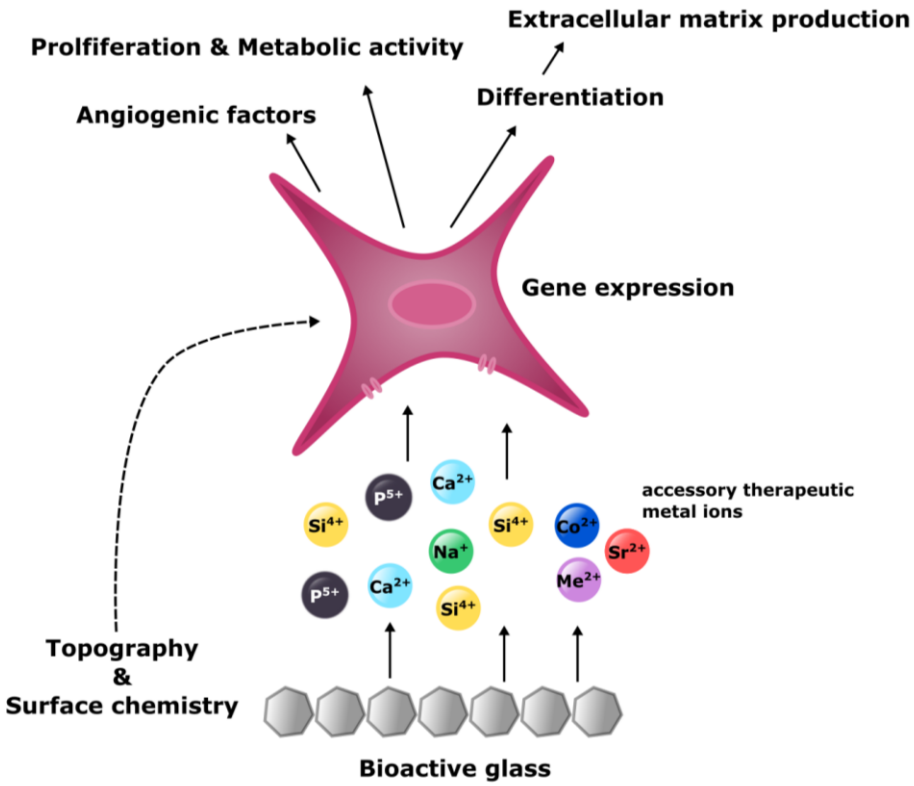


Figure 1.3: Regulation of cell behaviour by bioactive glasses. The cell response to bioactive glasses is regulated by a combination of factors, i.e. topography and surface chemistry of the graft and the ionic dissolution products. Interaction of cells with bioactive glasses and their dissolution products activates intracellular signalling pathways mediating changes in gene transcription. Adapted from Hoppe *et al.* and Jell and Stevens[146, 157].

1.6.2 Strontium

Strontium is the 15th most abundant element on earth and a natural constituent of the human diet[158]. Once taken up into the body, the bulk of strontium is deposited in bone or teeth where it makes up 0.335% of the cation content. There is evidence that strontium is preferably localised to mineralised bone or in close proximity thereof[159, 160]. While high doses of strontium (>4 g/l) in the diet have been reported to disturb bone mineralisation in rats, low doses of strontium (<4 g/l) have been found to have a beneficial effect on both bone formation and trabecular bone density[158]. The increased bone formation rate has been attributed to a higher osteoblastic activity which results in an increase in the amount of osteoid[161]. Interestingly, it has recently been reported that exposure to 1 M $SrCl_2$ *in vitro* increased the stiffness, hardness and toughness of bone, hence suggesting an influence on intrinsic bone material properties[162]. In this study, bone specimens excised from female rats were exposed to $SrCl_2$ as well as $BaCl_2$ and $CaCl_2$ ion solutions to assess specificity. Bone hardness was only significantly increased in the $SrCl_2$ treated specimens, while elastic modulus was increased by all ion solutions. Notably, when bone specimens collected from ovariectomised (OVX) mice were exposed to 1 M $SrCl_2$, material level

property changes regarding stiffness, hardness and re much more pronounced than in control animals. *In vitro* studies of murine and human bone marrow derived MSCs have shown that strontium at a concentration of 3 mM has an influence on the commitment of the MSCs, favouring the osteogenic over the adipogenic lineage[163, 164]. The underlying mechanisms of the mode of action of strontium remain ill defined; however, one study suggests that strontium mediates its effects via WNT/β-catenin signalling[165].

1.6.2.1 Effects of SrR in vitro and in vivo

Osteoporosis is characterised by an imbalance of bone formation and bone resorption resulting in low bone mass and microarchitectural deterioration of bone tissue[166]. Since 2004, strontium ranelate (SrR) has been used as anti-osteoporosis treatment. SrR significantly reduces the incidence of vertebral and non-vertebral fractures in post-menopausal women suffering from osteoporosis[167, 168]. In animal studies using OVX rats, a model for post-menopausal osteoporosis, SrR treatment resulted in improved bone parameters in terms of mass, microarchitecture and strength[169]. Unlike other anti-osteoporosis drugs, there is evidence from animal studies and studies on bone cells *in vitro* that SrR has the ability to both enhance bone formation[170, 171] and decrease bone resorption[172]. Indeed, *in vitro* studies have shown that SrR stimulates osteoblast differentiation and function while suppressing osteoclast differentiation and resorptive activity[173]. However, the underlying mechanisms that account for the anabolic and anti-catabolic actions of SrR remain largely unknown and the "dual action" of SrR has lately been challenged[174]. An intriguing study suggests that SrR inhibits Nf-kB activation, uncoupling it from TNF alpha signalling[175]. Interestingly, the individual components of SrR, sodium ranelate and strontium chloride, had no influence at the concentration studied on NF-kB highlighting that SrR and strontium ions are not necessarily interchangeable[175].

Another study provided evidence that SrR induced nuclear factor of activated T cells (NFAT)-mediated Wnt signalling and subsequent osteoblast proliferation and differentiation[176]. From a mechanistic viewpoint, the beneficial effects of SrR would be at least partly attributed to activation of the Calcium-sensing receptor (CaSR)[177, 178]. Using osteoblasts from CaSR knockout [CaSR(-/-)] and wild-type [CaSR(+/+)] mice it was shown, however, that SrR maintained its positive effect on cell replication indicating that CaSR is not the only target of SrR[179].

Apart from osteoblasts and osteoclasts, SrR likewise seems to have an influence on the differentiation of MSCs. Treatment of rat bone marrow MSCs with SrR significantly enhanced the mRNA expression of key osteogenic markers i.e. RUNX2, bone sialoprotein, and osteocalcin in osteogenic medium and significantly repressed the expression of key adipogenic markers, i.e. peroxisome proliferator-activated receptors γ (PPARG), adipocyte lipid-binding protein 2, and lipoprotein lipase in adipogenic medium compared to control respectively[180]. Another study confirmed that SrR increased the expression of RUNX2 in human MSCs at day 4 which may indicate a facilitated differentiation towards the osteogenic lineage[181].

1.6.2.2 Strontium-containing bioactive glasses

Considering the promising results obtained by treating osteoporosis with SrR, bioactive glasses substituted with strontium (SrBG) may be highly interesting for bone regeneration applications. Bioactive glasses provide the opportunity of a slow, preferably controlled, release of therapeutically relevant ion species such as strontium. Moreover, SrBG grafts would allow the local delivery of strontium minimising undesired side effects. To investigate the influence of strontium substitution in the system 49.46 mol% SiO_2, (23.08 - X mol%) CaO, X mol% SrO, 26.38 mol% Na_2O, 1.07 mol% P_2O_5 on glass structure, physical properties and cell response, 0 – 100 % of the calcium were substituted on a molar basis with strontium (0, 10, 50 or 100 %)[128]. Regarding the physical properties, substitution of calcium by strontium did not alter the glass network structure itself; yet, the network was expanded due to the larger ionic radius of strontium[128, 182]. Furthermore, the substitution by strontium increased glass dissolution and hence ion release which was attributed to the expanded glass network[128]. Interestingly, apatite formation was significantly enhanced by 100% strontium substitution[128]. In agreement, it has been reported that strontium addition in phosphosilicate glasses favoured the formation of apatite on the surface of the glass *in vitro*[183]. In contrast, the introduction of strontium in the 38.49 mol% SiO_2, (36.07 mol% − X mol%) CaO, X mol% SrO, 19.24 mol% MgO, 5.61 mol% P_2O_5, 0.59 mol% CaF_2 system resulted in a decreased apatite formation in SBF[182]. A study by Gentlemen *et al.* has nicely dissected the effects of strontium substitution in the above mentioned SiO_2, P_2O_5, CaO, SrO, Na_2O system[184]. Saos-2 cells, a human osteosarcoma cell line, has shown enhanced metabolic activity after two weeks of culture in medium containing SrBG ionic dissolution products compared to Saos-2 cells cultured in standard medium or standard medium containing bioactive glass dissolution products with no strontium. When Saos-2 cells were directly seeded on SrBG discs, a significant increase in total ALP activity and DNA abundance which correlated with increasing strontium content was observed after two weeks of culture. In accordance with the *in vitro* results obtained for SrR, treatment of osteoclasts with SrBG dissolution products resulted in decreased tartrate-resistant acid phosphatase activity and erosion pit area on CaP-coated glass slides, a known indicator to test osteoclast activity. Yet, the SrBG dissolution products did not suppress erosion pit formation to the same extent as pamidronate, a bisphosphonate.

Taken together, strontium is a highly attractive bioactive moiety with a possible disease modifying effect on osteoporosis. Incorporation of strontium enhances the bioactivity of bioactive glasses and may benefit bone repair applications.

1.6.3 Cobalt

Cobalt, a transition group metal, is present as trace element in the human body. Cobalt is naturally taken up through the diet and can be detected in drinking water, vegetables and fish. The mean daily cobalt uptake ranges between 11 to 45 µg[185, 186]. The European Food Safety Authority deemed a daily cobalt

intake of <600 µg as harmless while the United Kingdom Expert Group on Vitamins and Minerals stated that ingestion of up to 1400 µg of cobalt-containing supplements per day was unlikely to cause adverse health effects[187-189]. Although cobalt is a cofactor of vitamin B_{12} (hydroxocobalamin) it is acutely toxic in larger amounts. Similarly, long-term exposure to lower levels of cobalt can cause adverse health effects such as cobalt asthma or cobalt cardiomyopathy[190]. Cobalt-based alloys such as the cobalt–chromium–molybdenum system are frequently used in the medical industry for the manufacture of bone and dental implants[191]. Yet, metal debris from such implants has been associated with inflammation and aseptic implant lossening[192]. The underlying mechanisms of cobalt toxicity remain largely elusive but may be linked to the ion's 1) similarity to calcium which could affect calcium-dependent signalling mechanisms, 2) high affinity to sulfhydryl groups which may inhibit enzymes implicated in oxidative respiration, 3) ability to displace other metal ions from the active centre of metal-dependent enzymes and 4) ability to generate reactive oxygen species via Fenton-like reactions.

Despite the reported adverse effects, cobalt was successfully used to treat anaemia in the 1950s and marketed in the US under the name Roncovite, however, due to high renal toxicity the drug was later retracted[193]. More recently, the administrations of cobalt chloride ($CoCl_2$) for several weeks at a dose of 500 - 1200 µg/day to treat hyperexcretion of oestrogen during hormone replacement therapies has been suggested[194]. To date, cobalt containing supplements are available on the US market (Gammadyn Mn-Co (Unda Seroyal)[193]. A recent study investigated the impact of continuous $CoCl_2$ ingestion (1000 µg/day) for one month on healthy adults[189]. Despite a pronounced increase in cobalt levels in whole blood samples after 31 days of treatment (0.5 µg/L baseline versus (vs.) 33.3 µg/L (mean value female volunteers); 16.3 µg/L (mean value male volunteers)), no adverse health effects were observed. Furthermore, results from animal studies suggest $CoCl_2$ supplementation as viable tool for tissue protection. *In vivo* experiments in rats have shown that pre-conditioning with $CoCl_2$ prior to hypoxic conditions had a protective effect on the heart[195, 196], kidney[197] and brain[198]. The tissue protective effect was linked to up-regulation of HIF-1α and its target genes including heme oxygenase-1 and erythropoietin. Interestingly, rats were continuously treated with $CoCl_2$ for 7[196, 198], 14[197] or up to 43[195] days with no apparent adverse effects on the health of the animals.

In the human body, cobalt is preferentially taken up in the kidneys and liver and excreted through the urinary system over time[190]. Cellular uptake of cobalt appears to be mediated by active and passive transport mechanisms. The intracellular cobalt concentration was shown to correlate with the extracellular $CoCl_2$ level and, notably, to accumulate over time up until a saturation point after 12 h of continuous exposure was reached[199]. Yet the authors only analysed Co^{2+} uptake kinetics for up to 24 h so that long term data on Co^{2+} accumulation is lacking. Cobalt has been identified as potent hypoxia-mimicking agent. To understand the implications of that characteristic, the mechanisms of cellular oxygen sensing will be discussed.

1.6.3.1 Oxygen sensing in cells

Cells adapt to changes in oxygen tension by activating a plethora of signalling cascades. The hypoxia-inducible factor-1 (HIF-1) pathway is the key mediator of the cells' complex response to hypoxia and essential for cell survival. Apart from the HIF-1 pathway, the cellular response to hypoxia is orchestrated in part by mammalian target of rapamycin (mTOR) kinase signalling and activation of the unfolded protein response (UPR)[200]. Considering the scope of this literature review, the HIF-1 independent O_2-sensitive signalling pathways will not be discussed.

HIF-1 is a heterodimeric transcription factor first described by Semenza *et al.* in 1991 as hypoxia-inducible nuclear factor binding to the enhancer region of the erythropoietin (EPO) gene[201]. HIF-1 is composed of an oxygen-regulated hypoxia inducible factor-1 alpha (HIF-1α) subunit and a constitutively expressed hypoxia inducible factor-1 beta (HIF-1β) subunit. HIF-1β was originally termed aryl hydrocarbon receptor nuclear translocator (ARNT). Two paralogs of HIF-1α have been identified, HIF-2α and HIF-3α. While HIF-1α is ubiquitously expressed throughout the body, HIF-2α is not found in all tissues[202]. HIF-2α is closely related to HIF-1α as it shares 48% amino acid sequence identity and hence biochemical and structural characteristics such as the ability to dimerise with HIF-1β and to associate to hypoxia responsive elements (HRE) in the promoter region of HIF-1 target genes[203]. HIF-3α shares the ability to dimerise with HIF-1β and to bind to HRE with the other two HIF-α's, yet there are studies suggesting a negative regulatory role of HIF-3α on the HIF-1 pathway[204].

HIF proteins belong to the superfamily of basic helix-loop-helix (bHLH) transcription factors that must dimerise prior to transactivation of gene expression. More specifically, HIF proteins are distinguished by the presence of a PER-ARNT-SIM (PAS) motif that ensures specific dimerisation among the bHLH/ PAS family[205, 206] (Fig. 1.4). Two transactivator domains, N-terminal (N-TAD) and carboxy-terminal (C-TAD), localised in the carboxy-terminal half of HIF-1α, were identified which mediate the association with coactivators including CBP (cyclic-AMP responsive element binding (CREB)-binding protein)/ p300 to activate gene transcription[207].The HIF-α proteins are further characterised by an oxygen-dependent degradation domain (ODDD) that is responsible for the oxygen tension-regulated stability.

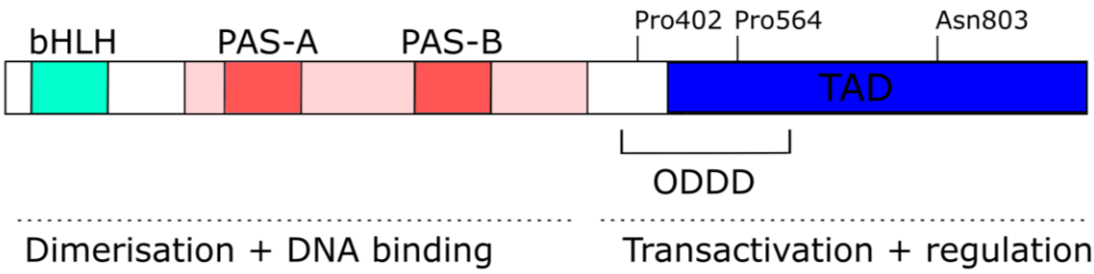


Figure 1.4: Structure of hypoxia inducible factor-1α (HIF-1α). The structure of HIF-1α is shown with the basic helix-loop-helix (bHLH) and the two PER-ARNT-SIM (PAS) domains that are necessary for dimerisation and DNA binding. On the C-terminus HIF-1α further contains a transactivation domain (TADs) that is constituted of two internal units, N-TAD and C-TAD. The hydroxylation of specific proline residues (Pro402 and Pro564) within the oxygen-dependent degradation domain (ODDD) targets HIF-1α for degradation via proteasome. Figure adapted from Semenza and Simon and Keith[208, 209].

In normoxic conditions, HIF-1α is rapidly hydroxylated at two conserved proline residues (Pro402 and Pro564, or for HIF-2α, Pro405 and Pro530) located within the ODDD domain. HIF-specific 2-oxogluterate dependent prolyl hydroxylases, termed prolyl hydroxylase domain containing (PHD1, 2 and 3), are responsible for this reaction which requires oxygen as well as iron and ascorbate as cofactors (Fig. 1.5)[210]. During the reaction, one oxygen atom is transferred to the proline residue while the other reacts with 2-oxogluterate to produce succinate and carbon dioxide. Among the PHDs, PHD2 has been identified as the critical oxygen-sensing enzyme responsible for HIF-1α degradation in normoxic coditions[211]. Hydroxylated HIF-1α is rapidly bound by the von Hippel Lindau protein (pVHL) which mediates the recruitment of an E3 ubiquitin ligase complex resulting in poly-ubiquitylation and subsequent proteasomal degradation of HIF-1α. In a process reminiscent of the proline hydroxylation in the ODDD domain, the asparagine residue 803 within the C-TAD region is hydroxylated in normoxic conditions abolishing the interaction of HIF-1α with its co-factors. Hydroxylation of the asparagine residue is performed by factor inhibiting HIF (FIH) and activity of FIH is reduced in hypoxic conditions[212]. In ambient conditions, HIF-1α is continuously produced but has a short half-life of approximately $t_{1/2}$ = 5 min[213]. Extensive study of the regulation of HIF-1α protein has revealed a complex network of oxygen dependent and independent mechanisms. Although the opinion persists that HIF-1α function is mainly coordinated on a protein level, there are studies reporting a differential regulation of HIF-1α transcription levels in response to changes in oxygen availability[214].

In hypoxic conditions, degradation of HIF-1α is abrogated so that the protein can translocate to the nucleus where it dimerises with HIF-1β. The HIF-1 heterodimer binds to HREs that contain a conserved HIF-binding sequence (5'-RCGTC-3' with "R" being a purine residue) within the promoter or enhancer region of oxygen-responsive genes. Interaction of the C-TAD domain with co-activators

such as CBP/p300 enhances activation of gene transcription and is thought to be required for full HIF activity[207]. Notably, HIF-1α stabilisation in HeLa cells was found to increase almost exponentially when oxygen concentrations fell below 6%[215]. HIF-1α levels as well as DNA binding activity peaked at 0.5% O_2. Yet, the kinetics and likely the extent of HIF-1α stabilisation has been shown to be organ-specific[216]. To adapt to changes in oxygen supply and ensure cellular survival, HIF-1α transactivates the expression of a variety of genes which can be grouped in the following categories: angiogenesis, glucose metabolism, erythropoiesis, cell survival and apotosis[213]. A study in arterial endothelial cells demonstrated a differential regulation of 2.6% of all tested genes by hypoxia or constitutive stabilisation of HIF-1α[217]. The largest group of regulated genes encoded for transcription factors suggesting that the HIF-1 pathway activates a network of downstream transcriptional responses. Among the most famous HIF-1 regulated genes are VEGF and EPO.

1.6.3.2 Cobalt's hypoxia-mimicking properties

Different mechanisms have been proposed to explain cobalt's hypoxia mimicking properties (Fig. 1.5). Epstein *et al.* were the first to fully characterise the PHDs and to hypothesise that cobalt exerts its function by replacing the iron in the iron-binding centre of PHDs directly inactivating the enzymes[210]. Previously Wang *et al.* had observed that cobalt ions stabilised HIF-1α in ambient air[206]. Yuan *et al.* further demonstrated that cobalt ions can bind directly to the conserved proline residues in the ODDD domain of HIF-1α, inhibiting the hydroxylation of HIF-1α by PHDs and/or the interaction of hydroxylated HIF-1α with pVHL[218]. A third mechanism links cobalt-triggered generation of reactive oxygen species (ROS) to an increase in HIF-1α concentration. Following treatment with 100 μM $CoCl_2$, increased ROS levels were measured in HeLa cells[219]. ROS production was independent from mitochondrial function and induced stabilisation of HIF-1α in a mechanism that seemed to depend on phosphatidylinositol 3-kinase (PI3K). In keeping with these results, a study using smooth airway muscle cells showed that $CoCl_2$ increased HIF-1α levels by producing ROS that in turn activated PI3K signalling pathway possibly leading to the up-regulation of HIF-1α mRNA translation[214]. Interestingly, the efficiency of cobalt ions to produce ROS via Fenton-like reactions was characterised as very low unless they are appropriately chelated[220]. Yet, the role of cobalt mediated ROS production in HIF-1α up-regulation has been questioned[221, 222]. Another possible pathway may be the depletion of cellular ascorbate by cobalt causing an inhibition of PHDs[223]. To date, the ability of cobalt ions to increase the cellular protein level of HIF-1α has been demonstrated in a number of cell types for concentrations ranging from 50 μM to 400 μM[224, 225]. Although cobalt successfully enhances the transcription of known HIF-1 pathway target genes there is evidence that cobalt-induced hypoxia does not fully recapitulate low oxygen tensions. Proteomic analysis of human leukemic cells (U937) after culture in hypoxic conditions or in presence of 50 μM $CoCl_2$ identified 62 and 16 proteins respectively that were differentially regulated compared to the normoxic control[226]. 11 of the 16 proteins modulated by $CoCl_2$ treatment matched with protein profiles in hypoxic conditions while the remaining 5 were exclusively

regulated indicating that $CoCl_2$ induced some hypoxia-mimicking mechanisms but also cobalt-dependent effects. While the work in this thesis is focused on the effect of HIF-1α stabilisation, HIF-2α should similarly be affected by the cobalt mediated inhibition of PHDs. Therefore some of the observed effects may indeed be due to HIF-2α signalling.

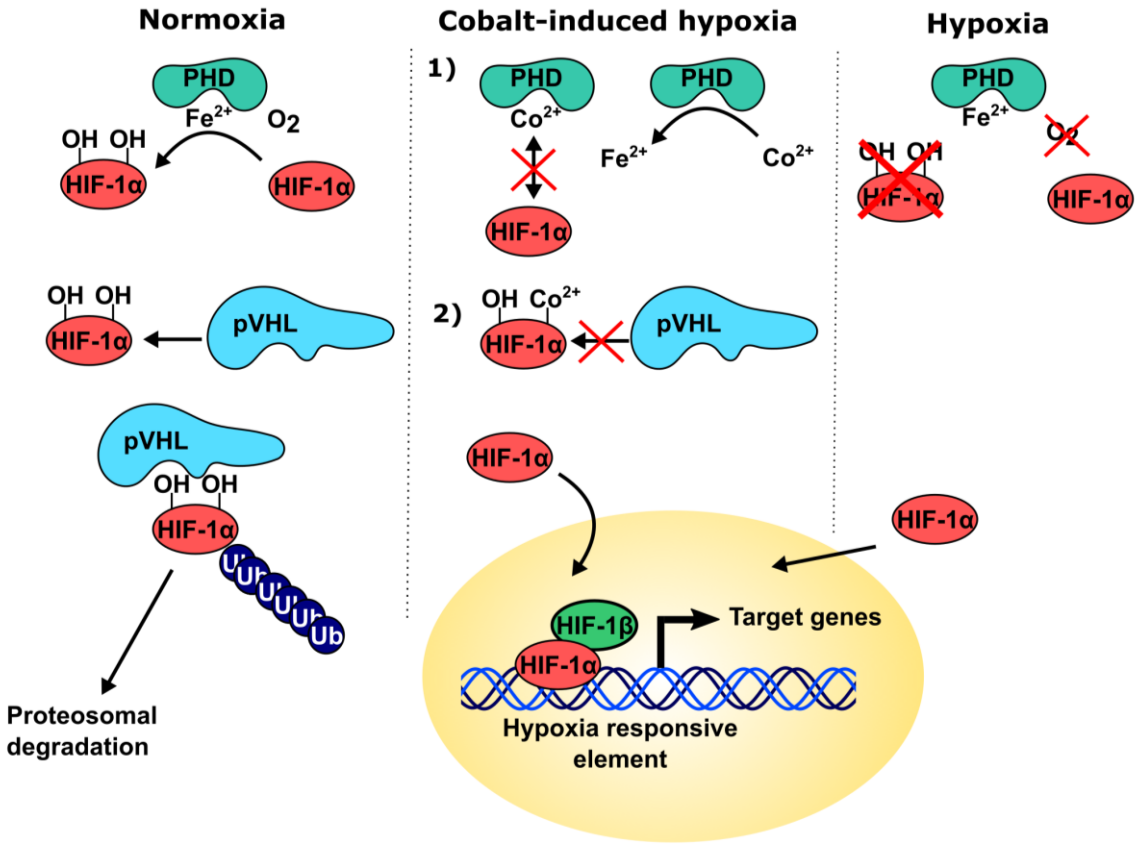


Figure 1.5: Regulation of the HIF-1 pathway. In ambient air, cellular oxygen sensors termed prolyl hydroxylases (PHD) mediate the hydroxylation of conserved proline residues within the oxygen-dependent degradation domain of HIF-1α. The E3 ligase von Hippel-Lindau protein (pVHL) binds to hydroxylated HIF-1α and mediates its subsequent poly- ubiquitylation and degradation by the 26S proteasome pathway. In presence of cobalt, the iron in the iron binding centre of PHDs is replaced by cobalt, inactivating the enzyme. Alternatively, cobalt ions can bind to the specific proline residues of HIF-1α, inhibiting the interaction with pVHL. Stabilised HIF-1α can translocate to the nucleus where it dimerises with HIF-1β and binds to hypoxia responsive elements (HRE) in the promoter or enhancer region of its target genes. In hypoxic conditions, the scarcity of oxygen leads to inactivity of PHDs and hence accumulation of HIF-1α. As the role of ROS in HIF-1α regulation is a subject of ongoing debate, it was omitted from the figure. Figure adapted from Maes *et al.*[227].

1.6.3.3 The use of cobalt in tissue engineering

Considering cobalt's known hypoxia mimicking properties it comes with no surprise that a growing body of research tries to exploit the ion's potential for tissue engineering purposes by incorporating the element into biomaterials. In most cases cobalt incorporation was performed to confer pro-angiogenic properties to a biomaterial; mainly but not exclusively for bone regeneration applications. Successful

bone regeneration necessitates angiogenesis at a relatively early stage as a functional blood supply is pivotal for the repair process of bigger defects and/or to provide engineered tissue with nutrients[228]. Yet, to date angiogenesis presents a challenge for synthetic bone grafts, especially when applied to larger defects[229]. Several approaches such as pre-vascularisation of constructs or the controlled release of growth factors from materials are being investigated. Generally, these approaches are rather complex, costly and, in case of growth factors, associated with a short half-life, instability as well as safety issues[230]. Therefore, the transition metal cobalt presents an attractive alternative due to its stability, low cost and relative ease of use.

Fan *et al*. showed that $CoCl_2$ pre-treated human hMSCs enhanced vascularisation and ultimately osteogenesis in a co-culture model with osteogenic pre-differentiated hMSC in a skull bone defect in SCID mice[231]. The authors attributed this beneficial effect to secretion of the pro-angiogenic VEGF which may, apart from its obvious function, have stimulated osteogenesis in the hMSC-derived osteoblasts. In a study by Kulanthaivel *et al.* cobalt-doped hydroxyapatite was synthesised and found to increase VEGF protein expression in an osteosarcoma cell line[232]. Yet, the paper did comment on the final cobalt concentration that the cells were exposed to which makes any comparison with other studies difficult. Similarly, 2 mol% and 5 mol% cobalt substituted β-tricalcium phosphate (Co-TCP) ceramics were prepared by Zhang *et al.*[229]. Extracts prepared from 5% Co-TCP significantly enhanced the VEGF production by hMSCs compared to control medium or 2% Co-TCP. Yet extracts prepared from 2% Co-TCP performed best in an *in vitro* angiogenesis assay using HUVECs suggesting cell type dependent differences. The amount of cobalt in the extracts was relatively low with 12 µM (5% Co-TCP) and 1.5 µM (2% Co-TCP) compared to $CoCl_2$ concentrations routinely used to induce hypoxia. In a follow-up study it was shown that extracts prepared from Co-TCP enhanced hMSC osteogenesis compared to extracts prepared from β-TCP[233]. Yet, the authors neither stated if 2% or 5% Co-TCP was used nor commented on the final cobalt content in the medium. Interestingly, Co-TCP extracts up-regulated inflammatory markers in RAW264.7 cells, a macrophage cell line. When hMSCs were exposed to RAW cell conditioned Co-TCP extracts the previously obtained observations were reversed with a down-regulation of osteogenic marker gene expression as well as ALP protein abundance and activity. An *in vivo* bone defect model in rats further highlighted that in presence of Co-TCP new bone formation was impaired compared to β-TCP, an effect that was contributed to immunomodulation.

Perez *et al.* incorporated Co^{2+} as pro-angiogenic factor in a collagen/alginate core-shell hydrogel system for bone regeneration applications[228]. 1 mM $CoCl_2$ was used for the preparation of the hydrogel, which corresponded to a Co^{2+} release of 15 µM, a value much lower than the frequently used 100 µM to induce hypoxia. Exposure to release products of the collagen/alginate scaffolds had a dose dependent effect on murine MSCs and significantly reduced the viability when higher cobalt concentrations (150 µM) were used. Interestingly, up-regulation of angiogenic factors as well as osteogenic markers were observed in response to indirect culture with the collagen/alginate scaffolds suggesting that relatively low amounts of cobalt can induce hypoxia-like effects in cells. While the most

favourable results regarding angiogenic and osteogenic markers were obtained with cobalt releasing collagen/alginate scaffolds *in vitro*, bone formation was reduced *in vivo* in a rat calvarial defect model compared to control scaffolds lacking cobalt. Yet, co-delivery of cobalt with BMP2 achieved the best bone formation indices compared to control or BMP2 only releasing scaffolds. Recently, polylactic acid (PLA) particles were coated with CaP and Co^{2+} to study blood vessel formation after intramuscular implantation in goats[234]. Cobalt incorporation into the coating enhanced the size and number of newly formed blood vessels compared to PLA particles and PLA particles coated with CaP in the absence of cobalt. Notably, relatively low amounts of cobalt were used (0.1 and 20 μM) to prepare the coatings. Interestingly, the inflammatory response was found to be comparable between all groups. Unfortunately, the ion release from the particles was not measured. Beyond angiogenesis, recently, the use of cobalt or its incorporation into scaffold systems to support chondrogenesis has been an up-coming notion. To support chondrogenic differentiation, human adipose tissue derived MSCs were cultured in cobalt/calcium alginate beads in a study by Focaroli *et al.*[235] An up-regulation of chondrogenic markers in the absence of any chondrogenic growth factors was observed which depended on the presence of cobalt but varied with regards to the amount of cobalt in the initial gelling bath. Unfortunately, the cobalt concentration within the beads or indeed the actual cobalt content of the beads was not measured.

1.6.3.4 Cobalt-containing bioactive glasses

As discussed previously, bioactive glasses are ideal carriers for bioactive ions due to their superior capacity to be modified in their composition. Furthermore, bioactive glasses allow the delivery of such bioactive ions in a controlled and relatively sustainable manner that can be tuned according to the requirements of the application. Much like for other biomaterials, cobalt was incorporated into bioactive glasses to design scaffolds with therapeutic pro-angiogenic and pro-osteogenic potential. To this end, Lee *et al*. prepared a series of cobalt-doped titanium phosphate-based bioactive glasses with increasing cobalt incorporation (0, 5, 10 and 15 mol%)[236]. Biological evaluation showed that the number of osteosarcoma cells seeded on discs prepared from all bioactive glasses was comparable after three days of culture. After seven days, the cell number on discs lacking cobalt seemed to be increased while the growth rate of osteosarcoma cells cultured on cobalt-doped discs was reduced in a dose-dependent manner. Metabolic activity of cells followed a similar trend. Interestingly, VEGF protein production was increased in response to all bioactive glasses compared to tissue culture plastic suggesting a general underlying mechanism. Cell culture on bioactive glass discs containing 5 or 10 mol% cobalt had a tendency to enhance the VEGF production albeit only to a small degree.

Wu *et al*. further developed the idea of a cobalt-doped biomaterial for tissue engineering applications and prepared cobalt containing 3D mesoporous bioactive glass (Co-MBG) scaffolds for bone tissue engineering[237]. HIF-1α protein was up-regulated in hMSCs cultured on the Co-MBG scaffolds indicating hypoxia-mimicking properties of the material. Furthermore, *VEGF* and *osteocalcin* gene expression as well as secretion of VEGF were enhanced in response to culture on the Co-MBG

scaffolds compared to the cobalt free MBG scaffold control[237]. A mild inhibitory effect of cobalt on cell viability was observed with 5 mol% substituted Co-MBG while no significant differences were found for 2 mol% Co-MBG compared to the MBG control after 7 days of culture. Hoppe and colleagues developed a cobalt releasing 13-93 BG scaffold and showed that cell viability and metabolic activity depended on the extent of cobalt incorporation[146, 238].

With the aim to design hypoxia-mimicking bioactive glasses for skeletal tissue engineering a series of cobalt-containing glasses with increasing cobalt substitution (0, 0.5, 1, 2 or 4 mol%) were developed by M.M. Azevedo *et al*. in the laboratory of the Stevens group[239, 240]. Medium containing ionic extracts of the cobalt-containing glasses enhanced HIF-1α activity in hMSCs after 8 h of culture[240]. Gene expression of hypoxia-responsive genes was shown to be up-regulated in hMSCs after 24 h of culture in cobalt-doped bioactive glass-conditioned medium further underscoring the hypoxia-mimicking properties of the developed glasses. To confer pro-angiogenic properties to a collagen-glycosaminoglycan (CG) scaffold system for bone tissue engineering, cobalt-doped bioactive glass particles (38 μm and 100 μm) were incorporated[241]. Bioactive glass/ CG scaffolds with 100 μm enhanced VEGF protein production by endothelial cells and conditioned medium prepared from the scaffolds increased tubule formation by HUVECs compared to the bioactive glass free scaffold control. The cobalt-containing bioactive glass/ CG scaffolds were further shown to promote osteogenesis enhancing the ALP activity in pre-osteoblast cells compared to cobalt-free bioactive glass/CG or glass free scaffolds.

In summary, the hypoxia-mimicking properties of cobalt confer a unique modulatory capacity to the ion and make it highly interesting for tissue engineering applications. Hypoxia fulfils crucial functions not only during embryonic development but also in the adult body. Beyond cobalt's demonstrated value for angiogenesis and osteogenesis, it is therefore a potent bioactive ion that can elicit a plethora of signalling mechanisms in cells.

1.6.4 Magnesium and other bioactive ions

The development of magnesium-containing bioactive glasses for tissue engineering purposes has lately received growing attention owing likely to the ion's numerous functions as signalling molecule in the body and its role in bone growth and maintenance. In a rat model, a reduction of dietary magnesium by only 50% reduced the bone mineral content. Furthermore, a low magnesium diet in mice caused a decrease in the number of osteoblasts while the number of osteoclasts was increased. For a comprehensive review on magnesium-containing bioactive glasses, please refer to Diba *et al.*[242]. The incorporation of magnesium into a bioactive glass system has been shown to induce complex structural changes in the glass network that remain to be fully elucidated. Yet, literature agrees that the presence of magnesium ions delays the formation of the HCA layer which likely owes to inhibition of crystal growth by occupation of crystal growth sites[107]. The influence of magnesium incorporation on the

degradation kinetics of bioactive glasses is less clear as both an increase and a decrease has been reported[242]. The influence of magnesium incorporation on bioactive glass properties may thus depend on the glass composition. A number of studies have evaluated the effect of magnesium-doped bioactive glasses for bone regeneration applications. Generally, the incorporation of magnesium in a given glass composition did not cause any cytotoxic effects. In contrast magnesium-doped bioactive glasses tended to enhance proliferation of osteoblasts and MSCs and increased the expression of osteogenic markers[134, 243]. In a study by Wang *et al.* the bioactive glass scaffolds with the highest magnesium incorporation (2.25 mol% Mg) increased both proliferation and ALP activity of murine MSCs compared to the control glass scaffold with no magnesium[244]. Yet, most studies lacked a magnesium-free reference in the same bioactive glass system making it difficult to relate the observed changes to magnesium. In summary, magnesium containing bioactive glasses are highly interesting materials for bone repair applications, however, further clarification of the influence of magnesium ions within bioactive glasses and their dissolution products is needed.

Taking it one step further, several studies have investigated the effect of single ion species on cell response. It has been shown that solutions containing silicon ions potently enhance bone formation, increase osteoblast proliferation as well as ALP activity and the secretion of osteocalcin[245]. In agreement, a study has demonstrated that orthosilic acid at concentrations of 10 µM and 20 µM stimulated type I collagen synthesis, increased ALP activity and enhanced osteocalcin secretion in a human osteosarcoma cell line[246]. In addition, the effect of calcium has been investigated. Calcium concentrations of 6 - 8 mM had a favourable effect on osteocalcin expression and matrix production by osteoblasts. Interestingly, these effects are observed at significantly lower concentrations in 3D culture[247]. Finally, phosphate ions specifically enhance the expression of osteopontin, a protein involved in mineralisation, and matrix gla protein in osteoblasts[248, 249]. Hence, the bioactivity of bioactive glass can at least partly be attributed to the joined effects of single ion species on cell metabolic activity.

1.7 Conclusion

Tissue engineering is a rapidly evolving field whose findings have not yet fully translated to clinical applications. This chapter has aimed to give a brief overview of the current challenges and state of knowledge in this area. In particular, this chapter introduces the osteochondral system with its most important cell types and discusses bioactive glasses as versatile carriers of bioactive, therapeutic ions. Finally, key bioactive ion species are introduced and their influence on the cell response described to highlight how simple ion incorporation can impact cell behaviour. A better understanding of cell-biomaterial interactions and of how cell behaviour can be modified by the introduction of bioactive moieties is crucial for the design of novel scaffolds to overcome the current limitations of tissue engineering. The motivation of this work was to investigate the responsiveness of human mesenchymal stem cells to bioactive glass ionic dissolution products.

1.8 Hypothesis and aims of the thesis

The underlying hypothesis of this work is that incorporation of key ion species into bioactive glasses can be used to guide cell behaviour. The overall aim of this PhD was to understand the influence of ions released from bioactive glasses on human bone marrow-derived mesenchymal stem cells. In particular, the aims were to understand the relationship between the presence of strontium or cobalt ions within the bioactive glass extracts and hMSC behaviour as well as chondrogenic differentiation. To that end, different glass compositions were used to obtain bioactive-glass conditioned medium for the culture of hMSCs. The work done to address these aims is divided into four chapters.

Chapter 2 was based on the hypothesis that up-regulation of the isoprenoid pathway on a gene level by the presence of strontium within bioactive glass would trigger a biological response and modify hMSC behaviour. More specifically, it was hypothesised that strontium-containing bioactive glasses would affect the cell membrane as the isoprenoid pathway is responsible for the production of cholesterol. The aim of this chapter was to investigate functional effects of the strontium-bioactive glass-triggered up-regulation of the isoprenoid pathway with special respect to the plasma membrane.

Chapter 3 was based on the hypothesis that a change in the composition of bioactive glasses would modify hMSC chondrogenesis. In particular, it was hypothesised that strontium incorporation into bioactive glass would enhance hMSC chondrogenic differentiation and cartilaginous tissue production. The aim of this chapter was to identify bioactive glass compositions with a beneficial effect on hMSC chondrogenic lineage commitment.

Chapter 4 was based on the hypothesis that incorporating cobalt into bioactive glasses would enhance hMSC chondrogenesis by mimicking hypoxia. The aims of this chapter were to test this hypothesis and to identify an optimum cobalt concentration within bioactive glass extracts to support chondrogenic differentiation of hMSCs.

Chapter 5 was based on the hypothesis that cobalt incorporation into bioactive glasses would enhance the stem cell-like properties of hMSCs by mimicking hypoxia. The aim of this chapter was to understand the influence of cobalt-containing bioactive glass dissolution products on hMSC behaviour.

CHAPTER 2

The Influence of Strontium-containing Bioactive Glasses on the Isoprenoid Pathway in hMSCs

(The data reported in this chapter has been previously published in Autefage H, Gentleman E, Littmann E, Hedegaard MAB, Von Erlach T, O'Donnell M, Burden FR, Winkler DA, and Stevens MM, Sparse feature selection methods identify unexpected global cellular response to strontium-containing materials. Proceedings of the National Academy of Sciences (PNAS). 2015;112:4280-5.)

All data presented in this chapter were collected by me unless explicitly stated otherwise.

2.1 Introduction

In the field of tissue engineering the formation of new, functional tissue is the ultimate goal by definition. (Bio)materials are a centre piece of most approaches to accomplish the regeneration and repair of tissue. Currently, the mechanisms that drive biomaterials-based repair *in vivo* are often still largely elusive. Usually, the *in vitro* evaluation of such biomaterials is focussed on the desired outcome; (stem) cell survival, proliferation and differentiation to an appropriate lineage. While it is, of course, imperative to know if a material will enable a desired outcome, a lot of useful information may be lost by concentrating exclusively on the predicted result. Hence, the global cell response to the majority of biomaterials remains incompletely understood and underlying pathways that govern cell-biomaterial interactions *in vitro* and particularly *in vivo* are not fully identified. Therefore, the study by Autefage *et al.* aimed at unravelling the cell response to strontium-containing bioactive glasses pursuing an unbiased approach[250]. Such an unbiased approach may yield novel insights into cell-biomaterial interactions opening up new possible investigation avenues.

Strontium was chosen as a bioactive moiety as numerous studies have demonstrated its ability to enhance osteogenesis *in vitro* and *in vivo* when incorporated within biomaterials or as the active component of SrR[168, 184, 251-253]. Bioactive glasses are particularly attractive biomaterials for bone regeneration purposes due to their osteoinductive/osteproductive properties. Furthermore, bioactive glasses are excellent carrier systems for therapeutic ions as their composition can be tailored to the application. Characteristically, bioactive glasses undergo partial dissolution/re-precipitation reactions on their surface upon exposure to biological fluids thereby releasing ions from their network into their surroundings. Yet, not all ions that are released re-precipitate to form a HCA layer but some remain in solution modifying the local ionic microenvironment. Such bioactive glass ionic dissolution products can influence the biological response in their own right and are, in part, responsible for the bioactive properties of bioactive glasses[146]. In the study by Autefage *et al.*, which was performed in the Stevens Group laboratory, conditioned medium prepared from strontium-containing bioactive glass was chosen to evaluate the biological response of hMSCs to strontium within a mix of other known bioactive ions such as calcium and silicon[250]. To avoid any bias towards a certain outcome a whole genome microarray was performed to study the response of hMSCs to the incorporation of strontium into the classic 45S5 BG composition[250]. The resulting data set was analysed using functional annotation clustering as well as a sparse feature selection method. Strikingly, genes encoding for enzymes of the mevalonate and sterol/steroid biosynthesis pathways were by far the strongest differentially regulated cluster by the presence of strontium-containing bioactive glass-conditioned media. Following on from these exciting results obtained with the mRNA microarray, the cell response to strontium-containing bioactive glass ionic dissolution products was further studied on mRNA and protein levels as well as with respect to systemic changes in the cell.

The focus of the research presented in this chapter was to investigate the influence of strontium-containing bioactive glass ionic dissolution products on the metabolic activity of hMSCs with a special emphasis on the mevalonate and sterol/steroid biosynthesis to assess whether the strong regulation of these pathways, observed at the gene level by microarray analysis, induced significant changes at the cellular level. hMSCs were chosen for this study for a number of reasons: (1) hMSCs are widely used for (bone) tissue engineering purposes, (2) hMSCs are recruited to the defect site *in vivo* and play a role in the physiological bone fracture healing process, a mechanism which may further be exploited and enhanced by third generation biomaterials, (3) strontium has been suggested to influence hMSC lineage commitment and (4) the clarification of hMSC metabolism is of interest from a basic science point of view.

2.1.1 Gene expression profiling of hMSCs after strontium-containing bioactive glass extract exposure

The mRNA microarray performed by Autefage *et al.* highlighted the influence of bioactive ions released from strontium-containing bioactive glasses on the regulation of a series of genes involved in hMSC metabolism[250]. The following paragraph will describe the design of the strontium-containing bioactive glass microarray study and summarise its findings. In order to dissect the influence of strontium incorporation within a biomaterial, increasing amounts of strontium were incorporated into the 45S5 BG composition (46.13 mol% SiO_2, 26.91 mol% CaO, 24.36 mol% Na_2O, 2.6 mol% P_2O_5) by substitution for calcium on a molar basis (0%, 10%, and 100% strontium for calcium substitution). The strontium-doped bioactive glasses with 0%, 10% and 100% strontium substitution will be referred to as Sr0, Sr10 and Sr100, respectively or BG when all three compositions are concerned.

BG-conditioned medium was prepared by incubating 0.1 mm - 1.0 mm glass particles for 24 h in hMSC growth medium (PromoCell GmbH, Germany). To investigate the influence of the ions released from the BGs on gene expression, hMSC from three different donors were incubated with the filtered BG-conditioned media or growth medium (Fig. 2.1). Growth medium was added as a condition to assess gene expression in "normal" cell culture conditions in order to better understand the impact of the BG extracts. At different time points (T0, 30 min, 2 h, 4 h, 48 h, 5 days and 10 days), mRNA from all groups were isolated and cDNA were subsequently prepared and labelled with the Ambion WT kit. Samples were hybridised on Affymetrix Human Gene 1.0 ST arrays and the arrays were scanned. Statistical analysis revealed that exposure to all BG-conditioned media had a profound effect on the regulation of hMSC gene expression. More than 1,000 genes were found to be differentially expressed in presence of Sr100 dissolution products compared to growth medium (Fig. 2.1B). While all glass compositions triggered a change in gene expression compared to growth medium, strontium dose-dependently further increased the overall number of genes as well as the amount of highly significant differentially expressed (DE) genes (Fig. 2.1C). This observation pointed towards a special role of

strontium within the BG dissolution products with regards to the response of hMSCs.

The gene expression data set was further analysed to identify key genes and pathways that were regulated by the BG dissolution products using functional annotation clustering as well as sophisticated sparse feature selection methods. Surprisingly, genes associated with the mevalonate and sterol/steroid biosynthesis pathways scored the highest *p*-values when the differential gene expression between hMSCs cultured in Sr100-conditioned and growth medium were analysed. Specifically, functional annotation clustering of the DE genes indicated a very strong regulation of the sterol/steroid biosynthesis and metabolic processes with a *p*-value smaller than 10^{-10} in response to treatment with Sr100 when compared to the growth medium condition. Furthermore, Kyoto Encyclopaedia of Genes and Genomes (KEGG) pathway analysis revealed that all genes associated with these pathways were differentially regulated following Sr100 treatment. While the mRNA expression levels of these genes were increased by all BGs compared to growth medium only, the mRNA expression levels in the Sr100 group were significantly higher not only compared to growth medium (p-values < 0.01) but also to Sr0 (p-values < 0.05). A closer look at individual gene expression profiles allowed the conclusion that all enzyme-coding genes involved in the mevalonate and sterol/steroid biosynthesis pathways were dose-dependently up-regulated with increasing strontium substitution. Sparse feature selection methods identified the enzyme farnesyl-diphosphate farnesyltransferase 1 (squalene synthase, FDFT1) as one of the key discriminators between conditions. FDFT1 is the first specific enzyme committed to sterol biosynthesis. Its strong regulation on a gene level by the BGs in a strontium dose-dependent manner reinforced the influence of strontium within the BG dissolution products on the sterol/steroid biosynthesis pathway. Yet, while gene expression levels increased with higher strontium ion concentrations, the observed influence on gene expression was unlikely solely dependent on strontium but rather a joined effect of the ions in the medium. Following on from these findings, a deeper investigation of the effects of the bioactive glass-mediated regulation of the mevalonate and sterol/steroid biosynthesis pathways was performed.

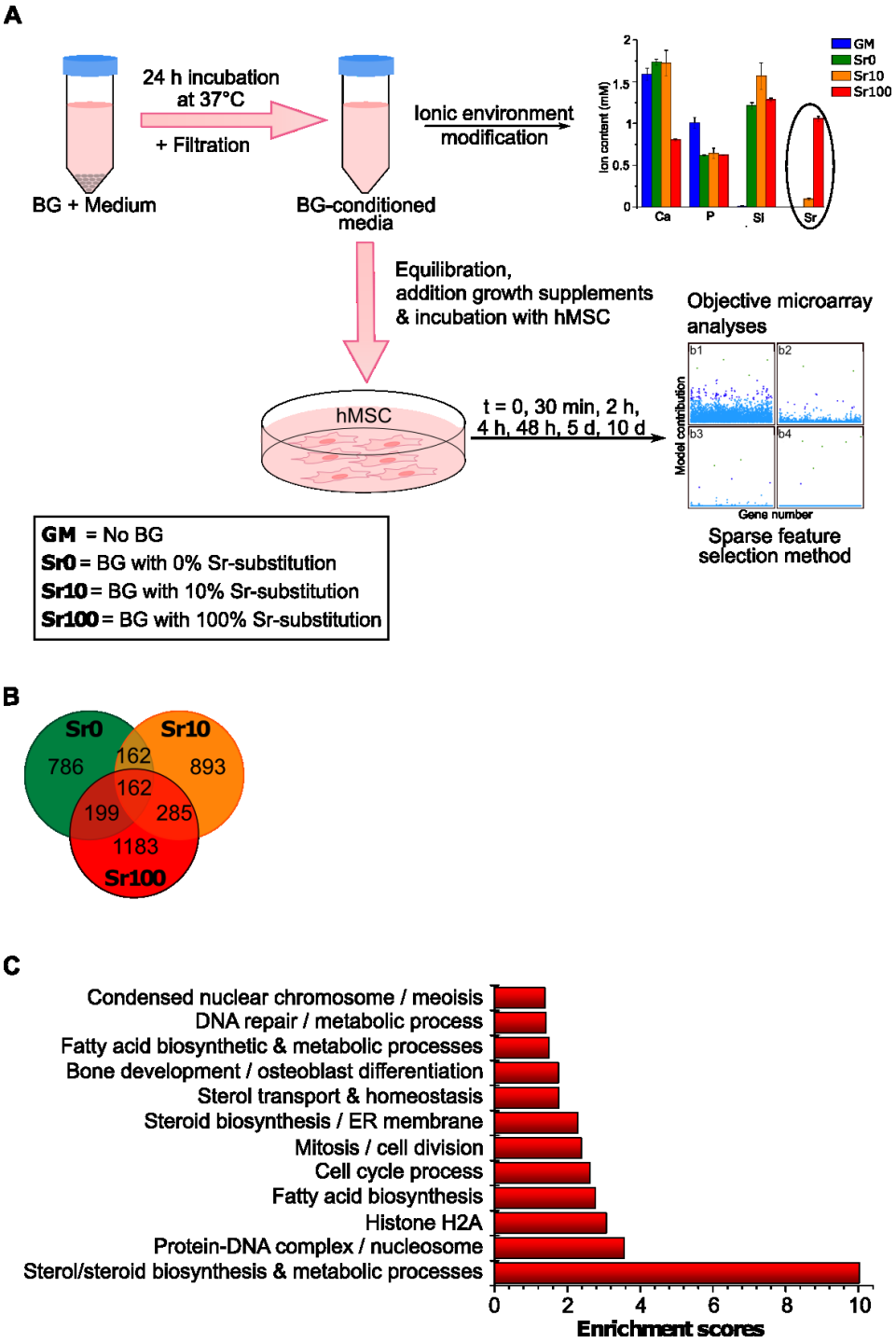


Figure 2.1: Overview of the BG microarray study design and results. A) Increasing amounts of strontium were incorporated into the 45S5 BG composition by substitution for calcium (0, 10 and 100%). BG-conditioned media were prepared and used to culture hMSCs for up to 10 days. To study the impact of BG dissolution products on hMSCs, a whole genome microarray was performed (Affymetrix ST 1.0). B) Illustration of the number of differentially expressed genes (p<0.05) in presence of BG dissolution products compared with the growth medium only (GM) group presented in a Venn diagram. C) Visual representation of the results of the functional annotation clustering comparing differential gene expression between hMSCs cultured in Sr100-conditioned or GM medium. A high enrichment score of the mevalonate and sterol/steroid biosynthesis pathways was revealed. BG = bioactive glass. Reproduced and adapted from Autefage *et al.*[250].

2.1.2 Mevalonate and sterol/steroid biosynthetic pathways

The isoprenoid pathway is an essential metabolic pathway as it provides cells with vital molecules that play key roles in a number of cellular processes (Fig. 2.2). The isoprenoid pathway can be divided into the mevalonate biosynthesis pathway and the sterol/steroid biosynthesis pathway. In mammals, this pathway is used exclusively for the biosynthesis of isoprenoids from mevalonate[254]. Products of the isoprenoid pathway can be grouped as sterol and non-sterol isoprenoids and serve as precursors for molecules that participate in a multitude of cellular processes, among them steroid biosynthesis, protein prenylation, cell membrane maintenance, and protein N-glycosylation[255, 256]. Initially, 3-hydroxy 3-methylglutaryl-CoA (HMG-CoA) is converted to mevalonic acid by HMG-CoA reductase (HMGR). HMGR is the rate-limiting enzyme of the mevalonate pathway and tightly regulated by the cell's demand for sterol and non-sterol isoprenoids. Mevalonic acid is subsequently converted to farnesyl pyrophosphate (farnesyl-PP) through multistep enzymatic reactions. Bisphosphonates inhibit the farnesyl-PP synthase (FDPS) thereby reducing the production of downstream metabolites. Farnesyl-PP is the branching point of the mevalonate pathway as it can be used as precursor for either non-sterol isoprenoids or sterols. FDFT1, also known as squalene synthase, is the first enzyme exclusively committed to the cholesterol synthesis. It catalyses the conversion of farnesyl-PP to squalene which is then further metabolised through a chain of enzymatic reactions to cholesterol. Thus, FDFT1 plays a crucial role in directing the flow of the farnesyl-PP metabolite either to the sterol or non-sterol branch of the isoprenoid pathway. Following the non-sterol branch, farnesyl-PP can either serve as a substrate for protein farnesylation or can be further converted to geranylgeranyl pyrophosphate (geranylgeranyl-PP) or dolichyl phosphate[255]. Both isoprenoids are crucial substrates for protein prenylation and N-glycosylation of growth factor receptors[257]. Prenylation is a process in which hydrophobic molecules, typically C-15 isoprene farnesyl or C-20 isoprene geranygeranyl groups, are covalently attached to the C-terminal end of certain proteins including small GTP-binding proteins. Prenylation fulfils the purpose to equip such proteins with a hydrophobic lipid anchor to attach to cell membranes and to enable protein-protein interactions[258].

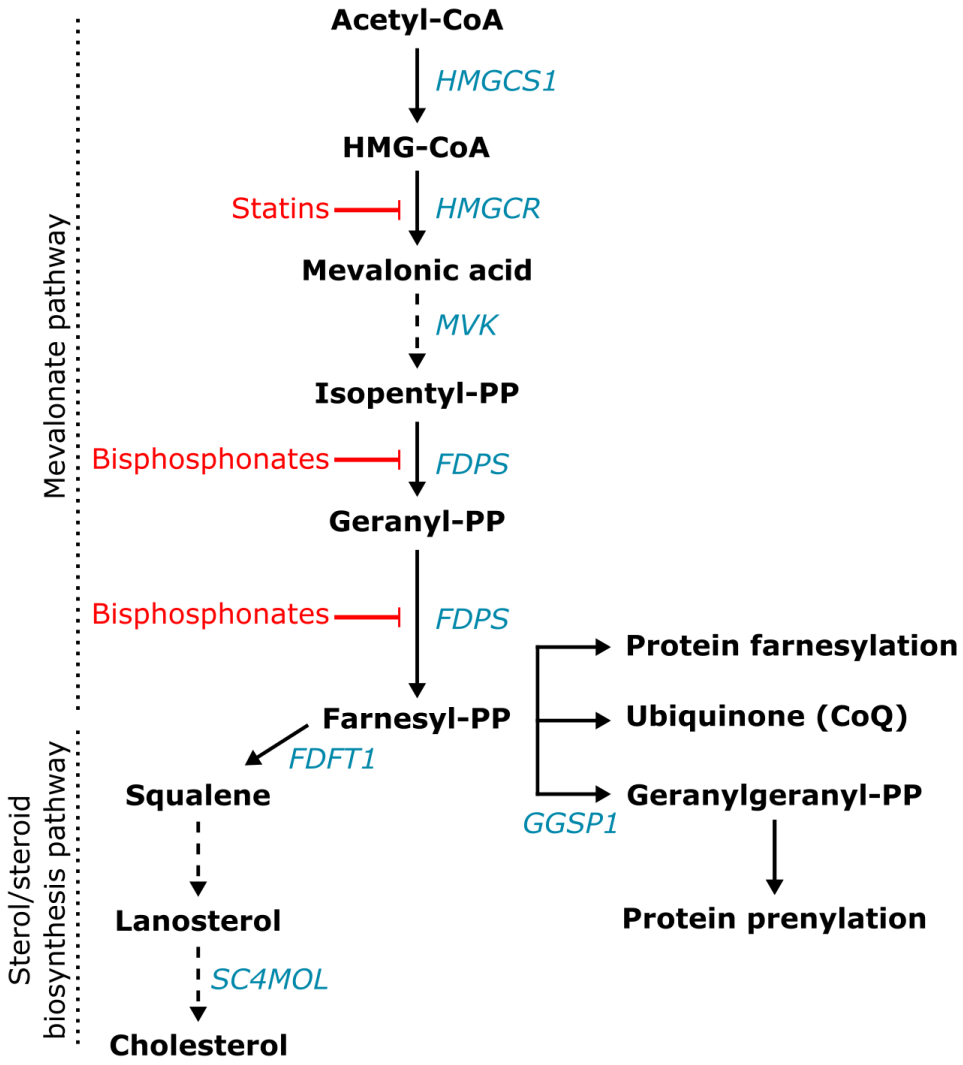


Figure 2.2: Overview of the isoprenoid pathway and its inhibitors. The mevalonate and sterol/steroid biosynthesis pathways with selected key enzymes (blue) are shown. Inhibitors of the pathway are highlighted in red. For a complete reproduction of the isoprenoid pathway, please refer to Buhaescu and Izzedine[256] or the KEGG pathway (http://www.genome.jp/kegg-bin/show_pathway?map00900). FDPS = Farnesyl-diphosphate synthase, GGPS1 = Geranylgeranyl pyrophosphate synthase, FDFT1 = Farnesyl-diphosphate farnesyltransferase 1, SC4MOL = Methylsterol monooxygenase 1. Adapted from Goldstein and Brown[259].

Cholesterol is one of the most important end products of the mevalonate and sterol/steroid biosynthesis pathways. Apart from being a precursor for steroid hormones and numerous other important (signalling) molecules, cholesterol serves as pivotal part of the lipid bilayer of mammalian cell membranes and plays an indispensable role in the regulation of cell membrane properties such as rigidity and fluidity (Fig. 2.3)[260]. Cholesterol and phospholipids are the main constituents of the lipid bilayer of mammalian cells[261]. According to the fluid mosaic model proposed by Jonathan Singer and Garth Nicholson in

1972, the lipids in the bilayer are in a dynamic state and viewed as “two-dimensional fluids” in which receptors, transporters and enzymes are inserted[262]. The finding of detergent resistant entities within membranes, termed lipid rafts, expanded the original mosaic model of membrane organisation[263]. Lipid rafts are commonly defined as cholesterol- and sphingolipid (sphingomyelin and glycosphingolipids)-enriched dynamic microdomains in the exoplasmic leaflet of the plasma membrane. Proteins frequently associated to rafts include glycosylphosphatidylinositol (GPI)-anchored proteins, α-subunits of heterotrimeric G proteins and cholesterol-coupled proteins such as Hedgehog[264]. These dynamic assemblies segregate and concentrate membrane proteins, thus creating signalling platforms by virtue of controlling the co-localisation of receptor-ligand complexes[265, 266]. Changes in the cholesterol content of the plasma cell membrane have been found to alter the structure and composition of lipid rafts. The composition of lipid rafts and specifically the cholesterol content influence the localisation of receptor proteins thereby inducing changes in cellular signalling cascades[265, 267, 268]. Since the introduction of the lipid raft hypothesis, the idea of floating entities in the plasma membrane, cholesterol and its homeostasis have received considerable attention.

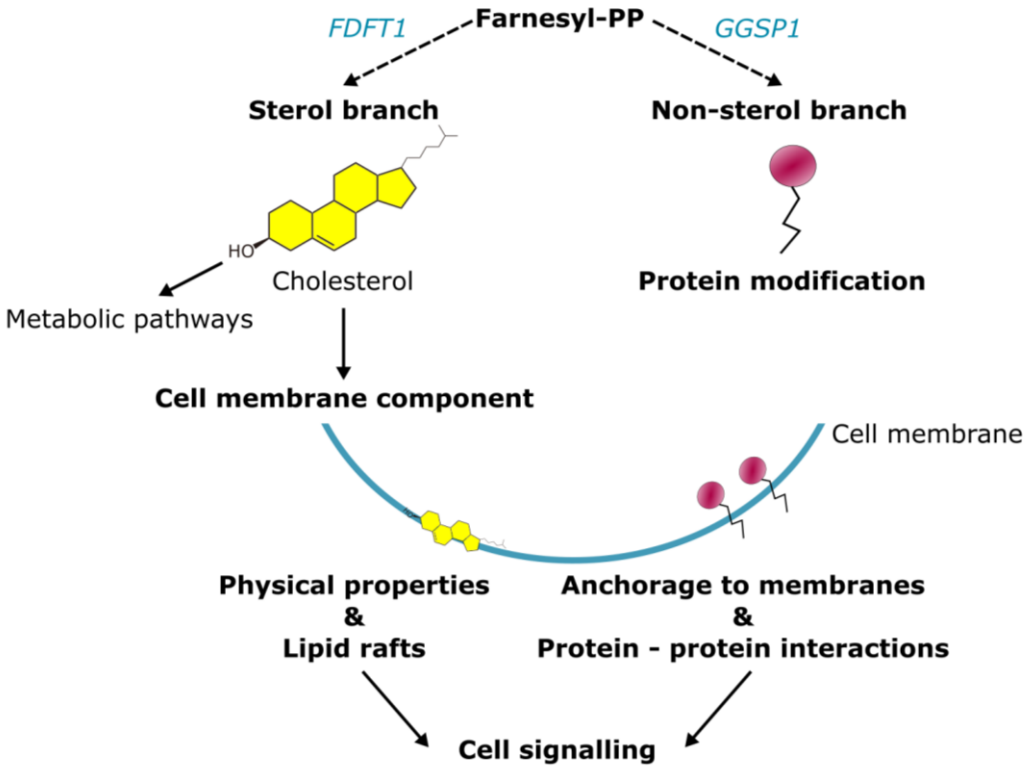


Figure 2.3: Influence of sterol/steroid pathway products on cell signalling mechanisms at the plasma membrane. Schematic depicting how products of the isoprenoid biosynthesis pathway affect cell signalling at the plasma membrane. With regards to the sterol branch, cholesterol is an integral constituent of the cell membrane conferring structural rigidity. Furthermore, it is part of the so-called lipid rafts signalling platforms in the cell membrane. The non-sterol branch is responsible for the prenylation of proteins. The lipid modification allows proteins to insert into cellular membranes and enables protein-protein interactions. GGPS1 = Geranylgeranyl pyrophosphate synthase 1, FDFT1 = Farnesyl-diphosphate farnesyltransferase 1.

As the mevalonate pathway is a key player in controlling a multitude of cellular processes, it has received considerable attention as a therapeutic target. Statins competitively inhibit the HMGCR by occupying its HMC-CoA binding site, hence abolishing the production of downstream products such as cholesterol (Fig. 2.2)[256]. In fact, statins are one of the most frequently sold drugs worldwide today owing to their ability to decrease cardiovascular morbidity and cardiovascular disease-associated mortality. The other prominent group of therapeutic agents used to manipulate the mevalonate pathway are bisphosphonates (BP). BPs hinder bone loss by inhibiting the resorptive activity of osteoclasts which results in a reduced bone turnover, increased bone mass and improved bone mineralisation in patients with osteoporosis. BPs bind potently to hydroxyapatite, especially in regions of bone turnover and remodelling where bone mineral becomes exposed to the surrounding fluids[269]. Bone-bound BPs are taken up by the bone-resorbing osteoclasts via endocytosis. Once internalised, nitrogen-containing BPs potently inhibit the FDPS thereby preventing the prenylation of small GTPase proteins[270, 271]. In

osteoclasts, this causes a disruption in the actin skeleton and impaired formation of the tight-sealing zones or ruffled borders which are necessary for bone reabsorption[269]. Ultimately, this was shown to cause osteoclast apoptosis[270].

Taken together, the mevalonate and sterol/steroid biosynthesis pathways are crucial for the production of key metabolites in cells. The non-sterol branch results in the production of substrates for protein modification and the synthesis of e.g. ubiquinone, while the sterol branch is responsible for the synthesis of cholesterol and its downstream products. Cholesterol fulfils important functions in cellular membranes and as a precursor for signalling molecules within the cell.

In summary, the mechanisms underlying cell-material interactions *in vitro* and especially *in vivo* remain largely elusive. Yet, for the successful design of scaffolds for tissue engineering purposes a clear understanding of such mechanisms is needed. To study the influence of strontium incorporation within the classic 45S5 BG composition on the global response of hMSCs a gene expression microarray study was performed. Surprisingly, a strong up-regulation of the mevalonate and sterol/steroid biosynthesis pathways was observed and the strontium content within the bioactive glasses seemed to play a pronounced role. Continuing from these findings, it was sought to address the question if the observed changes on a gene level translated into systemic changes in the cell and how such modifications could affect cell behaviour. In particular, there was an interest in the cellular plasma membrane which is essential for the communication of the cell with its environment and thus plays an important role in signal transmission and processing.

2.1.3 Aims and objectives

The aim of this chapter was to identify functional effects of the strontium bioactive glass-triggered up-regulation of the isoprenoid pathway in hMSCs with special respect to the plasma membrane. The objectives were to:

- Validate the data obtained with the microarray with respect to the differential regulation of gene expression of enzymes of the isoprenoid pathway;
- Investigate whether changes on a gene level translated to differential protein expression;
- Evaluate if strontium-containing bioactive glass extracts had an effect on the cell membrane of hMSCs;
- Investigate if strontium-containing bioactive glass extracts influenced hMSC lineage commitment.

2.2 Materials & Methods

2.2.1 Glass synthesis

All bioactive glass compositions were produced using a melt-quench route as previously described[128]. Strontium was incorporated into the classic 45S5 BG composition (46.13 mol% SiO_2, 26.91 mol% CaO, 24.36 mol% Na_2O mol%, 2.6 P_2O_5 mol%) by substitution for calcium on a molar basis. 0%, 10% and 100 % of the calcium in the composition were substituted by strontium resulting in 2.69 mol% strontium in the Sr10 composition and 26.91 mol% strontium in the Sr100 composition (Table 2.1). From here onwards, the glasses will be referred to as Sr0, Sr10 and Sr100 or as BG if all three glass compositions are concerned. SiO_2 (99.8%; Tarmac Ltd., UK), Na_2CO_3, Na_3PO_4, $CaCO_3$, and $SrCO_3$ (all >99%; Sigma-Aldrich, UK) were used to prepare the glasses. In brief, the precursor materials were mixed and melted in a platinum-gold crucible for 90 min at 1,400°C. Afterwards, the compositions were rapidly quenched into deionised water (dH_2O) to avoid crystallisation. The batch size was 150 g on average. Particle sizes of 0.1 - 1.0 mm in diameter were used. The particle size range of 0.1 - 1.0 mm was chosen to mimic the shape of commercially available bioactive glass products. Glass synthesis and particle preparation were kindly carried out by Miss Anu Solanki and Dr. Matthew O'Donnell.

Table 2.1: Glass compositions (mol%) and strontium for calcium substitution (%).

Glass	Sr^{2+} for Ca^{2+} substitution	SiO_2	Na_2O	CaO	SrO	P_2O_5
Sr0	0	46.13	24.36	26.91	/	2.6
Sr10	10	46.13	24.36	24.22	2.69	2.6
Sr100	100	46.13	24.36	/	26.91	2.6

2.2.2 Preparation of bioactive glass-conditioned medium

To obtain BG-conditioned medium, 6 mg/mL of Sr0, Sr10 and Sr100 particles were incubated in hMSC growth medium (GM) (PromoCell GmbH, Germany) at 37°C under constant agitation for 24 h. The concentration of particles as well as the incubation time had previously been optimised by Dr. Eileen Gentleman and Dr. Hélène Autefage. These initial experiments showed that the ion release from the glasses into the medium reached a stable equilibrium by 24 h. Furthermore, the concentration of ion release products in the medium were shown to be in a plateau phase at this time point. To remove remaining glass particles, the BG-conditioned medium was passed through a 0.2 μm filter (Sartorius, UK) under sterile conditions and kept at 4°C until use. To determine the elemental concentrations of calcium, phosphorus, silicon and strontium resulting from the partial dissolution of the BGs, medium samples were analysed by inductively coupled plasma optical emission spectrometry (ICP-OES) using an iCAP6000 Series ICP spectrometer (Thermo Scientific, UK). Prior to addition to cells, the medium

was supplemented with 10% (v/v) hMSC growth medium supplement (PromoCell GmbH, Germany) and equilibrated in a controlled humidified chamber (37°C, 5% (v/v) CO_2) for at least 4 h. After equilibration, the pH of the BG-conditioned media was similar to growth medium as measured by H. Autefage. After incubation in a controlled humidified chamber (37 °C, 5% (v/v) CO_2) for 6 h the obtained values for the pH were: GM = 7.65, Sr0 = 7.74, Sr10 = 7.73, Sr100 = 7.70.

2.2.3 Cell culture

Human bone marrow-derived hMSCs were purchased from PromoCell GmbH, Germany and cultured in standard cell culture conditions (37°C, 5% (v/v) CO_2). The hMSCs were expanded in PromoCell growth medium including 10% (v/v) serum supplement (PromoCell GmbH, Germany). Upon 70 - 90% confluency, cells were detached with 0.05% (w/v) Trypsin-EDTA solution (Gibco®, UK), counted using a haemocytometer and re-seeded at density of 4,000 cells/cm^2 for culture expansion. For this study, hMSCs were used between passages 4 and 8. To evaluate pre-commitment of hMSCs in the presence of BG-conditioned medium, cells were treated with a 1:1 (v/v) mix of adipogenic and osteogenic hMSC differentiation medium containing 10% (v/v) serum supplement (all PromoCell GmbH, Germany). A representative image showing the morphology of the purchased hMSCs cultured on tissue culture plastic is shown below (Fig. 2.4).

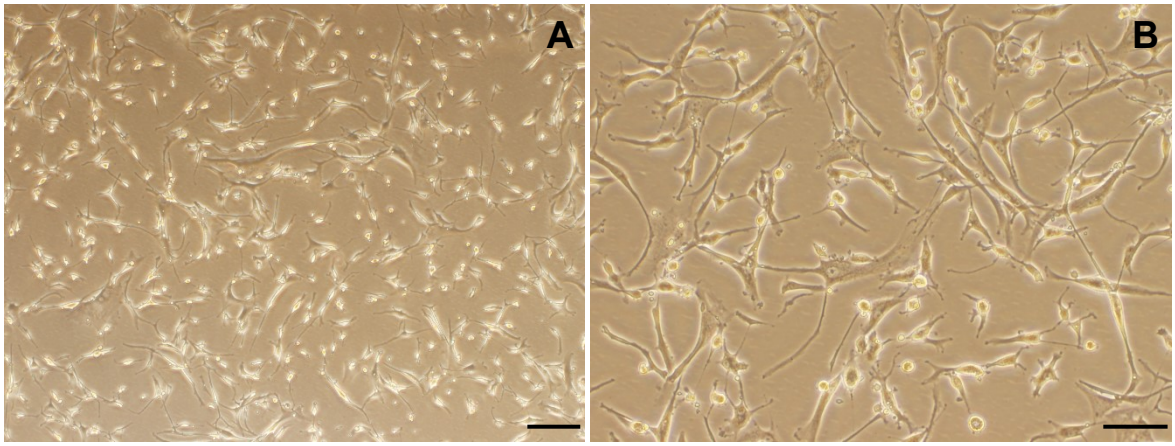


Figure 2.4: Human mesenchymal stem cells (hMSC) at passage 5. Representative image of hMSCs cultured in hMSC growth medium. (A) 4x magnification, scale bar = 200 µm (B) 10x magnification, scale bar = 100 µm.

2.2.4 Quantitative real time PCR (qPCR) analysis of genes involved in the isoprenoid pathway

hMSCs in growth medium were seeded at a density of 20,000 cells/cm^2 in 6-well plates. After 24 h the medium was replaced with growth medium, BG-conditioned medium (Sr0, Sr10 or Sr100) or growth medium supplemented with either calcium chloride dehydrate ($CaCl_2$) (Sigma-Aldrich, UK) (at concentrations of 1 mM and 3 mM) or strontium chloride hexahydrate ($SrCl_2$) (Sigma-Aldrich, UK) (at concentrations of 1 mM and 3 mM). Moreover, pamidronate disodium salt hydrate (Sigma-Aldrich, UK) (at concentrations of 1 μM and 10 μM) and methyl-β-cyclodextrin (MβCD) (Santa Cruz Biotechnologies, USA) (at a concentration of 0.5 mM) were added to growth medium as additional conditions. All conditions were prepared in triplicates and three independent repeats of the experiment were performed. In this chapter, the time of the first medium change was defined as T0. The medium was replaced every second day. After 5 days of treatment, cells were harvested for total RNA isolation using the RNeasy® Plus Mini Kit (Qiagen, UK), according to supplier's instructions. The RNA concentration and quality of each sample were assessed by light absorbance at 260 nm and by calculating the A260/A280 ratio, detected by a Nanodrop 2000c spectrophotometer (Thermo Scientific, UK). One microgram of total RNA of each sample was reverse transcribed into cDNA using the QuantiTect Reverse Transcription Kit (Qiagen, UK) according to the manufacturer's instructions. For qPCR analysis, the cDNA was diluted 1:10 in RNAse free water (Sigma, UK).

For each sample, the total reaction volume was 10 μL containing 300 nM of each primer and 5 μL of QuantiTect SYBR Green PCR Master Mix (Qiagen, Germany). A Corbett Rotorgene 6000 (Qiagen, UK) was used to perform the qPCR reactions. Each sample was run in triplicates. Sequences and cycling conditions of primers used in this study are listed in Table 2.2. Each condition was run for 40 cycles. The primers for *RPL32, HMGCS1, HMGCR, FDPS* and *SC4MOL* were previously described and ordered from Invitrogen (UK), while *GAPDH, RUNX2* and *PPARG* were purchased from Qiagen (QuantiTect® Primer Assay Qiagen, UK)[272]. RPL32 is a ribosomal protein and is deemed to be an appropriate housekeeping gene for qPCR analysis[273]. The efficiency of all primers has been confirmed to be between 0.9 and 1.1.

Data were analysed by the comparative Ct method. Ct is an abbreviation for threshold cycle and is defined as the intersection between an amplification curve and a (pre-)defined threshold line. In brief, delta Ct (ΔCt) values are calculated by normalising the gene expression levels of genes of interest to the expression of the endogenous reference or housekeeping gene (i.e. *RPL32* or *GAPDH*). Thus, ΔCt represents the difference in threshold cycles for target and housekeeping gene.

(1) $\Delta Ct = Ct_{target\ gene} - Ct_{housekeeping}$

ΔΔCt values are equal to the difference in ΔCt for the sample and a chosen calibrator. In this chapter, ΔΔCt represents the target gene expression of the sample relative to the expression level of cells grown in growth medium for 24 h (T0) prior to the initial replacement with BG-conditioned medium.

(2) $\Delta\Delta Ct = \Delta Ct_{sample} - \Delta Ct_{sample\ at\ T0}$

The presented fold change corresponds to the amount of the target, normalised to the endogenous reference and relative to a calibrator as calculated using

(3) $2^{-\Delta\Delta Ct}$ [274].

Table 2.2: Sequences and cycling conditions of primers used in qPCR.

	Gene name	Primer sequence (5'-3')	Cycling conditions
Housekeeping genes	*RPL32*	TTCCTGGTCCACAACGTCAAG TGTGAGCGATCTCGGCAC	95°C for 15 s 60°C for 30 s 72°C for 30 s
	GAPDH	QuantiTect® Primer Assay Qiagen QT00079247)	95°C for 15 s 55°C for 30 s 72°C for 30 s
Isoprenoid pathway	*HMGCS1*	GGGCAGGGCATTATTAGGCTAT TTAGGTTGTCAGCCTCTATGTTGAA	95°C for 15 s 60°C for 30 s 72°C for 30 s
	HMGCR	GGCCCAGTTGTGCGTCTT CGAGCCAGGCTTTCACTTCT	
	FDPS	TCAGACCAGTCGCAGTTTCG CTGCGTTGCGCATTTCC	
	SC4MOL	GAAAAGCCGGCACCAAGA TCAAAGAGAGAATCAGCTCAAACTG	
Lineage markers	*RUNX2*	QuantiTect® Primer Assay Qiagen QT00020517	95°C for 15 s 55°C for 30 s 72°C for 30 s
	PPARG	QuantiTect® Primer Assay Qiagen QT00037793	

2.2.5 In-Cell Western analysis

Utilising *in situ* western blotting, a method termed In-Cell Western, protein expression levels were quantified. The hMSCs were cultured in 48-well tissue culture plates at an initial seeding density of 20,000 cells/cm^2. After 24 h the medium was replaced with growth medium or BG-conditioned medium (Sr0, Sr10 or Sr100). All conditions were prepared in quadruplicates and three independent repeats of the experiment were performed. After 5 days of treatment, cells were fixed with 3.7% (v/v) paraformaldehyde (PFA) in phosphate buffered saline (PBS) for 15 min followed by three washes in PBS. Cells were permeabilised using 0.25% (v/v) Triton-X-100/PBS for 2 - 3 min, rinsed three times with PBS and blocked with 3% (w/v) bovine serum albumin (BSA) in 0.1% (v/v) Tween-20 (Tw) in PBS (PBSTw) for 45 min to 1 h at room temperature (RT) under constant agitation. Primary antibodies, mouse anti-FDFT1 (Abcam, UK, ab119267, 1:200), mouse anti-GGPS1 (Novus Biologicals, USA,

NBP2-03037, 1:200) or rabbit anti-HMGCR (Abcam, UK, ab87246, 1:400), in 3% (w/v) BSA in PBSTw were incubated for 90 min at RT. The cells were then washed three times with PBSTw. Anti-mouse (Li-Cor Biosciences, USA, 1:400) or Anti-rabbit (Li-Cor Biosciences, USA, 1:2000) IR800-labeled secondary antibodies in 3% (w/v) BSA in PBSTw were added to the cells for 1 h at RT under constant agitation and used to visualise the respective protein levels. The intensity values for each protein were normalised to the DNA content per well using the far-red fluorescent DNA dye DRAQ5™ (New England Biolabs, USA, 1:2,000) in 3% (w/v) BSA in PBSTw. After rinsing three rimes with PBSTw, the fluorescent signal was collected and quantified using the Odyssey Infrared Imager (Li-Cor Biosciences, USA). Cells stained with secondary antibody only in the absence of DRAQ5™ were used as controls, and this background was subtracted from the signal.

2.2.6 Quality analysis of antibodies used for In-Cell Western analysis

To assure the specificity of the antibodies used for In-Cell Western analysis, Western blot analysis was carried out (Fig. 2.5). The anti-HMGCS1 antibody detected a protein band at the predicted molecular weight of HMGCS1, namely 57 kilo Dalton (kDa). Besides the band corresponding to HMGCS1, a very faint protein band just below 37 kDa was detected. Detection of the second band can either be due to splice variants or lower molecular weight HMGCS1 degradation products or due to unspecific binding. Considering that the band corresponding to full-length HMGCS1 was much more intense, the anti-HMGCS1 antibody was considered to be specific. Likewise, the anti-FDFT1 antibody detected a protein band corresponding to the predicted molecular weight of FDFT1, 48 kDa. There are three other, though fainter, protein bands visible with higher molecular weights. The presence of the bands may be explained by glycosylation of FDFT1 which would result in a higher molecular weight or unspecific binding, potentially to break down products of other proteins. In the event of cell lysis, proteins can be broken down despite cautionary measures, exposing sequences that may be similar to the target sequence of the antibody.

The antibody raised against GGPS1 detected a band corresponding to a molecular weight of approximately 60 kDa and a much fainter band just below 250 kDa. The predicted molecular weight of GGPS1 is 35 kDa. Even though GGPS1 is known to form a hexameric complex assembled from three dimers in solution, the complex should have been broken down by the denaturation step and the addition of SDS[275]. Reviewing the datasheets of commercially available anti-GGPS1 antibodies, the protein band corresponding to approximately 60 kDa is also detected by a number of other anti-GGPS1 antibodies; among them ab155584 (Abcam), H00009453-B01 (Novus Biologicals) and OAAB15893 (Aviva Systems Biology). Since the detected molecular weight is much higher than the predicted one, it cannot be explained by post-translational glycosylation of the protein but it is possible that the denaturation step did not fully disassemble the GGPS1 complex. In summary, all antibodies were deemed specific.

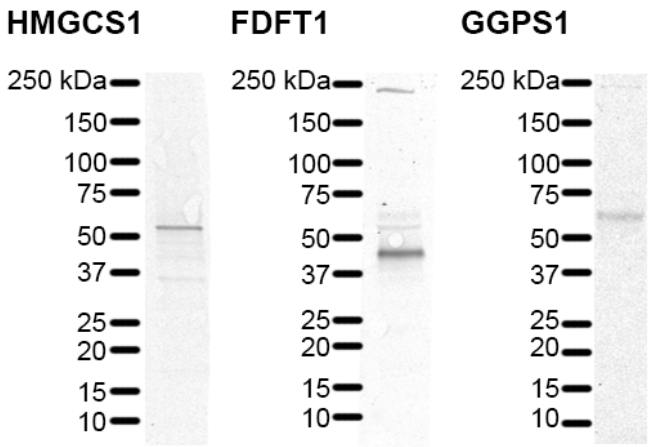


Figure 2.5: Antibody characterisation using Western blot analysis. Whole hMSC lysates were subjected to SDS-PAGE and immunoblotted with the indicated antibodies. Anti-HMGCS1, anti-FDFT1 and anti-GGPS1 antibodies were characterised. All antibodies were deemed specific.

2.2.6.1 Sodium dodecyl sulphate polyacrylamide gel electrophoresis (SDS-PAGE)

SDS-PAGE was performed on hMSC extracts to separate proteins according to their size using 4 - 20% gradient mini-PROTEAN® TGX™ precast polyacrylamide gel (BIO-RAD, UK) following standard procedures. Briefly, hMSCs were seeded at a density of 20,000 cells/cm^2 in 6-well plates and grown to confluency. Cells were washed once with ice-cold PBS prior sample lysis. Cell lysis was performed using Radio Immuno Precipitation Assay (RIPA) buffer (Santa Cruz Biotechnology, USA) containing 150 mM NaCl/1.0% (v/v) Triton X-100/0.5% (w/v) sodium deoxycholate as well as protease and phosphatase inhibitors (cOmplete mini EDTA-free tablets and PhosSTOP Phosphatase Inhibitor Cocktail Tablets, both Roche, UK). The hMSC extracts were transferred to pre-cooled microcentrifuge tubes and maintained at constant agitation for 30 min at 4°C. To separate cell debris, the cell suspension was centrifuged at 16,000 xg for 20 min in a 4°C pre-cooled centrifuge. The supernatant was transferred to a new pre-cooled microcentrifuge tube and used for further analysis. Samples were prepared with an equal volume of 2X Laemmli sample buffer (BIO-RAD, UK) and heated to 100°C for 5 min to reduce and denature the proteins. Afterwards, 20 µL of each sample was loaded onto the gel. The gels were run in running buffer (25 mM Tris-HCl, 190 mM glycine, 0.1% (w/v) SDS, pH 8.3) at 120V until the target protein had been sufficiently separated. Precision Plus Protein™ standards All Blue marker (BIO-RAD, UK) was used as a size marker.

2.2.6.2 Electroblotting of proteins to a nitrocellulose membrane

The proteins were transferred from the polyacrylamide gel onto a nitrocellulose membrane (GE Healthcare Life Sciences Whatman™, USA) by wet transfer in transfer (25 mM Tris-HCl, 190 mM

glycine), running for 90 min at 400 mA on ice. Upon completion of the electrophoretic transfer, membranes were blocked in 3% (w/v) BSA in PBSTw for 30 min at RT and subsequently washed thrice (5 min each) with PBSTw. Primary antibodies, mouse anti-FDFT1 (ab119267, 1:200), mouse anti-GGPS1 (NBP2-03037, 1:200) or rabbit anti-HMGCS1 (ab87246, 1:400), in 3% (w/v) BSA in PBSTw were incubated for 90 min RT. The membranes were then washed three times with PBSTw. Anti-rabbit (Li-Cor Biosciences, USA, 1:2000) or anti-mouse (Li-Cor Biosciences, USA, 1:400) IR800-labeled secondary antibodies were incubated for 1 h at RT and used to visualise the respective protein levels. Membranes were washed three times with PBSTw to remove unbound antibodies before being imaged using an Odyssey Infrared Imager (Li-Cor Biosciences, USA).

2.2.7 Immunofluorescence staining and imaging

Cells were grown on 10 mm glass slides placed in 48-well dishes or in chambered cover glass systems (Lab-Tek® Chambered #1.0 Borosilicate Coverglass System, UK) and were immunostained using standard procedures. Briefly, hMSCs were seeded in growth medium at a density of 4,000 cells/cm^2 on glass slides in 48-well plates or in chambered cover glass systems. After 24 h, BG-conditioned or growth medium was added. Medium was replaced every second day. After 5 days of treatment, cells were fixed with 3.0% (v/v) methanol-free PFA in PBS (Gibco®, UK) for 1 h at RT and subsequently washed three times with PBS. To quench the paraformaldehyde, cells were incubated with 0.15% (w/v) glycine in PBS, rinsed three times with PBS and then blocked with 3% (w/v) BSA in PBSTw for 1 h at RT.

2.2.7.1 Filipin fluorescence staining of free cholesterol in cultured cells

Filipin III is one of four isomeric polyene macrolides isolated from cultures of S. filipinensis. Due to filipin III's ability to bind specifically to cholesterol and its intrinsic fluorescence the compound has been widely used to detect cholesterol. After fixation and blocking, cells were incubated with 0.05 mg/mL of filipin III (Cambridge Bioscience CAY70440, UK) in 10% (v/v) foetal bovine serum (FBS) in PBS under constant agitation. After 4 h cells were rinsed three times with PBS.

2.2.7.2 Staining of lipid rafts with FITC-conjugated cholera toxin subunit β

Cholera toxin is the virulent protein complex secreted by Vibrio cholera that is responsible for the characteristics of a cholera infection in humans[276, 277]. The cholera toxin is comprised of an A and a B subunit characterising it as a member of the AB_5-subunit family of toxins[276]. Cholera toxin subunit B (CTβ) alone is non-toxic to cells and is widely used as a marker for membrane lipid rafts due to its G_{M1} ganglioside binding property[278]. FITC is a commonly used fluorochrome and derived from fluorescin. FITC-conjugated CTβ (Sigma C-1655, UK) was added at a concentration of 0.01 mg/mL in PBS and incubated over-night at 4°C under constant agitation[279]. Cells were washed three times with PBS and post-fixed with 2% (v/v) methanol-free paraformaldehyde for 15 min at RT. The nature of lipid rafts

necessitates post-fixation as the fluorescent molecules may otherwise drift. Afterwards, cells were rinsed three times with PBS.

2.2.7.3 Imaging

Imaging of both cholesterol and lipid rafts was achieved using total internal reflection fluorescence (TIRF) microscopy. TIRF microscopy is a highly sensitive technique to observe molecules at or near the plasma membrane due to a high signal-to-noise ratio and a resolution in the z direction ranging between 70-250 nm. While single fluorescent species in or near the cell membrane can be selectively excited when using TIRF microscopy, images obtained with epifluorescene or confocal microscopy are frequently obscured by a high background fluorescence. Due to these advantages, TIRF microscopy has emerged as method of choice to visualise cellular processes occurring at or near the cell membrane such as endo- and exocytosis[280]. Here, a Zeiss Axiovert 200 manual inverted microscope with a 488 nm laser diode, a 100x/1.45W Alpha Plan Fluar objective, and a back-illuminated EM-CCD camera (Hamamatsu C9100-13), which was provided by the Imperial College London FILM facility, was used to image cholesterol and lipid raft staining in the cellular plasma membrane. Fluorescence was excited using a 488 nm laser and images were analysed using ImageJ. Initially, any background staining was subtracted before the 16 bit raw images were transferred into binary 8 bit files. Subsequently, based on visual examination, an area of interest was defined as well as the intensity threshold adjusted for the binary images. For quantitation purposes, the fluorescent intensity of the stained area was calculated relative to the total area of interest. Imaging of samples and image analysis were performed by Dr. Thomas von Erlach.

2.2.8 Statistical analysis

Statistical analysis was performed using one-way analysis of variance (ANOVA) combined with a Tukey *post-hoc* test on data obtained from at least three independent experiments. The ANOVA was chosen to be able to compare all groups with each other in order to detect both general effects of bioactive glass dissolution products in comparison to extract free growth medium as well as to test for differences between the BG-conditioned medium groups to identify possible composition-dependent effects. Results with p-values lower than 0.05 were deemed significant. All data are expressed as mean ± standard deviation (SD).

2.3 Results

2.3.1 Effect of strontium incorporation on bioactive glass ion release

To obtain BG-conditioned medium, glass particles were incubated in hMSC growth medium for 24 h at 37°C. The medium was subsequently filtered to remove remaining glass particles. The elemental concentrations of the BG dissolution products calcium (Ca), phosphorous (P), silica (Si) and strontium (Sr) in hMSC media were determined by ICP-OES (Table 2.3). As observed previously, the strontium ion release increased corresponding to its molar content in the glasses (non-detectable (ND), 0.09 mM and 1 mM for Sr0, Sr10 and Sr100, respectively). The values for the release of silicon and phosphorous were comparable across all compositions save calcium[184]. Compared to growth medium only, the phosphorous ion content was decreased in BG-conditioned media which may be explained by partial precipitation of calcium phosphate (CaP)[281]. The decreased calcium concentration in Sr100-conditioned medium may owe to the fact that the partial loss of calcium by CaP precipitation could not be balanced by the ions released from the glass as 100% of the calcium were replaced by strontium. Hence, a general limitation of the BG-conditioned medium was that with increasing strontium content, the overall calcium content in the conditioned medium decreased. The amount of strontium ions detected in the conditioned medium is likely clinically relevant as the release from Sr10 corresponded to the strontium level found in the serum of patients treated with SrR for osteoporosis (0.12 mM)[251]. In cell culture experiments 1 mM strontium has been widely used as a reference concentration which is similar to the release from Sr100[173, 176].

Table 2.3: Ion content of strontium-substituted BG-conditioned media measured by inductively coupled plasma optical emission spectroscopy (ICP-OES). Elemental concentrations of BG ionic dissolution products (Si, Ca, P and Sr) in PromoCell hMSC growth medium are shown. Bioactive glass particles were incubated in growth medium for 24 h at 37°C under constant agitation. The ion content was measured by ICP-OES. Elemental concentrations are expressed as a mean ± standard deviation (SD) of 3 independent samples in ppm unless otherwise indicated. The ICP-OES was operated with the assistance of Dr. Hélène Autefage and Miss Anu Solanki. GM = Growth medium. Non-detectable = ND.

	Si	Ca	P	Sr	Sr (mM)
GM	ND	67.1 ± 7.1	31.2 ± 7.1	ND	ND
Sr0	31.1 ± 1.0	69.5 ± 1.5	19.1 ± 0.2	ND	ND
Sr10	44.0 ± 4.5	69.1 ± 6.2	19.9 ± 1.9	8.2 ± 0.9	0.09 ± 0.01
Sr100	36.0 ± 0.5	32.2 ± 0.4	19.2 ± 0.1	92.5 ± 2.6	1.06 ± 0.03

2.3.2 Effect of strontium-containing bioactive glass extracts on the isoprenoid pathway on a gene level

In a first step, the observations obtained with the mRNA microarray were confirmed by quantitative real-time PCR (qPCR). For this purpose, four representative genes exclusive to the mevalonate and sterol/steroid biosynthesis pathways were chosen, namely *HMG-CoA synthase 1 (HMGCS1), HMG-CoA reductase (HMGCR), farnesyl diphosphate synthase (FDPS)* and *methylsterol monooxygenase (SC4MOL)*. HMGCS1 and HMGCR are the first two enzymes of the mevalonate pathway with HMGCR activity being the rate limiting step of the mevalonate pathway. HMGCR expression is regulated in parts by feedback mechanisms. FDPS is the last enzyme of the mevalonate pathway before it branches into the sterol and non-sterol arms of the isoprenoid biosynthesis pathway. SC4MOL is dedicated to the synthesis of cholesterol. Hence, different stages of the isoprenoid biosynthesis pathway were appropriately represented by the chosen genes. The hMSCs were exposed to the various BG-conditioned media (Sr0, Sr10 or Sr100) for 5 days in order to evaluate their influence on the expression of key genes of the mevalonate and sterol/steroid biosynthesis pathways. The 5 day time point was chosen on basis of the microarray results as the strongest differential gene expression in response to the BG dissolution products (when compared to growth medium only) was measured after 5 days. To clarify whether the obtained results were due to strontium ions exclusively, strontium ions ($SrCl_2$ at concentrations of 1 mM and 3 mM) were added to growth medium. Correspondingly, growth medium was supplemented with calcium ions at the same concentrations ($CaCl_2$, 1 mM and 3 mM) to serve as controls. A strontium concentration of 1 mM corresponds to the strontium concentration in Sr100-conditioned medium. The gene expression results presented in this chapter were combined with additional, independent repeats for publication in Autefage *et al.*[250].

The expression of all selected genes was significantly increased by treatment with BG-conditioned medium compared to growth medium (Fig. 2.6). Interestingly, also Sr0 triggered a significant increase in the expression levels of *HMGCS1*, *FDPS* and *SC4MOL*. Yet, Sr100 treatment further significantly up-regulated the expression of all three genes compared to Sr0 and *HMGCS1* expression was significantly higher in Sr100-treated cells compared with the Sr0 and Sr10 groups indicating a strontium-dependent mechanism. In summary, the BG dissolution products significantly increased the gene expression of *HMGCS1, HMGCR, FDPS* and *SC4MOL*, suggesting that all stages of the mevalonate and sterol/steroid biosynthesis pathways were regulated on a gene level. Furthermore, replacing 100% of the calcium with strontium in the 45S5 BG composition correlated with enhanced gene expression values, implicating a pronounced role of strontium within the glass composition. Highlighting that the combination of BG ion release products was pivotal for the observed changes in gene expression, neither the Sr^{2+} nor the Ca^{2+} controls alone increased gene expression levels. Overall, the results of the gene expression analysis corroborated the findings obtained with the whole genome

microarray emphasising the impact of both BG dissolution products and a single key bioactive ion species within a biomaterial composition.

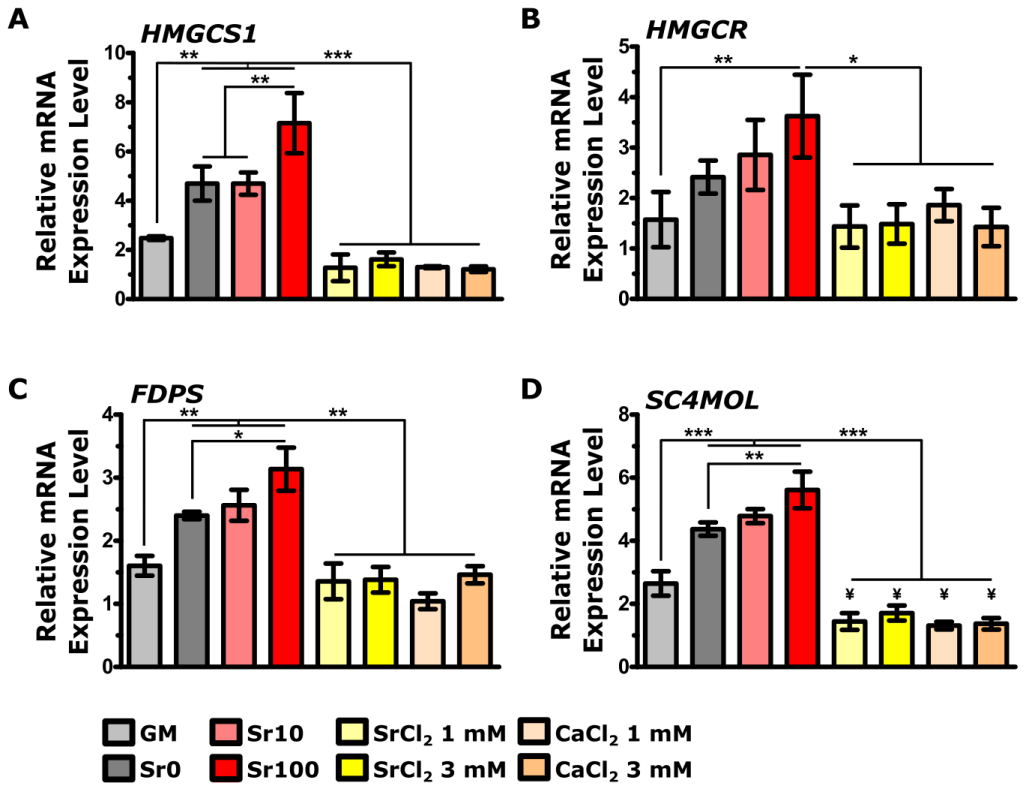


Figure 2.6: Effect of incorporating strontium into BG on isoprenoid biosynthesis-associated genes. hMSCs were continuously cultured in the presence of BG-conditioned (Sr0, Sr10 and Sr100) or growth (GM) medium in the presence or absence of $SrCl_2$ (1 mM and 3 mM), or $CaCl_2$ (1 mM and 3 mM) for 5 days prior to qPCR. The gene expression of *HMGCS1* (A), *HMGCR* (B), *FDPS* (C) and *SC4MOL* (D) was assessed. Data are represented as the mean ± standard deviation (SD) of 3 independent experiments. Significance was assessed by a one-way ANOVA combined with a Tukey *post-hoc* test. (*p<0.05; **p<0.01; ***p<0.001). D) For visual display, significant differences in *SC4MOL* expression between GM and the $SrCl_2$ and $CaCl_2$-conditioned media are indicated separately (¥ p<0.05). Sr0, Sr10 and Sr100 represent strontium-doped bioactive glasses with 0%, 10% and 100% strontium substitution for calcium, respectively.

As additional conditions, pamidronate (at concentrations of 1 µM and 10 µM) and methyl-β-cyclodextrin (at a concentration of 0.5 mM) were added to growth medium. As pamidronate is a bisphosphonate and a known inhibitor of FDPS there was an interest to study whether treatment of cells with pamidronate would elicit similar results as ions released from the BGs. Furthermore, it was sought to investigate whether the removal of cholesterol from the cell membrane had an influence on the mevalonate and sterol/steroid biosynthesis pathways. As cholesterol is one of the main downstream products of the mevalonate pathway, it was evaluated whether a positive feedback mechanism would be activated after its depletion in the cellular membrane causing an up-regulation on gene level. Methyl-

β-cyclodextrin (MβCD) is widely used to sequester cholesterol from cellular membranes and was used for that purpose accordingly[282]. The supplementation of pamidronate or MβCD did not affect gene expression levels of the selected target genes (Fig. 2.7). This result allows the conclusion that inhibition of FDPS by pamidronate does not result in a gene up-regulation as observed after treatment with the BG ionic dissolution products. Thus, BGs and pamidronate differ in their mode of action. Likewise, MβCD treatment did not increase the expression of any of the studied genes. As the mevalonate and sterol/steroid biosynthesis pathways are partly regulated by a feedback loop, an up-regulation of some of the genes could have been expected upon cholesterol depletion. However, since MβCD selectively removes cholesterol from the cell membrane, the conventional feedback mechanism via the sterol regulatory element-binding protein (SREBP) may not be activated as quickly[283]. Another explanation may be that MβCD was not supplemented at a concentration sufficient to properly deplete membrane cholesterol, as the use of concentrations greater than 1 mM has been reported in the literature[282, 284]. The concentration of 0.5 mM was chosen based on preliminary tests that had been carried out in the Stevens group. To assure that long term administration of MβCD was non-toxic for the cells, different concentrations had been evaluated. Long term exposure to MβCD concentrations higher than 0.5 mM had a cytotoxic effect.

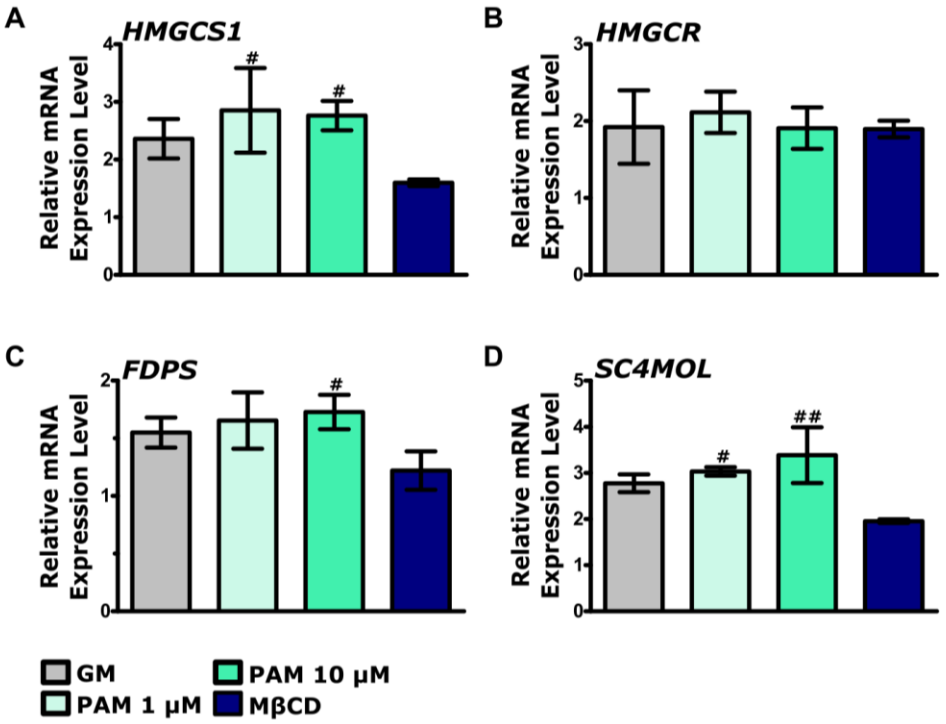


Figure 2.7: Effect of pamidronate (PAM) and methyl-β-cyclodextrin (MβCD) on isoprenoid pathway-associated genes. hMSCs were continuously cultured in growth (GM) medium in absence or presence of pamidronate (1 µM and 10 µM) or MβCD (0.5 mM) for 5 days prior to qPCR. The gene expression of *HMGCS1* (A), *HMGCR* (B), *FDPS* (C) and *SC4MOL* (D) was examined. Data are represented as the mean ± SD of 3 independent experiments. Statistical significance was assessed by a one-way ANOVA combined with a Tukey *post-hoc* test. #$p<0.05$, ##$p<0.01$ vs. MβCD.

2.3.3 Effect of strontium-containing bioactive glass extracts on the expression of proteins of the isoprenoid biosynthesis pathway

To evaluate whether the up-regulation of isoprenoid biosynthesis pathway-associated genes in presence of BG dissolution products translated into changes at the protein level, In-Cell Western analysis was performed. hMSCs were cultured in BG-conditioned medium prepared from Sr0, Sr10 or Sr100 for 5 days. As an additional condition, growth medium was supplemented with MβCD. As representatives for the isoprenoid biosynthesis pathway, protein expression levels of HMGCS1, squalene synthase (FDFT1) and geranylgeranyl pyrophosphate synthetase 1 (GGPS1) were quantified (Fig. 2.8). FDFT1 and GGPS1 are key enzymes at the branching point of the isoprenoid pathway[255, 259, 285, 286]. FDFT1 is the first specific enzyme exclusively dedicated to cholesterol biosynthesis while GGPS1 is a member of the prenyltransferase family crucial for the C20-prenylation of proteins; hence FDFT1 and GGPS1 represent different arms of the isoprenoid pathway. The amount of HMGCS1 protein was comparable between the various conditions, despite the differential expression observed at a gene level (Fig. 2.8A). This may be due to a tight regulation on a post-transcriptional level keeping the abundance of HMGCS1

protein constant. GGPS1 protein abundance was significantly increased in presence of Sr100-conditioned medium compared to the Sr0 condition indicating a strontium-dependent effect (Fig. 2.8B). Furthermore, GGPS1 protein levels were increased in the presence of all BG dissolution products compared to growth medium only. Addition of MβCD had no effect on GGPS1 abundance compared to growth medium which correlated with the gene expression results. Assessment of FDFT1 expression showed that FDFT1 was significantly increased in all BG groups compared to growth medium (Fig. 2.8C). Differences in FDFT1 protein abundance among the different bioactive glass compositions were not statistically significant even though the fluorescence intensity detected for FDFT1 was consistently higher in the Sr10 condition compared to both Sr0 and Sr100 in all three independent repeats. In-Cell Western analysis might not have been sufficiently sensitive to pick up differences in FDFT1 content between the BG groups that would allow a statistical significant result. To investigate whether there is a Sr/Ca ratio-dependent influence, more independent repeats need to be performed to determine if statistically significant differences can be observed. Taken together, all BG dissolution products caused a significant increase in GGPS1 and FDFT1 protein abundance compared to growth medium only while the HMGCS1 protein level was comparable across all conditions. The presence of strontium within the Sr10 and Sr100 dissolution products had a less clear effect on protein expression compared to the previous gene expression results. Only GGPS1 was significantly up-regulated by Sr100-conditioned medium compared to Sr0.

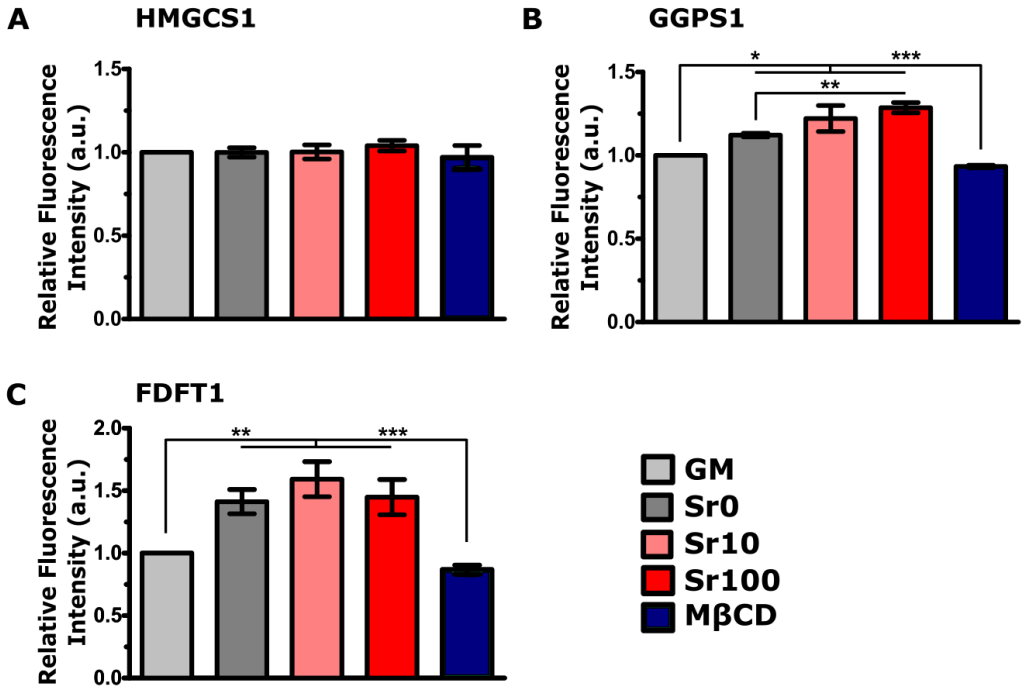


Figure 2.8: Effect of incorporating strontium into BG on protein abundance of isoprenoid pathway-associated enzymes. hMSCs were treated with BG-conditioned (Sr0, Sr10 and Sr100) or growth (GM) medium in the presence or absence of methyl-β-cyclodextrin (MβCD, 0.5 mM) for 5 days. The protein expression of HMGCS1 (A), FDFT1 (B) and GGPS1 (C) was measured by In-Cell Western analysis. Values were normalised to the DNA content and are presented relative to GM. Data are represented as the mean ± SD of 3 independent experiments. Significance was assessed by a one-way ANOVA combined with a Tukey *post-hoc* test (*p<0.05, **p<0.01, ***p< 0.001). Sr0, Sr10 and Sr100 represent strontium-doped bioactive glasses with 0%, 10% and 100% strontium substitution for calcium, respectively. A.u. = arbitrary units.

2.3.4 Effect of strontium-containing bioactive glass extracts on membranous cholesterol in hMSCs

Following on from the previous results, the impact of strontium within the BG extracts on downstream products of the mevalonate and sterol/steroid biosynthesis pathways was studied. Cholesterol is one of the most well-known products of the isoprenoid biosynthesis pathway and fulfils several crucial functions in the cell. Raman spectroscopy mapping of Sr100-treated hMSCs indicated an increased cholesterol and lipid content compared to hMSCs cultured in growth medium suggesting a change in sterol metabolite level (published in Autefage *et al.)*[250]. Building on this finding it was decided to focus on the impact of such an increase in sterol metabolites on the cell membrane. Cholesterol is one of the key constituents of the cellular plasma membrane where it is involved in the regulation of physical properties of the lipid bilayer and of membrane protein clustering within lipid rafts[260]. Considering the up-regulation of genes coding for enzymes of the sterol branch of the isoprenoid pathway as identified

by the whole genome microarray and confirmed by qPCR for *FDFT1* and *SC4MOL* (data presented in 2.3.2), it was sought to quantify the amount of cholesterol in the plasma membrane of hMSCs. After 5 days of exposure to growth or BG-conditioned media, cells were fixed and stained with filipin III, a molecule that specifically binds to non-esterified cholesterol[287]. In order to exclusively visualise and quantify the cholesterol content in the substrate-facing plasma membrane, TIRF microscopy was used (Figure 2.9A, B). Filipin III staining intensity was significantly higher in Sr100-treated hMSCs than in hMSCs exposed to either Sr0-conditioned or growth medium (Fig. 2.9A). This observation supports a role of ion dissolution products derived from strontium-containing bioactive glasses in the regulation of cholesterol content in the cellular plasma membrane. Notably, there was evidence that the presence of strontium ions within the bioactive glass composition was essential for this effect in the conditions of the experiments presented in this chapter, as the values obtained for Sr0 were not significantly different from growth medium only. Representative TIRF images of hMSCs treated with growth or BG-conditioned media (Sr0, Sr10 and Sr100) for 5 days prior to staining with filipin III are shown in Figure 2.9B.

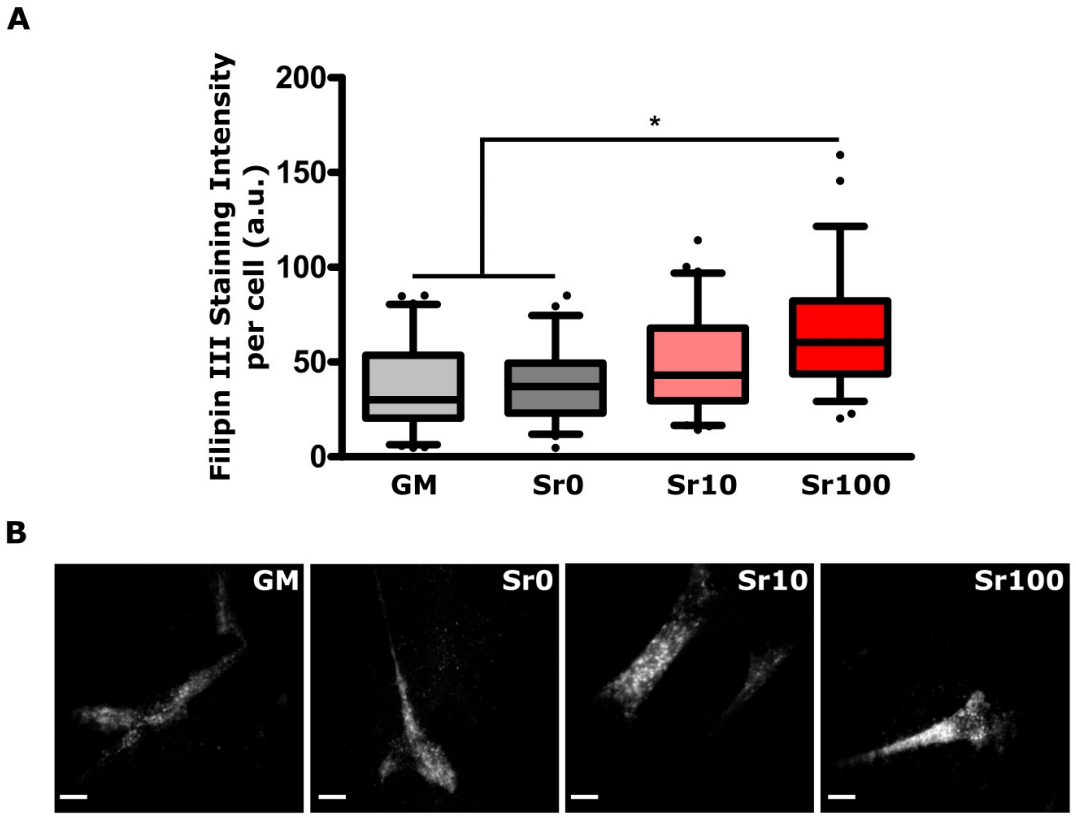


Figure 2.9: Effect of incorporating strontium into BG on the membranous cholesterol content in hMSCs. A) The cholesterol content in the plasma membrane of hMSCs was determined by quantification of filipin III staining after treatment with different BG-conditioned media (Sr0, Sr10 and Sr100) or growth medium (GM) for 5 days. Data are expressed as box plots representing analysis of at least 30 cells per group over 3 independent experiments. The whiskers indicate the 5th and 95th percentile, outliers are highlighted as dots. B) Representative TIRF images for GM and BG-treated hMSCs (scale bar = 10 µm). Croppings of these images also appear in Autefage *et al.*[250]. Significance was assessed by one-way ANOVA combined with a Tukey *post-hoc* test (*p<0.05). Sr0, Sr10 and Sr100 represent strontium-doped bioactive glasses with 0%, 10% and 100% strontium substitution for calcium, respectively. Image acquisition and data analysis were performed by Dr. Thomas von Erlach.

2.3.5 Effect of strontium-containing bioactive glass extracts on lipid-raft abundance in hMSCs

Based on the previously described up-regulation of FDFT1, a protein associated to membrane lipid raft composition, together with the increased cholesterol content in the cell membrane, it was speculated that strontium-containing bioactive glasses affected the cellular lipid raft abundance[286]. These raft-signalling platforms have been shown to be important for numerous signalling pathways and cell functions[264]. To test this hypothesis, TIRF microscopy was used to visualise and quantify lipid rafts in response to BG extract treatment (Fig. 2.10). The intensity of FTIC-conjugated CTβ staining served as a measure for the amount of lipid rafts in the plasma membrane. Analysis of CTβ staining revealed a

significantly higher staining intensity in hMSCs treated with Sr100-conditioned medium compared to Sr0 and growth medium (Fig. 2.10A). The staining intensity measured in Sr0 and growth medium was comparable, indicating that the incorporation of strontium within the 45S5 BG composition affected the lipid raft content in the cellular plasma membrane. Hence, these results suggest that the amount or the composition of lipid rafts was modified in presence of BG dissolution products in a strontium-dependent manner. Considering the plethora of signalling mechanisms that depend upon lipid rafts, these observations highlight how biomaterials may affect cell behaviour. Representative TIRF images of hMSCs treated with growth or BG-conditioned medium (Sr0, Sr10 and Sr100) for 5 days prior to staining with CTβ are shown in Figure 2.10B.

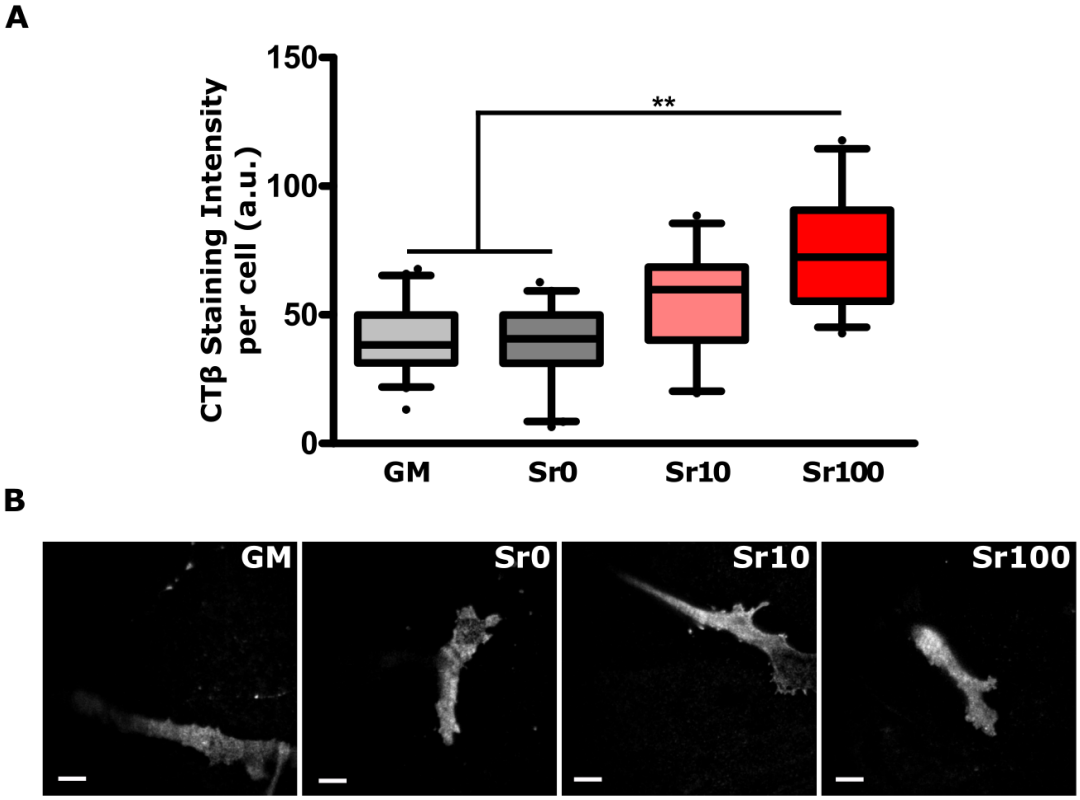


Figure 2.10: Effect of incorporating strontium into BG on the lipid raft content in hMSCs. A) The lipid raft abundance in the plasma membrane of hMSCs was determined by cholera toxin subunit β (CTβ) staining after treatment with growth (GM) or BG-conditioned medium (Sr0, Sr10 and Sr100) for 5 days. Data are expressed as box plots representing analysis of at least 30 cells per group over 3 independent experiments. The whiskers indicate the 5th and 95th percentile, outliers are highlighted as dots. B) Representative TIRF images for growth medium and BG-treated hMSCs (scale bar = 10 µm). Croppings of these images also appear in Autefage *et al.*[250]. Significance was assessed by a one-way ANOVA combined with a Tukey *post-hoc* test (**p< 0.01). Sr0, Sr10 and Sr100 represent strontium-doped bioactive glasses with 0%, 10% and 100% strontium substitution for calcium, respectively. Image acquisition and data analysis were performed by Dr. Thomas von Erlach.

2.3.6 Influence of strontium-containing bioactive glass extracts on the pre-commitment of hMSCs

Analysis of the microarray data had only pointed towards a mild regulation of osteogenic differentiation of lineage-associated genes by BG-conditioned hMSC growth medium. Generally, strontium either incorporated in biomaterials or in form of SrR, is thought to promote hMSC osteogenic lineage commitment[288-291]. Since the hMSC growth medium is designed to maintain the stem cell-like properties of hMSCs it may have suppressed differentiation. Therefore, it was sought to investigate whether strontium-containing BG-conditioned medium had an influence on the pre-commitment of hMSCs. For 5 days, hMSCs were cultured in BG-conditioned medium (Sr0, Sr10 and Sr100) as previously

described. On day 5, the medium was replaced by a 1:1 (v/v) mix of osteogenic and adipogenic media. The media mix was chosen to expose the cells with equal amounts of adipogenic and osteogenic supplements, thus clarifying if exposure to the BG ionic dissolution products induced cell signalling mechanisms that favoured or facilitated commitment to either lineage[292, 293]. *RUNX2* and *PPARG* served as representative genes for the osteogenic and adipogenic lineage commitment respectively. Gene expression levels were determined by qPCR. All values were normalised to the housekeeping gene *GAPDH* and expressed as fold change to the respective gene expression in the growth medium group at day 5 (Fig. 2.11A, B). Cells cultured in growth medium for 5 days were treated for 2 days with the osteogenic/adipogenic media mix along with the other conditions.

There were no significant differences in *RUNX2* expression level between groups or time points (Fig. 2.11A). In particular, there were no apparent differences between the BG-treated groups, suggesting that a putative effect of the BG-conditioned media on *RUNX2* expression was not strontium-dependent. To ascertain the effect of BG extracts on *RUNX2* expression in hMSCs, more repeats of the experiment and more time points would be necessary. An increase in *RUNX2* expression on day 7 could have been expected, at least in the growth medium only group, as the osteogenic medium supplements should enhance osteogenic lineage-associated gene expression. This may suggest that the chosen time point was not appropriate for the assessment of *RUNX2* gene expression. Overall, the *RUNX2* expression levels remained quite low and differences were subtle.

PPARG expression was comparable in all groups and all time points (Fig. 2.11B). A previous study has shown that the supplementation of SrR in adipogenic medium resulted in a decreased differentiation of MSCs towards the adipogenic lineage[180]. Even though a decrease was not observed in this study, *PPARG* expression was not increased on day 7 after treatment with the 1:1 (v/v) mix of osteogenic and adipogenic medium. Considering the presence of adipogenic supplements an increase in *PPARG* could have been expected. However, from the results obtained in this study no conclusion can be drawn whether BG dissolution products decreased adipogenic differentiation.

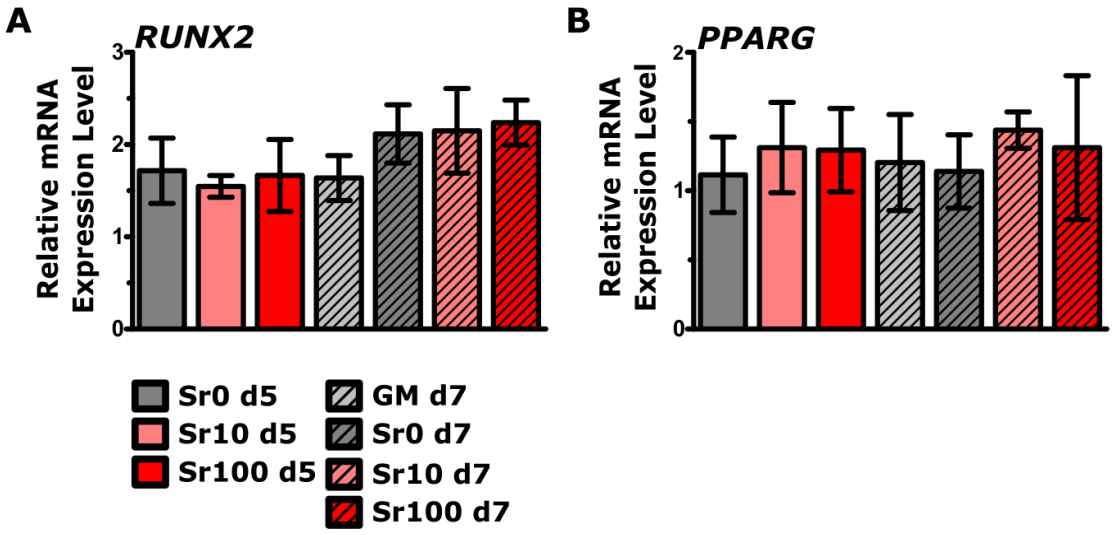


Figure 2.11: Influence of strontium incorporation into BG on the pre-commitment of hMSCs. hMSCs were continuously cultured in BG-conditioned or growth (GM) medium for 5 days prior to treatment with a 1:1 mix of osteogenic and adipogenic differentiation medium for 48 h. Pre-commitment of hMSCs was assessed by means of qPCR of *RUNX2* (A) and *PPARG* (B). Data are represented as the mean ± SD of 3 independent experiments and are expressed relative to the gene expression of the growth medium group on day 5. Significance was assessed by a one-way ANOVA combined with a Tukey *post-hoc* test. Sr0, Sr10 and Sr100 represent strontium-doped bioactive glasses with 0%, 10% and 100% strontium substitution for calcium, respectively.

2.4 Discussion

Strontium occurs naturally as a trace element in the human body and has received considerable attention as anti-osteoporotic agent in form of SrR. Considering the promising results reported with SrR, strontium has been incorporated into biomaterials with the aim of developing novel, smart, osteogenic materials. Bioactive glasses are particularly attractive carrier systems for therapeutic ions such as strontium owing to their inherent osteinductive/osteoproductive properties. Whereas the osteogenic potential of SrR and strontium-containing biomaterials has been widely studied, the global influence of strontium-substituted biomaterials on cells has remained largely elusive. In order to address this question, a whole genome microarray was performed on hMSCs after culture in Sr0, Sr10 or Sr100-conditioned medium[250]. Following on from the unexpected results obtained with the mRNA microarray, the main aim of the research presented in this chapter was to clarify the influence of BG ionic dissolution products on the mevalonate and sterol/steroid biosynthesis pathways in hMSCs with a special emphasis on the role of strontium.

In summary, the results corroborate a role of BG ionic dissolution products in the regulation of the mevalonate and sterol/steroid biosynthesis pathways. Furthermore, there is evidence that the incorporation of strontium into 45S5 BG was pivotal for this regulatory function in the conditions of the experiments presented in this chapter. All BG dissolution products had an influence on the gene expression of enzymes involved in the mevalonate and sterol/steroid biosynthesis pathways with Sr100 further increasing the expression levels compared to Sr0. Interestingly, no up-regulation of isoprenoid pathway-associated genes was observed for growth medium supplemented with $SrCl_2$. A concerted action of strontium ions together with the other bioactive ion species derived from BG may be causative; however, this cannot be deduced from the results presented in this study. Either the other bioactive ions fulfil a supporting but in itself insufficient role to induce the observed changes or strontium released from BGs acts differently to the strontium supplemented as $SrCl_2$. To dissect this issue further, medium could have been supplemented with different ion combinations derived from BGs (Si, Ca, Sr and P).

In line with the gene expression analysis, protein levels of isoprenoid biosynthesis pathway-associated enzymes were increased by treatment with BG-conditioned medium compared to growth medium. The obtained results for FDFT1 and GGPS1 expression showed a significant up-regulation of protein expression in BG-treated cells. Treatment with Sr100-conditioned medium significantly enhanced GGPS1 protein expression further compared to the Sr0 group. Thus, BGs were shown to regulate both sterol- and non-sterol-committed branches of the isoprenoid pathway. HMGCS1 abundance was comparable between all conditions and did not seem to be influenced by BG ion dissolution products. Thus, while the effect of bioactive glass dissolution products was marked, the influence of strontium ions was less pronounced compared to the changes on gene expression level. This likely owes to the fact that differences observed on gene expression level do not translate into protein level in a linear manner. Protein expression is not only regulated by the transcription rate, but

complex post-transcriptional mechanisms control the translation of mRNAs into proteins. Another explanation may be that In-Cell Western analysis was not sensitive enough to detect subtle changes in protein concentration. Overall, differences observed at the protein level are expected to be less marked compared to the gene level, thus making it more difficult to detect differential expression levels. The up-regulation of enzymes associated with the mevalonate and sterol/steroid biosynthesis pathways on gene and protein levels was likely indicative of changes in cellular content of cholesterol and its downstream products.

Continuing from these findings, the influence of treatment with strontium-containing bioactive glasses on cholesterol and lipid raft content of the cellular plasma membrane was studied. Indeed, the changes in gene and protein expression levels translated into an increase in membranous cholesterol content. The increase in cholesterol abundance in the conditions of the work described in this chapter depended on the presence of strontium within the bioactive glass composition as significantly higher values for filipin III staining intensity were obtained in Sr100-treated hMSCs compared to Sr0 and growth medium only. Cholesterol plays an important role in lipid raft assembly and maintenance. Therefore, it was hypothesised that lipid raft abundance might be altered by treatment with strontium-containing BG-conditioned medium. Lipid rafts are particularly interesting in this context as they are important signalling platforms mediating the signal transduction across the cell membrane. Changes in lipid raft properties may thus induce possible modifications in cell signalling. Supporting the hypothesis that strontium-containing bioactive glasses may mediate their effects via changes in lipid raft-dependent signalling, the staining for lipid rafts was found to be significantly increased in hMSCs exposed to Sr100 dissolution products compared to Sr0 and growth medium. Taken together with the results obtained for cholesterol, there is evidence that strontium within the BG dissolution products influenced the composition of the plasma membrane of hMSCs. Considering the importance of lipid rafts for cellular signalling events and cell-cell communication, the impact of such changes can be manifold and may influence cell-biomaterial interactions.

Further work by Autefage *et al.* revealed an increase in phosphorylated myosin II light chain (pMLC) content in Sr10 and Sr100-treated hMSCs[250]. Lipid-raft associated signalling cascades are regulated through interactions with the cellular actin cytoskeleton[294]. pMLC is one of the proteins responsible for the communication between lipid rafts and the actin/myosin meshwork[150]. Therefore, the hypothesis that strontium-substituted bioactive glasses influence cell signalling processes at the cell membrane was further strengthened. In this context, the observed increase in GGPS1 protein is particularly interesting as GGPS1 is responsible for the prenylation of a group of small molecules called GTPases. GTPases govern the interaction between lipid rafts and the cytoskeleton which can further modulate signalling cascades[294]. Changes in the actin/myosin meshwork were previously linked to hMSC commitment[148, 150]. Whether ions released from BGs influence the pre-commitment of hMSCs by favouring the differentiation towards the osteogenic lineage needs to be further investigated. In this context, however, strontium incorporation did not influence the outcome. In terms of functional

outcome, the work presented in this chapter was focussed on the plasma membrane. Yet, the isoprenoid biosynthesis pathway with its numerous products can influence cell behaviour through multiple pathways which all likely influence the response of cells to strontium-containing biomaterials.

At the onset of the study it had been decided to culture the hMSCs in hMSC growth medium and not like in the majority of studies in osteogenic medium. Osteogenic medium pushes the cells towards the osteogenic lineage using a number of (growth) factors, making it difficult to dissect specifically the effects of the BG ionic dissolution products. On the other hand, hMSC growth medium maintains the stem cell-like character of the hMSCs possibly overruling any osteogenic effects of the ions. Therefore rather subtle changes in the expression of differentiation markers were likely. Considering the variability between samples, small changes in expression values are frequently not significant by qPCR analysis. To confirm these preliminary results and gain statistical power further independent repeats need to be performed. Strontium is widely accepted to enhance osteogenic differentiation of hMSCs; however, most studies are conducted in osteogenic medium. In an interesting study by Santoclides-Romero *et al.* hMSCs were cultured in 50% and 100% strontium-substituted 45S5 BG-conditioned medium in the presence or absence of osteogenic supplements[288]. Gene expression analysis of key osteogenic markers revealed different patterns depending on the presence or absence of osteogenic supplements. In the absence of osteogenic factors, *RUNX2* and *COL1A1* expression were up-regulated after 3 and 6 days of culture by all glass compositions (Sr0, Sr50 and Sr100) which is in agreement with the observations described in this chapter. Thus, a longer culture period may have led to significant differences in *RUNX2* regulation in presence of (strontium-containing) bioactive glass dissolution products compared to control. Notably, in the study by Santoclides-Romero *et al.* Sr50 and Sr100-conditioned medium further enhanced the gene expression of *Bmp2*, *Alpl* and *Spp1* (osteopontin) compared to Sr0 only in presence of osteogenic factors[288]. A possible hypothesis to explain this phenomenon may be that MSCs require a certain degree of pre-commitment to the osteogenic lineage to be further stimulated by strontium. Strontium signalling can be divided into calcium sensitive receptor (CaSR)-dependent and CaSR independent signalling mechanisms. As strontium shares many characteristics with calcium it is considered to be able to cross-activate the CaSR. CaSR expression has been confirmed in human osteoblasts and osteoclasts[295, 296]. In the regulation of osteoblast development and bone formation, CaSR signalling has been shown to serve a pivotal function[297]. Yet, there is contradicting literature concerning the presence of CaSR in MSCs. While CaSR expression has been detected in equine umbilical cord MSCs[298], another study has highlighted that CaSR expression in hMSCs is strongly depended upon the culture conditions[299]. Strikingly, hMSCs that were cultured in medium lacking FBS supplementation did not express CaSR even though the medium was supplemented with human platelet lysate instead. Therefore, the expression of CaSR in the hMSCs used for the experiments presented in this chapter is not guaranteed.

Interestingly, it has been suggested that the isoprenoid pathway with its intermediates is crucial for proper differentiation of MSCs into osteoblasts[300]. Specifically, oxysterols have been identified as

potent osteoinductive molecules which, among other properties, synergistically enhance ALP activity together with BMP2 and BMP7[301, 302]. In agreement, it has been reported that cholesterol treatment of murine MSCs increased mRNA and protein levels of osteogenic lineage markers, ALP activity and number of mineralised nodules in presence of osteogenic supplements[303]. Recently, it was reported that phosphoinositide 3-kinase (PI3K)/Akt signalling was required for hMSC osteogenesis *in vitro*[304]. Baker *et al.* further showed that the localisation of Akt in cholesterol-rich membrane rafts was required for Akt activation and hMSC lineage commitment. In this context, SrR has been shown to increase Akt phosphorylation and thus activation in primary human osteoblasts[179]. Taken together, several links between metabolites of the mevalonate and sterol/steroid biosynthesis pathways and osteogenic differentiation of MSCs have been established possibly connecting the osteogenic effects of strontium-containing biomaterials with the results obtained by the microarray and the work presented in this chapter.

2.4.1 Limitations

A disadvantage of the bioactive glass system used for the experiments described in this chapter was that a 100% strontium substitution for calcium resulted in lower calcium concentrations in the Sr100-conditioned medium (approximately 32.2 mg/L (Ca^{2+})) compared to all other conditions (around 68.57 mg/L (Ca^{2+})). Thus, the results obtained with Sr100-conditioned medium could have been due to a lower calcium level rather than the presence of strontium. To fully rule a calcium concentration-dependent effect out, calcium ions could have been supplemented to the Sr100-conditioned medium to compensate for the reduced calcium concentration. However, the addition of calcium ions may have led to precipitation of CaP and thus may not have increased the overall calcium concentration in the solution. Alternatively, a bioactive glass with a strontium substitution between 10% and 100% (e.g. 50%) that allows the maintenance of the calcium level whilst releasing a similar amount of strontium as Sr100 could have been used to ascertain a strontium-dependent effect.

Furthermore, Sr0-conditioned medium supplemented with 1 mM Sr^{2+} would have been an interesting additional condition to assess if cells treated with Sr100-conditioned medium behaved comparable to cells treated with strontium supplemented Sr0-conditioned medium. By supplementing the amount of strontium that was released from Sr100 into the medium, it would have been possible to ascertain the role of strontium within the mix of other ion release products in the up-regulation of the isoprenoid pathway and its downstream mediators. As the concentration of ions in the medium is based on an equilibrium, it would have been important to assess possible modifications in ion contents for calcium, phosphorous and silicon as a result of the addition of an external source of strontium.

As previously discussed, the choice to use stem cell growth medium for the experiments likely had an effect on the outcome of the gene expression profiling. It would have been interesting to repeat the experiment in osteogenic conditions to investigate whether the up-regulation of the isoprenoid

pathway was still observed in presence of pro-osteogenic factors.

To better understand the influence of BG-conditioned medium on hMSC (pre-)commitment, the gene expression of other markers, apart from *PPARG* and *RUNX2*, such as *COL1A1* would be interesting to assess. Since no big changes in gene expression were observed with the time points chosen for this study, using later time points instead would allow to better assess a differential regulation. Additionally, it would have been preferable to include positive controls for the studied lineages to establish what expression levels can be expected at the respective time points. Apart from gene expression analysis, performing functional assays such as ALP or Alizarin red staining at later time points would complement the assessment of hMSC differentiation in presence of strontium-containing bioactive glasses.

2.5 Conclusion

In conclusion, the work described in this chapter demonstrated how simple ion incorporation can have a profound impact on the global cell response to a biomaterial. Replacing 100% of the calcium with strontium in the 45S5 BG composition significantly up-regulated the gene expression of isoprenoid pathway-associated genes, as well as increased the cholesterol and lipid raft contents in the cellular plasma membrane of hMSCs compared to un-substituted 45S5 BG. A clear understanding of cell-biomaterial interactions and especially of how cells respond to certain cues is essential for the design of scaffolds for tissue engineering purposes. The previously undescribed influence of strontium-containing bioactive glass dissolution products on the isoprenoid pathway in hMSCs was uncovered by using an unbiased "global" approach as opposed to an analysis limited to a desired or expected outcome. This study exemplified how biomaterials can affect cell behaviour via unexpected mechanisms opening up possible future avenues of investigation.

CHAPTER 3

Strontium and Magnesium-containing Bioactive Glasses for Osteochondral Repair

(*Some of the work in this chapter is in preparation for publication in "The composition of the ionic environment differentially affects hMSC chondrogenesis" by Littmann E, Autefage H, Solanki AK, You A, Jones JR, Alini M, Peroglio M and Stevens MM*)

All data presented in this chapter were collected by me unless explicitly stated otherwise.

3.1 Introduction

Classically, bioactive glasses have been used for bone regeneration applications. However, bioactive glasses are increasingly recognised as versatile biomaterials not only for hard but also for soft tissue repair as reviewed by Miguez-Pacheco *et al.* and Baino *et al.*[305, 306]. This trend can be, at least in part, attributed to the influence of bioactive glass dissolution products on cells and eventually tissue regeneration.

Stemming from their well-described osteconductive/osteoinductive properties, bioactive glasses have been suggested as bone-facing component of multi-layered scaffolds for the repair of osteochondral defects. Yet, through the release of ions from the bioactive glasses, not only the subchondral bone but also the cartilage layer may benefit from rationally designed bioactive glass compositions. In this chapter, the influence of bioactive glass dissolution products on hMSC chondrogenesis in a pellet culture model was assessed. While there are numerous studies investigating the effect of such bioactive glass dissolution products on the osteogenic lineage commitment of hMSCs, data on hMSC chondrogenic differentiation is scarce. In particular, the question was pursued whether the modification of bioactive glass compositions would affect cell behaviour. To test this hypothesis, two compositions were chosen; the classic 45S5 BG (Comp1) and a second composition designed and prepared in collaboration with Professor Julian Jones's group at Imperial College London. The second composition, referred to as Comp2, was initially designed to obtain a melt-derived bioactive glass that can be used for the fabrication of 3D porous scaffolds. The composition of Comp2 contains magnesium which has been shown to enhance cartilage repair *in vivo*. Both compositions were modified by strontium incorporation. There was a special interest in strontium as clinical studies suggested that SrR attenuated the progression of OA and concomitant cartilage degeneration[307, 308].

3.1.1 The use of bioactive glasses for cartilage regeneration

To date, a limited number of studies have evaluated the effect of bioactive glasses on cartilage repair. Early studies demonstrated that bioactive glass discs supported the attachment and proliferation of foetal rat chondrocytes *in vitro*[309] and the growth of newly formed cartilage with mostly hyaline-like features in osteochondral defects in the rabbit femur[310]. Yet, considering the latter study, empty control defects healed as well, limiting the interpretation of the data provided. Aho *et al.* introduced osteochondral defects in the knee joint of the distal femur of rabbits to investigate the performance of injectable composites of bioactive glass and poly(ε-caprolactone-co-D,L-lactide)[311]. Newly formed cartilaginous tissue covered up to 82% of filled defects and had a higher quality than the cartilage found in empty controls. Interestingly, mature chondrocytes were localised in close proximity to the composite surface. Yet, newly formed bone and fat cells were found in the nascent cartilage layer as well, warranting further evaluation. Similar to the results obtained in animal models, human chondrocytes were shown to attach to and proliferate on 45S5 BG discs[312]. The human chondrocytes proceeded to

form cartilage nodules accompanied by positive type II collagen staining indicative of re-differentiation as hypothesised by the authors. In patients there is evidence for the growth of cartilage with hyaline-like features on top of bioactive glass[313].

Several studies have evaluated the use of bioactive glasses as bone substrate of bi- or multi-layered osteochondral scaffolds. Classically, such scaffolds consist of a cartilage-facing layer, usually made of a cell-seeded hydrogel, and a bone-facing component. In an interesting study, Bal *et al.* assessed the influence of the subchondral support material of bi-layered scaffolds on the repair of a critical sized ostechondral defect in the trochlear groove and medial condyle of rabbits[314]. To that end, a polyethylenglycol (PEG) hydrogel was attached to a porous cylinder consisting of allograft bone, 13-93 bioactive glass (13-93 BG) or porous tantalum metal. The PEG hydrogel was either acellular or seeded with chondrogenic pre-differentiated MSCs. After 6 weeks, cell-seeded hydrogels connected to either allograft or 13-93 BG constructs promoted a significantly greater formation of cartilage-like matrix in the defects than all other groups. Assessment of the quality of the newly formed tissue by immunohistochemical detection of type I and type II collagen showed that the matrix formed on top of cell-seeded hydrogels joined to 13-93 BG resembled normal hyaline cartilage most closely compared to all other conditions. Thus, in the conditions used for the study, the nature of the subchondral material affected the repair of the chondral portion of the defect. Overall, 13-93 BG outperformed the other bone-facing components with regards to cartilage repair. The authors hypothesised that the enhanced cartilage-like tissue regeneration in presence of 13-93 BG was linked to suitable mechanical properties. In a subsequent pilot study, a bovine chondrocyte seeded agarose layer was joined with a 13-93 BG subchondral substrate to obtain a bi-layered scaffold for osteochondral repair[315]. After 42 days of culture the sGAG content of the cell-seeded agarose layer connected to 13-93 BG appeared higher than the cell-seeded agarose layer only control, however, the difference was not significant. The authors went on to investigate whether ions released from 13-93 BG constructs had an influence on the chondrocyte-seeded agarose layer[315]. A 13-93 BG cylinder was placed next to the chondrocyte-seeded agarose layer throughout the culture period (days 0 - 42), at the beginning of the culture period (days 0 - 14) or at the end of the culture period (days 28 - 42). Interestingly, the most favourable results, both in terms of sGAG and collagen production as well as mechanical properties, were obtained when the agarose layer was cultured adjacent to 13-93 BG constructs at the end of the culture period (days 28 - 42). However, also the other exposure protocols had a tendency to improve extracellular matrix production and mechanical properties compared to the untreated control alluding to a pronounced role of bioactive dissolution products.

Bioactive glasses have also been combined with polymers to form composite materials with improved bioactivity for osteochondral applications. Jiang *et al.* used sintered polylactide-co-glycolide (PLGA)/45S5 BG composite microspheres in combination with agarose hydrogel to create stratified scaffolds[316]. The interface region of the PLGA/45S5 BG composite with the agarose gel was designed to promote the formation of a stable calcified cartilage layer. As outlined by the authors, a functional

and stable calcified cartilage layer functions as physical barrier to prevent bony ingrowth and is key to lasting cartilage repair. Interestingly, the incorporation of 45S5 BG particles increased both the ALP activity and sGAG synthesis of chondrocytes significantly when the cells were seeded directly on the PLGA/45S5 BG composite compared to the PLGA only control[316]. When the whole stratified construct was seeded with chondrocytes and osteoblasts respectively and cultured for 20 days, mineralisation was apparent in the interface and bone-facing region in a 45S5 BG-dependent manner suggesting that the presence of bioactive glass facilitated the deposition of mineral.

A recent study modified polylactide-based knitted and rolled 3D scaffolds with chitosan and/or 13-93 BG[317]. Chondrogenic lineage commitment of adipose tissue-derived hMSCs was mildly enhanced both in terms of sGAG production and cartilage marker gene expression in presence of 13-93 BG when compared to the plain polylactide control but was inferior to chitosan modified scaffolds. Interestingly, the presence of 13-93 BG had no significant effect on osteogenic marker expression suggesting a low or absent osteostimulative activity on the adipose tissue derived hMSCs in the conditions used for the study.

In summary, previous studies demonstrate that bioactive glasses are suitable substrates for chondrocyte culture *in vitro* and are able to enhance cartilage regeneration *in vivo*. Furthermore, bioactive glasses have been recognised as attractive bone-substrate of multi-layered osteochondral scaffolds and there is one study reporting an influence of bioactive glass dissolution products on cartilaginous ECM production.

3.1.2 Mechanisms by which therapeutic ions influence cartilage repair

Thus, while bioactive glasses have been described as suitable substrates for chondrocyte culture and have been shown to support chondrogenic differentiation of MSCs, little is known about the effects of bioactive glass dissolution products. Apart from the study by Jayabalan *et al.* there is only one other study that indirectly investigated and supported a modulation of chondrocyte behaviour by bioactive glass dissolution products. Here, using a medium composition facilitating endochondral ossification, rat nasal chondrocytes were cultured in presence of either 45S5 BG or the less reactive 60S BG particles[318]. While some of the cells in culture were in direct contact with the bioactive glass particles, the majority was likely only affected by the ions released from the particles. In presence of 45S5 BG, the gene expression of *RUNX2*, *Indian hedgehog* and *type X collagen (COL10A1)* were up-regulated which is indicative of chondrocyte hypertrophic differentiation. In keeping, ALP activity was enhanced in presence of 45S5 BG compared to the 60S BG control. Unfortunately, the authors neither measured the ion release from the particles nor the pH of the medium rendering a comparison between the two groups difficult.

While bioactive ions in general have the ability to modulate cell behaviour, here, evaluating the

role of strontium and magnesium was deemed particularly interesting. Both ions have individually been shown to improve cartilage extracellular matrix production *in vitro* and cartilage repair *in vivo*.

3.1.2.1 The impact of strontium on cartilage repair

Compelled by the suggested dual action of SrR on bone remodelling, Henrotin *et al.* studied the influence of SrR treatment on chondrocytes isolated from either healthy or osteoarthritic donors[319]. SrR (0.5-1 mM) significantly increased proteoglycan secretion from normal and osteoarthritic human chondrocyte pellets as well as proteoglycan accumulation in healthy chondrocyte pellets after 72 h compared to the control. Treatment with 2 mM $SrCl_2$ enhanced proteoglycan secretion to a similar degree suggesting that the effects were independent of ranelic acid. Yet, also treatment with 1 mM CaR increased proteoglycan secretion. Interestingly, CaR but not SrR or $SrCl_2$ enhanced the activity of MMP3, a proteinase linked to cartilage degeneration and OA. Therefore, the authors argued that SrR was a more suitable agent to enhance cartilage repair. When total proteoglycan production was considered all tested substances (SrR, CaR, $SrCl_2$) had significant stimulatory effects on normal and OA chondrocytes. Furthermore, SrR (1 mM) and $SrCl_2$ (2 mM) enhanced production of sGAG compared to control. Unfortunately, CaR was not included in this experiment.

Following on from this study, Wang *et al.* sought to investigate further how SrR influenced chondrocyte behaviour[320]. Therefore, rat chondrocytes were exposed to SrR at different concentrations (1 mM to 5 mM) for up to 72 h. Type II collagen gene expression was significantly increased on all tested time points (24 h, 48 h, 72 h) in presence of 3 mM and 5mM SrR. SrR at both concentrations similarly enhanced insulin growth factor I (IGF-I) expression after 24 h and 48 h of culture but significantly decreased IGF-I levels after 72 h compared to control. Gene expression of both type II collagen and IGF-I was not affected by culture with 1 mM SrR, indicating a dose-dependent effect. MMP13, a major type II collagenase, was down-regulated at all time points by all SrR concentrations. Considering that MMP13 was found to be up-regulated in OA, this result merits special attention. Quantification of the respective protein levels showed similar trends as on the gene level. Analysis of hydroxyproline abundance as indicator of collagen synthesis revealed a significant increase in a strontium dose-dependent manner after 72 h for all concentrations. Considering the promising results obtained with SrR treatment of chondrocyte cultures, Okita *et al.* assessed the effect of strontium supplementation on adipose-derived dedifferentiated fat cells (DFAT) and a hMSC cell line[321]. DFAT cells were cultured in chondrogenic medium supplemented with either 0.15 mM $SrCl_2$ or 1.5 mM $SrCl_2$. After 14 days in monolayer culture, 1.5 mM $SrCl_2$ increased Alcian blue staining as marker for chondrogenic lineage commitment in DFAT cells. Strontium supplementation had no effect on the hMSC cell line; however, as Alcian blue staining was nearly absent, the monolayer culture model might not have been suitable to assess chondrogenesis in hMSCs. Gene expression analysis in DFAT cells showed that 1.5 mM $SrCl_2$ seemed to induce type II collagen, while hypertrophic and osteogenic markers were unchanged compared to control. Interestingly, inhibition of calcium sensitive receptor

(CaSR) reduced Alcian blue staining, indicating a function in chondrogenic differentiation.

While there are only a number of *in vitro* studies on the influence of strontium on chondrocytes and MSC chondrogenesis available, clinical data provide compelling evidence of SrR's beneficial effect on cartilage (repair). Unfortunately, most studies were primarily focused on SrR treatment for osteoporosis and therefore did not necessarily evaluate relevant parameters for cartilage repair nor represented an unbiased patient group. Carboxy-terminal telopeptides of type II collagen (CTX II) are a biomarker for cartilage turnover and elevated CTX II levels have been associated with cartilage degeneration[322]. The CTX II levels in urine samples of osteoporotic women treated with SrR or placebo were measured over a 3 year period[322]. SrR reduced the CTX II level as early as 3 months after treatment commenced by approximately 20% compared to the start of the study and the placebo control. The CTX II level remained significantly lower than the placebo group throughout the measurement period. Since the main focus of the study had been on osteoporosis, OA parameters were not assessed so that no direct conclusions on the effect of SrR on OA (progression) could be drawn. Yet, a *post-hoc* analysis of two large trials performed on 1105 women with osteoporosis and radiological spinal OA was able to shed some light on the impact of SrR on OA progression[323]. Indeed, SrR was found to attenuate the progression of radiographic features of spinal OA in osteoporotic women after a three year treatment period compared to placebo[323]. A large clinical double blind placebo controlled study further underscored a beneficial effect of SrR on OA. Here, patients suffering from knee OA were treated with either 1 g/day or 2 g/day SrR[308]. After three years, treatment with SrR attenuated clinical signs for OA such as joint space narrowing and there were fewer progressors in the SrR patient cohort as identified by radiology. In line with previous findings, patients treated with SrR had significantly lower levels of CTX II in their urine. Furthermore, it was found that knee OA patients treated with SrR had fewer bone marrow lesions and decreased cartilage volume loss compared with the placebo group[307].

Apart from clinical trials, *in vivo* data from animal models further underscores an effect of SrR on cartilage. Using an experimental OA model in dogs, Pelletier *et al.* investigated the influence of treatment with SrR for 12 weeks[324]. A significant, SrR dose-dependent, decrease in lesion depth and size was observed. In cartilage, gene expression of key catabolic factors (MMPs) associated with cartilage degeneration were significantly decreased by the highest tested SrR dose (75 mg/kg). As previously observed, SrR reduced the level of CTX II secretion. A study using an experimental OA rat model obtained similar results[325]. SrR attenuated cartilage lesions compared to the untreated OA control and reduced chondrocyte apoptosis. Furthermore, mechanical properties of the subchondral bone were improved suggesting that SrR had an effect on both, cartilage and the underlying bone. Interestingly, SrR enhanced the study parameters at a relative high dose (1800 mg/kg) while the lower dose (625 mg/kg) had little or no effect. Considering both studies using OA animal models, there seems to be a threshold for SrR as beneficial effects on cartilage/subchondral bone were only seen at higher concentrations. Yet, the studies were relatively short with 12[324] and 6 weeks[325] while the clinical studies

lasted at least 3 years. SrR likely needs to reach a certain serum level to exert its action. Therefore, shorter studies may require higher doses to obtain statistically significant results.

3.1.2.2 The impact of magnesium on cartilage repair

Magnesium is an alkaline earth metal and an essential element in the human body fulfilling numerous intracellular functions. In vertebrates, magnesium is the fourth most common cation with 50 - 60% bound as substitute in the mineral component of bone. On an intracellular level, magnesium is the second most abundant cation after potassium and serves as cofactor in more than 300 enzymatic reactions[326]. Magnesium deficiency or hypomagnesaemia can affect heart function and the central nervous system and lead to clinical symptoms such as cardiac arrhythmia and depression.

Notably, magnesium availability appears to be crucial for proper cartilage development as a magnesium-deficient diet during postnatal development of rats was shown to cause cartilage lesions[327]. In addition, a magnesium deficient diet altered the morphology of articular cartilage and reduced the proteoglycan content in juvenile rats after 6 months of treatment[328]. Interestingly, immunolocalisation of SOX9 was likewise lower in magnesium-deficient rats compared to the control group and might be the underlying reason for the observed changes in morphology as hypothesised by the authors[328]. Further evidence suggests that magnesium has a protective effect on cartilage growth and repair beyond postnatal development. Intra-articular injections of magnesium sulphate ($MgSO_4$) were demonstrated to reduce OA and alleviate nociception in an experimental OA model in rats[329]. Furthermore, OA-induced chondrocyte apoptosis was attenuated through a mechanism likely linked to inhibition of the N-methyl-D-aspartate receptor (NMDA) receptor by magnesium ions. *In vitro* experiments using human articular chondrocytes showed that 10 mM $MgSO_4$ enhanced proliferation significantly while 20 mM decreased cell number over time[330]. Supplementation of 10 mM $MgSO_4$ to control medium, however, did not enhance sGAG production. Similarly, sGAG synthesis by goat costal fibrochondrocytes was not affected by magnesium ion concentrations of up to 20 mM. Interestingly, 20 mM $MgSO_4$ but not 20 mM $MgCl_2$ significantly increased the type II /type I collagen ratio compared to control. This suggests at least a supporting role of the sulphate anion. Duo *et al.* assessed the response of porcine chondrocytes, either in monolayer culture or encapsulated in alginate hydrogel, to magnesium microspheres[331]. The microspheres degraded over time in the medium, releasing magnesium ions into their surroundings. This method was chosen to mimic fluctuating magnesium concentrations during degradation of magnesium alloys *in vivo*. Assessment of porcine chondrocyte metabolic activity showed that 20 mM $MgCl_2$ caused a significant decrease in monolayer culture but not in 3D possibly indicating that diffusion of magnesium ions into the alginate hydrogel was limited. In monolayer culture, the addition of 250 µg/mL magnesium microspheres to the medium (peak concentration of magnesium ions 10 mM on day 3) or supplementation of 5 mM or 10 mM $MgCl_2$ significantly enhanced sGAG secretion compared to control on day 14. In contrast, high concentrations of extracellular magnesium (20 mM) decreased sGAG release significantly. In 3D alginate culture,

magnesium ions significantly decreased sGAG production at concentrations of 10 mM and 20 mM, however, sGAG abundance appeared overall low. Gene expression analysis of chondrogenic markers did not indicate magnesium-concentration dependent changes in porcine chondrocytes. Yet, also a reduction in GAG production and chondrogenic marker expression has been observed in the prechondrogenic cell line ATDC5 after treatment with 4.2 mM $MgCl_2$[332]. In contrast, calcium supplementation increased GAG accumulation and chondrogenic marker expression and this effect was abrogated by addition of magnesium. In the same study, the supplementation of 4.2 mM $MgCl_2$ to culture medium containing excess calcium inhibited calcium-induced matrix-mineralisation. This is particularly interesting for cartilage tissue engineering applications as mineralization is generally not desired in cartilaginous tissue.

Overall, *in vitro* experiments using chondrocytes, either in monolayer or 3D culture, have not been able to offer an insight into the beneficial effects of magnesium administration on cartilage (repair) *in vivo*. Thus, the influence of magnesium observed *in vivo* could be due to indirect alterations in cell-cell or cell-material interactions that are not easily replicated by *in vitro* experiments. Magnesium ions are known to enhance the binding of integrins to their respective ligands. Integrins are heterodimeric transmembrane receptors responsible for cell-cell or cell-ECM interactions that bind to specific amino acid motifs such as RGD[333]. Upon ligand binding, a complex process is initiated involving the recruitment of the cellular actin cytoskeleton to form focal adhesions. Such focal adhesions, together with growth factor receptors, are thought to orchestrate complex signalling cascades affecting cell growth and differentiation[333]. Indeed, several studies have linked changes in MSC behaviour in response to magnesium ions to the binding affinity and expression of integrins.

The proliferation of bone-marrow derived hMSCs was found to be increased in response to treatment with 2.5 - 10 mM magnesium ions after 72 h[334]. In the same study, the gene expression of integrin subunits α2 and α3 but not β1 was assessed after exposure to 2.5 - 10 mM magnesium ions for up to 4 h and found to be up-regulated. When integrin subunits α2 and α3 were knocked-down by siRNAs, no magnesium-associated increase in hMSC proliferation was observed indicating that α2 and α3 integrin function was crucial. A study by Shimaya *et al*. investigated the effect of magnesium ions on hMSC chondrogenesis and adherence to osteochondral defects[335]. Medium supplementation with 5 mM magnesium enhanced sGAG production by synovial fluid-derived hMSC in 3D pellet culture[335]. The same study demonstrated that synovial fluid-derived hMSCs adhered better to osteochondral defects *in vitro* and *in vivo* in presence of magnesium ions. These magnesium-dependent effects were likely mediated through integrins as neutralising antibodies to integrins α2 and/or β1 reduced matrix accumulation and adherence to the control level. In line with the previous studies, extracts prepared from magnesium alloys were found to enhanced the proliferation of hMSCs[336]. When magnesium but not the alloy extracts was added to chondrogenic medium, hMSC chondrogenesis tended to be enhanced compared to control as measured by aggrecan staining after 21 days of culture.

In summary, treatment with magnesium ions did not negatively affect chondrocyte viability or proliferation up to concentrations of 20 mM. The effect of magnesium ions on chondrocyte extracellular matrix production is less clear. In contrast, magnesium ions appear to increase MSC proliferation as well as chondrogenesis in a process likely mediated through integrins.

3.1.3 Choice of bioactive glass compositions

Thus far, the influence of bioactive glass (dissolution products) on MSC chondrogenesis has been studied mainly with a focus on the classic compositions 45S5 and 13-39. In this chapter, it was sought to investigate whether differences in the glass composition and thus nature of the respective glass extracts affected hMSC chondrogenesis with a particular emphasis on strontium. There was a particular interest in the novel composition 44.5 mol% SiO_2, 17.8 mol% CaO, 17.8 mol% SrO, 4.0 mol% Na_2O, 4.0 mol% K_2O, 7.5 mol% MgO, 4.5 mol% P_2O_5 (herein termed Comp2-Sr) which had previously been designed in a collaboration between Prof. Stevens's and Prof. Jones's research groups. The composition was designed to allow 3D scaffold formation whilst releasing strontium in a biologically relevant range. A 50% substitution of strontium for calcium was shown to fulfil both requirements. An *in vivo* study using an ovine model demonstrated that Comp2-Sr 3D scaffolds supported osteogenesis and formation of high quality newly-formed bone when compared to 45S5 BG particles (Autefage *et al.*, paper under review). Based on these findings, Comp2-Sr might represent an interesting material for the bone-facing layer of osteochondral scaffolds. To assess the role of strontium within the ion release products, the same composition without strontium incorporation was included in the study (44.5 mol% SiO_2, 35.6 mol% CaO, 4.0 mol% Na_2O, 4.0 mol% K_2O, 7.5 mol% MgO, 4.5 mol% P_2O_5, herein termed Comp2-Ca). As the 45S5 composition remains the most widely used bioactive glass in the clinic, it was added as an additional condition (herein referred to as Comp1-Ca). To analyse if the presence of strontium ions had an effect on hMSC chondrogenesis that was independent from the other dissolution products, 50% of the calcium in the 45S5 BG composition were replaced by strontium resulting in a fourth composition, termed Comp1-Sr. A substitution of 50% of the calcium was chosen to be consistent with Comp2-Sr. Bioactive glass-free medium was added as a reference for the chondrogenic differentiation potential of the hMSCs in standard conditions and to assess the general effect of the bioactive glass dissolution products.

3.1.4 Aims and objectives

Taken together, both magnesium and strontium ions appear to have a beneficial influence on cartilage maintenance and repair especially with respect to *in vivo* data from previous studies. Furthermore, bioactive glasses have been identified as attractive bone substrate for multi-layered osteochondral scaffolds and their release products seem to influence cartilage-like ECM production. In light of these findings, it seems important to study if the composition of bioactive glasses and their extracts

respectively, differentially affect chondrogenic lineage commitment of MSCs. In particular, strontium- and/or magnesium-containing bioactive glasses merit evaluation for treatment of osteochondral defects.

The aim of the work presented in this chapter was to identify bioactive glass compositions with a beneficial effect on hMSC chondrogenic lineage commitment, with a special emphasis on the impact of strontium incorporation. The objectives were to:

- Assess chondrogenic differentiation of hMSCs in presence of bioactive glass extracts derived from two different bioactive glass base compositions;
- Evaluate if incorporation of strontium into bioactive glass enhanced chondrogenic differentiation.

3.2 Materials & Methods

3.2.1 Glass synthesis

To evaluate the impact of different bioactive glass compositions on hMSC chondrogenic differentiation and cartilaginous tissue formation, the classic 45S5 BG composition, which will be referred to as Comp1-Ca (46.1 mol% SiO_2, 26.9 mol% CaO, 24.4 mol% Na_2O, 2.6 mol% P_2O_5), and a novel glass composition (Comp2-Ca) (44.5 mol% SiO_2, 35.6 mol% CaO, 4.0 mol% Na_2O, 4.0 mol% K_2O, 7.5 mol% MgO, 4.5 mol% P_2O_5) were chosen (Table 3.1). Strontium was incorporated into both compositions by replacing 50% of the calcium on a molar basis resulting in a strontium content of 13.45 mol% and 17.80 mol%, respectively (Table 3.1). The strontium-containing compositions were termed Comp1-Sr and Comp2-Sr accordingly. The bioactive glasses were prepared using the precursor materials SiO_2 (Prince Minerals, UK), Na_2CO_3, $CaCO_3$, $SrCO_3$, K_2O, MgO and P_2O_5, (all Sigma-Aldrich, UK). The precursor materials were mixed, melted at 1,400°C in a platinum-gold crucible for 90 min and quenched into deionised water. The resulting glass frit was allowed to dry between 120 - 150°C over-night before milling in a planetary ball mill at 500rpm for 5 min. Glass powder was sieved to <38 µm and stored in a desiccator. A particle size of <38 µm is widely used for the preparation of bioactive glass-conditioned medium[128, 184, 337]. Glass synthesis and processing were kindly performed by Miss Anu Solanki and Dr. Hok Man Tang.

Table 3.1: Glass compositions (mol%).

Glass	SiO_2	Na_2O	CaO	SrO	K_2O	MgO	P_2O_5
Comp1-Ca	46.13	24.36	26.9	/	/	/	2.6
Comp1-Sr	46.13	24.36	13.45	13.45	/	/	2.6
Comp2-Ca	44.50	4.00	35.6	/	4.00	7.50	4.50
Comp2-Sr	44.50	4.00	17.80	17.80	4.00	7.50	4.50

3.2.2 Preparation of bioactive glass-conditioned medium

Bioactive glass-conditioned (BG-conditioned) medium was obtained by incubating 1.5 mg/mL of bioactive glass particles in high glucose Dulbecco's Modified Eagle Medium (DMEM) (Gibco®, UK) containing 100 units (U)/mL penicillin and 100 µg/mL streptomycin (Gibco®, UK) as well as 20 mM (4-(2-hydroxyethyl)-1-piperazineethanesulfonic acid) (HEPES) (Gibco®, UK) under constant agitation at 37ºC for 4 h. The medium was subsequently passed through a 0.2 µm filter (Sartorius, UK) under sterile conditions to remove remaining bioactive glass particles. The BG-conditioned medium was

stored at 4°C. Following the standard operation procedure at AO Foundation Davos, HEPES buffer was added to the medium to improve the buffer capacity in order to allow a more stable pH, especially with respect to pellet culture in microcentrifuge tubes. In contrast to Chapter 2, high glucose DMEM medium was used as it is the gold standard medium for chondrogenic differentiation. Prior to treatment of cells, the medium was equilibrated in a cell culture incubator at 37°C/ 5% (v/v) CO_2 for at least 4 h or over-night. The elemental concentrations of calcium, phosphorus, silicon, magnesium and strontium in the conditioned medium were determined by ICP-OES using an iCAP6000 Series ICP spectrometer (Thermo Scientific, UK) on at least three independent samples. The ICP-OES was operated with the assistance of Miss A. Solanki.

The concentration of bioactive glass particles and the length of incubation had previously been optimised for the preparation of conditioned medium from glass particles with a diameter of <38 µm by members of the Stevens group[128, 184, 239]. For the glass compositions Comp1-Ca, Comp2-Ca and Comp2-Sr specifically, the optimisation was carried out by Dr. Hélène Autefage and Hortense Le Ferrand (published in the Master thesis of Hortense Le Ferrand "Cell response to complex osteochondral scaffold", Swiss Federal Institute of Technology Zurich and Imperial College London). Overall, the release profiles showed a stabilisation in ion concentration after 4 h of incubation in DMEM high glucose medium. A concentration of 1.5 mg/mL particles resulted in a similar concentration of ions in the medium after 4 h as incubating a 3D Comp2-Sr scaffold in medium for 24 h and was thus chosen for further experiments.

3.2.3 Cell culture

Bone marrow-derived human mesenchymal stem cells (hMSCs) were isolated from human bone marrow obtained from the Hospital of Davos, Switzerland after approval by the local ethical commission (KEK-ZH-NR: 2010-0444/0). The human bone marrow was harvested from the femoral heads of five patients. Commonly, MSCs are isolated from bone marrow aspirates from the iliac crest; yet, a previous study has demonstrated the osteogenic and chondrogenic differentiation potential of hMSCs harvested from femoral bone marrow[338]. After bone marrow homogenisation, hMSCs were isolated by Ficoll® gradient centrifugation and adherence to tissue culture plastic as previously described[339]. Isolation of hMSCs was performed by the permanent staff at AO Foundation Davos. The details for each donor are listed in Table 3.2 and a representative bright field image of donor #4 is shown in Figure 3.1. As the isolation of hMSCs is a routine procedure at AO Foundation Davos, only few donors are characterised by flow cytometry. To assure the right phenotype of the hMSCs used for experiments presented in this thesis, donor #4 was characterised by flow cytometry analysis as a representative for all donors. Donor #4 derived cells at passage 2 stained positive for the surface markers CD73, CD105, CD90, CD44 but were negative for the haematopoietic markers CD45, CD34 and CD14. On basis of this result, the isolated cells were deemed hMSCs. Flow cytometry analysis was performed

with the assistance of Dr. Jennifer Bara and Dr. Ursula Menzel (both AO Foundation Davos).

Cells were expanded in Minimum Essential Medium Eagle alpha (α-MEM) (Gibco®, UK) containing 10% (v/v) FBS (SeraPlus, Pan-Biotech, Germany), 5 ng/mL basic fibroblast growth factor (bFGF) (Fitzgerald, USA), 100 U/mL penicillin and 100 µg/mL streptomycin (Gibco®, UK) in a standard cell culture incubator (37°C, 5% (v/v) CO_2). In Chapter 2 hMSCs were cultured in PromoCell hMSC growth medium (PromoCell GmbH, Germany). Here, the hMSCs were cultured in the above outlined supplemented α-MEM medium to follow the standard procedures at AO Foundation Davos. Upon 70 - 90% confluency, cells were detached as outlined in 2.2.3 and re-seeded at a density of 3000 cells/cm^2 for culture expansion. For chondrogenic differentiation, 2 x 10^6 passage 1 hMSCs were thawed and passaged twice before they were subjected to pellet culture. For initial cell viability and proliferation assays, bone marrow-derived hMSCs purchased from PromoCell GmbH, Germany and Lonza, UK at passages 5 - 6 were used.

Table 3.2: Details of hMSC donors used for assessment of chondrogenic differentiation in various BG-conditioned media. hMSCs (donors #1 - #5) were isolated from human bone marrow at AO Foundation Davos. The age refers to the age of the respective donor when the hMSCs were isolated. F = female, m = male. *Donor #6 was commercially obtained from Lonza, UK.

Donor	Age (years)	Gender
#1	69	F
#2	56	M
#4	58	M
#5	73	F
#6*	29	F

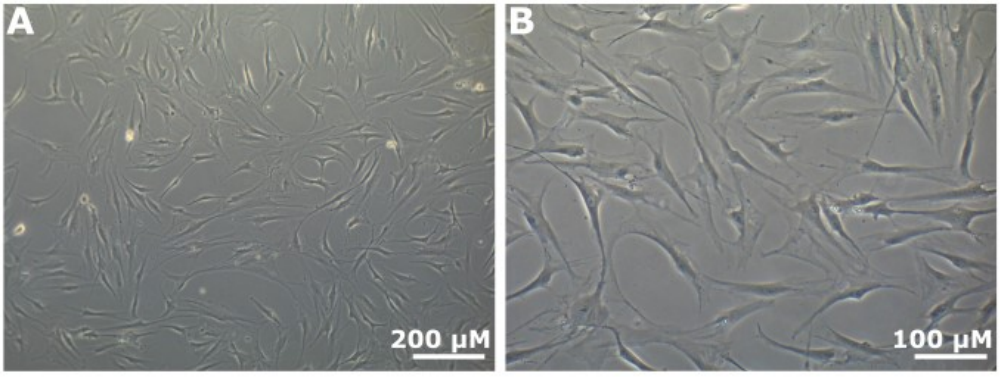


Figure 3.1: Primary human mesenchymal stem cells (hMSC) isolated at AO Foundation Davos. Representative images of donor #4 hMSCs at passage 1. (A) 10x magnification, scale bar = 200 µm (B) 20x magnification, scale bar = 100 µm.

3.2.4 MTT assay

The MTT assay was performed to assess the effect of the various BG-conditioned media on hMSC metabolic activity. In brief, 1.5 x 10^4 cells/cm^2 of passage 5 - 6 hMSCs were seeded in 96-well plates. After 24 h the medium was replaced by DMEM or BG-conditioned DMEM medium containing 10% (v/v) FBS (Seraplus, Pan-Biotech, Germany), 100 U/mL penicillin and 100 µg/mL streptomycin (Gibco®, UK) and 20 mM HEPES (Gibco®, UK). After 24 h, 3 days and 7 days, respectively, medium was removed and cells were washed once with PBS prior to addition of 5 mg/mL of MTT (Thiazolyl Blue Tetrazolium bromide, M2128, Sigma®, UK) in phenol-free high glucose DMEM (Gibco®, UK). After 2 h the MTT solution was thoroughly removed and replaced by 100 µL of dimethylsulphoxide (DMSO) (Sigma-Aldrich, UK) to solubilise the formed formazan crystals. Absorbance was measured at a wavelength of 570 nm with a reference wavelength of 620 nm using a microplate reader (SpectraMax M5, Molecular Devices, UK). Three independent repeats of the experiment were performed each time using a different donor. Each condition was run in quadruplicates.

3.2.5 CyQUANT® Direct Cell Proliferation Assay

Cell growth in the presence of BG-conditioned medium was assessed using the CyQUANT® Direct Cell Proliferation Assay (Life technologies, UK). The assay was performed according to the manufacturer's instructions. In brief, 5 x 10^3 cells/cm^2 of passage 5 - 6 hMSCs were seeded in 96-well plates. To avoid confluency throughout the 7 day culture period, a lower cell density compared to the MTT assay was chosen. After 24 h the medium was replaced by DMEM or BG-conditioned DMEM medium containing 10% (v/v) FBS (Seraplus, Pan-Biotech, Germany), 100 U/mL penicillin and 100 µg/mL streptomycin (Gibco®, UK) and 20 mM HEPES (Gibco®, UK). The medium was changed every other day over the course of the experiment. After 24 h, 4 days and 7 days respectively, medium was removed and cells were washed once with PBS prior to addition of CyQUANT® Direct Cell Proliferation Assay kit in phenol-free high glucose DMEM (Gibco®, UK). After 1 h of incubation fluorescence was excited at 480 nm and emission was quantified at 535 nm using a microplate reader (SpectraMax M5, Molecular Devices, UK). Three independent repeats of the experiment were performed each time using a different donor. Each condition was run in quadruplicates.

3.2.6 Chondrogenic differentiation of hMSCs

To induce chondrogenic differentiation in hMSCs, hMSCs were cultured as pellets in chondrogenic medium for up to 21 days. Bone marrow-derived hMSCs at passage 3 were re-suspended in chondrogenic medium consisting of high glucose DMEM (Gibco®, UK) containing 20 mM HEPES (Gibco®, UK), 10 ng/mL TGF-β1 (Fitzgerald, USA), 100 nM dexamethasone (Sigma, UK), 50 µg/mL ascorbic acid-2-phosphate (Sigma, UK), 1% (v/v) non-essential amino acids (Gibco®,UK), 1% (v/v) insulin, transferrin, sodium selenite (ITS) + premix (BD biosciences, UK) and 100 U/mL penicillin and

100 µg/mL streptomycin (Gibco®, UK). HEPES was added to the medium to ensure a stable pH during cell medium changes in pellet culture. Furthermore, HEPES was added with respect to the increase in pH caused by partial dissolution of the bioactive glasses during preparation of the BG-conditioned medium.

For pellet culture, 250,000 hMSCs were re-suspended in 1 mL of chondrogenic medium, placed into sterile conical mircocentrifuge tubes (Eppendorf, UK) and spun at 400 xg for 10 min. To allow hMSC condensation, cells were incubated in a controlled humidified chamber (37°C, 5% (v/v) CO_2) for three days prior to the first medium change. On the day of the first medium change (day 0), 1 mL of either chondrogenic medium, Comp1-Ca, Comp1-Sr, Comp2-Ca or Comp2-Sr-conditioned medium, all containing chondrogenic supplements, was added to the respective tubes. Medium was changed every 2 - 3 days for a total culture period of 21 days. Medium was retained to quantify the sGAG release throughout the experiment. The DNA content and sGAG production were measured in three independent experiments using different donors (#2, #4 and #5). Each condition was run in triplicates for each independent experiment.

3.2.7 Biochemical analysis of hMSC pellets

After pellet formation (day 0) or after 21 days, hMSC pellets were washed twice in PBS prior to digestion in 0.5 mg/mL proteinase-K (PK) (2.5 U/mg, chromozyme assay; Roche, Germany) at 56ºC for 16 h. The digested samples were stored at -20ºC until further use. The DNA content per pellet was measured spectrofluorometrically using Hoechst 33258 dye[340]. In brief, 40 µL of the PK digested sample were incubated with 160 µL of 0.1% (w/v) Hoechst 33258 (Sigma, Germany) in PBS for 20 min in the dark. Fluorescence intensity was measured at 360 nm excitation/ 465 nm emission. The standard curve was generated with calf thymus DNA (Invitrogen, Germany).

The sGAG content for each sample and in medium was determined by 1,9-Dimethyl-methylene blue dye (DMMB) binding assay[341]. In brief, 200 µL of DMMB solution (16 mg DMMB in 1 L water containing 3.04 g glycine and 2.37 g NaCl at pH 3.0) were added to 20 µL of PK digested sample and immediately measured at 538 nm absorbance using a Victor3 Micro Plate Reader (Perkin Elmer, USA). For detection of sGAG in medium, the digestion step was not necessary so that 200 µL of DMMB solution were directly added to 50 µL of retained medium per sample. The standard curve was generated with chondroitin 4-sulphate sodium salt from bovine trachea (Fluka BioChemika, Germany).

3.2.8 Gene expression analysis of key differentiation markers by qPCR

200,000 hMSCs were used to obtain pellets as previously described in section 3.2.6 and treated with BG extract free chondrogenic medium or BG-conditioned medium containing chondrogenic factors for up to 7 days. The medium was changed every 2 - 3 days. After the formation of pellets (day 0) as well as after 3 and 7 days of treatment, cells were harvested for total RNA isolation using either TRIzol®

(Invitrogen, UK) or RLT buffer containing 1% (v/v) β-mercaptoethanol (Qiagen, UK). Pellets were homogenised in the respective buffer with RNase free pestels followed by RNA extraction using the RNeasy® Plus Mini Kit (Qiagen, UK), according to supplier's instructions. The amount of total RNA per sample was measured by light absorbance at 260 nm using a Nanodrop 2000c spectrophotometer (Thermo Scientific, UK). RNA quality was assessed by calculating the A260/ A280 ratio. For cDNA generation, up to 100 ng of total RNA of each sample were reverse transcribed into cDNA using the QuantiTect Reverse Transcription Kit (Qiagen, UK) following manufacturer's instructions. For gene expression analysis by qPCR, RNAse free water (Sigma, UK) was used to dilute the cDNA 1:5.

For qPCR, the total reaction volume was 10 µL containing 300 nM of each primer and 5 µL of EXPRESS SYBR® GreenER™ qPCR Supermix, with premixed ROX (Life technologies, Invitrogen, UK) for each sample. The QuantStudio™ 6 Flex Real-Time PCR System (Applied Biosystems™, UK) was used to perform the qPCR reactions. Each sample was run in triplicates. Sequences and cycling conditions of primers used in this study are listed in Table 3.3. Each condition was run for 40 cycles. All primers were custom-designed by Dr. Hélène Autefage and Dr. Jean-Philippe St.-Pierre and ordered from Invitrogen, UK. Data analysis was performed according the ΔΔCt method outlined in Chapter 2 (2.2.4). Data are presented relative to the first medium change after pellet formation (day 0) unless otherwise stated. For differentiation marker gene expression analysis, three donors (#1, #5 and #6) were analysed. Each condition was run in triplicates for each independent experiment.

Table 3.3: Primer sequences and cycling conditions.

	Gene name	Primer sequence (5'-3')	Cycling conditions
Housekeeping gene	*18S*	GTAACCCGTTGAACC CCATCCAATCGGTAGTAGTAGCG	95°C for 15 s 61°C for 30 s 72°C for 30 s
Lineage marker genes	*SOX9*	AACGCCGAGCTCAGCAAG ACGAACGGCCGCTTCTC	95°C for 15 s 62°C for 30 s 72°C for 30 s
	ACAN	GCTACCCTGACCCTTCATC AAGCTTTCTGGGA TGTCCAC	
	COL2A1	CATCCCACCCTCTCACAGTT GTCTCTGCCTTGACCCAAAG	95°C for 15 s 60°C for 30 s 72°C for 15 s
	COL1A1	CATTAGGGGTCACAATG GTC TGGAGTTCCA TTTTCACCAG	
	RUNX2	CCGCCTCAGTGATTTAGGGC GGGTCTGTAATCTGACTCTGTCC	95°C for 15 s 61°C for 30 s 72°C for 30 s

3.2.9 Histology

To study the quality of *in vitro* formed tissue in presence of BG-conditioned medium containing chondrogenic factors or BG extract-free chondrogenic medium, pelleted hMSCs were cultured for up to 21 days as previously described in 3.2.6 and assessed by histology. Samples for histology were fixed in 70% (v/v) methanol in H_2O and stored at 4°C. At least 24 h prior to cryo-sectioning, samples were transferred to 5% (w/v) sucrose (Fluka, Germany) in PBS to aid the penetration of the optimal cutting temperature (OCT) medium on the next day. Prior to sectioning, samples were incubated in OCT (Jung Tissue Freezing Medium, Leica Biosystems, Germany) for at least 10 min before being fast frozen at -56°C. For histological staining and immunohistochemistry, 10 µm sections of hMSC pellets were prepared using a cryostat at -24°C (Microm HM 560, Thermo Fisher Cryostat Series, USA). Generally, it was aimed to obtain sections from the centre of the pellets. The sample sections were collected on

Menzel-Glaeser Superfrost® Plus slides (Thermo Fisher, Germany) and stored until further use at -20°C. Donors #4 and #5 were subjected to histological assessment.

3.2.9.1 Toluidine Blue staining

Toluidine Blue is a basic metachromatic dye with a high affinity for acidic tissue components[342]. Toluidine Blue staining of tissues is based on the phenomenon of metachromasia as the dye changes colour depending on its binding partners and surroundings. Characteristically, the cytoplasm of cells stains light blue, the nuclear region dark blue, and proteoglycans purple.

Slides were selected and allowed to reach RT to enhance the binding of tissue sections to the slide. The OCT medium was removed by rinsing the slides for at least 10 min in dH_2O. Sections were stained in a 0.1% (w/v) Toluidine Blue solution in MilliQ water containing 0.1% (w/v) sodium tetraborate (Fluka, Germany). After 1 min the sections were washed in dH_2O until all excess Toluidine Blue was removed. Sections were dried for at least 30 min prior to transfer to xylene. Sections were mounted with Eukitt (Fluka, Germany). After at least 24 h, the sections were observed using an Olympus BX51 epifluorescence microscope equipped with an Olympus DP70 digital camera under visible light. Image processing was performed using GIMP 2.8.

3.2.9.2 Safranin O/ Fast Green staining

Safranin O staining allows the detection of cartilage-like tissue as it binds to the negatively charged glycosaminoglycans. Using this method, proteoglycans will be stained orange/red. Fast Green, which serves as the counter stain of Safranin O, binds strongly to the amino group of proteins by virtue of a sulphate group-containing motif.

Slides were selected and allowed to reach RT to enhance the binding of sections to the slide. The OCT medium was removed by rinsing the slides for at least 10 min in dH_2O. To stain the nuclei, sections were exposed to Weigerts Haematoxylin (Merck, Germany) for 12 min followed by 10 min incubation in running, lukewarm tap water. Sections were rinsed once in dH_2O and stained in a 0.02% (w/v) Fast Green (Fluka, Germany) solution in MilliQ water containing 0.1% (v/v) acetic acid for 6 min. Remaining Fast Green was rinsed off in a 1% (v/v) acetic acid solution before the slides were exposed to a 0.1% (w/v) Safranin O (Polysciences Inc, Warrington, USA) solution in MilliQ water for 15 min. To remove remaining Safranin O, sections were briefly washed in water before being dehydrated for 2 min each in 70% EtOH, 96% EtOH, 96% EtOH, 100% EtOH and 100% EtOH. Afterwards, the sections were exposed to Xylene for a total of 10 min and mounted with Eukitt (Fluka, Germany). After at least 24 h, the sections were observed using an Olympus BX51 epifluorescence microscope equipped with an Olympus DP70 digital camera under visible light. Image processing was performed using GIMP 2.8.

3.2.10 Immunohistochemistry

Immunohistochemical staining (IHC) was used to visualise the distribution of type I, type II and type X collagens in hMSC pellets. For the preparation of pellet sections please refer to 3.2.9. Sections of bovine cartilage were used as positive controls (Appendix A). For IHC, cryosections of pellets were selected and allowed to reach RT. To remove the cryo-compound, cells were washed for 10 min in dH_2O. To block the endogenous peroxidase, the sections were incubated in 1% (v/v) 30% H_2O_2 (Sigma, UK) in methanol (Sigma, UK) for 30 min. Afterwards, the slides were washed twice in PBS and transferred to 0.05 U/mL hyaluronidase (Sigma, UK) in PBSTw for 30 min at 37°C for antigen retrieval. The slides were washed three times in PBS and subjected to Avidin/Biotin blocking (Avidin D/Biotin Blocking Kit, Vektor Laboratories, UK). Therefore, slides were placed in a humidified chamber and incubated with avidin D prior to incubation with biotin for 15 min each. After removal of biotin, the slides were washed twice in PBS. The sections were blocked with 5% (v/v) goat serum (Dako, UK) in PBS for 1 h at RT. The sections were immunostained with the primary antibodies mouse anti-collagen I (Sigma C2456, 1:500), rabbit anti-collagen II (abcam ab34712, 1:150) and rabbit anti-collagen X (GeneTex GTX37732 1:150) in 5% (v/v) goat serum in PBS at 4°C over-night. For the negative control, sections were incubated in 5% (v/v) goat serum in PBS at 4°C over-night (Appendix A). After three washes with PBSTw, all sections were incubated with the secondary horseradish peroxidase (HRP)-coupled antibodies, goat anti-mouse (Dako P044801-2 1:100) or anti-rabbit (Dako P044701-2, 1:100) in 5% goat serum (v/v) in PBS for 1 h at RT. The sections were washed three times with PBSTw and subjected to the 3,3'-diaminobenzidine kit (DAB) (Vector Labs, UK) following the manufacturer's instructions. The HRP-DAB system is a widely used method in IHC to detect the presence of a desired antigen, as the resultant staining can be viewed with traditional microscopy and stored for extended periods of time without signal loss. The method relies on the ability of the enzyme HRP to oxidise DAB in the presence of hydrogen peroxide thereby producing a dark-brown insoluble precipitate which indirectly visualises the location of the antigen. Once the reaction was deemed to be sufficient, samples were washed for 10 min to terminate the reaction. The sections were counterstained with Harris' Haematoxylin for 3 s and subsequently washed under running tap water for 5 min. Haematoxylin is a basic dye used to visualise the nuclei of cells as it forms an insoluble salt with DNA and RNA, staining them red. By washing the slides in tap water, the dye is "blued" which results in the characteristic purple/blue staining of nuclei. The sections were then dehydrated for 2 min each in 70%, 90%, 100%, 100% EtOH and 5 min each of three Histo-Clear (Fisher Scientific, UK) baths. All sections were briefly soaked in Xylene and mounted with Eukitt (Sigma, UK). After at least 24 h, the sections were observed using an Olympus BX51 epifluorescence microscope equipped with an Olympus DP70 digital camera under visible light. Image processing was performed using GIMP 2.8. Donors #4 and #5 were subjected to IHC analysis.

3.2.11 Fourier transform infrared spectroscopy (FTIR) of hMSC pellet sections

To further assess tissue formation in presence of BG-conditioned medium containing chondrogenic factors or BG extract-free chondrogenic medium, pelleted hMSCs were cultured as previously described in 3.2.6 for 21 days and subsequently subjected to FTIR analysis. Donors #4 and #5 were used for FTIR analysis. Samples for FTIR analysis were fixed in 70% (v/v) methanol in H_2O and stored at 4°C. At least 24 h prior to cryo-sectioning, samples were transferred to 5% (w/v) sucrose (Fluka, Germany) in PBS to aid the penetration of the OCT (Jung Tissue Freezing Medium, Leica Biosystems, Germany) medium on the next day. Prior to sectioning, samples were embedded and incubated in OCT medium for at least 10 min before being fast frozen at -56°C. For FTIR analysis, 5 µm sections of hMSC pellets were prepared using a cryostat at -24°C (Microm HM 560, Thermo Fisher Cryostat Series, USA). Generally, it was aimed to obtain sections from the centre of the pellets. The sample sections were collected on calcium fluoride (CaF_2) slides (Global Optics, UK) and stored until further use at -20°C. Prior to FTIR analysis, pellet sections were carefully washed with MilliQ water to remove remaining OCT. Donors #4 and #5 were subjected to FTIR and two sections per donor and condition were analysed.

FTIR maps of pellets were acquired on an Agilent Cary 670-IR spectrometer coupled with a Cary 620-IR imaging microscope (Agilent Technologies, CA) with a 128 x 128 MCT focal plane array (FPA) detector. The FTIR maps were obtained in transmission mode with a 15 x objective with a numerical aperture of 0.62. Spectral resolution was set to 4 cm^{-1}. 16 spectral scans were co-added for background whereas 4 spectral scans were co-added for the sample. All pre-processing and analysis of the FTIR spectroscopic data were performed in Matlab version R2015a (MathWorks, Natick, MA, USA) and PLS toolbox version 8.0 (Eigenvector Technologies, Manson, Washington, USA). The raw FTIR spectra were cropped to the biological "fingerprint" region (1000 - 1825 cm^{-1}) for Multivariate Curve Resolution (MCR). Wavenumbers below 1000 cm^{-1} are beyond the detection limit of the FPA detector. After that the data was pre-processed by Savitzky-Golay smoothing (9 points), weighted least squares polynomial baseline correction (4^{th} order) and normalisation to area under the curve. MCR analysis was applied to the pre-processed data to estimate the pure component spectra and respective concentrations of each pure component within each spectrum (scores). Heat maps of each pure component were then plotted with the MCR scores (normalised across all the samples). For visual display, K-means clustering was used to segment the pellet regions removing the surrounding background area. FTIR imaging and data analysis were performed in collaboration with Miss Amanda You.

3.2.12 Statistical analysis

To determine statistical significance, a one-way ANOVA combined with Tukey *post-hoc* test was used for experiments with one time point. For experiments with multiple time points, a two-way ANOVA followed by Bonferroni *post-hoc* test was used. Results with *p*-values lower than 0.05 were deemed significant. All data are expressed as mean ± standard deviation (SD).

3.3 Results

Previous studies have evaluated the use of bioactive glasses as bone facing substrates of multi-layered osteochondral scaffolds. So far, only the classic bioactive glass compositions and in particular 45S5 BG and 13-93 BG have been studied for such applications and the influence of bioactive glass dissolution products on the chondrogenic differentiation of hMSCs remains largely unknown. Modifying bioactive glass compositions to aid chondrogenic differentiation is a novel approach, which remains to be explored.

To study the impact of key bioactive ion species on hMSC chondrogenic lineage commitment, two compositions (Comp1 and Comp2) were chosen (Table 3.1). Comp1-Ca is the classic 45S5 BG composition while Comp2-Ca was designed and fabricated by the Stevens group in collaboration with Prof. Jones's group. Comp2 contains magnesium and potassium which are known to influence the glass transition temperature allowing the fabrication of 3D scaffolds. Strontium was incorporated into both compositions by replacing 50% of the calcium on a molar basis resulting in a molar strontium content of 13.45 mol% (Comp1-Sr) and 17.80 mol% (Comp2-Sr).

3.3.1 Ionic composition of strontium and/or magnesium-containing BG-conditioned media

Particles prepared from all compositions (Comp1-Ca, Comp1-Sr, Comp2-Ca and Comp2-Sr) were incubated in high glucose DMEM medium containing 20 mM HEPES for 4 h at 37°C under constant agitation and subsequently filtered to remove remaining particles. The elemental concentrations of silicon, calcium, phosphorous, strontium and magnesium in BG-conditioned or BG-free DMEM medium were determined using ICP-OES (Table 3.4). The silicon content in all BG-conditioned media was comparable. The calcium content was similar for Comp1-Ca and Comp2-Ca as well as for Comp1-Sr and Comp2-Sr. The ion concentration of phosphorous was similar in all samples; however, it tended to be slightly lower for Comp1. The strontium release into the medium was comparable for the strontium-containing compositions and was with around 1.75 mM in the range of strontium concentrations used for *in vitro* experiments[176, 319]. The concentration of strontium in blood of osteoporotic patients, both male and female, treated with SrR was determined to be 0.12 mM[251, 343]. The magnesium concentration was found to be comparable between BG-free and Comp1-conditioned medium. The magnesium release from Comp2 into the medium doubled the basal concentration (0.8 mM to 1.65 mM). Supplementation of 5 mM $MgCl_2$ has been shown to enhance *in vitro* chondrogenesis of human synovial MSCs[335] while 10 mM $MgSO_4$ supported proliferation of human articular chondrocytes[330]. While the magnesium concentration in the Comp2-conditioned media was below the levels used in literature, the long-term exposure and the interaction with other bioactive ions may suffice to stimulate chondrogenesis in hMSCs.

Table 3.4: Ion content of BG-conditioned DMEM medium. Elemental concentrations of bioactive glass ionic dissolution products (Si, Ca, P, Sr, Mg) in DMEM high glucose medium are shown. Bioactive glass particles were incubated in DMEM for 4 h at 37°C under constant agitation. Ion release was measure by ICP-OES. Elemental concentrations are expressed as mean ± SD of 3 independent experiments (in ppm). The ICP-OES was operated with the assistance of Miss Anu Solanki. ND = non-detectable.

	Si	Ca	P	Sr	Mg
DMEM	ND	65 ± 7	26 ± 6	ND	20 ± 3
Comp1-Ca	65± 3	155 ± 20	14 ± 6	ND	17 ± 2
Comp1-Sr	65 ± 2	98 ± 11	22 ± 7	147 ± 11	17 ± 2
Comp2-Ca	63 ± 1	166 ± 21	23 ± 7	ND	41 ± 3
Comp2-Sr	64 ± 1	104 ± 13	29 ± 8	168 ± 15	40 ± 2

The partial dissolution of bioactive glasses in aqueous buffers and the concomitant release of ions are known to increase the pH. The rise in pH is caused by H^+ consumption during initial ion exchange reactions[126]. As a high pH is linked to cellular cytotoxicity, the BG-conditioned medium was equilibrated for at least 4 h or over-night in a standard cell culture incubator (37°C, 5% (v/v) CO_2) prior to addition to cells. The pH was measured before and after equilibration (Table 3.5). Equilibration resulted in a decrease in pH for Comp1-conditioned media, while differences in pH before and after equilibration for Comp2 were subtle. The pH of all BG-conditioned media were comparable after equilibration. The pH of the DMEM control increased. After equilibration, the difference in pH between BG extract-free and BG-conditioned media was markedly reduced.

Table 3.5: pH values of DMEM and BG-conditioned DMEM medium before and after equilibration. DMEM and BG-conditioned media were equilibrated under standard cell culture conditions (37°C, 5% (v/v) CO_2) for at least 4 h or over-night. pH values are expressed as a mean ± SD of two independent experiments.

	pH before	pH after
DMEM	7.23 ± 0.07	7.70 ± 0.11
Comp1-Ca	8.07 ± 0.13	7.86 ± 0.14
Comp1-Sr	8.05 ±0.16	7.86 ± 0.11
Comp2-Ca	7.88 ± 0.13	7.85 ± 0.13
Comp2-Sr	7.87 ± 0.12	7.84 ± 0.10

3.3.2 Metabolic activity and hMSC cell number in presence of BG dissolution products

Generally, bioactive glasses have been shown to enhance cell metabolic activity[184, 337, 344]. To assess the influence of the BG-dissolution products used in this study on the cell metabolic activity and development of cell number over time, hMSCs were treated with the various BG-conditioned media for up to 7 days (Fig. 3.2). The metabolic activity of hMSCs was determined using the MTT assay on days 1, 4 and 7 of culture (Fig. 3.2A). There were no significant differences in metabolic activity between hMSCs cultured in the various BG-conditioned media. Thus, the incorporation of strontium or the use of different base compositions (Comp1 and Comp2) had no significant influence on cell metabolic activity. On day 7, Comp1-Sr ($p<0.05$), Comp2-Ca ($p<0.01$) and Comp2-Sr ($p<0.05$) dissolution products significantly enhanced hMSC metabolic activity compared to BG extract-free DMEM medium. In presence of all bioactive glass dissolution products but not BG extract free DMEM medium, the metabolic activity increased significantly over time when day 1 was compared to day 4 ($p<0.01$ for Comp1-Ca, Comp2-Ca and $p<0.001$ for Comp1-Sr, Comp2-Sr) and day 7 (all $p<0.001$). There was no significant difference in metabolic activity between days 4 and 7 which may be indicative of a near-confluent cell layer on day 4.

The change in cell number over time was assessed using the CyQUANT® Direct Cell Proliferation Assay on days 1, 4 and 7 of culture (Fig. 3.2B, Appendix B). Due to donor variability, the results are presented separately for each donor. The cell number increased for all donors when comparing days 1 and 4. For donor #1 and the hMSCs purchased from PromoCell, cell number was comparable on days 4 and 7 (Fig. 3.2B, Appendix B). Considering donor #6, cell number further increased when comparing day 4 to day 7 (Appendix B, Fig. A). There are several possible explanations for this observation. Firstly, passage 6 hMSCs may have lost some of their proliferative potential. Especially the donor #1 hMSCs which were obtained from an individual undergoing total hip replacement, might not have had the same replicative potential as the hMSCs purchased from Lonza (donor #6). Secondly, the hMSCs were expanded in the presence of bFGF while the experiments were conducted without bFGF. As bFGF is known to support hMSC cell proliferation it was not supplemented to the media during the experiments to focus on the influence of the BG extracts. Yet, withdrawal from bFGF might have reduced the cell proliferation[345].

Lastly, due to donor-dependent differences in the size of hMSCs, cells might have reached near confluency prematurely at 4 days of culture. After 4 and 7 days of culture, the various BG extracts increased cell number compared to BG extract-free DMEM for all donors. Considering these results, all conditions allowed or supported hMSC growth, proliferation and metabolic activity.

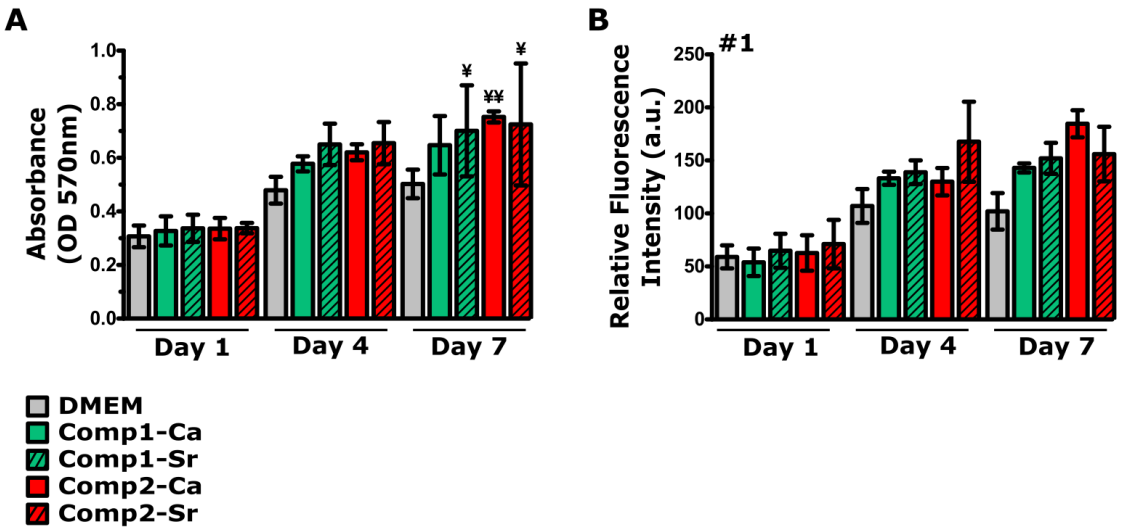


Figure 3.2: Effect of various BG extracts on hMSC metabolic activity and cell number. BG-conditioned or DMEM medium was used to culture hMSCs for up to 7 days. At the indicated time points, A) metabolic activity was measured by the MTT assay and B) cell proliferation over time was assessed using the CyQUANT® Direct Cell Proliferation Assay. A) Data are expressed as mean ± SD of 3 independent experiments using different donors. Statistical significance was assessed using two-way ANOVA followed by Bonferroni *post-hoc* test. ¥$p<0.05$, ~~¥¥~~$p<0.01$ versus DMEM only at the same time point. Statistically significant changes over time are not indicated in the figure. Over time, metabolic activity increased significantly for all media containing bioactive glass extracts but not DMEM when days 1 and 4 ($p<0.01$ for Comp1-Ca, Comp2-Ca and $p<0.001$ for Comp1-Sr, Comp2-Sr) and days 1 and 7 (all $p<0.001$) were compared. B) Cell abundance over time is shown representatively for donor #1. Data are expressed as mean ± SD of 4 biological replicates. As only one donor is displayed, no statistical analysis was performed.

3.3.3 sGAG production of hMSCs in response to BG dissolution products

Once all bioactive glass dissolution products were deemed biocompatible, the influence of BG-conditioned medium on hMSC chondrogenic lineage commitment was assessed. In pellet culture for *in vitro* chondrogenesis, hMSCs were exposed to BG-conditioned medium containing chondrogenic supplements or chondrogenic medium only as a reference for up to 21 days. The DNA content per pellet after 21 days of culture was similar in all conditions and not significantly different from day 0 (D0) (Fig. 3.3A). Quantification of sGAG showed that the accumulation of the extracellular matrix protein by the pellets normalised according to their respective DNA content was significantly increased compared to day 0 for all conditions save Comp2-Sr (Fig. 3.3B). There were no significant differences between the various BG extract conditions on day 21. Since some of the synthesised sGAG is known to be released from pellets, the sGAG content in the medium was quantified over time (Fig. 3.3C). The amount of sGAG in the culture medium per pellet increased over time for all conditions except Comp2-Sr indicating a progressive commitment to the chondrogenic lineage during the culture period. The level

of sGAG detected in the retained medium was significantly higher for all conditions save Comp2-Sr when days 15 - 21 were compared to days 1 - 7 ($p<0.05$ for chondrogenic medium, Comp1-Sr, Comp2-Ca, $p<0.01$ for Comp1-Ca). Thus, in contrast to all other conditions, hMSCs cultured in Comp2-Sr-conditioned medium neither accumulated a significantly higher amount of normalised sGAG after 21 days compared to day 0 nor did the sGAG release into the medium increase significantly over the three week culture period. The sGAG release from hMSCs cultured in Comp2-Sr was significantly lower compared to Comp1-Ca when days 15 - 21 were compared. However, since the sGAG release did not statistically differ between Comp2-Ca and Comp2-Sr, no conclusions can be drawn regarding the role of strontium. The results for the individual donors are shown in Appendix C.

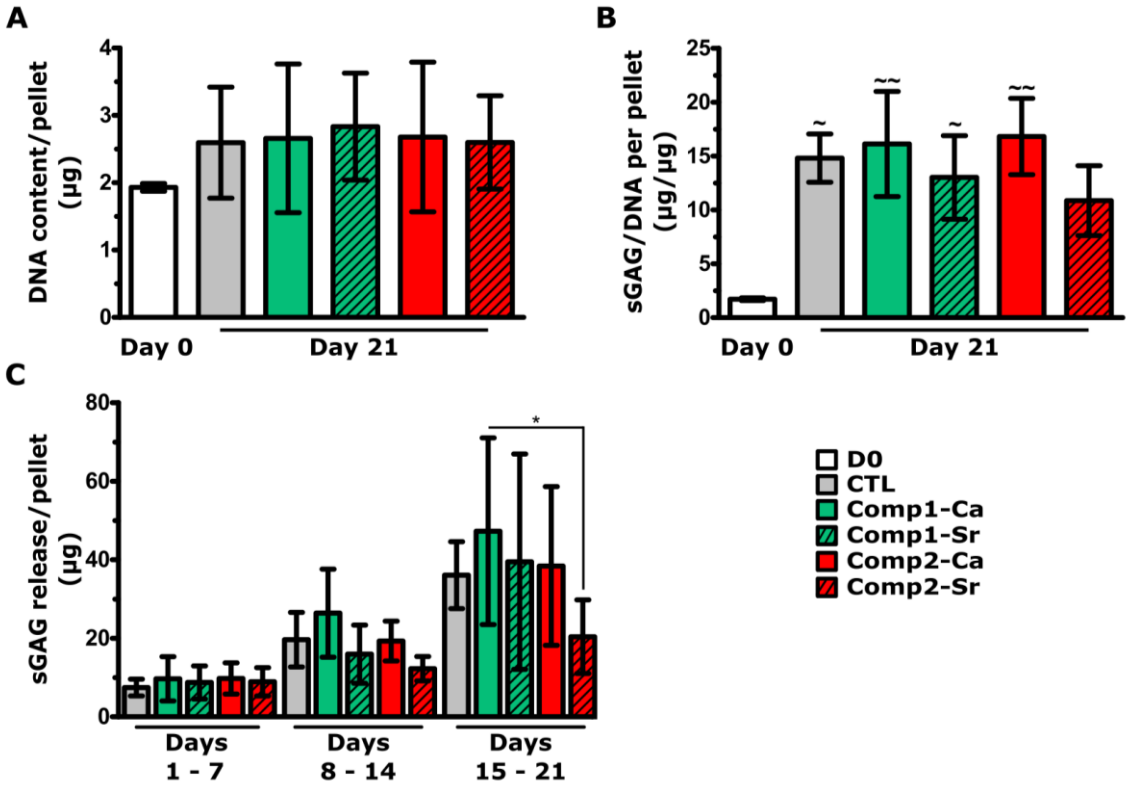


Figure 3.3: Effect of various BG extracts on hMSC chondrogenic differentiation. A - C) hMSC pellets were cultured in BG-conditioned medium in the presence of chondrogenic supplements or chondrogenic medium (CM) for up to 21 days prior to quantification of A) DNA by Hoechst or B) sulphated glycosaminoglycans (sGAG) by DMMB. C) Media samples were retained to assess sGAG released to media during the 21 day culture period. Data are expressed as mean ± SD of 3 independent experiments using different donors. Statistical significance was assessed A), B) using one-way ANOVA followed by Tukey *post-hoc* test and C) using a two-way ANOVA combined with Bonferroni *post-hoc* test. ~p<0.05, ~~p<0.01 (vs. day 0), *p<0.05. Statistically significant changes over time are not indicated in the figure. Comparing days 1 - 7 with days 15 - 21, sGAG release increased significantly for CM, Comp1-Sr, Comp2-Ca (all p<0.05) and Comp1-Ca (p<0.01).

3.3.4 Key chondrogenic marker gene expression in hMSCs during treatment with bioactive glass extracts

Since there were no pronounced differences in cartilage-like ECM production between conditions after 21 days in culture, it was sought to investigate whether bioactive glass dissolution products affected the early phase of hMSC chondrogenic lineage commitment. Therefore, the gene expression levels of key differentiation markers on days 3 and 7 of pellet culture in BG-conditioned medium in the presence of chondrogenic supplements or chondrogenic medium only were analysed. As pellets prepared from donor #4 for gene expression analysis did not properly form, they were excluded from analysis (data not shown). Instead, the experiment was repeated using donor #6. Donor #6 was commercially obtained from Lonza, UK. The expression levels of all genes were normalised to the housekeeping gene, *18S*, and are expressed relative to day 0, except for type II collagen (*COL2A1*). As the gene expression level

of type II collagen was below the detection level on day 0, data was normalised to chondrogenic medium only on day 3. Due to donor variability, the gene expression results are presented separately and need to be considered with caution.

Treatment with chondrogenic medium only, Comp1-Ca or Comp2-Ca-conditioned medium resulted in similar gene expression levels of the chondrogenic markers *SOX9*, *ACAN* and *COL2A1* (Fig. 3.4A, D, G). While Comp1-Ca and Comp2-Ca appeared to promote *SOX9* and *ACAN* expression in donors #5 and #6 beyond chondrogenic medium only, chondrogenic medium performed better than Comp1-Ca (but not Comp2-Ca) with respect to donor #1. The gene expression patterns of *RUNX2* and *COL1A1* were similar between conditions except for Comp2-Ca which appeared to mildly up-regulate the mRNA levels of both osteogenic markers. When the two time points were compared, the gene expression of all tested genes was higher on day 7. This trend was particularly pronounced for *ACAN* and *COL2A1* suggesting a progressive lineage commitment. Overall, the relative gene expression level of *SOX9* was rather low which may suggest that the chosen time points were either too early or too late to observe a peak in *SOX9* mRNA level. Overall, strontium incorporation reduced the gene expression levels of chondrogenic lineage marker genes.

Taken together, gene expression analysis of pellet culture of donor #5 followed a trend reminiscent of donor #1. For both donors, Comp2-Ca seemed to particularly enhance chondrogenic marker gene expression but also *COL1A1* compared to all other conditions. Yet, also Comp1-Ca and Comp2-Sr induced higher or at least similar gene expression levels of *SOX9*, *ACAN* and *COL2A1* compared to chondrogenic medium. Considering the day 3 time point, Comp1-Sr appeared to enhance *SOX9*, *ACAN* and *COL2A1* expression compared to chondrogenic medium only, however, this trend was not maintained on day 7. The up-regulation of chondrogenic markers was particularly pronounced in donor #6 likely owing to the relatively young age of the donor. The influence of bioactive glass dissolution products was particularly marked for donor #6 as Comp1-Ca and Comp2-Ca increased *COL2A1* expression levels more than 10 fold compared to chondrogenic medium only on day 7. Overall, Comp1-Ca and Comp2-Ca strongly up-regulated chondrogenic marker gene expression compared to BG extract-free chondrogenic medium for donor #6.

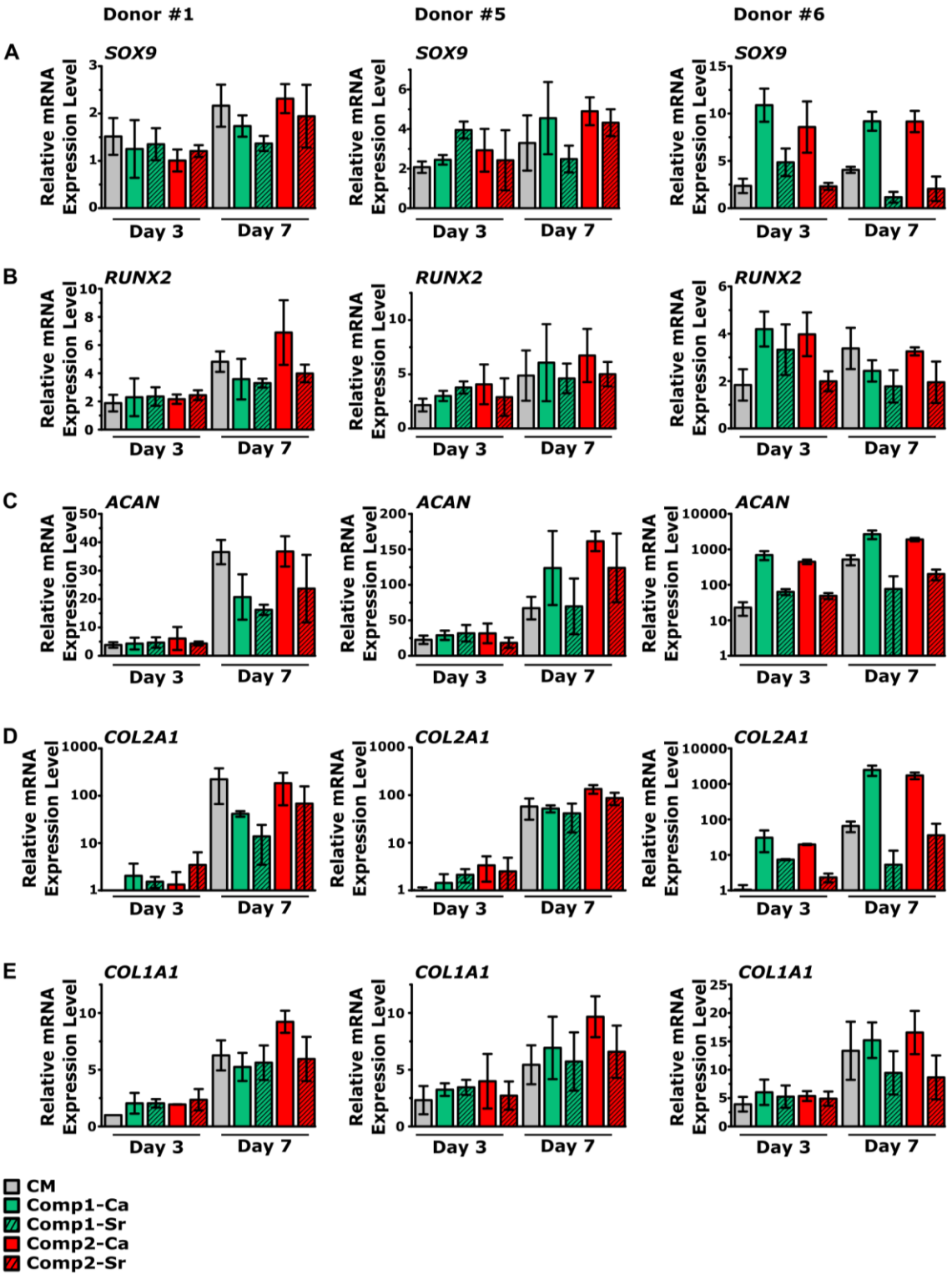


Figure 3.4: Effect of various BG extracts on chondrogenic and osteogenic lineage marker gene expression by hMSCs. Prior to qPCR, hMSCs were grown as pellets in BG-conditioned medium containing chondrogenic supplements or chondrogenic medium (CM) only for up to 7 days. A) *SOX9*, B) *RUNX2*, C) *ACAN*, D) *COL2A1* and E) *COL1A1* mRNA expression, respectively relative to D0 (or day 3 CM for *COL2A1*) in hMSC after 3 and 7 days as quantified by qPCR. Gene expression analysis was conducted for donors #1, #5 and #6. Data are expressed as mean ± SD of 3 biological replicates. As data for single donors are presented, no statistical analysis was performed.

3.3.5 *In vitro* tissue formation of hMSCs in BG-conditioned medium

To obtain a better understanding of (cartilage-like) tissue formation by hMSC pellets in BG-conditioned medium, the *in vitro* formed tissue was characterised by histology, immunohistochemistry and FTIR.

3.3.5.1 Histology

In a first step, the quality of extracellular matrix production by hMSCs in presence of bioactive glass dissolution products was assessed using histology. hMSCs were pelleted and cultured for 21 days in chondrogenic medium or BG-conditioned medium in presence of chondrogenic supplements as previously described.

Toluidine Blue is a metachromatic stain that changes colour from dark blue to a rich purple when bound to acidic proteins such as proteoglycans/glycosaminoglycans. Day 0 pellet sections stained only faintly for Toluidine Blue indicating little extracellular matrix (Fig. 3.5, left panel and Appendix D). After 21 days of culture, Toluidine Blue staining appeared dark purple suggesting the presence of proteoglycans/glycosaminoglycans in all conditions. In the centre of all pellets a fainter stained region was visible. This may point towards an undifferentiated core possibly due to the lack of sufficient nutrient and differentiation factor diffusion. Interestingly, in presence of Comp1-Sr dissolution products, the faintly stained core region was particularly pronounced and rounded (Fig. 3.5 and Appendix D). Culture in Comp2-Sr-conditioned medium led to smaller pellets relative to the other conditions and a smaller area of intense purple staining.

Safranin O similarly binds to proteoglycans/glycosaminoglycans giving rise to a bright red colour. Safranin O staining is thought to be proportional to proteoglycan content in healthy cartilage; however, the stain has been shown not to be sufficiently sensitive to detect low levels of glycosaminoglycans[346]. Fast Green is frequently used as the counter stain to Safranin O as it binds to other proteins such as collagens. No Safranin O staining on day 0 hMSC pellets was visible supporting the result obtained with Toluidine Blue (Fig. 3.5, right panel and Appendix D). After 21 days of culture, Safranin O staining of sectioned pellets was visible in all conditions indicating robust production of glycosaminoglycans. Cell nuclei in Safranin O stained regions appeared bigger and rounder suggesting chondrogenic lineage commitment. The central region of pellets did not show uniform Safranin O staining as observed with Toluidine Blue. The rim of all pellets was stained positive for Fast Green which was accompanied by tighter packed cells with flatter cell nuclei. Fast Green staining at the rim of pellet sections has also been observed elsewhere[347, 348]. The fibrocartilage-like layer was particularly pronounced in the Comp2-Sr condition. Interestingly, hMSC pellet growth appeared to be modulated by Comp2-Sr resulting in smaller, differently shaped pellets.

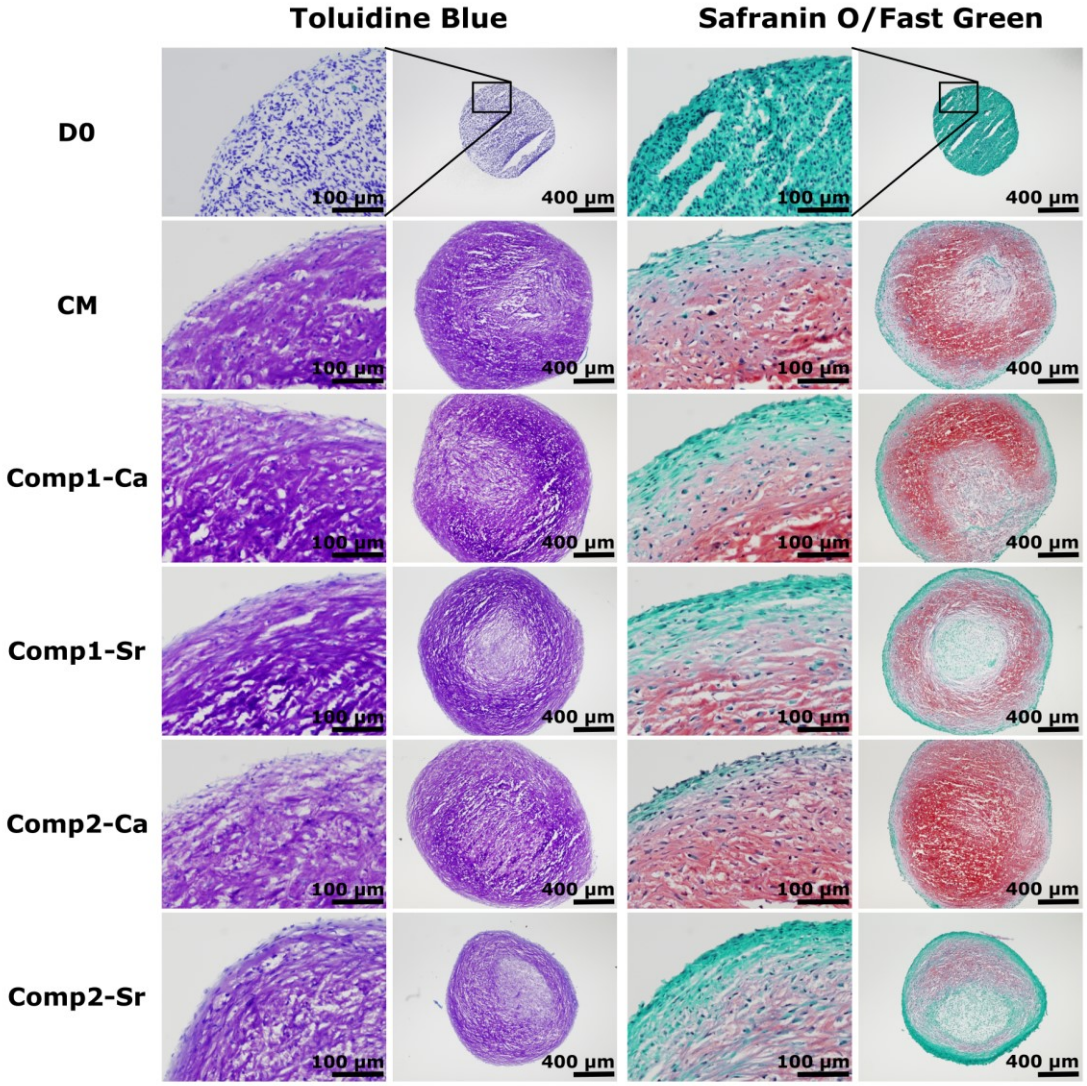


Figure 3.5: Effect of various BG extracts on *in vitro* cartilage-like tissue formation assessed by histology. Prior to histological assessment, hMSCs were grown as pellets in chondrogenic medium (CM) or BG-conditioned medium in chondrogenic conditions for up to 21 days. The presence of sulphated proteoglycans in the extracellular matrix of hMSC pellets was assessed by a) Toluidine Blue (purple metachromasia) and b) Safranin O staining. Fast Green stains collagens and other proteins. Representative images (donor #4) are shown.

3.3.5.2 Immunohistochemistry (IHC)

To further characterise cartilaginous tissue formation in presence of bioactive glass extracts, immunohistochemical detection of type I, type II and type X collagens was performed (Fig. 3.6 and Appendix D). Type I collagen is produced by undifferentiated hMSCs but is also regarded as indicator for fibrocartilage and osteogenic differentiation[84, 349]. Immunohistochemical detection of type I collagen was visible on pellet sections on day 0 (Fig. 3.6, left panel). After 21 days of culture, sectioned pellets of all conditions stained positive for type I collagen. Type I collagen was mainly localised to the rim of pellets in the region stained by Fast Green (Fig. 3.5) but was also visible throughout. Type II collagen

is indicative of chondrogenic differentiation and a crucial part of the hyaline cartilage ECM. Immunohistochemical detection of type II collagen on day 0 pellet sections was negative (Fig. 3.6, middle panel). After 21 days of culture, type II collagen was detected especially in the rim region of pellets but also throughout for all conditions. Especially for Comp2-Sr, type II collagen staining co-localised with Safranin O staining when the results for histology and IHC were compared. Type I and II collagen staining was faint or absent in the central region of pellets. Type X collagen is a marker for hypertrophic cartilage and is thought to support bone formation during endochondral ossification, in part through its ability to bind calcium[84]. Type X collagen staining was overall very faint (Fig. 3.6, right panel). Due to the faint staining, pellets were not exposed to haematoxylin as this would have masked the detection of type X collagen. Positive staining for type X collagen mainly localised to the outer rim of pellets. While type X collagen staining was nearly absent in presence of Comp2-Ca dissolution products, it tended to be slightly stronger in the fibrocartilage-like outer rim of pellets cultured in Comp2-Sr-conditioned medium. For the anti-type X collagen antibody there was a slight nonspecific background stain as observed in the negative control (Appendix A).

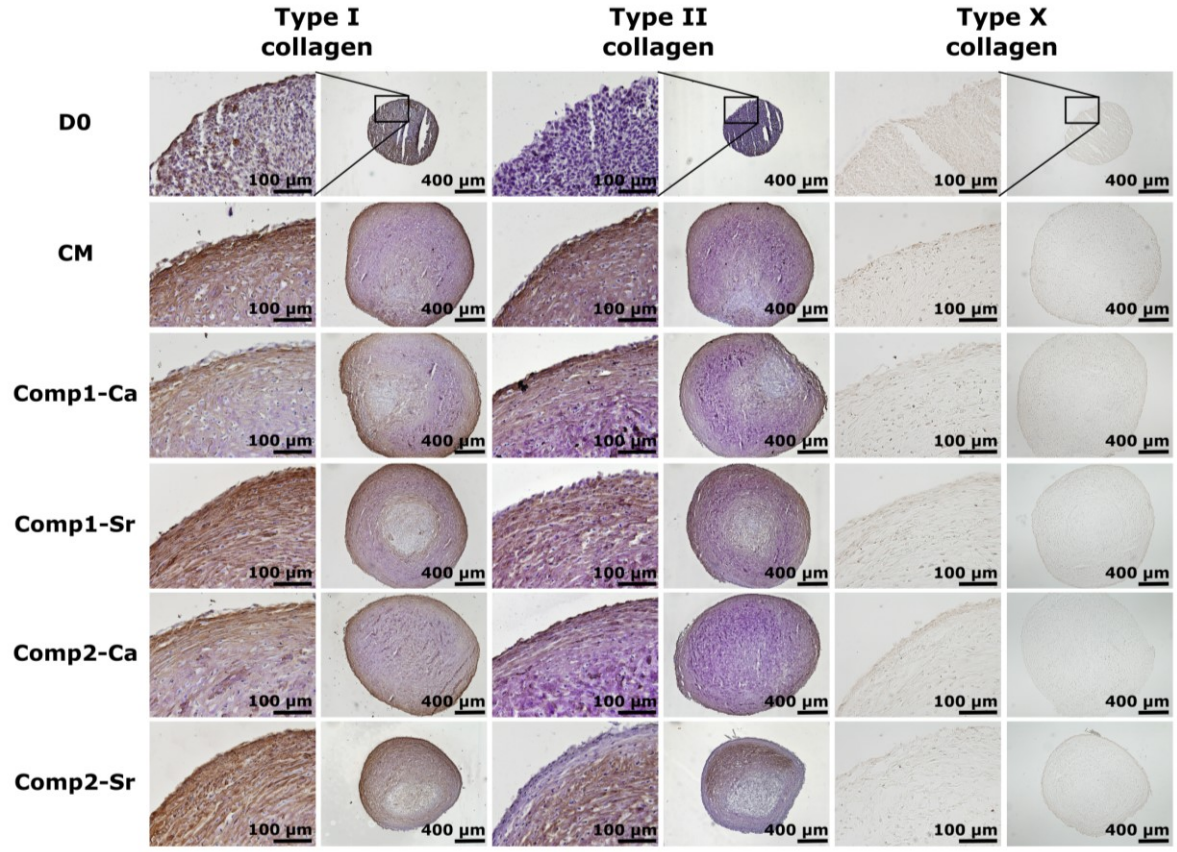


Figure 3.6: Distribution of type I, II and X collagens in hMSC pellets in presence of various bioactive glass extracts. Prior to immunohistochemistry, hMSCs were grown as pellets in chondrogenic medium (CM) or BG-conditioned medium in chondrogenic conditions for up to 21 days. Immunohistochemical staining of type I collagen (left panel), type II collagen (middle panel) and type X collagen (right panel). Representative images (donor #4) are shown.

3.3.5.3 Fourier transform infrared spectroscopy (FTIR)

Infrared (IR) spectroscopy is an analytical technique which is based on the interactions between infrared light and molecules. Chemical bonds within molecules absorb characteristic IR wavelengths which allow the molecular characterisation of samples. Fourier transform infrared (FTIR) imaging and spectroscopy have been used to study the chemical composition of various tissues including cartilage and bone[350]. The combination of FTIR technology with focal plane array (FPA) detectors opens up the possibility of collecting a large number of spectra simultaneously from relatively big sample areas. This development is especially interesting for the analysis of tissue samples[351]. Recently, hMSC pellets have been analysed by FTIR to monitor the state of chondrogenic differentiation[352].

In the work described in this chapter, hMSC pellets were subjected to FTIR analysis as an independent alternative method to observe the distribution of collagen. Multiplicative Curve Resolution (MCR) was used to extract the collagen spectrum in a spatially defined manner (Fig. 3.7). Heat maps of the MCR scores relating to collagen were then plotted[353, 354]. The heat maps showed a similar trend for collagen distribution as the results obtained with IHC supporting the previous observations. Collagen was detected throughout the pellet sections for all conditions. The relative signal intensity for collagen tended to be stronger at the rim of pellets which is in line with the results obtained by IHC. Overall, Comp2-Sr seemed to have the highest relative collagen signal intensity.

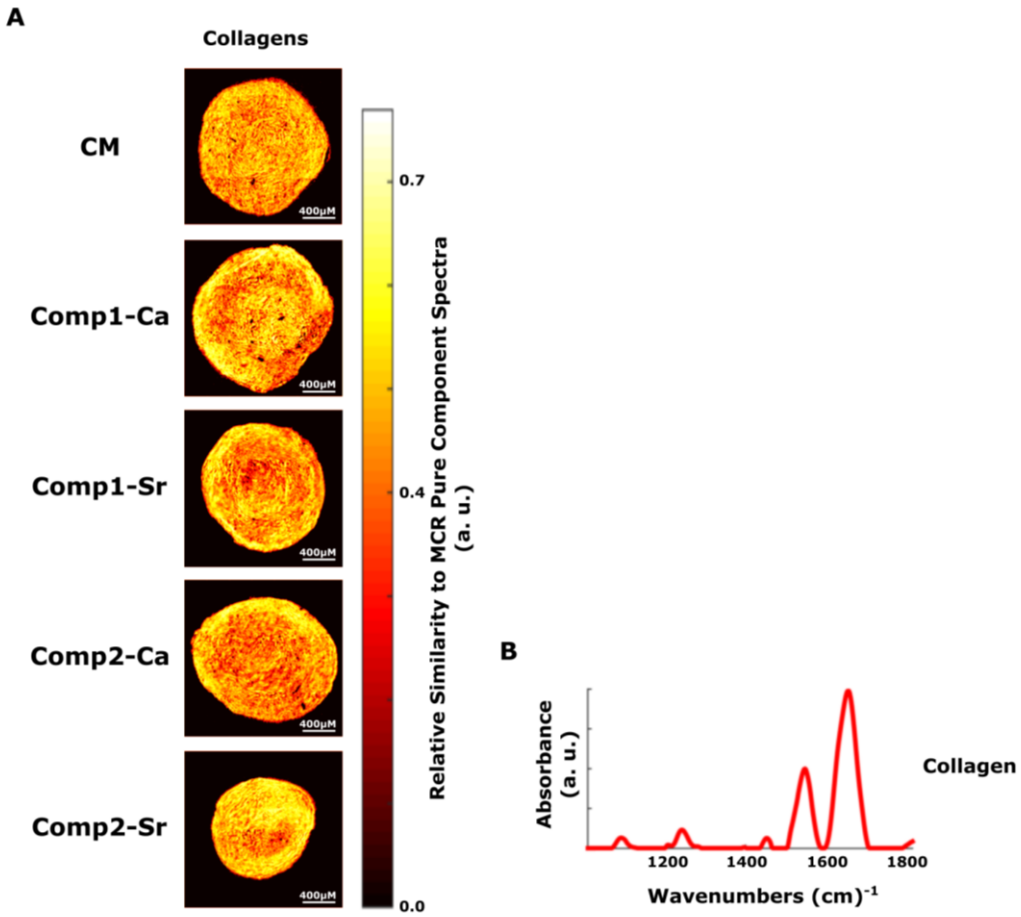


Figure 3.7: FTIR analysis of collagen distribution in hMSC pellets after culture in BG-conditioned media. Prior to FTIR, hMSCs were grown as pellets in chondrogenic medium (CM) or BG-conditioned medium in chondrogenic conditions for 21 days. A) Artificially coloured images from cross sections of hMSC pellets are shown. Multiplicative curve resolution (MCR)-determined collagen components are presented. The colour bar represents the scores by MCR. Representative images (donor #4) are shown. Scale bar = 400 µm. Pixel size = 5.5 µm x 5.5 µm. B) MCR pure component spectra of collagen. FTIR imaging and data analysis were performed in collaboration with Miss Amanda You.

Furthermore, FTIR opens up the possibility of detecting the presence of CaP depositions. As bioactive glasses have been shown to favour the formation of mineral, pellet sections were examined with respect to possible mineral depositions. In the context of (articular) cartilage regeneration, such depositions would be undesirable. Mineralised bone and cartilage are known to present a hydroxyapatite phosphate band at around 1000 to 1150 cm^{-1} [350]. In this study, no such peak was found in all samples, thus suggesting that there was no mineral deposition within the pellets (Fig. 3.8).

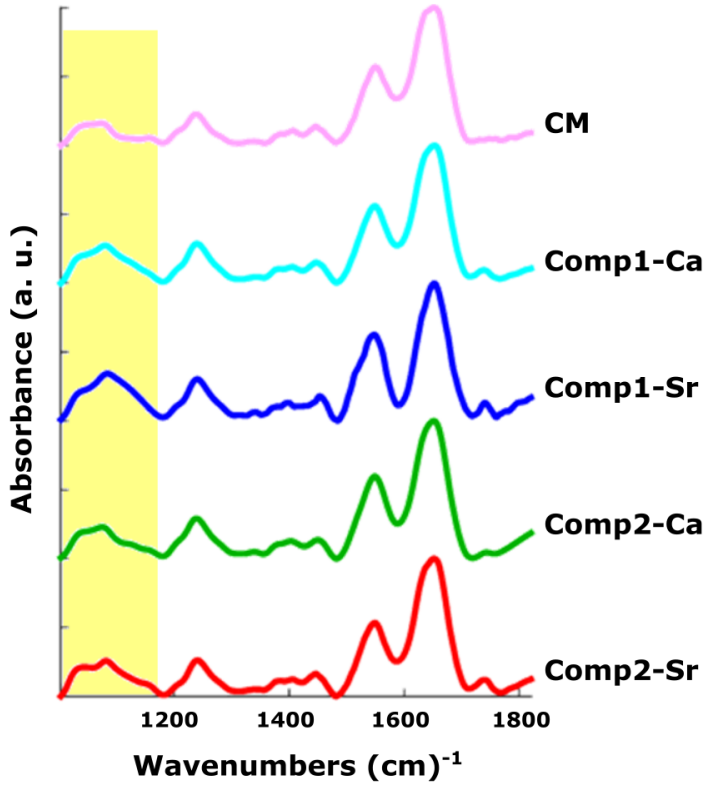


Figure 3.8: Effect of BG-conditioned media on the mean IR spectra of hMSC pellets. Prior to FTIR, hMSCs were grown as pellets in chondrogenic medium (CM) or BG-conditioned medium containing chondrogenic supplements for 21 days. The mean IR spectra for hMSC pellet sections for donor #4 are shown. Analysis of the mean IR spectra revealed no CaP depositions in hMSC pellets after culture in BG-conditioned media. Two sections per condition were analysed and the result for one representative section per condition is shown. The phosphate band (1000 to 1150 cm^{-1}) is highlighted. FTIR imaging and data analysis were performed in collaboration with Miss Amanda You.

3.3.6 Summary

In summary, it was demonstrated that bioactive glasses and their respective ionic dissolution products did not significantly affect sGAG accumulation. However, there was a composition-dependent effect on hMSC chondrogenesis when considering histological as well as immunohistochemical assessment. The incorporation of strontium into both studied compositions seemed to reduce chondrogenic lineage commitment in the conditions of this study. Further research is required to fully understand the influence of bioactive glass extracts on hMSC chondrogenesis and how single ion species within such ionic dissolution products can be used to promote chondrogenic differentiation.

3.4 Discussion

Bioactive glasses, either as granules, scaffolds or part of composites, are highly attractive materials for bone regeneration and beyond due to their bioactive properties. Owing to their superior bonding to bone and osteoconductive characteristics, bioactive glasses have been evaluated as bone substrate for multi-layered scaffolds for osteochondral repair. MSCs have emerged as the cell type of choice for tissue engineering applications in the osteochondral system and MSC-seeded scaffolds are widely being evaluated for osteochondral defects. Even though a couple of studies have reported a supporting role of bioactive glasses on cartilage repair *in vivo*, little is known about the effect of bioactive glasses on MSC chondrogenic differentiation. Here, it was aimed to shed light on the effect of bioactive glass ionic dissolution products on hMSC chondrogenesis in a pellet culture model. In particular, the question was addressed whether modification of bioactive glass compositions had an impact on hMSC differentiation and if hMSC commitment towards the chondrogenic lineage could be enhanced by incorporating key bioactive ions. To that end, two compositions were chosen; the classic 45S5 BG (termed Comp1) composition and a composition with a wider processing window that allows the formation of 3D scaffolds (Comp2). Strontium was incorporated by substitution for calcium into both compositions. Strontium was deemed especially interesting as previous *in vitro* and *in vivo* studies had suggested a positive effect of the ion on cartilage regeneration. Additionally, it was sought to evaluate a bioactive glass that would release magnesium ions. There was evidence from previous *in vitro* and *in vivo* studies for a beneficial effect of magnesium on cartilage regeneration. Therefore, Comp2 was included in the study.

The strontium content in Comp1-Sr and Comp2-Sr-conditioned medium was quite high with 147 ppm and 168 ppm. These values are higher than the 92 ppm measured in Sr100-conditioned medium in Chapter 2. Yet, Sr100 contains a higher amount of strontium with 26.91 mol% compared to 13.45 mol% (Comp1-Sr) and 17.80 mol% (Comp2-Sr). Generally, it needs to be stressed that the ion release from bioactive glasses depends on a multitude of factors, including glass composition, physical features of the glass and the characteristics of the medium the glass is immersed in. Furthermore, the release of ion species is not necessarily linear with respect to their content in the glass, as shown by Gentleman *et al.* for strontium[184]. As the silicon concentration in the BG-conditioned medium in Chapter 2 is below its solubility limit in solution with on average 36 ppm, it can be assumed that the overall ion release from the 0.1 – 1 mm particles used in Chapter 2 was lower than the ion release from the <38 μm particles used in this chapter where on average 65 ppm silicon were measured in the medium. This is likely due to several factors. Firstly, a smaller particle size has been associated with a higher rate of ion release due to a bigger surface area[355]. Secondly, the media used in Chapter 2 and Chapter 3, PromoCell hMSC growth medium and high glucose DMEM medium respectively, might have differentially influenced the ion release from the glasses. In a study by Gentleman *et al.*, the strontium ion release from strontium-containing glasses differed depending on the cell culture

medium[184]. Thirdly, addition of the buffer HEPES to the medium used in this chapter increased the ion concentration of calcium, strontium, magnesium and phosphate. While no conclusions can be drawn from the obtained ICP-OES results, the stronger regulation of the pH might have enhanced the ion release from particles or reduced the re-precipitation of ions. Without HEPES, the strontium concentration in Comp1-Sr and Comp2-Sr-conditioned medium was 67 ppm and 80 ppm, respectively (data not shown). Also the values for calcium and phosphate were about half of the values measured in the presence of HEPES in the medium.

Culture in BG-conditioned medium increased metabolic activity of hMSCs compared to DMEM medium only on day 7 and this may in part be attributed to an enhanced proliferation of hMSCs in presence of bioactive glass dissolution products. Yet, the influence of bioactive glass dissolution products on hMSC proliferation needs to be confirmed. There were no significant differences between BG compositions. Previous studies have shown an increase in osteoblast proliferation in response to bioactive glasses[147]. These observations are believed to be especially linked to the presence of silicon and calcium[247, 356]. Continuing from these promising findings, the effect of bioactive glass dissolution products on hMSC chondrogenesis was assessed in a pellet culture model. The hMSCs used for the differentiation study all originated from the femoral heads of patients undergoing total hip replacement surgery. After 21 days in culture, the DNA content of pellets was comparable between conditions and not significantly different from day 0. After condensation to pellets, hMSCs cease to proliferate and start to differentiate so that no substantial increase in DNA content was expected. In fact, several studies observed a decrease in DNA content per pellet over time[335, 347, 357]. The normalised sGAG content of hMSC pellets after 21 days of culture was significantly higher for all conditions, save Comp2-Sr, compared to day 0. In light of data in the literature, the normalised sGAG values presented in this chapter fall within the upper/normal range[358, 359]. Interestingly, several studies have investigated the use of various treatments, including hypoxic culture, to enhance sGAG production *in vitro*[358, 359]. In the following chapter, the use of hypoxia-mimicking agents to influence hMSC chondrogenic differentiation will be discussed. Quantification of sGAG release from hMSC pellets indicated a progressive lineage commitment throughout the culture period. There were no significant differences between the Comp1-Ca and Comp1-Sr or Comp2-Ca and Comp-Sr-conditioned media conditions. To obtain more pronounced differences between conditions, which would allow a clearer interpretation of the influence of the various BG-conditioned media, a longer culture period may be necessary. Apart from the standard 21 day time point chosen for this study, 28 days of culture are also routinely used to study chondrogenic differentiation[360]. As SrR administration enhanced cartilage repair in patients and promoted cartilage regeneration in *in vivo* experiments, the performance of Comp1-Sr and Comp2-Sr in the *in vitro* experiments described in this chapter were unexpected. The concentration of strontium in the blood of patients treated with SrR was determined to be 0.12 mM, which is considerably lower than the strontium ion levels in the BG-conditioned media used for the experiments presented in this chapter (around 1.75 mM). Therefore, the strontium ion concentration may have been too high in the

BG-conditioned media. Yet, previous studies showed that strontium ion concentrations of up to 5 mM increased ECM production by chondrocytes suggesting that a strontium ion level above 0.12 mM does not inhibit cartilage-like ECM accumulation per se. Moreover, most studies assessing the impact of SrR on chondrocytes *in vitro* used (at least) 1 mM of SrR, which equals 2 mM of strontium ions. In this context, the length of treatment may be critical as the endpoint of most *in vitro* studies was usually not longer than 72 h, which is significantly shorter than the 21 day culture period described in this chapter.

As there were no significant differences in sGAG production between conditions after 21 days, the question was pursued whether BG-dissolution products induced more subtle changes at earlier time points of hMSC lineage commitment. Therefore, the gene expression of key differentiation markers after 3 and 7 days of pellet culture was analysed. Due to variability on donor level, no definite conclusions can be drawn from the results and the data need to be interpreted with caution. An up-regulation of *ACAN* and *COL2A1* expression by all donors on day 7 indicated commitment to the chondrogenic lineage for all culture conditions. Overall, compositions Comp1-Ca and Comp2-Ca appeared to enhance expression of chondrogenic differentiation markers. Interestingly, gene expression levels of chondrogenic markers in hMSC pellets cultured in Comp2-Sr were similar to chondrogenic medium only. This may suggest that the reduced cartilage-like tissue formation observed by histological assessment on day 21 was due to a prolonged exposure to Comp2-Sr beyond the 7 day time point. There were no big differences in *SOX9* gene expression level for donors #1 and #5. Zhang *et al.* and Murdoch *et al.* did not observe a correlation between *SOX9* expression and extent of extracellular matrix production; however, different time points were chosen[360, 361]. With respect to donor #6, Comp1-Ca and especially Comp2-Ca increased gene expression of chondrogenic markers. Gene expression levels of chondrogenic marker genes correlated with pellet size and likely extracellular matrix production. In contrast to donors #1 and #5, which were isolated at AO Foundation Davos from femoral heads of patients undergoing total hip replacement, donor #6 was commercially obtained from Lonza, UK. According to the information supplied by the company, donor #6 was 29 years old at the time of cell isolation and female. All donors were of Caucasian origin. Hence, #donor 6 was significantly younger than the other donors used in this study which may account for the differences in gene expression values. Previously, donor age has been negatively correlated with differentiation capacity in both murine and human MSCs[362, 363]. Overall, the relative gene expression levels of all chondrogenic marker genes were higher and up-regulated at earlier time points indicating an earlier and stronger lineage commitment. The impact of bioactive glass dissolution products was likewise more pronounced than for the other donors; however, this could also owe to a donor and not age-dependent effect. Comp1-Ca and Comp2-Ca dissolution products particularly enhanced *SOX9*, *ACAN* and *COL2A1* expression compared to chondrogenic medium only and the strontium-containing conditions. Focusing on the day 3 time point, Comp1-Sr-conditioned medium seemed to increase *SOX9*, *ACAN* and *COL2A1* expression compared to chondrogenic medium only, albeit not to a similar degree as Comp1-Ca and Comp2-Ca.

In a preliminary experiment using donor #5 it was shown that gene expression of *COL10A1*

was below the detection level on both time points for all conditions (data not shown). However, the chosen time points may have been too early to detect an up-regulation of *COL10A1*. A previous study has reported the up-regulation of hypertrophic markers on day 7; notably, before the induction of *COL2A1* on day 14[84]. Yet, generally it is accepted that *COL2A1* up-regulation precedes hMSC maturation and hypertrophy[349].

Next, the quality of cartilage-like tissue formation was assessed by histology, IHC and FTIR. Toluidine Blue and Safranin O/Fast Green staining of pellet sections showed that a glycosaminoglycan-rich matrix was produced in all conditions. However, the area of glycosaminoglycan positive staining was smaller when hMSC pellets were cultured in presence of strontium-containing bioactive glass extracts. The outer layer of cells had a fibrocartilage-like phenotype. This phenomenon is not unusual for hMSC pellet culture and has been described elsewhere[50, 360]. Mechanical stresses at the outside of the pellets may be causative for this observation. In the central region of pellets, cells appeared undifferentiated which was accompanied by little cartilage-like ECM production. The presence of cells throughout the pellet argues against a necrotic core region. To ascertain the viability of cells in the central region of pellets, a TUNEL assay could have been performed[361]. Using the TUNEL assay, apoptosis of cells *in situ* can be visualised. In presence of either Comp1-Sr or Comp2-Sr, the outer fibrocartilage-like rim appeared thicker which may have caused a further reduction in nutrient and growth factor diffusion to the central region of the pellet. In turn, this may have led to a larger undifferentiated core. Characterisation of the *in vitro* formed tissue by IHC, showed the presence of both type I and type II collagens at the rim and throughout the pellet matrix. While this result warrants further confirmation, it seemed like, in the presence of Comp2-Sr dissolution products, type II collagen did not localise to the rim of pellets but was exclusively visible in regions also positive for Safranin O. Staining for type X collagen was overall very faint and mainly localised to the rim of pellets. Pellets cultured in Comp2-Ca-conditioned medium showed the faintest type X collagen staining while the rim of pellets cultured in Comp2-Sr had a tendency to be more intensely stained. Yet, both observations need to be further validated with more donors to be reliable. Generally, the expression of type X collagen and thus the development of a hypertrophic phenotype by hMSCs/chondrocytes are largely not desired in cartilage engineering. Yet, some studies suggest the guided formation of a confined calcified cartilage layer for osteochondral tissue repair[316]. Such a calcified interface is thought to function as a barrier between the articular cartilage and bone to prevent bony ingrowth into the newly formed cartilage layer. Previous studies have observed positive type X collagen staining in control conditions in pellet culture[50, 357]. Data presented in this chapter suggest a low level of type X collagen as visualised by IHC staining but with a longer culture period of e.g. 28 days, type X collagen abundance may have been more pronounced. Of note, Mueller and Tuan suggested that a combination of TGF-β withdrawal, a reduction of dexamethasone and addition of thyroid hormone (T3) in the culture medium was necessary to elicit a full hypertrophic maturation hMSCs[50].

FTIR analysis of tissues can provide information that is complimentary to histological

assessment and biochemical techniques. Preliminary analysis of pellet sections by FTIR confirmed the presence of collagens in all conditions. Collagen was detected throughout the pellet sections and showed a similar relative intensity pattern between conditions. The relative signal intensity for collagen tended to be higher around the rim of the pellets. Comparing the different culture conditions, the relative collagen signal intensity appeared to be increased for Comp2-Sr which is in line with IHC. As bioactive glass dissolution products are known to enhance hMSC differentiation towards the osteogenic lineage and support formation of mineral depositions, it was sought to ensure that hypertrophy was not promoted in chondrogenic-differentiated hMSCs. Indeed, immunohistochemical detection of type X collagen demonstrated that the pellets were only faintly positive for the hypertrophic marker. Furthermore, FTIR analysis showed that the pellets were free of mineral depositions as no phosphate band peak was detected. This result is encouraging; however, it would be necessary to repeat the experiment in presence of mineralisation inducing factors.

High density culture systems have been shown to provide an efficient support for hMSC chondrogenic differentiation *in vitro*. In particular, pellet culture is thought to provide a suitable 3D environment for hMSC chondrogenic differentiation that resembles the conditions MSCs encounter in pre-cartilage condensations during embryonic development. While pellet culture is the classic high density culture model to induce MSC chondrogenesis, lately micromass culture has emerged as possibly superior system. Pellet culture can lead to an undifferentiated or necrotised central region and facilitate the differentiation towards a fibrocartilage-like phenotype as characterised by type I and type X collagen expression [50, 360]. In the micromass culture system, a high density cell suspension in a small volume (for example 12.5 µL[361] or 20 µL[364]) is placed in a well of an i.e. 24-well plate. After an initial incubation period, chondrogenic medium is added and cells aggregate within the first 24 h. Extracellular matrix production and chondrogenic marker expression were found to be increased in micromass culture compared to pellets. Additionally, fibrocartilage and hypertrophy markers were decreased. The authors argued that better nutrient diffusion and a slightly lower cell density may be causative for the superior performance of the micromass system. A highly interesting question which was beyond the scope of this work is how bioactive glass dissolution products would affect the initial condensation of hMSC pellets or, respectively, the aggregation of hMSCs in a micromass system. Future work could address this matter by re-suspending hMSCs in BG-conditioned media prior to centrifugation of hMSCs for pellet formation/preparation of micromasses. Since magnesium ions are known to stimulate integrin binding and thus cell-cell interactions, compositions Comp2-Ca and Comp2-Sr may modulate cell behaviour to a greater extent than after pellet formation.

Taken together, data provided in this chapter reinforce the notion that bioactive glasses are suitable substrates for the bone facing component of multi-layered osteochondral scaffolds with respect to their influence on hMSC chondrogenesis. In the conditions of this study, strontium incorporation seemed to favour a more fibrocartilage-like phenotype with fewer sGAG accumulation as shown by histology and immunohistochemistry. This result was surprising since there is compelling clinical trial

and *in vivo* data which support a beneficial effect of strontium on cartilage maintenance and repair. However, the effect of strontium on hMSC chondrogenesis is largely unknown and the study presented in this chapter was the first to evaluate strontium-containing bioactive glasses with respect to chondrogenic lineage commitment of hMSCs. Since chondrogenic marker gene expression of hMSC pellets treated with Comp2-Sr was similar to chondrogenic medium only on days 3 and 7, prolonged exposure to the strontium-containing bioactive glass extracts may have eventually hampered a proper differentiation towards a chondrocyte phenotype. The remodelling of subchondral bone is a common phenomenon observed in osteoarthritis[307]. Therefore, strontium-substituted bioactive glasses would be especially interesting to use for osteochondral defects considering the well-described beneficial effects of strontium on bone remodelling in osteoporosis. Hence, a further evaluation of strontium-containing bioactive glasses merits consideration.

An up-coming notion in the field of bone tissue engineering is to pursue an endochondral ossification approach to mimic processes during development and injury repair as shown by e.g. Scotti *et al.*[365] and reviewed by Thompson *et al.*[91]. Bioactive glasses with a tailored composition and their respective dissolution products may prove useful in guiding MSCs along chondrogenic lineage commitment and subsequent maturation towards a hypertrophic phenotype. Indeed, previous studies have observed an up-regulation of chondrogenic and osteogenic markers in presence of bioactive glasses. Based on the results presented in this chapter, no definite conclusions can be drawn regarding an optimal composition for such an application. Hypertrophic differentiation of hMSCs is usually induced with a medium composition that differs from the chondrogenic medium used for experiments described in this chapter. Comp1-Sr appeared to mildly enhance type X collagen accumulation as shown by immunohistochemistry, which may point towards a hypertrophic phenotype. Pursuing the endochondral ossification approach, bioactive glasses may present a highly interesting material to use. Future studies could address this hypothesis and investigate whether the incorporation of key ions could facilitate such a strategy.

3.4.1 Limitations

In this chapter, HEPES was added to the medium to allow a stable pH during hMSC pellet culture in microcentrifuge tubes following the standard protocol at AO Foundation Davos. The addition of HEPES affected the ion concentration in the bioactive glass-conditioned media, increasing the values for calcium, magnesium, strontium and phosphorous compared to HEPES-free conditioned medium. As such this is not a problem as all conditions in this chapter were prepared the same way. Yet, a high osmolarity caused by the high concentration of ion species may influence cellular behaviour. In the context of this thesis, the results obtained in Chapter 2 cannot be directly related to those obtained in this chapter, as the ion contents of the conditioned media differed. More generally, it is difficult to draw definite conclusions from the results obtained with conditioned medium *in vitro* to a possible

performance *in vivo* as the composition of ion release products *in vivo* is unknown.

It is possible that the 21 day time point used in this study was too early to detect the effects of different bioactive glass compositions on hMSCs. It would be interesting to evaluate longer time periods, such as 28 or 35 days, to investigate whether or not the composition of BG-conditioned media would influence chondrogenesis.

3.5 Conclusion

In summary, this chapter shows that hMSCs cultured in BG-conditioned chondrogenic medium produce a similar amount of normalised sGAG compared to chondrogenic medium only. The incorporation of strontium within bioactive glasses did not enhance hMSC chondrogenic differentiation. In contrast, histology and immunohistochemistry pointed towards a reduction in cartilaginous matrix formation in presence of strontium in the conditions of this study. Further research is needed to clarify if tailored bioactive glasses containing key bioactive ion species can enhance hMSC chondrogenesis.

CHAPTER 4

The Influence of Cobalt-containing Bioactive Glasses on hMSC Chondrogenic Differentiation

(*Some of the work in this chapter is in preparation for publication in "Hypoxia-mimicking bioactive glasses reduce hMSC chondrogenesis despite HIF-1α stabilisation" by Littmann E, Autefage H, Solanki AK, Kallepitis C, Jones JR, Alini M, Peroglio M and Stevens MM*)

All data presented in this chapter were collected by me unless explicitly stated otherwise.

4.1 Introduction

The necessity of molecular oxygen for animal life was illustrated by Joseph Priestley as early as 1772[366]. In his famous experiment he placed a mouse along with a burning candle in a sealed bell jar with fatal consequences for the rodent. Since then much research has been undertaken to elicit the vital role of oxygen in an array of organisms ranging from bacteria to vertebrates. Molecular oxygen is required for many intracellular biochemical reactions as primary electron acceptor and, importantly, is essential for the generation of ATP in the mitochondrion (aerobic respiration). While the lack of a sufficient oxygen supply can have deleterious effects on living organisms, hypoxic microenvironments and oxygen gradients are, in fact, required for the proper development of embryos as well as tissue formation and repair at later stages of development and in the adult. For a review on the role of oxygen in embryonic development, please refer to the paper by Simon and Keith, 2008[209]. An important point to be made is that physiological normoxia for most cells in the adult body ranges between 2 - 11% of molecular oxygen and hence deviates strongly from ambient air (21%) and conditions cells encounter in any regular cell culture incubator.

Building on the knowledge that reduced oxygen tension can guide cellular differentiation events as well as tissue formation *in vivo*; researchers have sought to use hypoxia for tissue engineering purposes. In this context, cartilage appears as an obvious choice as it is avascular and hence inherently hypoxic. Due to the lack of vasculature, nutrients as well as oxygen must diffuse from the surface of the joint facing the synovial fluid into the cartilage tissue below[367]. *In vivo*, articular chondrocytes are thought to be exposed to 1 - 7% oxygen and there is evidence for a decreasing oxygen tension gradient from the surface of the articular cartilage layer to the subchondral bone[368, 369]. Treatment of cartilage lesions remains a challenge in the clinic and for the tissue engineering community owing to the limited self-repair capacity of cartilage. One of the main hurdles of using chondrocytes for cartilage repair applications is their relatively low number in cartilage explants necessitating substantial expansion *in vitro*. During expansion, chondrocytes tend to change their phenotype, a process termed dedifferentiation. This process is characterised by loss of aggrecan and type II collagen production and an increase in the synthesis of type I and type III collagens[370]. The extracellular matrix produced by such dedifferentiated chondrocytes has inferior biochemical properties to hyaline cartilage and thus is not desirable for cartilage repair applications.

Appreciating that chondrocytes reside in a hypoxic environment *in vivo*, culture of chondrocytes in hypoxic conditions *in vitro* has been studied to improve the outcome of expansion. In a study by Domm *et al.* dedifferentiated bovine chondrocytes were either cultured in a monolayer or in alginate beads under 5% or 21% O_2 in the absence of redifferentiation factors such as TGF-β[371]. While low oxygen tension had no effect on dedifferentiated chondrocytes in monolayer culture, it increased the expression of type II collagen and stimulated the production of extracellular matrix constituents in alginate culture compared to the ambient air control. The authors concluded that low oxygen tensions

induced redifferentiation of dedifferentiated cells in alginate bead culture. Likewise, the dedifferentiated state of adult human chondrocytes was reversed by culture in reduced oxygen conditions in absence of TGF-β in studies by Malda *et al*. and Murphy and Polak[372, 373]. Grimshaw and Mason demonstrated that extracellular matrix production was enhanced at 10% O_2 compared to 20% and anoxic conditions in bovine articular chondrocyte pellets[367]. Using a mathematical model, Li *et al.* predicted that oxygen tensions below 8% favoured proteoglycan production while higher levels of oxygen enhanced collagen production in human articular chondrocytes[374].

Due to the drawbacks associated with cell-based therapies using chondrocytes for cartilage repair including high donor site morbidity, MSCs have emerged as attractive alternative cell source[358]. One of the main advantages of using MSCs for tissue engineering applications is their potential to be readily expanded *in vitro*. Once a sufficiently large cell population is obtained, MSCs can be differentiated towards the adipogenic, osteogenic, chondrogenic and possibly other mesoderm-derived lineages[61, 62]. While MSC-based therapies for cartilage repair have been receiving growing interest, currently the number of clinical trials is still limited and their quality is often insufficient to draw conclusions, as reviewed by Filardo *et al.*[375]. Even though Pittenger *et al.* demonstrated the multilineage differentiation potential of MSCs, and particularly interesting in this context, the ability to give rise to cartilage-like tissue, almost 20 years ago, there is still no consensus on the optimal conditions for chondrogenic differentiation[63]. One of the main issues encountered with *in vitro* chondrogenic differentiation of MSCs is their tendency to adopt a hypertrophic chondrocyte phenotype which fails to produce a hyaline cartilage-like matrix[50]. Hypertrophic differentiation is characterised by the expression of terminal chondrocyte differentiation markers such as type X collagen and MMP13. Thus, during chondrogenic lineage commitment *in vitro*, the hMSC phenotype is unstable and tends to follow the endochondral ossification pathway[84, 376]. Considering the hypoxic environment during growth plate development and the finding that low oxygen tension promotes chondrocyte redifferentiation, several studies pursued the hypothesis that reduced oxygen tension might enhance chondrogenesis and cartilaginous extracellular matrix production by MSCs.

In agreement with the results obtained for chondrocytes, hypoxia was shown to promote MSC differentiation towards the cartilaginous lineage[377-380]. Using adipose-derived hMSCs Wang *et al.* demonstrated that 5% oxygen tension significantly enhanced the production of cartilage-associated ECM proteins such as collagens and proteoglycans[381]. Yet, this effect depended on the presence of chondrogenic medium suggesting that hypoxia alone was not sufficient to support chondrogenic differentiation *in vitro*. Similarly, hypoxic pellet culture of MSCs isolated from the infrapatellar fat pad of osteoarthritic patients increased the total and normalised sGAG production significantly, yet the total DNA content was reduced compared to the normoxic control[382]. In keeping with this, hypoxic culture (1% O_2) of pelleted hMSCs cultured in chondrogenic differentiation medium enhanced chondrogenesis compared to the normoxic control condition as shown by up-regulation of chondrogenic marker genes and more intense Alcian blue staining of pellet sections[383]. Notably, the gene expression of hypertrophy

markers *RUNX2* and *type X collagen (COL10A1)* was reduced in the hypoxic condition compared to the ambient air control. The authors linked the beneficial effects of hypoxic culture to activation of the PI3K/Akt/FoxO pathway. While most studies evaluated the effect of hypoxia during chondrogenic differentiation after MSC monolayer expansion in ambient air, the impact of hypoxic expansion on subsequent differentiation was likewise investigated. Interestingly, reduced oxygen tension during monolayer expansion up to passage 2 of ovine MSCs enhanced subsequent chondrogenic differentiation in pellet culture and in a type I collagen gel at ambient oxygen levels suggesting that hypoxic pre-culture primed the MSCs[359]. In contrast, Sheehy *et al.* showed that the oxygen pressure during porcine MSC expansion had only a mild effect on subsequent differentiation while reduced oxygen levels during differentiation proved as a strong promoter of chondrogenesis[380]. Yet another study showed that chondrogenic differentiation of hMSCs in pellet culture was inhibited by pre-conditioning with hypoxia[384]. Here, the most favourable results were obtained by applying hypoxia during pellet culture after cell expansion in normoxia. While MSCs in all studies mentioned above experienced at least a short period of culture in normoxic conditions during isolation or initial expansion, a well-designed study by Adesida *et al.* investigated the impact of hypoxic isolation and expansion of MSCs on subsequent chondrogenic differentiation[358]. Hypoxic culture conditions during expansion from passage 0 onwards positively affected differentiation in pellet culture and overruled the influence of oxygen tension during pellet culture similar to the observations made by Zscharnak *et al.*[358, 359]. Yet, the differentiation step was carried out in closed polypropylene tubes making it difficult to assess how much gas exchange took place during culture in the incubators. Interestingly, hypoxic conditions during differentiation significantly reduced *COL10A1* expression independent from the oxygen level during expansion. While the majority of studies demonstrate that hypoxic (pre-) treatment enhances MSC chondrogenic lineage commitment, there is also conflicting data[385, 386]. The discrepancies in outcome are likely owed to differences in experimental set-up (species, cell source, O_2 tension) and/or donor variability.

Kanichai *et al*. linked the beneficial effect of low oxygen environments on hMSC glycosaminoglycan and type II collagen production to the activation of HIF-1α[378]. Similarly, in the study by Khan *et al.*, the positive effect of hypoxia on extracellular matrix synthesis was linked to an up-regulation of key chondrogenic differentiation markers mediated by higher levels of HIF-1α and HIF-2α[382]. Further supporting the notion that hypoxic stabilisation of HIF-1α was responsible for enhanced chondrogenic differentiation, the transcription factor was identified as a positive regulator of the principal chondrogenic differentiation marker gene, *SOX9*[387, 388]. SOX9 is an essential transcription factor that governs hMSC condensation, the initial step of cartilage formation[81], as well as later stages of cell commitment to the chondrogenic lineage[82]. More specifically, SOX9 is known to activate specific enhancer elements in cartilage extracellular matrix genes such as type II collagen and aggrecan.

Overall, hypoxic pre-conditioning and/or hypoxic conditions during differentiation are associated with enhanced chondrogenic gene expression and cartilage-like extracellular matrix synthesis[378, 389]. Similarly, a beneficial effect on cartilage repair and chondrocyte redifferentiation has been attested to hypoxia[390]. The discovery of the role of HIF-1α in mediating the effects of hypoxia has sparked interest in modulating the activity of this transcription factor for therapeutic strategies.

4.1.1 The influence of cobalt on hMSC differentiation

While numerous studies have assessed the effect of low oxygen tension on MSC behaviour and differentiation, notably fewer studies describe the use of hypoxia-mimicking agents for tissue engineering applications. Yet, replacing reduced oxygen tension by hypoxia-mimicking agents has the advantage that special oxygen chambers are not required for *in vitro* cell culture. Even more importantly, hypoxia-mimicking moieties such as cobalt open up the avenue of incorporating such molecules into scaffolds, hence using them for *in vivo* tissue repair applications.

Interestingly, when human articular chondrocytes were exposed to 200 µM $CoCl_2$ for 24 h similar results to hypoxic culture were obtained[370]. Thus, the expression of cartilage marker genes (*SOX9*, *aggrecan and type II collagen (COL2A1)*) was significantly promoted by $CoCl_2$ treatment while the levels of type I and III collagens were reduced compared to the untreated control[370]. Analysis of the corresponding protein levels correlated with these findings. In keeping, Alcian blue staining indicated a higher level of GAG production by $CoCl_2$ treated human articular chondrocytes compared to control. Hence, Duval *et al.* demonstrated that the hypoxia-mimicking agent $CoCl_2$ had a similar influence on chondrocyte behaviour as physiological hypoxia, albeit the treatment duration with 24 h was rather short. In keeping with the results obtained by Duval *et al.*, treatment of primary rabbit chondrocytes with 150 µM $CoCl_2$ for 24 h increased the gene expression level of type II collagen and proteoglycan core protein[370, 391]. Concomitantly, cell viability was increased after treatment with 150 µM $CoCl_2$ for 12 h compared to the untreated control. Of note, it was demonstrated that the glucose uptake of equine chondrocytes in monolayer culture was increased when the cells were exposed to $CoCl_2$ concentrations of as little as 15 µM highlighting that $CoCl_2$ treatment has a profound effect on the cellular metabolism[392].

As outlined above, MSCs have been identified as a promising, more suitable cell type for cartilage repair and it is hence not surprising, that the influence of $CoCl_2$ on hMSC chondrogenesis has been evaluated. In a subsequent study by Duval *et al*., chondrogenic marker gene expression was shown to be higher in hMSCs treated with 200 µM $CoCl_2$ for 24 h than in the untreated control[393]. Apart from a significant up-regulation of *aggrecan*, *COL2A1* as well as *SOX9* and its downstream transcription factors *SOX5* and *SOX6* after 24 h, exposure to $CoCl_2$ reduced the expression of *COL10A1*. The gene expression pattern obtained with $CoCl_2$ treatment was similar to the gene expression profile of hMSCs constitutively expressing HIF-1α reinforcing the influence of cobalt-mediated HIF-1α stabilisation on

these effects. In line with these findings, Focaroli *et al.* stated that the expression of chondrogenic lineage associated genes was increased in adipose tissue-derived hMSCs cultured in cobalt/calcium alginate beads compared to the calcium alginate bead control[235]. Yet, when cobalt/alginate beads with different Co^{2+} contents were compared, no common trend in the regulation of gene expression was apparent and the fold change of gene expression differed quite considerably between conditions. Seo *et al.* similarly investigated the use of hypoxia mimicking agents to induce chondrogenesis in a clonal hMSC cell line[394].Yet, there is also conflicting data with a study by Jeon *et al.* reporting down-regulation of SOX9 on gene and protein level in response to $CoCl_2$ treatment (100 µM for 3 h) in hMSCs[395]. This decrease was linked to higher levels of miR-124a, a micro RNA that is known to suppress the expression of anti-neural proteins[395].

While cobalt ions are usually administered as $CoCl_2$, cobalt-containing biomaterials are of particular interest for *in vivo* applications and the design of bioactive scaffolds. As previously mentioned, the composition of bioactive glasses can be elegantly tailored to incorporate desired inorganic ions. Pursuing the incorporation of the hypoxia mimicking agent cobalt into a smart carrier system that would allow a controlled release, cobalt-doped bioactive glasses were prepared and characterised in the Stevens group by Azevedo *et al.*[239, 240]. To study the optimal amount of cobalt incorporation for bone tissue regeneration applications, increasing amounts of calcium were replaced by cobalt (0, 0.5, 1, 2, and 4 mol%) in a 49.46 mol% SiO_2, (23.08 – X mol%) CaO, X mol% CoO, 26.38 mol% Na_2O, 1.07 mol% P_2O_5 system. Cobalt-containing bioactive glass (CoBG)-conditioned medium prepared from these glasses was used to culture hMSCs for up to 7 days[240]. The CoBGs successfully induced a hypoxic state in the hMSCs as HIF-1α was shown to be activated in response to CoBG treatment after 8 h which was further corroborated by up-regulation of hypoxia target genes after 24 h[240]. In particular, *VEGF* gene expression was found to be up-regulated after 24 h of exposure to CoBG-conditioned medium and VEGF release was consistently increased up to 7 days underscoring a functional effect[240]. Following on from these encouraging findings, CoBG was incorporated in a previously optimised collagen-glycosaminoglycan (CG) scaffold system with the aim to design a scaffold for bone tissue engineering that would also support angiogenesis[241]. For the study CoBG with 4 mol% cobalt incorporation was chosen with particle diameters of either 38 µm or 100 µm. Scaffolds with smaller sized particles had a tendency to release more cobalt ions; yet, this trend was not significant. Cobalt-doped bioactive glass/CG scaffolds enhanced ALP activity of MC3T3 pre-osteoblasts compared to the bioactive glass free CG control and cobalt free bioactive glass/CG scaffolds suggesting a cobalt-dependent mechanism. Furthermore, the scaffolds supported an up-regulation of angiogenic markers as VEGF gene expression as well as protein production were enhanced and tubule formation by HUVECS in a functional assay was promoted. Interestingly, this beneficial effect was particularly pronounced in scaffolds containing larger CoBG particles highlighting that little differences in cobalt release may have a strong impact on the biological response.

4.1.2 Aims and objectives

Based on the benefits of hypoxic culture for chondrogenesis of MSCs together with promising results obtained with the hypoxia-mimicking agent cobalt, the hypothesis was explored whether cobalt-doped bioactive glasses might enhance chondrogenic differentiation of hMSCs. Considering the compelling results by Azevedo *et al.* and Quinlan *et al.,* cobalt-doped bioactive glasses might be especially interesting materials to use at the osteochondral interface[240, 241].

Thus, the aims of the work presented in this chapter were to investigate if cobalt-containing bioactive glasses enhanced chondrogenic differentiation of hMSCs and to identify an optimum cobalt concentration within bioactive glass to support chondrogenic differentiation. The objectives were to:

- Assess the influence of cobalt-containing bioactive glasses on chondrogenic differentiation of hMSCs pellets;
- Investigate the influence of cobalt-containing bioactive glasses on chondrogenic differentiation of hMSCs seeded on PCL membranes.

4.2 Materials & Methods

4.2.1 Glass synthesis

Glass synthesis and particle preparation were performed as previously described[33,34]. Cobalt was incorporated into the bioactive glass composition 49.46 mol% SiO_2, (23.08 – X mol%) CaO, X mol% CoO, 26.38 mol% Na_2O, 1.07 mol% P_2O_5 by substitution with calcium on a molar basis (where X equals 0, 1, 1.5 or 2 mol% cobalt substitution) (Table 4.1). Increasing amounts of cobalt were incorporated into the composition to identify an optimal cobalt concentration to support chondrogenesis. In future, the bioactive glasses will be referred to as 0%CoBG, 1%CoBG, 1.5%CoBG and 2%CoBG according to their molar cobalt content or as CoBGs if all glass compositions are concerned. The CoBGs were prepared using SiO_2 (Prince Minerals, UK), Na_2CO_3, P_2O_5, $CaCO_3$, and $CoCO_3$ (all Sigma-Aldrich, UK) as precursor materials. The precursor materials were mixed, melted at 1,400°C in a platinum-gold crucible for 90 min and quenched into deionised water. The resulting glass frit was allowed to dry between 120 - 150°C over-night before milling in a planetary ball mill at 500rpm for 5 min. The glass particle size used in this study was <38 μm in diameter (d = 0.9). Glass synthesis and processing were performed by Miss Anu Solanki.

Table 4.1: Glass compositions (mol%).

Glass	SiO_2	Na_2O	CaO	CoO	P_2O_5
0%CoBG	49.46	26.38	23.08	/	1.07
1%CoBG	49.46	26.38	22.08	1.00	1.07
1.5%CoBG	49.46	26.38	21.58	1.50	1.07
2%CoBG	49.46	26.38	21.08	2.00	1.07

4.2.2 Preparation of bioactive glass-conditioned medium

To obtain bioactive glass-conditioned medium, 1.5 mg/mL of CoBG particles were added to high glucose Dulbecco's Modified Eagle Medium (DMEM) (Gibco®, UK) containing 100 U/mL penicillin and 100 μg/mL streptomycin (Gibco®, UK) as well as 20 mM HEPES (Gibco®, UK). After 4 h of incubation under constant agitation at 37ºC, the solution was subsequently passed through a 0.2 μm filter (Sartorius, UK) under sterile conditions to remove remaining glass particles. The CoBG-conditioned medium was stored at 4°C until further use. Prior to treatment of cells, the medium was equilibrated at 37°C, 5% (v/v) CO_2 for at least 4 h or over-night. As described in Chapter 3 (3.2.2), the preparation of CoBG-conditioned medium followed a protocol previously established in the Stevens Group. Specifically, the concentration of <38 μm particles and the incubation time for bioactive glass compositions in the system 49.46 mol% SiO_2, (23.08 – X mol%) CaO, X mol% CoO, 26.38 mol%

Na_2O, 1.07 mol% P_2O_5 were optimised by Dr. Maria Azevedo (Maria M. Azevedo PhD Thesis "Hypoxia-mimicking bioactive materials for skeletal tissue engineering", Imperial College London, Department of Materials, 2012 and Azevedo *et al.*[239]). Cobalt-containing bioactive glass particle concentrations of higher than 1.5 mg/mL were shown to reduce viability of SaOs2 cells. The incubation time of 4 h was chosen as the ion release from particles was in a stable plateau phase at this time point. The elemental concentrations of calcium, phosphorous, silicon and cobalt in the bioactive glass-conditioned medium were determined by ICP-OES using an iCAP6000 Series ICP spectrometer (Thermo Scientific, UK) on at least three independent samples. The ICP-OES was operated with the assistance of Miss A. Solanki.

4.2.3 Cell culture

Bone marrow-derived human mesenchymal stem cells (hMSCs) were isolated from human bone marrow obtained from the Hospital of Davos, Switzerland after approval by the local ethical commission (KEK-ZH-NR: 2010-0444/0). The human bone marrow was harvested from the femoral heads of five patients. After bone marrow homogenisation, hMSCs were isolated by Ficoll® gradient centrifugation and adherence to tissue culture plastic as previously described[339]. Isolation of hMSCs was performed by the permanent staff at AO Foundation Davos. The details for each donor are listed in Table 4.2. To assure the right phenotype of cells, donor #4 was characterised by flow cytometry as described in Chapter 3 (3.2.3). Cells were expanded in Minimum Essential Medium Eagle alpha (α-MEM) (Gibco®, UK) containing 10% (v/v) FBS (SeraPlus, Pan-Biotech, Germany), 5 ng/mL bFGF (Fitzgerald, USA), 100 U/mL penicillin and 100 µg/mL streptomycin (Gibco®, UK) in a standard cell culture incubator (37°C, 5% (v/v) CO_2). Upon 70 - 90% confluency, hMSCs were trypsinised at previously described and plated at 3000 cells/cm^2 for expansion. For all chondrogenic differentiation studies, 2 x 10^6 passage 1 hMSCs were thawed and passaged twice before they were subjected to chondrogenic differentiation. For initial cell viability assays, hMSCs purchased from PromoCell GmbH, Germany/ Lonza, UK at passages 5 - 6 were used.

Table 4.2: Details of hMSC donors used for assessment of chondrogenic differentiation in CoBG-conditioned media. hMSCs were isolated from human bone marrow at AO Foundation Davos. The age refers to the age of the respective donor when the hMSCs were isolated. F = female, m = male.

Donor	Age (years)	Gender
#1	69	F
#2	56	M
#3	46	M
#4	58	M
#5	73	F

4.2.3 AlamarBlue® viability assay

The alamarBlue® assay (Invitrogen, UK) is routinely used to quantitatively assess cell metabolic activity. The active component of alamarBlue® is the water-soluble blue dye resazurin that can permeate the cell membrane without being toxic. Upon entering the cellular cytosol, resazurin is converted to its reduced form, resorufin, a red fluorescent dye, by mitochondrial enzyme activity. Prolonged monitoring of cell viability is possible as viable cells continuously reduce resazurin to resorufin. The alamarBlue® assay was performed according to the manufacturer's instructions. In brief, 1.5 x 10^4 cells/cm^2 were seeded in 96-well plates. 24 h after seeding, the growth medium was replaced by CoBG-conditioned or DMEM medium containing 10% (v/v) FBS (SeraPlus, Pan-Biotech, Germany), 100 U/mL penicillin and 100 µg/mL streptomycin (Gibco®, UK) and 20 mM HEPES (Gibco®, UK). After 24 h or 48 h, the CoBG-conditioned or DMEM medium was removed and the cells were washed once with PBS. 200 µL of 10% (v/v) alamarBlue® in DMEM (Gibco®, UK) were added per well using empty wells as a control. After 2 h incubation in a cell culture incubator, 50 µL of the solution were transferred to a black 96-well plate in triplicates for each sample. Fluorescence was measured at an excitation wavelength of 540 nm and an emission wavelength of 585 nm using a microplate reader (SpectraMax M5, Molecular Devices, UK). Three independent repeats of the experiment were performed each time using a different donor. Each condition was run in quadruplicates.

4.2.6 Chondrogenic differentiation of hMSCs

Bone marrow-derived hMSCs at passage 3 were re-suspended in chondrogenic medium consisting of high glucose DMEM medium (Gibco®, UK) containing 20 mM HEPES (Gibco®, UK) and supplemented with 10 ng/mL TGF-β1 (Fitzgerald, USA), 100 nM dexamethasone (Sigma, UK), 50 µg/mL ascorbic acid-2-phosphate (Sigma, UK), 1% (v/v) non-essential amino acids (Gibco®, UK), 1% (v/v) insulin, transferrin, sodium selenite (ITS) + premix (BD biosciences, USA), and 100 U/mL penicillin and 100 µg/mL streptomycin penicillin–streptomycin (Gibco®, UK). HEPES was added to the medium to ensure a stable pH during medium changes, in particular for the pellet culture. Furthermore, the HEPES was added with respect to the increase in pH caused by partial dissolution of the CoBGs during preparation of the CoBG-conditioned medium.

4.2.6.1 Pellet culture

For chondrogenesis in pellet culture, 200,000 hMSCs were re-suspended in 1 ml of chondrogenic medium, placed into sterile conical mircocentrifuge tubes (Eppendorf, Germany), and spun at 400 xg for 10 min. Cells were incubated in a controlled humidified chamber (37°C, 5% (v/v) CO_2) for 3 days to allow condensation of hMSCs prior to the first medium change. On the day of the first medium change (day 0), 1 mL of either chondrogenic medium, 0%CoBG, 1%CoBG, 1.5%CoBG or 2%CoBG-conditioned medium, all containing chondrogenic supplements, was added to the respective tubes.

Medium was changed every 2 - 3 days for a total culture period of 21 days. Medium was collected to quantify the sGAG release throughout the 21 day culture. The DNA content and sGAG production were measured in 5 independent experiments, each using a different donor. Medium for sGAG release quantification was retained throughout 4 of the independent experiments with different donors. Each condition was run in triplicates for each independent experiment.

4.2.6.2 Culture on poly(ε-caprolactone) (PCL) membranes

In parallel, 200,000 hMSCs were seeded on a poly(*ε*-caprolactone) (PCL) fibrous membrane. To prepare fibrous PCL membranes, 12% (w/v) PCL (average number molecular weight M_n: 80,000, Aldrich, UK) in hexafluorisopropanol was electrospun in random orientation onto a rotating mandrel at 100rpm with an applied potential difference of 16V. The distance between the 16-gauge blunt-tip needle and the rotating mandrel was 10 cm. The resulting PCL membranes were ~ 200 µM in thickness. To restrict cells to the PCL membrane, a 6 mm circular shape was generated using a biopsy punch. The PCL fibrous membrane was then immobilised by placing it between custom fabricated holders made from 200 µL microtubes[396, 397]. The construct was sterilised by incubation in 70% ethanol (EtOH) for 30 min. After 3 washes in PBS, the scaffolds were incubated in 0.01% (w/v) BSA in PBS over-night. Prior to cell seeding, scaffolds were washed twice in sterile PBS and once in sterile MilliQ water. The scaffolds were placed in 6-well plates (2 scaffolds/well) in 1.5 mL of chondrogenic medium. 200,000 hMSCs were seeded in 50 µL on top of the PCL membrane. 24 h after cell seeding, the medium was replaced by 3 mL of CoBG extract-free chondrogenic medium or CoBG-conditioned medium containing chondrogenic supplements. To allow medium exchange from both sides it was ensured that there were no air bubbles trapped at the bottom of the scaffold by carefully turning the scaffolds in the medium after the initial 24 h incubation period. The medium was changed three times per week for a total culturing period of 21 days. The DNA content and sGAG production were measured in three independent experiments each using a different donor (donors #1, #2 and #3). Each condition was run in triplicates for each independent experiment.

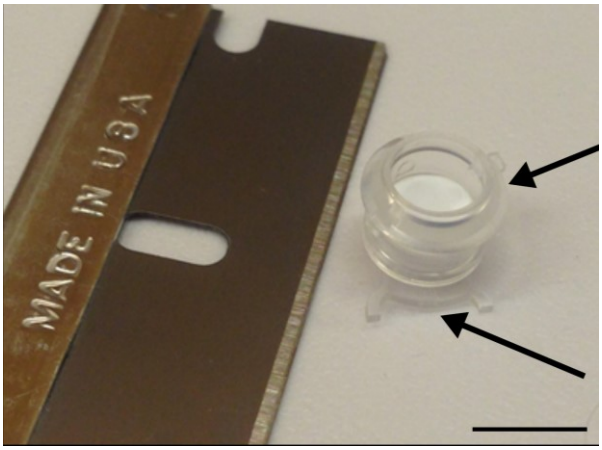


Figure 4.1: Fibrous PCL membrane immobilised between holders. Electrospun PCL fibres were cut into a 6 mm circular shape using a biopsy punch and placed between custom fabricated holders. The holders consisted of parts of 200 µL tubes and the respective tube lids (arrows). Scale bar = 1 cm.

4.2.7 Biochemical analysis of hMSC-derived tissue in chondrogenic conditions

Cell-seeded PCL membranes or hMSC pellets were rinsed twice in PBS and digested with 0.5 mg/mL proteinase-K (PK) (2.5 U/mg, chromozyme assay; Roche, Germany) at 56ºC for 16 h. Prior to washing, the plastic parts of the scaffold construct were removed. The DNA content per pellet or scaffold was measured spectrofluorometrically using Hoechst 33258 dye. In brief, 40 µL of the PK digested sample were incubated with 160 µL of 0.1% (w/v) Hoechst 33258 (Sigma, Germany) in PBS for 20 min in the dark. Fluorescence was measured at 360 nm excitation/465 nm emission. The standard curve was generated with calf thymus DNA (Invitrogen, UK). The sulphated glycosaminoglycan (sGAG) content for each sample and in medium was determined by 1,9-Dimethyl-methylene blue dye (DMMB) (Sigma-Aldrich, Germany) binding assay. In brief, 200 µL DMMB solution (16 mg DMMB in 1 L H_2O containing 3.04 g glycine and 2.37 g NaCl at pH 3.0) were added to 20 µL of PK digested sample and immediately measured at 538 nm absorbance using a Victor3 Micro Plate Reader (Perkin Elmer, USA). For detection of sGAG in medium, the digestion step was not necessary so that DMMB was directly added to 50 µL of retained medium per sample. The standard curve was generated with chondroitin 4-sulphate sodium salt from bovine trachea (Fluka BioChemika, Germany).

4.2.8 Gene expression analysis of key lineage markers by qPCR

To study lineage marker gene expression, 200,000 hMSCs were seeded on PCL fibrous membranes as previously described in section 4.2.6.2 and treated with CoBG extract-free chondrogenic medium or CoBG-conditioned medium containing chondrogenic supplements for 7 days. The medium was changed every 2 - 3 days. After culturing the cells on the membranes over-night (day 0) as well as after 7 days of treatment, cells were harvested for total RNA isolation using RLT buffer (Qiagen, UK)

followed by the RNeasy® Plus Mini Kit (Qiagen, UK), according to supplier's instructions. In brief, the scaffolds were washed twice in PBS prior to transfer to RNase/DNase free Eppendorf tubes containing 350 µL RLT buffer (Qiagen, UK). The tissue was lysed using the TissueLyser II (Qiagen, Germany) with 6 mm diameter stainless steel balls at 25Hz for 3 min. Subsequently, the samples were spun down at 12000 xg for 10 min to remove cell debris and the supernatant was subsequently transferred to a new tube followed by total RNA extraction using the RNeasy® Plus Mini Kit (Qiagen, UK). The amount of total RNA per sample was measured by light absorbance at 260 nm using a Nanodrop 2000c spectrophotometer (Thermo Scientific, UK). RNA quality was assessed by calculating the A260/A280 ratio.

For cDNA generation, 250 ng of total RNA of each sample were reverse transcribed into cDNA using the QuantiTect Reverse Transcription Kit (Qiagen, UK) following manufacturer's instructions. For gene expression analysis by qPCR, RNAse free water (Sigma, UK) was used to dilute the cDNA 1:10. The total reaction volume was 10 µL containing 300 nM of each forward and reverse primer and 5 µL of QuantiTect SYBR® Master Mix (Qiagen, Hilden, Germany) for each sample. A Qiagen Rotor-Gene Q (Qiagen, UK) was used to perform the qPCR reactions. Each sample was run in triplicates. Sequences and cycling conditions of primers used in this study are listed in Table 4.3. Each condition was run for 40 cycles. The primers for *SOX9*, *RUNX2* and *GAPDH* were purchased from Qiagen (QuantiTect® Primer Assay Qiagen, UK), while the second *GAPDH* and *OCT4* primers were custom-designed and ordered from Invitrogen, UK by Dr. Christine Horejs (Table 4.3). Data analysis was performed according to the ΔΔCt method outlined in Chapter 2 (2.2.4). Data are presented relative to the time of seeding (T0).

Table 4.3: Primer sequences and cycling conditions.

	Gene Name	Primer sequence (5'-3')	Cycling conditions
Housekeeping gene	*GAPDH*	(QuantiTect® Primer Assay) or TGGTATCGTGGAAGGACTCATGA ATGCCAGTGAGCTTCCCGTTCAG	95°C for 15s 55°C for 30s 72°C for 30s or 95°C for 15s 62°C for 30s 72°C for 30s
Lineage marker genes	*SOX9*	QuantiTect® Primer Assay	95°C for 15s 55°C for 30s 72°C for 30s
	RUNX2	QuantiTect® Primer Assay	
	OCT4	AGTTGGCGTGGAGACTTTGC CAGGGCTTTCATGTCCTGG	95°C for 15s 62°C for 30s 72°C for 30s

4.2.9 Histology

To study the quality of *in vitro* formed tissue in presence of CoBG-conditioned medium containing chondrogenic supplements or CoBG extract-free chondrogenic medium, pelleted hMSCs were cultured for up to 21 days as previously described and assessed by histology. Tissue generated from pellet and scaffold cultures was washed once in PBS prior to fixation in 70% (v/v) methanol and storage at 4°C. At least 24 h prior to cryo-sectioning, samples were transferred to 5% (w/v) sucrose (Fluka, Germany) in PBS to aid the penetration of the OCT medium on the next day. In order to section the samples, they were embedded in OCT (Jung Tissue Freezing Medium, Leica Biosystems, Germany). The samples were incubated in OCT medium for at least 10 min before being fast frozen at -56°C. For histological staining, 10 µm sections of hMSC pellets and 8 µm sections of cell-laden PCL membranes were prepared using a cryostat at -24°C (Microm HM 560, Thermo Fisher Cryostat Series, USA). Generally, it was aimed to obtain sections from the centre of the pellets and PCL membranes. The sample sections were collected on Menzel-Glaeser Superfrost® Plus slides (Thermo Fisher, Germany) and stored until further use at -20°C.

4.2.9.1 Toluidine Blue staining

As mentioned in Chapter 3, Toluidine Blue is a basic metachromatic dye with a high affinity for acidic tissue components[342]. Toluidine Blue staining of tissues is based on the phenomenon of metachromasia as the dye changes colour depending on its binding partners and surroundings. Characteristically, the cytoplasm of cells stains light blue, the nuclear region dark blue, and proteoglycans purple. According to the protocol described in 3.2.9, slides were selected and allowed to reach RT to enhance the binding of the sections to the slide. The OCT medium was removed by rinsing the slides for at least 10 min in dH_2O. Sections were stained in a 0.1% (w/v) Toluidine Blue (Fluka, Germany) solution in MilliQ water containing 0.1% (w/v) sodium tetraborate (Fluka, Germany). After 1 min the sections were washed in dH_2O until all excess Toluidine Blue was removed. Sections were dried for at least 30 min prior to transfer to xylene. Sections were mounted with Eukitt (Fluka, Germany). After at least 24 h, the sections were observed using an Olympus BX51 epifluorescence microscope equipped with an Olympus DP70 digital camera under visible light. Image processing was performed using GIMP 2.8.

4.2.9.2 Safranin O/ Fast Green staining

Safranin O staining allows the detection of cartilage-like tissue as it binds to negatively charged glycosaminoglycans. Using this method, proteoglycans will be stained orange/ red. Fast Green, which serves as the counter stain of Safranin O, binds strongly to the amino group of proteins by virtue a sulphate group-containing motif. Slides were selected and allowed to reach RT to enhance the binding of sections to the slide. The OCT medium was removed by rinsing the slides for at least 10 min in dH_2O. To stain the nuclei, sections were exposed to Weigerts Haematoxylin (Merck, Germany) for 12 min followed by 10 min incubation in running, lukewarm tap water. Sections were rinsed once in dH_2O and stained in a 0.02% (w/v) Fast Green (Fluka, Germany) solution in MilliQ water containing 0.1% (v/v) acetic acid for 6 min. Remaining Fast Green was rinsed off in a 1% (v/v) acetic acid solution before the slides were exposed to a 0.1% (w/v) Safranin O (Polysciences Inc, Warrington, USA) solution in MilliQ water for 15 min. To remove remaining Safranin O, sections were briefly washed in water before being dehydrated for 2 min each in 70% EtOH, 96% EtOH, 96% EtOH, 100% EtOH and 100% EtOH. Afterwards, the sections were exposed to xylene for 10 min total and mounted with Eukitt (Fluka, Germany). After at least 24 h, the sections were observed using an Olympus BX51 epifluorescence microscope equipped with an Olympus DP70 digital camera under visible light. Image processing was performed using GIMP 2.8.

4.2.10 Raman spectroscopy of hMSC pellet sections

To further assess tissue formation in presence of CoBG-conditioned or CoBG extract free chondrogenic medium, pelleted hMSCs (donor #1) were cultured as previously described for 21 days and subsequently subjected to Raman spectroscopic analysis. As an additional control, control medium was supplemented with $CoCl_2$ to obtain a final concentration of 100 µM. Cobalt (II) chloride hexahydrate

(Sigma-Aldrich, UK) was used to prepare a 10 mM $CoCl_2$ stock solution in MilliQ water. Samples for Raman spectroscopic analysis were fixed in 4% (v/v) PFA in PBS for 20 min. Pellets were rinsed repeatedly and stored in PBS at 4°C. Samples were incubated in OCT (Jung Tissue Freezing Medium, Leica Biosystems, Germany) for at least 10 min prior to being snap frozen in a pre-chilled isopentane bath cooled with liquid nitrogen. For Raman analysis, 10 μm sections of hMSC pellets were prepared using a cryostat (Model OT, Bright Instruments, Huntington, UK) at -21°C specimen temperature. Generally, it was aimed to obtain sections from the centre of the pellets. The sample sections were collected on magnesium fluoride (MgF_2) slides (Global Optics, UK) and stored until further use at -20°C. Prior to Raman analysis, pellet sections were carefully rinsed with MilliQ water to remove remaining OCT. Raman imaging and data analysis were performed in collaboration with Mr. Charalambos Kallepitis.

4.2.10.1 Confocal Raman spectral imaging

Raman imaging was performed on a confocal Raman microscope (alpha300R+, WITec, Ulm, Germany). A 532 nm laser was used with the application of a 10 x dry microscope objective lens. Scattered light was directed through a 100 μm fibre to the spectrometer. Imaging of cell pellet sections was performed in a continuous mode and Raman spectral images of ~1500 x 1500 μm for large and ~1100 x 1100 μm for small pellets were collected. A ~650 nm spatial resolution and 0.3 s integration time were used.

4.2.10.2 Multivariate data analysis

Each Raman image was processed using in-house written analytical methods through Matlab software (2016, MathWorks). Each Raman spectral image was first pre-processed by undergoing a third order polynomial baseline correction, Principal Component Analysis (PCA) assisted cosmic rays removal/outlier and Savitzky–Golay smoothing. K-means clustering was used to segment the pellet regions removing the surrounding background area. Multivariate Curve Resolution (MCR) was used to identify the spectral signatures dominating the data variation (i.e. collagen, GAG and lipid bodies). Afterwards, spectra of pure collagen, GAG and lipids were obtained (Appendix H) and a non-negative least-squares curve fitting analysis was used to calculate abundance values for these components in each pixel of the Raman images. Using the abundance values a semi-quantification and comparison between the different culture conditions was possible.

4.2.11 Statistical analysis

To determine statistical significance, a one-way ANOVA combined with Tukey *post-hoc* test was used for experiments with one time point. For experiments with multiple time points a two-way ANOVA followed by Bonferroni *post-hoc* test was used. A p-value of <0.05 was deemed significant.

4.3 Results

In order to study the influence of cobalt-containing bioactive glass dissolution products on hMSC chondrogenic differentiation, bioactive glasses based on the composition 49.46 mol% SiO_2, (23.08 – X mol%) CaO, X mol% CoO, 26.38 mol% Na_2O, 1.07 mol% P_2O_5 (where X equals 0, 1, 1.5 or 2 mol% cobalt substitution) were prepared. The resulting glass compositions were termed 0%CoBG, 1%CoBG, 1.5%CoBG and 2%CoBG respectively. In particular, there was an interest in identifying an optimal cobalt concentration window or threshold to guide hMSC differentiation events, thus increasing amounts of cobalt were incorporated into the CoBG composition. To obtain results relevant for a patient population, hMSCs of 5 different donors undergoing total hip replacement surgery were used for this study. For chondrogenic differentiation, hMSCs were either cultured as pellets, the gold standard to induce chondrogenesis in hMSCs, or on fibrous PCL membranes for up to 21 days in DMEM or CoBG-conditioned DMEM medium containing chondrogenic supplements.

The fibrous PCL membranes were used to mimic a scaffold system with a multi-layered osteochondral scaffold in mind and were based on the previously published work of McCullen *et al.* and Steele *et al.*[398, 399]. PCL is a FDA-approved, degradable polymer which has found wide application in the field of tissue engineering as scaffold material. PCL is a versatile material that allows the fabrication of scaffolds with varying geometries and mechanical properties whilst being easy to process. Using bovine chondrocytes McCullen *et al.* demonstrated cell proliferation and sGAG deposition on homogeneous or trilaminar composite electrospun PCL scaffolds[398]. The trilaminar composite scaffolds were prepared by sequential electrospinning of PCL resulting in a superficial, middle and deep layer with the aim to mimic the zonal organisation of cartilage. PCL fibres of the superficial zone were aligned while middle and deep zone fibres were randomly oriented. The DNA and (normalised) sGAG contents of constructs increased significantly over time. Bovine chondrocytes seeded on homogeneous scaffolds with fibres either aligned or randomly oriented were shown to proliferate and produce sGAG to a similar degree as on the trilaminar scaffolds. In agreement with an increase in sGAG deposition, *ACAN* and *COL2A1* gene expression were up-regulated over time; however, there were no significant differences between the different scaffolds. Steele *et al.* further developed the idea of a multi-layered scaffold for cartilage repair by combining a layer of aligned PCL fibres with a particulate-templated PCL layer[399]. Over time, chondrocytes seeded in the fibre layer proliferated and produced cartilaginous matrix as shown by biochemical analysis and histology. Taken together, electrospun PCL fibres present an interesting option for the top layer of a multi-zonal scaffold. Since McCullen *et al.* did not observe a significant difference between aligned and randomly oriented fibres, for simplicity, a membrane of PCL fibres with random orientation was chosen for the project presented in this thesis.

4.3.1 Ionic composition of CoBG-conditioned DMEM medium

Increasing amounts of cobalt ions were incorporated into the bioactive glass composition 49.46 mol% SiO_2, (23.08 – X mol%) CaO, X mol% CoO, 26.38 mol% Na_2O, 1.07 mol% P_2O_5 by substitution for calcium on a molar basis (X = 0, 1, 1.5 or 2 mol%) to evaluate their influence on hMSC chondrogenic differentiation (Table 4.1). Preliminary experiments using bovine chondrocytes indicated that the cobalt release from 1%CoBG was not sufficient to induce HIF-1 associated effects on extracellular matrix production (data not shown). Yet, while an increased cartilage-like extracellular matrix synthesis was observed in presence of 2%CoBG, cell density appeared reduced. Therefore, 1.5 mol% calcium were replaced by cobalt to introduce an intermediate condition.

CoBG-conditioned medium was prepared by incubation of CoBG particles in DMEM medium for 4 h at 37°C. The elemental concentrations of silicon, calcium, phosphorous and cobalt in conditioned or DMEM medium were assessed by ICP-OES (Table 4.4). The cobalt ion release into DMEM medium increased corresponding to its molar content in the bioactive glasses. The cobalt release from all cobalt containing compositions (119 µM, 170 µM and 254 µM for 1%CoBG, 1.5%CoBG and 2%CoBG, respectively) was within the range of concentrations routinely used in *in vitro* experiments to mimic hypoxia (100 - 300 µM)[224, 393, 400]. The ion concentrations of silicon, calcium and phosphorous in the medium were comparable between all glass compositions. The calcium concentration in control medium was markedly lower than in CoBG-conditioned medium while the phosphate content was higher. As expected, there was no silicon in the CoBG extract free DMEM medium. The lower amount of phosphorous present in the CoBG-conditioned medium compared to DMEM medium only was most likely due to partial precipitation of calcium phosphate.

Table 4.4: Ion content of CoBG-conditioned DMEM medium. Elemental concentrations of CoBG ionic dissolution products (Si, Ca, P and Co) in DMEM high glucose medium. CoBG particles were incubated in high glucose DMEM for 4 h at 37°C under constant agitation. Ion release was measured by ICP-OES. Elemental concentrations are expressed as mean ± SD of four independent experiments (in ppm unless otherwise stated). The ICP-OES was operated with the assistance of Miss Anu Solanki. ND = non-detectable.

	Si	Ca	P	Co	Co (µM)
DMEM	ND	66 ± 6	29 ± 3	ND	ND
0%CoBG	64 ± 8	142 ± 22	14 ± 2	ND	ND
1%CoBG	65 ± 6	144 ± 18	17 ± 1	7 ± 0	119
1.5%CoBG	66 ± 9	145 ± 16	18 ± 3	10 ± 1	170
2%CoBG	66 ± 4	145 ± 17	16 ± 4	15 ± 1	254

Partial dissolution of bioactive glasses increases the local pH and, in this case, of the CoBG-conditioned medium. The rise in pH is due to H^+ consumption during initial ion exchange reactions[126]. As a high pH can negatively affect cell viability, the CoBG-conditioned medium was equilibrated for at least 4 h or over-night in a standard cell culture incubator (37°C, 5% (v/v) CO_2). After equilibration, the pH of conditioned medium remained slightly higher than in CoBG extract-free DMEM (less than + 0.2) but the difference was deemed acceptable and was similar in all CoBG conditions (Table 4.5).

Table 4.5: pH values of DMEM and CoBG-conditioned DMEM medium before and after equilibration. DMEM and CoBG-conditioned media were equilibrated under standard cell culture conditions (37°C, 5% (v/v) CO_2) for at least 4 h or over-night. pH values are expressed as a mean ± SD of 3 independent experiments.

	pH before	pH after
DMEM	7.47 ± 0.20	7.62 ± 0.03
0%CoBG	8.18 ± 0.17	7.79 ± 0.02
1%CoBG	8.04 ±0.10	7.78 ± 0.02
1.5%CoBG	8.14 ± 0.14	7.79 ± 0.02
2%CoBG	8.11 ± 0.16	7.8 ± 0.02

4.3.2 hMSC metabolic activity in presence of CoBG dissolution products

To assess cell metabolic activity in presence of CoBG dissolution products, hMSCs were seeded on tissue culture plates and their ability to reduce the active component of alamarBlue®, resazurin, was measured after 24 and 48 h. The majority of studies report a cobalt dose- and exposure time-dependent decrease in cell number and metabolic activity[241, 400, 401], yet an increase has been observed as well[240, 391]. There were no statistical differences in metabolic activity after 24 h between conditions. After 48 h, cells cultured in 1.5%CoBG-conditioned medium had a significantly higher alamarBlue® activity than cells cultured in 0%CoBG-conditioned medium. There was no significant increase of cell metabolic activity over time which may indicate that the initial seeding density was too high. Incubating hMSCs with the alamarBlue® solution for 2 h did not result in any visible change in colour by eye, however, warranting careful evaluation of the results. As the hMSCs seemed to tolerate CoBG dissolution products and based on the results obtained by Azevedo *et al.*, the influence of CoBGs on hMSC differentiation was studied[240].

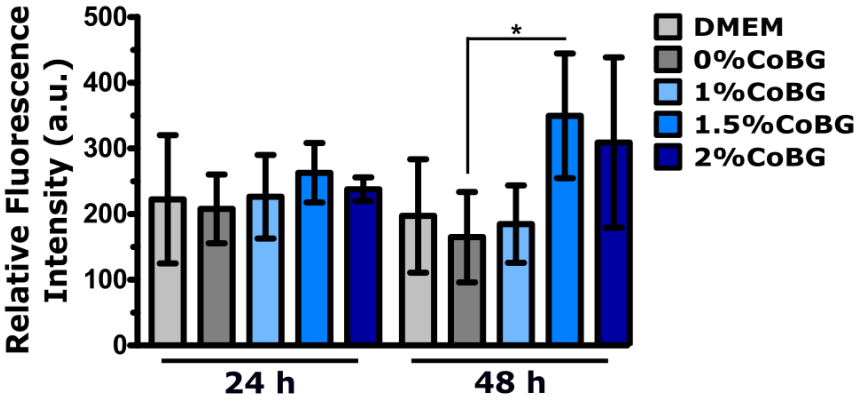


Figure 4.2: Effect of CoBG dissolution products on hMSC metabolic activity at early time points. Cell metabolic activity was assessed after 24 h and 48 h of culture in CoBG-conditioned or DMEM medium using the alamarBlue® assay. Data are represented as the mean ± SD of 3 independent experiments using different donors. Statistical significance was assessed using a two-way ANOVA combined with Bonferroni *post-hoc* test. *p<0.05. There was no significant increase of cell metabolic activity over time.

4.3.3 Downstream effect of CoBG dissolution products on hMSC chondrogenic differentiation

Building on previous studies which showed a beneficial effect of hypoxic (pre-)culture on hMSC chondrogenic differentiation, it was hypothesised that CoBG might enhance chondrogenic lineage commitment of hMSCs in a similar fashion. Moreover, a study by Duval *et al.* demonstrated that $CoCl_2$ treatment resulted in higher gene expression levels of chondrogenic markers further strengthening this hypothesis[393]. To evaluate whether the presence of CoBG dissolution products had a similar effect on hMSC differentiation towards the chondrogenic lineage, hMSCs were cultured in chondrogenic medium or CoBG-conditioned medium supplemented with chondrogenic factors for up to 21 days. For hMSC culture two different systems were used: a) pellet culture, the gold standard for chondrogenic differentiation of hMSCs and b) a fibrous PCL membrane to mimic cell culture on a multi-layered osteochondral scaffold. For both systems, hMSCs were cultured for up to 21 days in chondrogenic medium in the presence or absence of CoBG ionic dissolution products.

4.3.3.1 Accumulation and release of sGAG in hMSC pellet culture model

The amount of DNA and sGAG in hMSC pellets was determined on day 0 (D0) and at the endpoint of the study after 21 days (Fig. 4.3A, B). The release of sGAG from pellets into the medium was monitored over the entire culture period (Fig. 4.3C). Here, D0 marks the day of the first medium change after pellet formation. There was no significant difference in DNA content between conditions and compared to D0 (Fig. 4.3A). Quantification of sGAG accumulation normalised to DNA content in pellets cultured in bioactive glass extracts, showed a cobalt dose-dependent decrease in sGAG production (Fig. 4.3B).

The normalised sGAG/DNA contents in the 0%CoBG condition and in CoBG extract-free chondrogenic medium were significantly higher than on day 0 ($p<0.01$) suggesting successful chondrogenic differentiation in both groups. The considerable error bar for the 0%CoBG condition owed to some degree of donor variability. While 0%CoBG dissolution products had no or a beneficial effect on sGAG production by donors #1, #4 and #5 compared to chondrogenic medium, sGAG accumulation by donors #2 and #3 was reduced when compared to the chondrogenic medium only reference (Appendix E). In contrast, the normalised sGAG content in presence of 1%CoBG, 1.5%CoBG and 2%CoBG was not significantly different compared to day 0. In presence of 1.5%CoBG and 2%CoBG dissolution products, the normalised sGAG content was significantly lower compared to 0%CoBG on day 21. The difference in sGAG synthesis of pellets cultured in 2%CoBG-conditioned medium compared to 0%CoBG was highly significant ($p<0.01$) indicating a cobalt dose-dependent mechanism. The normalised sGAG values for 1%CoBG, 1.5%CoBG and 2%CoBG were also significantly lower compared to CoBG extract-free chondrogenic medium further indicating a reduction in chondrogenic differentiation. The sGAG release followed a similar trend as observed for sGAG accumulation (Fig. 4.3C). The sGAG release over time from pellets cultured in 0%CoBG-conditioned or in CoBG extract-free chondrogenic medium was significantly increased when days 1 - 7 were compared to days 15 - 21 ($p<0.01$ and $p<0.05$ respectively) suggesting a progressive commitment to the chondrogenic lineage. Overall, the extent of sGAG release followed a similar, cobalt-dose dependent trend as observed for sGAG accumulation with significantly lower values for 2%CoBG compared to 0%CoBG and CoBG extract-free chondrogenic medium when days 15 - 21 were considered.

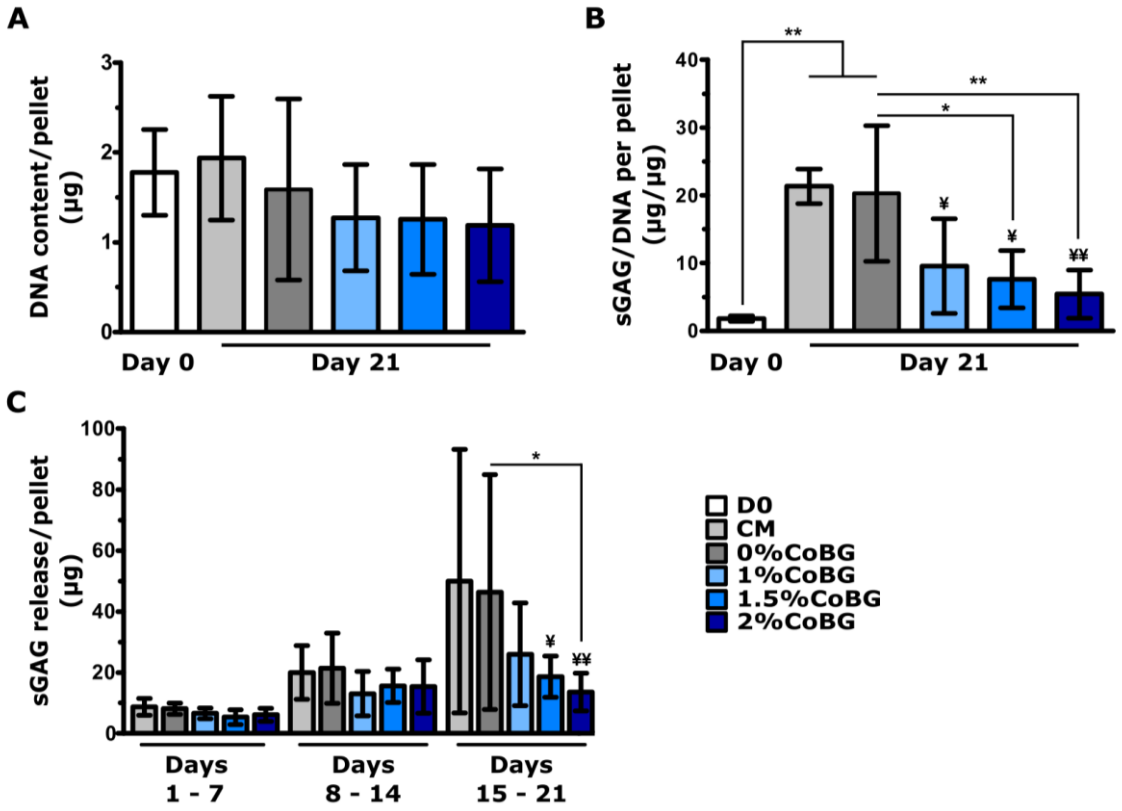


Figure 4.3: Effect of CoBG dissolution products on sGAG production and release by hMSCs in pellet culture. hMSC pellets were cultured in chondrogenic medium (CM) or CoBG-conditioned medium containing chondrogenic supplements for 21 days prior to quantification of A) DNA by Hoechst or B) sulphated glycosaminoglycans (sGAG) by DMMB. C) The sGAG release from pellets was measured in medium retained throughout the culture period. A, B) Data are expressed as mean ± SD of 5 independent experiments using different donors. Significance was assessed by a one-way ANOVA combined with Tukey *post-hoc* test. C) sGAG release profile of hMSC pellets cultured in CoBG-conditioned medium over the 21 days culture period. Data are expressed as mean ± SD of 4 independent experiments using different donors. Statistical significance was assessed by two-way ANOVA combined with Bonferroni *post-hoc* test. *p<0.05, **p<0.01. B, C) For visual display, significant differences compared to CM are indicated separately, ¥p<0.05 (vs. CM), ¥¥p<0.01. Statistically significant changes over time are not indicated in the figure. C) The amount of sGAG in retained medium from days 15 - 21 was significantly higher than in medium from days 1 - 7 for 0%CoBG (p<0.05) and CM (p<0.01).

4.3.3.2 Accumulation of sGAG in hMSC-seeded PCL membrane model

hMSCs from three donors (#1, #2, and #3) were subjected to culture on PCL membranes in presence of CoBG-conditioned medium supplemented with chondrogenic factors or CoBG extract free chondrogenic medium prior to biochemical analysis (Fig. 4.4). The DNA and sGAG contents of hMSC/PCL constructs were quantified after 7, 14 and 21 days of culture and on day 0 (D0). In this system, the first medium change occurred 24 h after seeding of the hMSCs on the PCL constructs (defined as D0). To illustrate that the response of hMSCs to CoBG ionic dissolution products had a

strong donor dependent component, the three donors are presented separately. For all three donors, the amount of DNA peaked at day 7 which may be explained by a reduction of cell proliferation during differentiation of progenitor cells (Fig. 4.4A, C, E). For all donors, the presence of cobalt within the bioactive glass extracts dose-dependently lowered the values for DNA compared to the 0%CoBG condition cultured for the same time period. There was a slight difference in seeding efficiency between donors, as the DNA content of scaffold constructs of donor #1 was almost doubled compared to donors #2 and #3. While all donors responded comparably to CoBG-dissolution products regarding the DNA content, there was no common trend for normalised sGAG production (Fig. 4.4B, D, F). Quantification of sGAG accumulation normalised to DNA showed that chondrogenic differentiation of donor #3 was not successful as indicated by very low sGAG/DNA values for all conditions (Fig. 4.4F). Even though the amount of DNA remained constant, the sGAG/DNA accumulation appeared to decline over time with overall low values. Pellet culture of hMSCs from donor #3 resulted in markedly higher values for normalised sGAG accumulation (Appendix E) suggesting that the lack of differentiation in the PCL membrane system was either due to the culture method itself or a technical error. Therefore, the discussion will focus on donors #1 and #2 only from here onwards.

The normalised sGAG values for donors #1 and #2 were higher for all conditions at all time-points compared to day 0. There was a slight increase in normalised sGAG from day 7 to day 14 suggesting a progressive chondrogenic differentiation in all conditions by both donors. Quantification of normalised sGAG synthesis of donor #1 showed a similar trend as observed with the pellet culture model (Fig. 4.4B). Comparison of the normalised sGAG values between conditions revealed a pronounced cobalt dose-dependent reduction that was apparent at all chosen time points. Overall, donor #1 produced the highest amounts of sGAG compared to donors #2 and #3 in the scaffold culture model. Analysis of normalised sGAG production of donor #2 revealed an inconsistent trend with fluctuating results between conditions and time points (Fig. 4.4D). While chondrogenic medium only performed well on days 7 and 14, the amount of sGAG/DNA dropped on day 21 which may allude to a technical problem with the samples, either during the last week of culture or during processing. The sGAG/DNA values in presence of 0%CoBG were much lower than in CoBG extract-free chondrogenic medium; however, this result was to some extent consistent with pellet culture of donor #2 (Appendix E). Surprisingly, sGAG accumulation seemed similar if not enhanced in presence of 1%CoBG dissolution products compared to CoBG extract-free chondrogenic medium on days 14 and 21. In pellet culture, 1%CoBG performed similarly to 0%CoBG but not as good as chondrogenic medium (Appendix E).

Overall, biochemical assessment of hMSC/PCL membranes showed that only donors #1 and #2 successfully differentiated towards the chondrogenic lineage. There was a considerable variability between donors #1 and #2 regarding their response to CoBG-conditioned media. While donor #1 differentiated well over time and showed a similar trend as obtained with pellet culture, sGAG/DNA quantification of donor #2 gave rise to inconsistent results especially regarding the CoBG extract-free chondrogenic medium and the 1%CoBG condition. The sGAG/DNA synthesis by donor #3 did not

increase over time and was overall low suggesting a very limited differentiation. Whether the discrepancies between pellet and scaffold culture obtained for donors #2 and #3 owed to the culturing technique or a technical error cannot be deduced from this data.

Taken together, donor #1 hMSCs cultured as pellets or on PCL membranes responded similarly to the CoBG-conditioned medium. A comparable trend for DNA and normalised sGAG content was observed with a cobalt dose-dependent decrease in DNA and cartilage-like extracellular matrix production. In contrast, donor #2 hMSCs gave inconsistent results with respect to the normalised sGAG content when seeded on PCL membranes. Comparing the two culture systems for all donors, hMSCs cultured as pellets produced more sGAG suggesting a stronger commitment to the chondrogenic lineage.

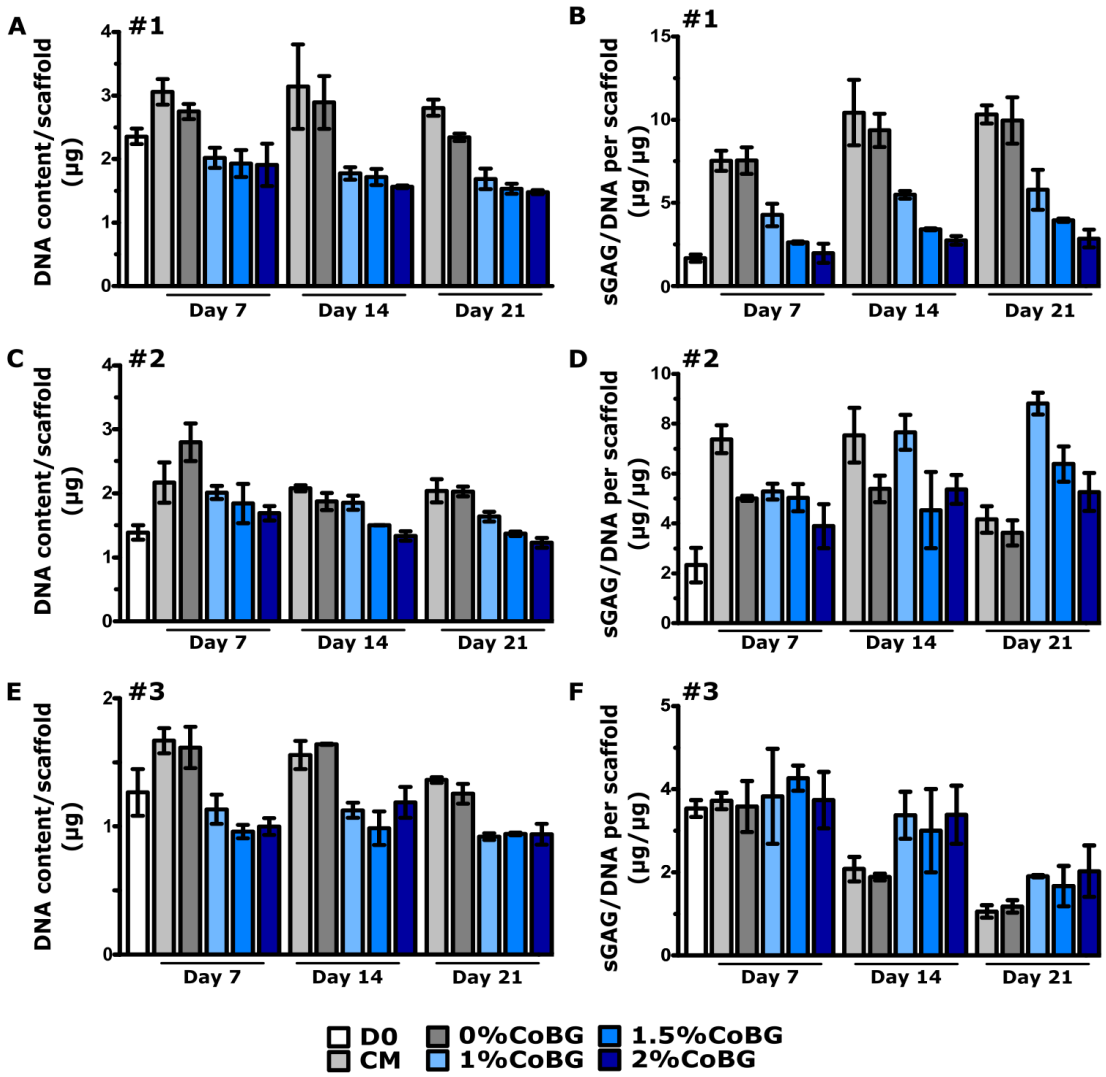


Figure 4.4: Effect of CoBG dissolution products on sGAG production by hMSCs seeded on PCL membranes. hMSCs were cultured on PCL membranes in chondrogenic medium (CM) or CoBG-conditioned medium in presence of chondrogenic supplements for up to 21 days prior to quantification of A, C, E) DNA by Hoechst or B, D, F) sulphated glycosaminoglycans (sGAG) by DMMB. Data are expressed as mean ± SD of 3 biological replicates. A, B) donor #1, female born in 1944, (C, D) donor #2, male born in 1958, (E, F) donor #3, male born in 1968. As the results for the different donors are presented separately, no statistical analysis was performed.

4.3.3.3 Gene expression of key differentiation markers at early time points of hMSC chondrogenic culture on PCL membranes

To further characterise the lineage commitment of hMSCs, the gene expression of key lineage markers was studied by quantitative real-time PCR (Fig. 4.5). hMSCs were cultured on PCL membranes in chondrogenic medium or CoBG-conditioned medium in presence of chondrogenic supplements. Since donor #3 failed to differentiate in scaffold culture, only donors #1 and #2 were subjected to gene expression analysis. For this purpose, *SOX9*, *RUNX2* and *OCT4* were chosen to represent the

chondrogenic and osteogenic lineage as well as the undifferentiated stem cell phenotype, respectively. The principal chondrogenic differentiation marker gene, *SOX9*, has been identified as target gene of HIF-1α. After 7 days of culture, total RNA was isolated and subjected to gene expression analysis. Gene expression levels were normalised to the housekeeping gene *GAPDH* and presented relative to T0 (time of seeding). There were no significant differences in the expression levels of all tested genes which likely owed to the fact that only two donors were used for the analysis. To gain statistical power, the experiment needs to be repeated with more donors. Considering the overall low expression levels of *RUNX2* and *OCT4* as well as the fact that only two donors were used, the gene expression results need to be considered as preliminary. In particular, since chondrogenic differentiation on scaffolds was inferior to the pellet culture model, it would be interesting to investigate differentiation marker gene expression in hMSC pellets in presence of CoBG dissolution products. An up-regulation of *OCT4* by cobalt ions would present a highly interesting result opening up avenues for tissue engineering applications.

Some studies have identified *GAPDH* as hypoxia responsive gene, although this effect appears to be cell type specific. While *GAPDH* expression in nucleus fibrosus cells was independent of oxygen availability, *GAPDH* was up-regulated in HeLa cells in response to hypoxia[402]. In endothelial cells, *GAPDH* expression was regulated by HIF-2α while in a hepatoma cell line, HIF-1α and HIF-2α contributed equally to *GAPDH* expression[403]. Since *GAPDH* has been used as housekeeping gene in previous studies assessing the effect of hypoxia on hMSCs it was chosen for normalising gene expression values in the present experiment[404].

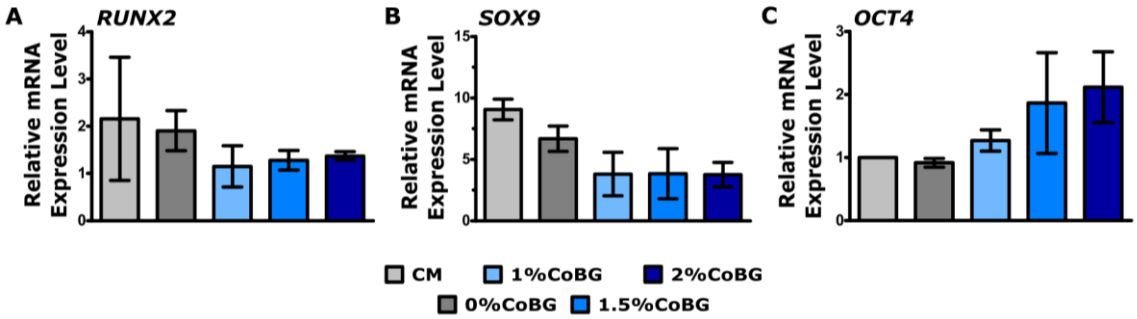


Figure 4.5: Effect of CoBG dissolution products on lineage marker gene expression. hMSCs were cultured on PCL membranes for 7 days in chondrogenic medium (CM) or CoBG-conditioned medium prior to RNA isolation. Gene expression levels of A) *RUNX2*, B) *SOX9* and C) *OCT4* were assessed, representing the osteogenic and chondrogenic lineage and the undifferentiated state, respectively. The relative mRNA expression was normalised to the housekeeping gene *GAPDH* and the fold increase expressed relative to T0 (time of seeding). Data are represented as the mean ± SD of 2 independent experiments (donors #1 and #2). Statistical significance was assessed by a one-way ANOVA combined with a Tukey *post-hoc* test. Data were not statistically different.

4.3.4 Cartilage-like tissue formation by hMSC in CoBG-conditioned medium

To further analyse and visualise the cartilaginous tissue formation by hMSCs in presence of CoBG dissolution products, pellets and hMSC/PCL constructs were subjected to histological assessment after 21 days in culture.

4.3.4.1 Characterisation of extracellular matrix production in hMSC pellet culture by histology

Visual examination of hMSC pellets at day 21 showed that the size of pellets was reduced in presence of cobalt-containing bioactive glass extracts. Histological characterisation of hMSC pellets by Toluidine Blue and Safranin O/ Fast Green staining confirmed a cobalt-dependent reduction of cartilage-like extracellular matrix production by hMSCs (Fig. 4.5 and Appendix F). For donors #2 and #3, cartilage-like extracellular matrix production was reduced in presence of all bioactive glass extracts which is in line with the results obtained by biochemical analysis (4.3.3.1 and Appendix E, F). The following discussion of the results obtained by histology is focussed on donors #1, #4 and #5. Pellets cultured in chondrogenic and 0%CoBG-conditioned medium demonstrated a strong positive staining for sGAGs, thereby suggesting a cobalt-dependent effect within the bioactive glass dissolution products on cartilaginous extracellular matrix production. Toluidine Blue, a metachromatic stain, appears light purple in presence of acidic extracellular matrix proteins such as GAGs. In absence of such negatively charged proteins, Toluidine Blue adopts a dark blue colour as seen in the staining of pellet sections on day 0. 0%CoBG and chondrogenic medium only both appeared light purple corroborating the results obtained by biochemical analysis. With increasing cobalt concentration in the CoBG-conditioned media, the staining of pellet sections turned continuously darker, more resembling the colour of day 0 than 0%CoBG.

Similarly, Safranin O staining, which gives rise to a red colour when bound to acidic sGAGs, was visible throughout the pellet sections of the chondrogenic medium and 0%CoBG-conditioned medium conditions but only faintly visible in presence of cobalt ions and located near the rim regions of the pellets. While there was some positive staining for cartilage-like matrix production in the 1%CoBG and 1.5%CoBG conditions, pellets cultured in presence of 2%CoBG dissolution products lacked Safranin O staining and appeared to be very condensed indicating a cobalt-dependent effect.

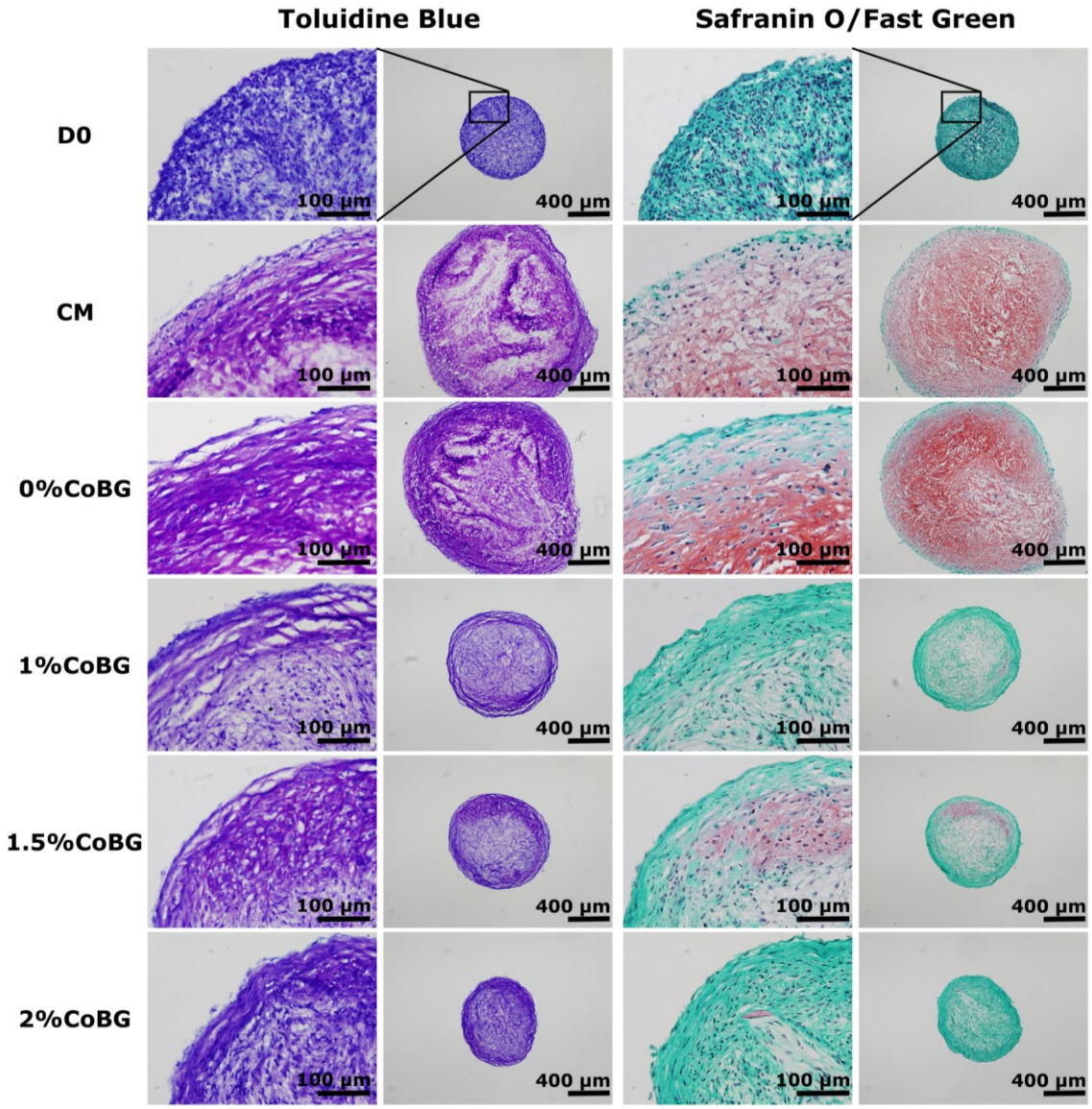


Figure 4.6: Effect of CoBG dissolution products on *in vitro* cartilage-like tissue formation by hMSC pellets. Prior to histological analysis, hMSCs were grown as pellets in chondrogenic medium (CM) or CoBG-conditioned medium containing chondrogenic supplements for 21 days. Proteoglycan deposition in the extracellular matrix was assessed by a) Toluidine Blue (purple metachromasia) and b) Safranin O staining. Fast Green stains collagens and other proteins. Representative images (donor #5) are shown.

4.3.4.2 hMSC chondrogenesis in PCL membrane model

Histological assessment of the hMSC/PCL constructs revealed a thin layer of tissue consisting of several layers of cells on the PCL membrane for all conditions after 21 days of culture (Fig. 4.7). Whilst the majority of the cells localised on top of the membrane, few cells appeared to have infiltrated into the PCL fibres. The cell layer was thinner and appeared denser with fewer extracellular matrix in the presence of cobalt ions from the CoBG dissolution products. Moreover, the cells seemed elongated and more flattened than in the chondrogenic medium and 0%CoBG-conditioned medium conditions. Compared to the pellet culture model, significantly less cartilaginous tissue formation was visible, further corroborating the results obtained by biochemical analysis. While Toluidine Blue staining, indicative of sGAGs, was light purple in the 0%CoBG-conditioned and chondrogenic medium conditions, there was no positive Safranin O staining. This lack of staining was not due to a technical error during staining, as the chondrogenic medium condition for another donor (#2) showed some red staining (Appendix G), but was more likely related to an insufficient amount of sGAGs present to give rise to positive Safranin O staining for donor #1. For the pellet culture model, Safranin O/ Fast Green staining was in line with the results obtained by biochemical analysis. Yet, in conditions with a relatively low sGAG content such as in presence of cobalt in the pellet culture system or, indeed, in the hMSC/PCL construct culture model, Safranin O staining was absent. This confirmed previous findings, that Safranin O fails to stain tissues with a low sGAG content and may thus not be sufficiently sensitive[346, 405].

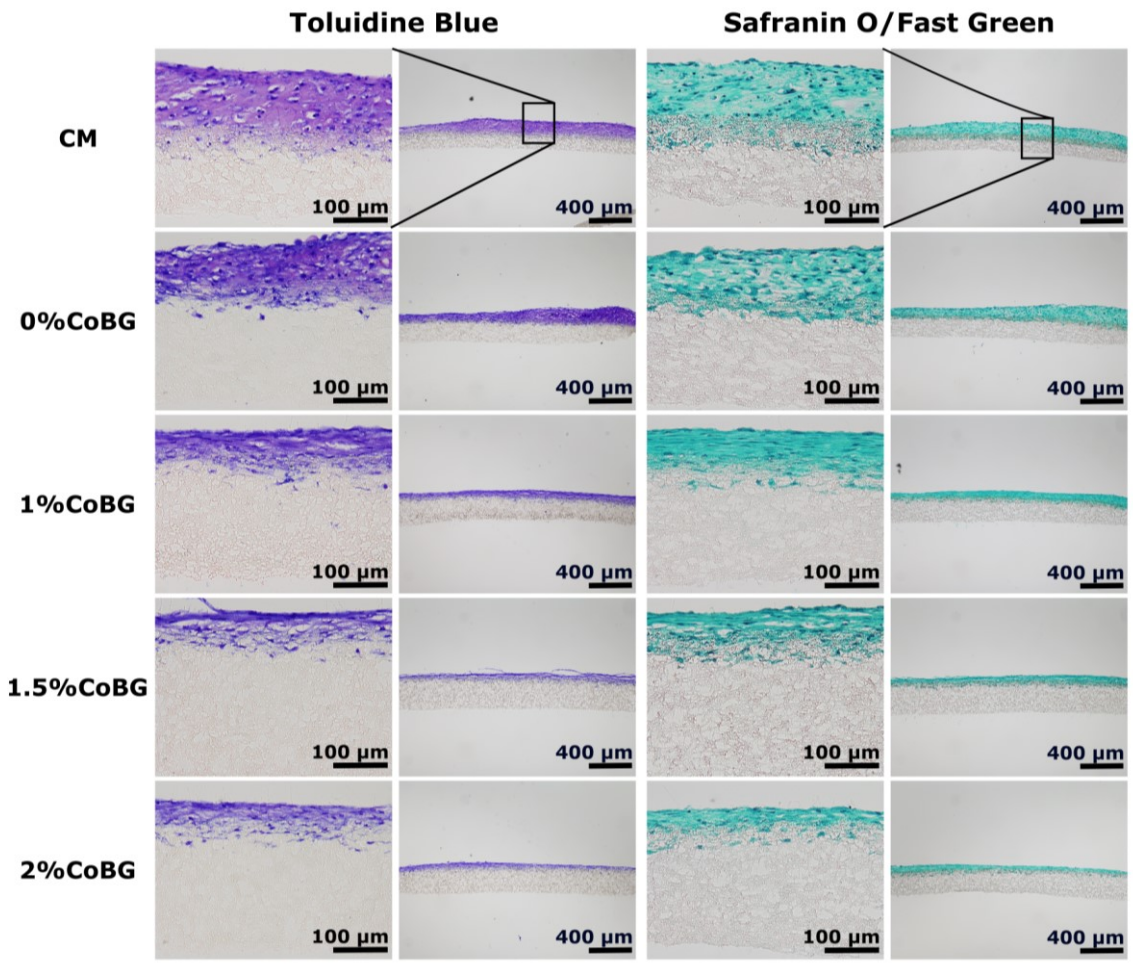


Figure 4.7: Effect of CoBG dissolution products on *in vitro* cartilage-like tissue formation by hMSCs seeded on PCL membranes. Prior to histological analysis, hMSCs seeded on PCL membranes were cultured in chondrogenic medium (CM) or CoBG-conditioned medium supplemented with chondrogenic factors for 21 days. Proteoglycan deposition in the extracellular matrix was assessed by a) Toluidine Blue (purple metachromasia) and b) Safranin O. Fast Green stains collagens and other proteins. Representative images (donor #1) are shown.

4.3.5 Raman spectroscopy mapping of hMSC pellet sections

So far, it was not clear whether the reduction in hMSC chondrogenesis observed in presence of cobalt-containing bioactive glass dissolution products was caused by a joined effect of cobalt with other bioactive ions or exclusively cobalt-dependent. To address this question, 100 µM $CoCl_2$ was added to chondrogenic medium as an additional condition. To further characterise the ECM produced by hMSC pellets cultured in the various CoBG-conditioned media and in $CoCl_2$ supplemented chondrogenic medium, Raman spectroscopy mapping was applied to hMSC pellet sections. Raman spectroscopy is a vibrational spectroscopic technique capable of providing detailed biochemical characterisation of live or fixed cells and tissues[250, 406, 407]. Raman spectroscopy presents a label-free and non-invasive alternative to conventional techniques which makes it an attractive tool especially for tissue

engineering. The Raman effect is a two photon inelastic light scattering event, caused by the interaction of a constant electric field with the vibrational state of chemical bonds of molecules that are located within the field. Chemical bonds can be identified by bond-specific differences in energy between incident and scattered photons. The Raman spectrum of chemical bonds in tissues or (single) cells provides a "biochemical fingerprint" that can be used to characterise them and uncover subtle differences in biochemical composition between sample groups[407]. Spectra of pure components, e.g. from collagen, can be used to create references of biochemical signatures which can facilitate a better characterisation of these components within cells. In particular, Raman spectroscopy is a valuable tool to identify cellular biopolymers such as nucleic acids, proteins, lipids and carbohydrates. Furthermore, it does not require any prior knowledge of the samples' chemical structure. Thus, Raman spectroscopy provides the whole spectrum of chemical bonds present in a sample thereby giving a complete view of a biological system which may help to uncover previously unknown tissue characteristics. In the context of this chapter, differences in the composition of the extracellular matrix of hMSC pellets cultured in the various media conditions were of particular interest.

hMSCs (donor #1) were pelleted and cultured for 21 days in the various media conditions in presence of chondrogenic supplements as previously described in this chapter. After 21 days, pellets cultured in CoBG extract-free chondrogenic medium or 0%CoBG-conditioned medium were markedly bigger than in presence of cobalt-containing bioactive glass extracts or $CoCl_2$ (Fig. 4.8A). Prior to Raman spectroscopy, hMSC pellets were sectioned as described in 4.2.10 and collected on MgF_2 slides. Raman spectral analysis on the pellet sections highlighted clear differences between the experimental conditions. The characteristic spectra that were identified by MCR clustering analysis were classified as GAGs, collagens, and lipids (Fig. 4.8A). Using spectra collected from pure GAG, collagen and lipid samples in combination with the non-negative least-squares curve fitting analysis allowed the semi-quantitative assessment of these discriminators (Fig. 4.8B). The GAG, collagen and lipid content was higher in the 0%CoBG and chondrogenic medium only condition than in all cobalt-containing media likely owing to an overall reduction in extracellular matrix production. The GAG signal appeared to decrease with increasing cobalt ion concentrations corresponding to the previously obtained results by biochemical analysis and histological stainings. Addition of $CoCl_2$ to chondrogenic medium induced a similar outcome as cobalt-containing bioactive glass extracts. The relative GAG signal in presence of $CoCl_2$ was higher than in the CoBG conditions but lower than the values for 0%CoBG and CoBG-free chondrogenic medium, possibly indicating a cobalt dose-dependent effect. As only one pellet section per condition was analysed the results warrant further confirmation and are preliminary; however, the results presented here are in line with histology and the biochemical analysis.

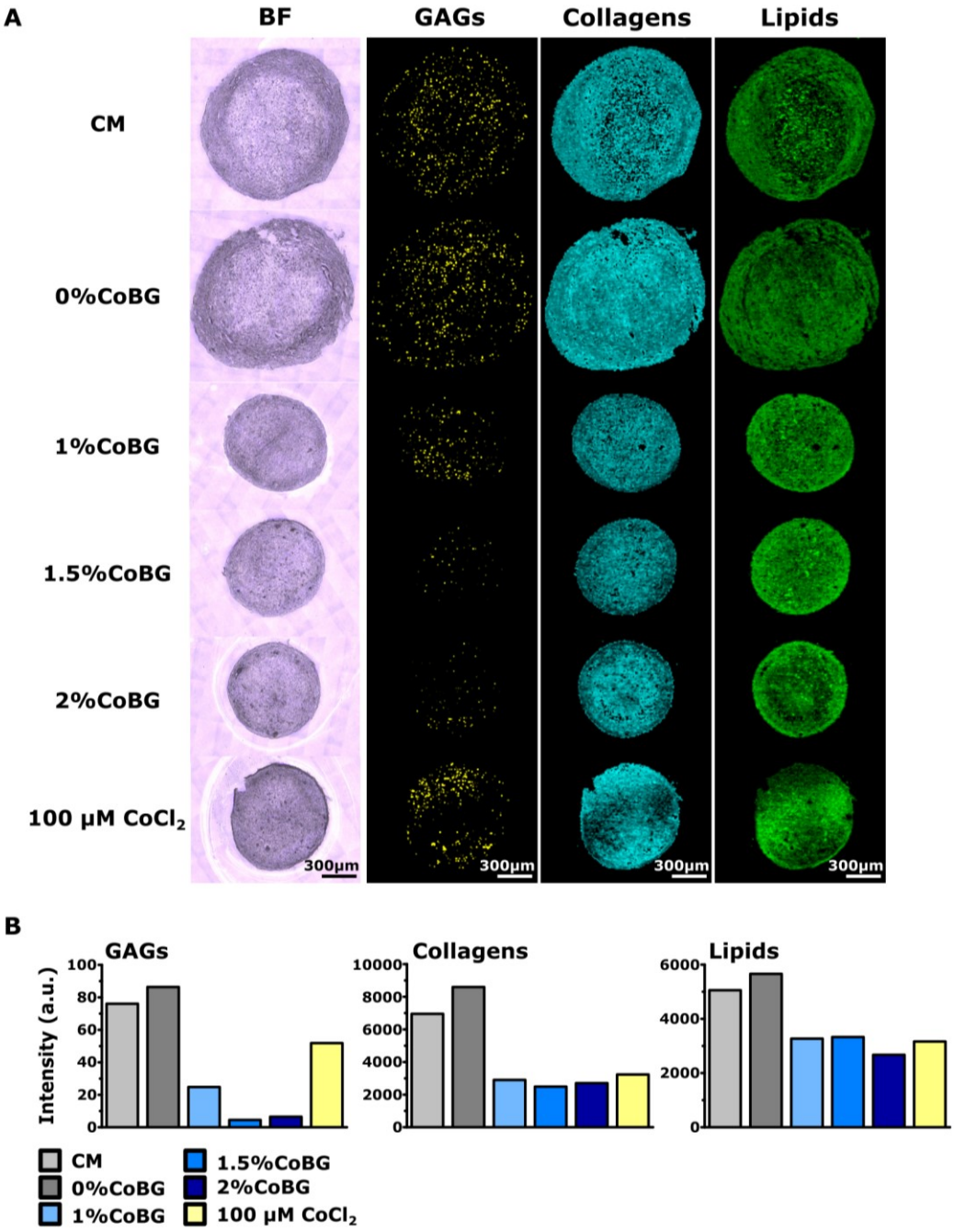


Figure 4.8: Extracellular matrix characterisation of hMSC pellets by Raman spectral analysis. Prior to Raman spectral analysis, pelleted hMSCs were cultured in chondrogenic medium (CM) or CoBG-conditioned medium containing chondrogenic supplements for 21 days. Additionally, chondrogenic medium was supplemented with 100 µM $CoCl_2$. A) Bright field (BF) images of respective pellet sections along with pseudo-coloured images of characteristic spectra within the hMSC pellet sections. Scale bars = 300 µm. (B) Semi-quantitative analysis of Raman spectra of one pellet section per condition. The intensity represents the number of pixels within each pellet section positive for the identified discriminator spectra (GAGs, collagens or lipids) multiplied by the respective signal intensity. Raman imaging and data analysis were performed in collaboration with Mr. Charalambos Kallepitis.

4.4 Discussion

In this study, the effect of CoBG dissolution products on hMSC chondrogenic differentiation was investigated. To induce hMSC chondrogenesis, two different models, the standard pellet culture and culture on a PCL fibrous membrane, to mimic the top layer of a stratified scaffold system, were adopted. The data presented in this chapter showed that the presence of CoBG dissolution products consistently reduced chondrogenic lineage commitment in a cobalt dose-dependent manner in both culture systems. In the chondrogenic and 0%CoBG-conditioned medium conditions, hMSCs differentiated well, albeit with some degree of donor variability, further underscoring a cobalt-dependent effect. In pellet culture, the amount of DNA was not significantly different compared to day 0 after 21 days of culture for all conditions. Such a result was expected in pellet culture as cells cease to proliferate once they commit to the chondrogenic lineage and has been reported previously[347, 357]. In the PCL membrane culture system, cells proliferated during the first week after which the DNA content peaked for the 0%CoBG-conditioned and CoBG extract-free chondrogenic medium conditions. The DNA content of hMSC/PCL constructs was lower in presence of cobalt within bioactive glass extracts in a dose-dependent manner correlating with the trend observed in pellet culture.

Quantification of sGAG accumulation normalised to the respective DNA content of pellets revealed a cobalt dose-dependent reduction that correlated with increasing concentrations of cobalt within the CoBG dissolution products. In chondrogenic medium and medium containing 0%CoBG dissolution products, hMSCs differentiated well as indicated by a satisfactory level of sGAG synthesis compared to values in the literature[358]. In presence of ion products derived from either 1%CoBG or 1.5%CoBG, pellets were slightly bigger than on day 0 with more extracellular matrix suggesting some degree of chondrogenic lineage commitment as visualised by histology. Yet, Safranin O staining was either negative or only localised to certain areas of the pellets. In presence of 2%CoBG dissolution products, there was little extracellular matrix and cells appeared to be densely packed after 21 days of culture. Exposure to 2%CoBG seemed to condense the pellets, with tightly packed nuclei beyond the morphology after initial pellet formation (D0) as observed by visual examination of the Toluidine Blue and Safranin O/Fast Green stained pellet sections. Similarly, the cell layer on the PCL membranes appeared more compact with cell nuclei closely packed on top of each other in the 2%CoBG condition.

Comparing the two different culture systems, the classic pellet culture proved as superior system to induce chondrogenic differentiation in hMSCs. The mean sGAG/DNA values were considerably higher in pellet culture indicating that chondrogenic differentiation on the PCL membranes was not as efficient. Pellet culture is designed to recapitulate the processes during growth plate development and in particular mesenchymal condensation[349]. It has been established by several early studies that chondrogenic differentiation of MSCs necessitates a high cell density both *in vivo* and *in vitro* as reviewed by DeLise *et al.*[349]. Considering the rather thin cell layer on the PCL membranes as visualised by histology, the seeding density of 200,000 hMSCs might not have been sufficient for 6 mm

in diameter membranes. Furthermore, concerted cell-cell and cell-matrix interaction patterns are thought to be crucial for MSC condensation and subsequent chondrogenesis during embryonic development. Culturing hMSCs as a layer may deprive the cells of some of the characteristics of condensation and may thus hinder a successful chondrogenic differentiation. Yet, initial seeding on the PCL membranes and cell attachment after 24 h were satisfactory considering the amount of DNA after 24 h (D0). The discussion will focus on the pellet culture model from here onwards.

The reduction of hMSC chondrogenic differentiation in 1%CoBG, 1.5%CoBG and 2%CoBG-conditioned medium was likely due to the cobalt ions within the bioactive glass dissolution products. Yet, at this point, no definite conclusion could be drawn as a joined effect of cobalt together with other bioactive ions was possible. Therefore, 100 µM $CoCl_2$ were added to chondrogenic medium as an additional condition. Pellets cultured in 100 µM $CoCl_2$-supplemeted chondrogenic medium were similar in size as the other cobalt-containing conditions and, importantly, smaller than the chondrogenic and 0%CoBG-conditioned medium conditions. Semi-quantitative analysis of Raman spectral imaging of pellet sections indicated a higher overall relative GAG content in the pellets cultured in chondrogenic and 0%CoBG-conditioned medium compared to all other conditions which is in line with the previous results. The relative GAG signal intensity was higher in the 100 µM $CoCl_2$ condition than in presence of all cobalt-containing bioactive glass dissolution products which may be due to cobalt-dose dependent effects. With respect to the cobalt ion concentration, supplementation with 100 µM $CoCl_2$ resembled 1%CoBG-conditioned medium (119 µM). Indeed, pellets cultured in these two conditions were similar in size and GAG signature albeit the latter was a bit higher in the 100 µM $CoCl_2$ group possibly owing to the slightly lower Co^{2+} content. The intensity for collagens and lipids was comparable between all cobalt-containing groups and differed from the chondrogenic medium and 0%CoBG-conditioned medium conditions. This trend is likely due to a higher overall amount of extracellular matrix in presence of 0%CoBG dissolution products and CoBG extract-free chondrogenic medium. Since Raman spectral imaging analysis was only performed on 1 section of 1 pellet (donor #1), the results need to be considered as preliminary and warrant further confirmation. The difference in pellet size between cobalt-free and all cobalt-containing conditions, however, was observed in at least one other pellet replicate by the same donor pointing towards a cobalt-dependent effect.

Since pellet culture was performed in closed 1.5 mL propylene tubes, the extent of gas exchange between the atmosphere in the tube and the incubator is difficult to estimate. Compared to data in the literature, the chondrogenic medium condition performed well both with respect to sGAG/DNA content as well as to histological assessment. Therefore, a hypoxic environment might have been unintentionally created in the closed propylene tubes. Most studies adopting the pellet culture method used 15 mL falcon tubes with a loosened cap for gas exchange[408, 409] or punctured the microcentrifuge tubes and then transferred pellets to low-binding 96-well plates[410]. Thus, an effect of an unintentionally created hypoxic environment during pellet culture in microcentrifuge tubes cannot be excluded. True hypoxia in combination with the artificial cobalt-induced hypoxia may have over-stimulated the HIF-1

pathway resulting in a downstream reduction of differentiation capacity of the hMSCs. Yet, the cobalt-dose dependent trend observed in pellet culture correlated well with the results obtained with scaffold culture, at least for donor #1, supporting a cobalt-dependent effect. Furthermore, Adesida *et al.* used the same microcentrifuge experimental set up as in the study described herein and observed differences in extracellular matrix production between groups cultured at different oxygen tensions indicating a gas exchange between the microcentrifuge tube and the atmosphere in the incubator[358]. However, the differences between groups were subtle so that a hindered gas exchange cannot be fully excluded based on that study.

Similar to other studies, we encountered some degree of donor variability[358]. Donors #1, #4 and #5 tended to have a superior chondrogenic capacity as characterised by higher sGAG/DNA values, pellet formation and more intense and uniform Safranin O staining compared to donors #2 and #3. Furthermore, donors responded differently to bioactive glass dissolution products in general which was most pronounced for the 0%CoBG condition (Appendices E, F). The sGAG /DNA accumulation in pellets cultured in 0%CoBG-conditioned medium had a tendency to be higher than in the control condition for donors #1, #4 and #5. For these donors, a pronounced reduction in chondrogenic differentiation with increasing cobalt concentration was observed. In contrast, the sGAG/ DNA contents of pellets prepared from donors #2 and #3 were markedly lower in presence of 0%CoBG dissolution products compared to chondrogenic medium only. Here, all bioactive glass-conditioned media, save 2%CoBG, had a similar effect on chondrogenesis. Thus, bioactive glass dissolution products in general appeared to reduce cartilaginous extracellular matrix production by donors #2 and #3 while cobalt had a subordinate effect only visible in presence of high doses (2%CoBG). This observation suggests that bioactive ions themselves can differently affect the donors possibly overruling the influence of single ion species (i.e. cobalt).

An interesting study by Malda *et al.* suggested that age might influence the cell's response to hypoxia based on the finding that chondrocytes derived from a younger donor (47 years) responded to hypoxic conditions with enhanced sGAG production while chondrocytes from an older donor (74 years) did not[372]. Yet, these observations could have been due to donor variability rather than age. The donors used for the experiments presented in this chapter varied both in age (48 to 75 years) and gender (2 female vs. 3 male). No gender or age related differences in differentiation capacity or response to CoBGs were observed. However, all donors underwent total hip replacement surgery alluding to some degree of morbidity in the osteochondral system; hence, none of the donors represented a young/ healthy population.

Based on the positive effect of hypoxic culture on hMSC chondrogenic differentiation as well as data reporting an up-regulation of chondrogenic markers in response to $CoCl_2$, the outcome of the current work was unexpected. Several factors can be responsible for the observed cobalt-dose dependent reduction in hMSC chondrogenesis. The study described in this chapter evaluated the long term effect of CoBG dissolution products on chondrogenic differentiation. Most studies assessing the effect of

$CoCl_2$ on chondrogenic markers focused on short time points of up to 24 h and did not monitor the effect of $CoCl_2$ beyond that treatment period. Apart from the length of exposure, the cobalt concentration may have been too high in the experimental set up described in this chapter. Yet, in the literature, concentrations between 100 µM to 200 µM $CoCl_2$ were used to assess the influence of cobalt-mediated HIF-1α stabilisation on chondrogenic marker gene expression or extracellular matrix accumulation either in chondrocytes or MSCs. These values correspond nicely to the amount of cobalt ions in the 1%CoBG (119 µM) and 1.5%CoBG (170 µM)-conditioned medium. Therefore, rather a combination of length of treatment and cobalt ion availability than the cobalt ion concentration in the CoBG-conditioned medium as such seems to be causative for the reduction in chondrogenic lineage commitment. Cobalt may exert its beneficial function within a tightly regulated concentration range when used for treatment beyond 24 h with lower cobalt ion concentrations likely being preferable. The synthesis of cartilaginous extracellular matrix by bovine and human articular chondrocytes has similarly been shown to be dependent on the precise availability of oxygen, with moderate hypoxic conditions of 5 - 10% O_2 being beneficial while anoxic conditions (<0.1%) compromised extracellular matrix production[367, 374]. With an average concentration of 119 µM Co^{2+} in 1%CoBG-conditioned medium, the Co^{2+} level might have already been too high for long term treatment of hMSCs. Previous studies suggest that cobalt exerts its beneficial action in a tightly regulated concentration window. In a study by Quinlan *et al*., differently sized particles of the same cobalt-containing bioactive glass composition were incorporated in a collagen/glycosaminoglycan composite scaffold system[241]. While there were no significant differences in cobalt ion release, functional differences in the response of HUVECS with regards to VEGF gene expression and protein production were observed indicating that subtle differences in cobalt release might induce changes in cell behaviour. Similarly, Focaroli *et al.* observed the most favourable outcome for their alginate bead/hMSC chondrogenesis model when using a 1.25 mM Co^{2+} gelling bath to prepare the beads as opposed to 2.5 mM or the cobalt free control[235]. When hMSCs were cultured on 2 mol% cobalt-containing mesoporous bioactive glass scaffolds (Co-MBG), the VEGF release was significantly increased compared to 5%Co-MBG and the cobalt free control[237].

Other studies evaluating the use of cobalt-doped bioactive glass-containing scaffolds for tissue engineering demonstrated their value for (bone) tissue engineering applications[237, 240, 241]. As bioactive glasses characteristically partially dissolve and re-precipitate on their surface, cells might not have been continuously exposed to high (≥100 µM) levels of cobalt which may explain the enhanced/ anticipated differentiation of cells towards the osteogenic lineage. In other biomaterial systems, regulatory effects of cobalt concentrations of as low as 1.5 µM were observed[229]. Considering that concentrations of 100 µM to 200 µM $CoCl_2$ induced an up-regulation of chondrogenic markers after 24 h, short-term treatment or pre-conditioning using CoBG dissolution products may prime hMSCs for subsequent (chondrogenic) differentiation processes. Yet, the use of biomaterials releasing high doses of cobalt ions for a continued period of time should be carefully considered in light of the findings presented in this chapter.

In the current study, CoBG-conditioned medium was added after formation of pellets. Future

studies could evaluate the influence of cobalt-containing bioactive glass extracts on pellet formation. The presence of such cobalt-containing bioactive glass dissolution products may prime the hMSCs for chondrogenic differentiation. After pellet formation, the medium could be replaced by CoBG extract free chondrogenic medium to limit the overall exposure duration to cobalt ions.

In the study presented in this chapter, it was not assessed whether the CoBG extracts indeed activated the HIF-1α pathway. Yet, in the study by Azevedo *et al.* it was shown that CoBG-conditioned media containing similar amounts of cobalt ions (90.74 μM, 178.93 μM and 389.57 μM compared to 119 μM, 170 μM and 254 μM in this study) activated the transcription factor HIF-1α leading to the up-regulation of *VEGF* gene expression after 24 h and VEGF protein release throughout the 7 days culture period[240]. The CoBG-conditioned media in the work by Azevedo *et al.* were based on the same bioactive glass system and the CoBG-conditioned medium was prepared according to the same protocol.

4.4.1 Limitations

One of the limitations of this chapter is that the $CoCl_2$ reference condition was not included in the experiments measuring the sGAG production and DNA content of pellets and hMSC-seeded PCL membranes. While the analysis with Raman spectral analysis suggested that addition of $CoCl_2$ to chondrogenic medium had a similar effect as CoBG extracts on hMSC chondrogenesis, including $CoCl_2$ in all other experiments as an additional condition would have allowed to better distinguish the effects resulting from the presence of cobalt itself and the effects of the combination of cobalt with bioactive glass dissolution products.

Furthermore, performing all experiments in parallel in hypoxic conditions would have allowed to directly compare the influence of cobalt-containing bioactive glass dissolution products and low oxygen tension on hMSC chondrogenesis. As the underlying rational of incorporating cobalt into biomaterials is to mimic hypoxia and ultimately to obtain the beneficial effects associated with hypoxic culture, culture in a hypoxic chamber would have been a valuable reference condition.

Finally, when assessing gene expression, target genes of the HIF-1α pathway along with more markers of the chondrogenic and osteogenic lineages would have been interesting to study to better clarify the influence of CoBG dissolution products on hMSC behaviour. Considering the poor chondrogenic differentiation of hMSCs on the PCL membranes even in standard chondrogenic conditions, gene expression analysis of hMSC pellets would have been more informative.

4.5 Conclusion

Overall, it was demonstrated that hMSC chondrogenesis was reduced in presence of cobalt-containing bioactive glass dissolution products but not in the 0%CoBG condition. Raman spectroscopic analysis suggested that 100 μM $CoCl_2$ had a similar effect on hMSC chondrogenesis as cobalt-containing CoBG dissolution products strengthening the hypothesis of a cobalt-dependent effect. Considering previous studies using Co^{2+} for pre-conditioning of MSCs, shorter exposure periods or a cobalt-containing bioactive glass with lower cobalt incorporation/release may stimulate MSC chondrogenic lineage commitment. Even though HIF-1α activation was not assessed in this context, previously obtained data by Azevedo *et al*. demonstrated stabilisation of HIF-1α and downstream activation of its target genes such as *VEGF* by CoBG-conditioned medium[240]. Since the outcome of the study presented in this chapter was unexpected, it was sought to address 1) if the CoBG-conditioned medium used for the experiments described in this chapter was capable of stabilising HIF-1α and 2) how the ions released from CoBGs influenced hMSC behaviour beyond chondrogenic differentiation. The experiments that were conducted to clarify these questions are presented in the next chapter (Chapter 5).

CHAPTER 5

The Influence of Cobalt-containing Bioactive Glasses on hMSC Behaviour

(*Some of the work in this chapter is in preparation for publication in "Hypoxia-mimicking bioactive glasses reduce hMSC chondrogenesis despite HIF-1α stabilisation" by Littmann E, Autefage H, Solanki AK, Kallepitis C, Jones JR, Alini M, Peroglio M and Stevens MM*)

All data presented in this chapter were collected by me unless explicitly stated otherwise.

5.1 Introduction

Mesenchymal stem cells (MSC) have found broad application in tissue engineering due to their relative ease of isolation and multilineage differentiation potential[63, 66, 411]. Moreover, MSCs can exert their beneficial function indirectly by releasing anti-inflammatory or growth factors[71, 412]. Using MSCs for tissue engineering applications necessitates considerable *in vitro* expansion as the cells merely account for 0.02% to 0.001% of mononuclear cells isolated from the bone marrow[63, 413]. The replicative potential of MSCs is one of their major advantages over further differentiated cells (i.e. osteoblasts and chondrocytes) for tissue engineering purposes. Yet, MSCs lose their stem cell properties during extensive expansion *in vitro* and eventually undergo replicative senescence limiting their therapeutic efficacy[414]. It is widely acknowledged that late passage MSCs have a reduced differentiation potential and cease to exert a protective effect in *in vivo* experiments[362, 415].

Hence, great efforts have been undertaken to identify "optimal" culture conditions to preserve stem cell properties while allowing considerable cell expansion as reviewed by Hoch and Leach.[416]. Among a number of approaches, the culture of MSCs in hypoxic conditions has emerged as relatively simple and cost-effective way to maintain MSC progenitor-like characteristics. In contrast to the atmospheric oxygen tension (21%) present in standard cell culture incubators, MSCs are exposed to hypoxic environments with oxygen tensions ranging from 1% to 7% in their physiological environment, the (bone marrow) stem cell niche[417].

Based on this knowledge many studies have evaluated the effect of low oxygen tensions on MSCs *in vitro* (reviewed by Das *et al.*)[418]. Hypoxic conditions are commonly thought to increase proliferation of hMSCs as well as to preserve and promote the undifferentiated, stem cell-like state[384, 404, 419-423]. Yet, not all studies demonstrate an enhanced proliferative potential of MSCs[424, 425]. An emerging hypothesis is that reduced oxygen tension positively selects for a pool of highly proliferative stem cell-like cells within the heterogeneous MSC population. This may explain an initial lag phase in proliferation in hypoxic conditions that was observed by Grayson *et al.*[426]. It is known that a population of (passaged) MSCs tends to be quite heterogeneous in that not all cells possess an early-progenitor phenotype. During expansion, MSCs readily lose their progenitor/stem cell phenotype as they are highly sensitive to the plating density[414]. The ability to form CFU-F is used as a measure for the replicative potential of cells and can indicate the preservation of stem-cell like properties. It is frequently used to identify mesenchymal stem cells among a population of freshly isolated mononucleated cells isolated from the bone marrow but can also be applied to passaged or expanded MSCs. Among other factors, the CFU-F forming efficiency is dependent on the donor as well as the passage number of the cells. Assessment of CFU-F formation by hMSCs isolated from different donors showed that at passage 4 the colony forming ability ranged between less than 5% to 25%[414]. At passage 12, hardly any colonies formed. In a study by Park *et al.*, less than 1% of cells formed colonies under standard conditions[404].

Previous studies demonstrated that hMSCs displayed greater colony forming activity when exposed to low oxygen levels (1 - 5%)[384, 420, 426]. Notably, the results differed with respect to the hypoxic treatment protocols; a) expansion in normoxic conditions, CFU-F assay in hypoxic conditions, b) expansion in hypoxic conditions, CFU-F assay in normoxic conditions and c) both expansion and CFU-F assay in hypoxic conditions. In a study by Park *et al*., the number of colonies more than doubled when the hMSCs were expanded in low oxygen environments prior to the CFU-F assay at ambient oxygen levels. Reduced oxygen tension during the CFU-F assay after expansion in hypoxia increased the number of colonies only slightly. Similarly, the expansion in hypoxic conditions had a greater influence on the subsequent culture conditions during the CFU-F assay in a study by Vertelov *et al.*[427]. In other studies, a significant beneficial effect of hypoxic culture during the CFU-F assay was observed[384, 428]. In contrast, CFU-F formation by hMSCs was decreased in presence of 1% O_2 compared to normoxic conditions in a study by Hung *et al*.[425].

Investigation of the influence of hypoxic culture on MSC osteogenic and adipogenic differentiation has yielded remarkably contrasting results; while a large number of studies showed a reduced lineage commitment[404, 420, 429], other studies demonstrated an enhanced commitment to at least one of the lineages[384, 430]. The diverging outcomes can be attributed to a variety of factors including donor variability, differences in experimental set up, especially regarding oxygen tension and exposure protocols, as well as the tissue source and origin of MSCs. Even though a large number of studies have evaluated the impact of hypoxia on MSC behaviour, the underlying mechanisms largely remain to be elucidated. Hypoxic culture of hMSCs either in monolayer or within 3D scaffolds increased the gene expression level of the stem cell marker *OCT4* which may account, in part, for the enhanced stem-cell like properties[426, 431, 432]. The up-regulation of *OCT4* might be mediated by HIF-2α, however, a causative link has yet to be established[431]. Martin-Rendon *et al*. assessed changes in hMSC gene expression after 24 h of hypoxic culture and found 45 genes to be differentially regulated by at least 1.75-fold[433]. A study evaluating the response of rat bone marrow-derived MSCs to 24 h of hypoxia found 135 genes to be differentially regulated by at least 3 fold[434]. In both studies pro-survival genes and genes associated with metabolic regulatory processes were increased. Both studies compared the MSC gene expression profile to either umbilical cord blood $CD133^+$ cells or marrow-derived mononuclear cells respectively and found substantial variations in expression profiles underscoring a cell-specific response to reduced oxygen tensions.

Considering the impact of oxygenation levels on MSC fate, oxygen-sensing pathways such as HIF-1 are likely causative for these observations. Low oxygen tension has been shown to enhance the abundance and activity of the transcription factor HIF-1α in MSCs and the up-regulation of HIF-1α target genes has been demonstrated[240]. Transfection with a constitutively stable HIF-1α vector mimicked the effects of the hypoxic control condition regarding CFU-F formation and differentiation behaviour in hMSCs cultured in ambient air suggesting that HIF-1α stabilisation was an adequate replacement for low oxygen tension at least to some extent[404]. Notably, constitutive HIF-1α stabilisation

did not enhance the overall cell proliferation as observed with the hypoxic control highlighting possible differences in mode of action. This result may also underscore the heterogeneous nature of hMSCs. Hypoxic environments/HIF-1α stabilisation may enhance the proliferation and CFU-F capacity of a subset of hMSCs but not the proliferative potential of the bulk population. Yet, the study was performed with only one hMSC donor warranting further confirmation.

Interestingly, beyond the evaluation of hypoxic conditions for cell expansion, its value for pre-conditioning of stem cells to enhance post-engraftment performance is increasingly recognised, as reviewed by Muscari *et al.*[435]. Stem cell-based therapies rely on the engraftment of stem cells to repair or replace damaged tissue. Hypoxic pre-treatment has been demonstrated to enhance MSC post-engraftment survival, retention and functional recovery of the host tissue[435]. Hypoxic pre-conditioning is based on the concept that the exposure to low oxygen tensions prepares cells for the subsequent transplantation to ischemic tissue sites by up-regulation of appropriate gene expression patterns. Therefore, pharmacological pre-treatment with PHD inhibitors has emerged as promising avenue to improve the efficacy of cell therapy, as reviewed by Esfahani *et al.*[436].

Transplantation of MSCs for tissue repair after stroke, cardiac infarction or kidney ischemia is emerging as promising treatment tool. Even though there is encouraging functional *in vivo* data, inefficient engraftment is currently limiting the clinical benefits of MSC transplantation. Poor MSC retention at the injury site is thought to be due to insufficient cell adhesion and/or migration[425]. The migration of MSCs to sites of (damaged) tissue is key to their natural role in tissue regeneration and is governed by a complex set of mechanisms. Interaction of the chemokine stromal derived factor 1 (SDF-1) and its receptor CXCR4 is thought be an important driver of MSC recruitment[437, 438]. During *in vitro* expansion of MSCs the CXCR4 expression declines which likely negatively affects the homing and engraftment efficiency of cultured MSCs in most cell therapy studies where cell expansion is necessary[439, 440].

While the SDF-1/CXCR4 axis is pivotal for homing of MSCs to bone marrow and their retention therein, the expression of SDF-1 can be selectively up-regulated in damaged or ischemic tissue, possibly in a HIF-1α dependent manner[438, 441, 442]. Similarly, CXCR4 is a target for the transcription factor HIF-1α and has been shown to be up-regulated on a gene and protein level in response to hypoxia in MSCs and other cell types[443-445]. Based on these findings, several studies evaluated whether hypoxic pre-conditioning would ameliorate subsequent engraftment and functional tissue repair. Indeed, hypoxic culture of MSCs improved their migratory activity towards SDF-1 or other soluble chemoattractants[427, 437, 446]. Furthermore, hypoxic pre-conditioning enhanced the expression of CXCR4 in hMSCs and their subsequent retention in chick embryos[425]. *In vivo* models for stroke[447], kidney ischemia[446, 448] or murine hind limb ischemia[449] showed an enhanced engraftment and functional recovery after hypoxic pre-conditioning of MSCs or constitutive CXCR4 expression.

Taken together, hypoxic culture conditions are starting to be recognised as a simple tool to enhance the proliferative potential and stem-cell like features of MSCs during expansion for tissue engineering purposes. Furthermore, low oxygen tension has emerged as versatile pre-treatment prior to cell engraftment.

5.1.1 The influence of cobalt on hMSC behaviour

After the discovery of cobalt's hypoxia-mimicking properties, researchers have sought to exploit the ion's characteristics for directing cell behaviour and fate. In this context, the up-regulation of angiogenic markers in order to enhance vascularisation and the pre-conditioning of cells prior to transplantation into low-oxygen environments have been the most commonly pursued applications. Yet, while hypoxia has been widely used to influence MSC behaviour, there is less data on the effect of cobalt on stem cell properties of MSCs. Therefore, cells with stem cell character or cells that are thought to have similar features as MSCs were included in the literature search.

$CoCl_2$ treatment induced stem cell marker expression in human periodontal ligament cells after 7 days of treatment while repressing osteogenic differentiation similar to the observations made for reduced oxygen tension[450]. The up-regulation of the stem cell marker *OCT4* was more enhanced in presence of higher $CoCl_2$ concentrations (100 µM vs. 50 µM) and seemed to rely on a HIF-1α dependent mechanism[450]. Concomitantly, osteogenic differentiation was more efficiently inhibited by treatment with 100 µM $CoCl_2$. Exposure to $CoCl_2$ had no effect on proliferation during the 7 day treatment period. Thus, the authors concluded that $CoCl_2$ might find its merit in preserving the stem-cell state in the laboratory. $CoCl_2$ has also been evaluated as pharmacological tool to enhance angiogenesis after dental pulp injury[451]. Viability and proliferation of human dental pulp cells were not affected in presence of up to 300 µM $CoCl_2$. Yet, only relatively short time points with 24 h and 6 h respectively were evaluated. The release of VEGF was successfully increased by exposure to $CoCl_2$. When human $CD133^+$ cells isolated from umbilical cord blood were exposed to $CoCl_2$, an increase in cell viability, migration and tubule-like structure formation was observed[452]. $CoCl_2$ treatment performed at least as good as the reduced oxygen tension control with the highest $CoCl_2$ concentration (200 µM) and the lowest oxygen tension (3%) inducing the most favourable outcome in all tested parameters.

Interestingly, the stabilisation of HIF-1α has been studied in the context of neurogenesis and $CoCl_2$ treatment has been shown to facilitate neuronal differentiation of MSCs[395, 400, 401]. HIF-1α stabilisation by $CoCl_2$ appeared to improve neuronal and dopaminergic differentiation by human mesencephalic neuronal progenitor cells (NPC) and to exert a protective effect on human dopaminergic neurons against treatment with a neurotoxin[453]. The enhanced dopaminergic differentiation by 100 µM $CoCl_2$ treatment outperformed the 3% O_2 control. Co^{2+} concentrations of up to 100 µM did not affect cell viability of human NPCs after 72 h of treatment, yet, cell death was enhanced from 5.1% (control) to 9.6% (100 µM $CoCl_2$) following 1 week of exposure. At the same time, there were more cells in the

S and G2/M phase of the cell cycle and fewer in the G0/G1 compared to control conditions suggesting an influence on the cell cycle. Similarly, exposure to 100 μM $CoCl_2$ for 72 h increased expression of neuronal markers in hMSCs[395]. Further supporting this notion, a study by Pacary *et al*. reported MSC differentiation towards neuron-like cells in the presence of $CoCl_2$[400]. These observations were accompanied by a reduction in cell proliferation that was completely inhibited after 72 h. Overall, these studies showed that whilst causing a reduction in cell proliferation, Co^{2+} enhanced differentiation marker expression highlighting the ion's potential to affect cell behaviour.

The study by Pacary *et al.* described a cobalt-associated up-regulation of the negative cell cycle regulator p21 on mRNA level[400]. Originally, p21, also known as p21WAF1/ Cip1, was identified as cell cycle inhibitor owing to its ability to arrest cell cycle progression by inhibition of cyclin-dependent kinase activity. In particular, p21 has been identified as marker for senescence, a state of permanent growth arrest in G1[454]. Lately, p21 function has been linked to a plethora of other pathways and mechanisms ranging from cell motility to stem cell differentiation. Activity and function of p21 might even differ depending on its sub-cellular localisation as reviewed by Coqueret[455]. Much like its function, regulation of p21 expression and activity is highly complex and is beyond the scope of this chapter. For an extensive review on the regulation of p21, please refer to Abbas and Dutta[454]. Here, the focus was laid on how p21 activity is regulated by HIF-1α dependent mechanisms. It is generally accepted that HIF-1α induces cell cycle and growth arrest via p21 activation[456]. However, the explicit mechanism of HIF-1α mediated p21 regulation remains controversial in the literature and has yet to be fully elucidated[457]. Generally, there is evidence that HIF-1α controls p21 through indirect pathways that depend neither on its transcriptional nor its DNA binding activity[458, 459]. Koshiji *et al.* suggested a mechanism involving Myc suppression and subsequent activation of p21 and He *et al.* further expanded this theory by linking HIF-1α mediated repression of Myc with reduced levels of the miRNAs miR-17/20a resulting in an enhanced p21 expression. Yet, most of the studies evaluating p21 expression emerged in the context of cancer research and there are few studies addressing its regulation in primary (stem) cells. Furthermore, p21 appears to fulfil some cell-type specific functions further complicating any generalisation or extrapolation of pathways[455].

HIF-1α has been identified as upstream player of p21 expression in human keratinocytes and while p21 expression is generally accepted to be up-regulated by hypoxia/HIF-1[400, 460, 461], there are some studies reporting a down-regulation of p21 in response to hypoxic stimuli[404, 405, 462]. Of note, p21 protein expression in hMSCs was shown to differ between donors and was found to be up-regulated in later passages[460]. Down-regulation of p21 in MSCs has previously been linked to enhanced expression of stemness markers and proliferation[460]. Knockdown of p21 in late-passage hMSCs appeared to reverse expansion-induced senescence and restored some of the stem-cell like properties. In keeping with these results, Tsai *et al.* attributed the maintenance of stem cell properties in hMSCs expanded in hypoxic conditions to HIF-1α mediated down-regulation of p21. Here, the down-regulation of p21 was explained by HIF-1α dependent up-regulation of TWIST, which was in turn thought to suppress p21 expression

via the inactivation of the transcription factor E2A. Similarly, Park *et al.* observed a lower level of p21 protein in hMSCs after culture in hypoxic environments for two days. In contrast, Grayson *et al.* did not observe a change in p21 protein expression in response to reduced oxygen levels in hMSCs[426]. In summary, p21 expression is thought to be regulated by HIF-1α. Yet, the underlying mechanism remains to be clarified. Furthermore, little is known about the interplay of HIF-1α and p21 in hMSCs.

Corresponding to the promising results with hypoxic pre-conditioning, the use of cobalt for similar applications was assessed. Treatment with the hypoxia-mimicking agents $CoCl_2$ or deferoxamine, an iron chelator, increased CXCR4 expression and enhanced MSC migration as assessed by scratch wound healing and transwell migration assays[448, 463]. $CoCl_2$ has been shown to up-regulate CXCR4 transcript and protein expression in microglia cells (150 µm, 16 h)[464]. Furthermore, pre-conditioning of bone marrow-derived rat MSCs with 200 µM $CoCl_2$ for 24 h enhanced the expression of CXCR4 on mRNA and protein level in a HIF-1α dependent manner and subsequently increased scratch wound healing[448]. Similarly, Liu *et al.* showed an up-regulation of CXCR4 in response to 100 µM $CoCl_2$ in murine MSCs which was accompanied by enhanced migration towards a SDF-1 gradient using a transwell system[463]. Interestingly, CXCR4 levels in normoxic conditions were nearly below the detection limit. Based on these findings, the effect of $CoCl_2$ pre-treatment on the ability of MSCs to attenuate acute kidney injury in a rat model was assessed. Pre-treated MSCs were more likely to be recruited to and retained in the ischemic kidney, which was associated with a reduction in kidney injury compared to the untreated MSC control group.

In summary, hypoxia has been identified as valuable tool to maintain the stemness of MSC during *in vitro* expansion and to pre-condition MSCs for subsequent engraftment. The use of $CoCl_2$ is emerging as potential alternative to reduced oxygen tension and has been evaluated in *in vitro* and *in vivo* experiments. $CoCl_2$ supplementation to medium is cheaper than the use of oxygen chambers and might be easier to standardise considering the numerous treatment protocols pursued for reduced oxygen tensions. Beyond $CoCl_2$ treatment, the incorporation of cobalt into biomaterials for tissue repair purposes is receiving growing interest. In particular, the development of cobalt-containing scaffolds for bone regeneration applications has been pursued[237, 240, 241]. In this context, bioactive glasses present attractive carrier systems due to their inherent osteogenic properties and the relative ease of modifying their composition. In presence of cobalt-containing bioactive glass extracts, HIF-1α activity was shown to be increased in hMSCs and hypoxia target genes were subsequently up-regulated demonstrating the delivery of cobalt ions at relevant concentrations[240]. Regarding pro-angiogenic properties of cobalt-containing bioactive glasses, the protein expression of VEGF was shown to be increased in hMSCs after either exposure to CoBG-conditioned medium or culture on cobalt-containing bioactive glass scaffolds[237, 240].

5.1.2 Aims and objectives

Considering the promising results obtained with cobalt-doped biomaterials in general and bioactive glasses in particular, it appears important to further characterise the response of hMSCs to such materials. In this chapter, the influence of cobalt-substituted bioactive glasses on hMSC behaviour and stem cell properties were investigated with a special respect to the cobalt ion concentration within the bioactive glass extracts. To assess whether there was an optimum concentration range of cobalt within the bioactive glass dissolution products, the previously introduced series of CoBGs, based on the system of Azevedo *et al.*, was used[239, 240]. With respect to Chapter 4, there was a particular interest in characterising the effect of CoBG dissolution products on hMSC behaviour to obtain a better understanding of the previously observed reduction in chondrogenic lineage commitment.

Thus, the aims of the work presented in this chapter were to understand the impact of cobalt-containing bioactive glasses on hMSC behaviour and to study if cell behaviour changed depending on the cobalt concentration within bioactive glass extracts. The objectives were to:

- Verify if HIF-1α was stabilised by the cobalt-containing bioactive glasses;
- Study the effects of cobalt-containing bioactive glass extracts on cell viability;
- Investigate the effect of cobalt-containing bioactive glass extracts on stem cell-like properties of hMSCs.

5.2 Materials & Methods

5.2.1 Glass synthesis

Glass synthesis and particle preparation were performed as previously described and outlined in Chapter 4 (4.2.1)[33,34]. To recapitulate, cobalt was incorporated into the bioactive glass composition 49.46 mol% SiO_2, (23.08 – X mol%) CaO, X mol% CoO, 26.38 mol% Na_2O, 1.07 mol% P_2O_5 by replacing calcium on a molar basis (where X equals 0, 1, 1.5 or 2 mol% cobalt substitution) (Table 5.1). To assess the influence of cobalt-containing bioactive glass dissolution products on hMSC behaviour, increasing amounts of cobalt were incorporated into the composition to identify cobalt dose-dependent effects. As previously introduced in Chapter 4, the glasses were termed 0%CoBG, 1%CoBG, 1.5%CoBG and 2%CoBG or referred to as CoBG if all glass compositions were concerned. The CoBGs were prepared using SiO_2 (Prince Minerals, UK), Na_2CO_3, P_2O_5, $CaCO_3$, and $CoCO_3$ (all Sigma-Aldrich, UK) as precursor materials. The precursor materials were mixed, melted at 1,400°C in a platinum-gold crucible for 90 min and quenched into deionised water. The resulting glass frit was allowed to dry between 120 - 150°C over-night before milling in a planetary ball mill at 500rpm for 5 min. The glass particle size used in this study was <38 μm in diameter (d = 0.9). Glass synthesis and processing were performed by Miss Anu Solanki.

Table 5.1: Glass compositions (mol%).

Glass	SiO_2	Na_2O	CaO	CoO	P_2O_5
0%CoBG	49.46	26.38	23.08	/	1.07
1%CoBG	49.46	26.38	22.08	1.00	1.07
1.5%CoBG	49.46	26.38	21.58	1.50	1.07
2%CoBG	49.46	26.38	21.08	2.00	1.07

5.2.2 Preparation of bioactive glass-conditioned medium

To obtain medium containing CoBG ionic dissolution products, 1.5 mg/mL of particles of CoBG were incubated in Minimum Essential Medium Eagle alpha modification (α-MEM) (Gibco®, UK) containing 100 U/mL penicillin and 100 μg/mL streptomycin (Gibco®, UK) as well as 20 mM HEPES (Gibco®, UK). After 4 h of incubation under constant agitation at 37ºC, the medium was passed through a 0.2 μm filter (Sartorius, UK) under sterile conditions to remove remaining glass particles. The CoBG-conditioned medium was stored at 4°C until further use. Prior to treatment of cells, the medium was equilibrated at 37°C, 5% (v/v) CO_2 for at least 4 h or over-night. As previously described, the elemental concentrations of calcium, phosphorus, silicon and cobalt in the conditioned medium were determined by ICP-OES using an iCAP6000 Series ICP spectrometer (Thermo Scientific, UK) on at least three

independent samples. The ICP-OES was operated with the assistance of Miss A. Solanki. If not defined otherwise, growth medium used in the experiments was defined as α-MEM (Gibco®, UK) containing 100 U/mL penicillin and 100 µg/mL streptomycin (Gibco®, UK) as well as 20 mM HEPES (Gibco®, UK). Cobalt (II) chloride hexahydrate (Sigma-Aldrich, UK) was used to prepare a 10 mM $CoCl_2$ stock solution in MilliQ water. For some experiments, growth medium was supplemented with $CoCl_2$ to obtain final concentrations of 100 µM and 200 µM as additional conditions.

5.2.3 Cell culture

Human bone-marrow derived MSCs (hMSCs) were expanded in α-MEM containing 10% (v/v) FBS (Seraplus, Pan-Biotech, Germany), 5 ng/µL bFGF (Fitzgerald, USA), 100 U/mL penicillin and 100 µg/mL streptomycin (Gibco®, UK). Upon 70 - 90% confluence hMSCs were passaged as previously described and re-seeded at a density of 3,000 cells/cm^2 for expansion. For most experiments, 1 hMSC donor isolated at AO Foundation Davos and 1 donor each from PromoCell GmbH, Germany and Lonza, UK were used to represent a mixed, unbiased population. All hMSCs were bone marrow-derived.

5.2.4 In-Cell Western analysis

The HIF-1α protein level in hMSCs in the presence of growth and CoBG-conditioned media was measured by In-Cell Western analysis. To assess the impact of CoBG-conditioned medium on HIF-1α protein content, hMSCs were cultured in CoBG-conditioned or growth medium for 4 h and 48 h, respectively. As additional controls, growth medium was supplemented with either 100 µM or 200 µM $CoCl_2$. To investigate CXCR4 protein expression in presence of CoBG dissolution products, hMSCs were cultured in growth or CoBG-conditioned medium for 24 h.

In brief, cells were seeded at a density of 20,000 cells/cm^2 and grown until confluency prior to treatment with the various CoBG conditioned-medium and reference conditions. After the respective time point, the previously described protocol was used (Chapter 2.2.5). Cells were incubated with the primary antibodies mouse anti-HIF-1-alpha [mgc3] (Abcam, ab16066, 1:200) or rabbit anti-CXCR4 (Abcam, ab124824, 1:250) in 3% (w/v) BSA in PBSTw for 90 min at RT under constant agitation. Anti-mouse or anti-rabbit (Li-Cor, 1:400) IR800-labeled secondary antibodies in 3% (w/v) BSA in PBSTw were added to the cells for 1 h at RT under constant agitation and used to visualise the respective protein levels. The intensity values for each protein were normalised to the DNA content per well using the far-red fluorescent DNA dye DRAQ5™ (New England Biolabs, 1:2,000) in 3% (w/v) BSA in PBSTw. The fluorescent signal was collected and quantified using the Odyssey Infrared Imager (Li-Cor Biosciences, USA). Cells incubated with secondary antibody only in the absence of DRAQ5™ were used as controls, and this background was subtracted from the signal. HIF-1α expression was measured in 4 (4 h time point) and 3 (48 h time point) independent experiments each using a different donor. The protein

expression of CXCR4 in hMSCs was assessed by In-Cell Western analysis in two independent experiments each using a different donor. All conditions were run in quadruplicates.

5.2.4.1 Quality analysis of antibodies used for In-Cell Western analysis

To assure the specificity of the antibodies used for In-Cell Western analysis, a traditional Western blot was carried out according to the protocol outlined below (5.2.5). The anti-HIF-1α and anti-CXCR4 antibodies detected a band corresponding to the molecular weight of the proteins and were deemed specific (116 kDa and 47 kDa respectively) (Fig. 5.1). In fact, the molecular weight of CXCR4 is predicted to be 40 kDa but commercially available antibodies detect bands with higher molecular weight for CXCR4, among them 47 kDa, which correspond to the glycosylated protein.

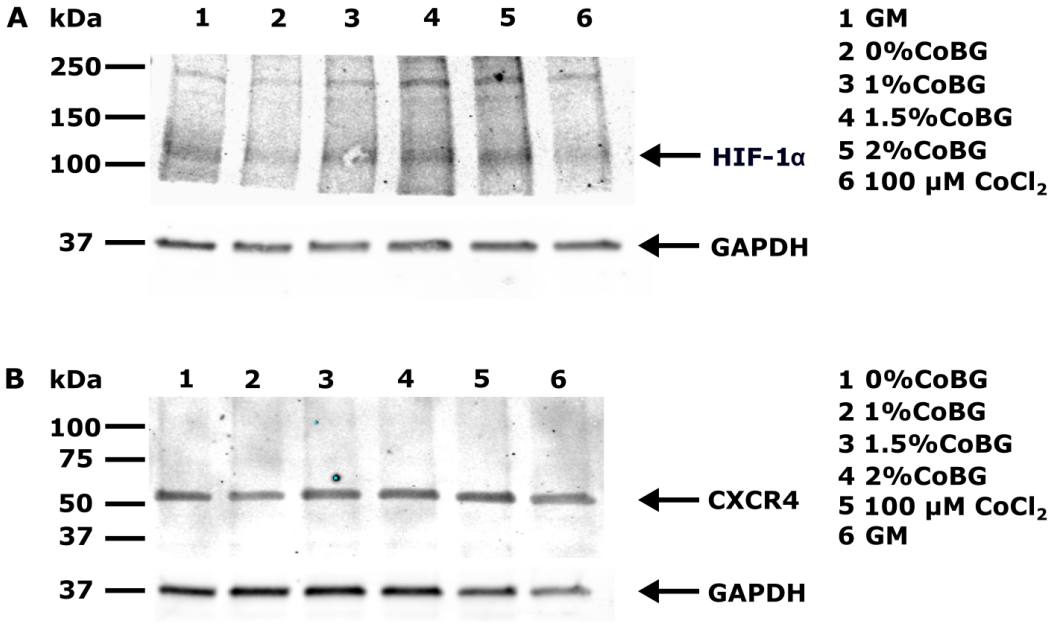


Figure 5.1: Antibody characterisation using Western blot analysis. Whole hMSC lysates were subjected to SDS-PAGE and immunoblotted with the indicated antibodies after 16 h of exposure to growth or CoBG-conditioned medium. A) The anti-HIF-1α antibody detected a band corresponding to the molecular weight of the protein (116 kDa). The intensity of bands was higher in presence of 1.5%CoBG and 2%CoBG dissolution products. B) The anti-CXCR4 antibody detected a band corresponding to the predicted molecular weight of the glycosylated protein (47 kDa). Considering affinity and specificity of the antibodies, anti-HIF-1α and anti-CXCR4 were deemed specific.

5.2.5 Sodium dodecyl sulphate polyacrylamide gel electrophoresis (SDS-PAGE)

Proteins from hMSC extracts were separated according to their size using SDS-PAGE with using 4 - 20% gradient mini-PROTEAN® TGX™ precast polyacrylamide gels (BIO-RAD, UK) following standard procedures. Briefly, hMSCs were seeded at a density of 20,000 cells/cm^2 in 6-well plates and grown to confluency prior to treatment with the various media for 16 h or 24 h. At the designated time point, cells were rinsed once with ice-cold PBS prior to sample lysis. Cell lysis was performed using Radio Immuno Precipitation Assay (RIPA) Lysis Buffer System (Santa Cruz, USA) including protease inhibitors. The hMSC extracts were transferred to pre-cooled microcentrifuge tubes and sonicated (three times for 5 s with an amplitude of 20%, interrupted by 20 s breaks) to disrupt and homogenise the cells. To separate cell debris, the cell extracts were centrifuged in pre-cooled microcentrifuge tubes (Eppendorf, UK) at 16,000 xg for 20 min in a 4°C pre-cooled centrifuge. The supernatants were transferred to new pre-cooled microcentrifuge tubes and used for further analysis. Samples were mixed with 4X Laemmli Sample Buffer (BIO-RAD, UK) containing 10% (v/v) 2-mercaptoethanol (Sigma-Aldrich, UK) and heated to 100°C for 5 min to reduce and denature the proteins. Afterwards, 38 µl of each sample was loaded onto the gel. The gels were run in running buffer (25 mM Tris-HCl, 190 mM glycine, 0.1% (w/v) SDS, pH 8.3) at 140V until the target proteins had been sufficiently separated. Precision Plus Protein™ standards All Blue marker (BIO-RAD, UK) was used as a size marker.

5.2.6 Electroblotting of proteins to a nitrocellulose membrane

Using wet transfer, the proteins were subsequently moved from the polyacrylamide gel onto Amersham Protran 0.2 µm nitrocellulose membranes (GE Healthcare Life Sciences Whatman™) in transfer buffer (25 mM Tris-HCl, 190 mM glycine) at 300mA for 90 min on ice. Upon completion of the electrophoretic transfer, membranes were blocked in 5% (w/v) non-fat milk (NFM) (Sigma, UK) /0.1% (v/v) Tween (Tw) in Tris-buffered saline (TBS) (TBSTw) for 1 h at RT and subsequently rinsed thrice (5 min each) with TBSTw. Membranes were immunostained with the primary antibodies, rabbit anti-p21 (Santa Cruz, sc-397, 1:200), mouse anti-p53 (Abcam, ab1101, 1:400), mouse anti-HIF1α (BD Biosciences 610958, 1:500), rabbit anti-CXCR4 (Santa Cruz, sc-9046, 1:200), or rabbit anti-GAPDH (Santa Cruz, sc-25778, 1:500), in 5% (w/v) NFM in TBSTw over-night at 4°C under constant agitation. Additionally, the specificity of the antibodies used for In-Cell Western analysis was tested. The primary antibodies mouse anti-HIF1α (Abcam, ab16066, 1:500) and rabbit anti-CXCR4 (Abcam, ab124824, 1:200) were used along with the other antibodies according to the protocol outlined above. After incubation, the membranes were rinsed three times with TBSTw. Anti-mouse or anti-rabbit (Li-Cor Biosciences, 1:600) IR800-labeled secondary antibodies in 5% (w/v) NFM in TBSTw were added to the membranes for 1 h at RT protected from light and used to visualise the respective protein levels. Membranes were washed thrice with TBST to remove any unbound antibodies before imaging using an Odyssey Infrared Imager (Li-Cor Biosciences, USA). Quantification of staining intensity was

performed using ImageJ software. To determine the protein expression of p21, p53 and CXCR4 in hMSC lysates after treatment with CoBG-conditioned or growth media, 3 different donors were independently assessed. 2 wells were pooled for each condition.

5.2.7 MTT assay

MTT assay was performed to assess the effect of CoBGs on hMSC metabolic activity. In brief, 1.5 x 10^4 cells/cm^2 of passage 5 - 6 hMSCs were seeded in 96-well plates. After 24 h the medium was replaced by growth (α-MEM) or CoBG-conditioned α-MEM medium containing 10% (v/v) FBS (Seraplus, Pan-Biotech, Germany), 100 U/mL penicillin and 100 µg/mL streptomycin (Gibco®, UK) and 20 mM HEPES (Gibco®, UK). As an additional control, α-MEM medium was supplemented with 100 µM $CoCl_2$. The medium was changed every other day over the course of the experiment. After 1, 4 and 7 days respectively, medium was removed and cells were gently washed once with PBS prior to addition of 0.5 mg/mL of MTT (Thiazolyl Blue Tetrazolium bromide, M2128, Sigma®, UK) in phenol-free high glucose DMEM (Gibco®, UK). Empty wells filled with the MTT solution served as background reference. After 2 h the MTT solution was gently removed and replaced by 100 µL of DMSO (Sigma-Aldrich, UK) to solubilise the formed formazan crystals. Absorbance was measured at a wavelength of 570 nm with a reference wavelength of 620 nm using a microplate reader (SpectraMax M5, Molecular Devices, UK). Three independent repeats of the experiment were performed each time using a different donor. Each condition was run in quadruplicates.

5.2.8 CyQUANT® Direct Cell Proliferation Assay

Changes in cell number over time in the presence of CoBG-conditioned or growth (α-MEM) medium were evaluated using the CyQUANT® Direct Cell Proliferation Assay (Life Technologies, UK). The assay was performed according to the manufacturer's instructions. In brief, 5 x 10^3 cells/cm^2 of passage 5 - 6 hMSCs were seeded in 96-well plates. After 24 h the medium was replaced by growth or CoBG-conditioned medium containing 10% (v/v) FBS (Seraplus, Pan-Biotech, Germany), 100 U/mL penicillin and 100 µg/mL streptomycin (Gibco®, UK) and 20 mM HEPES (Gibco®, UK). As an additional control, α-MEM medium was supplemented with 100 µM $CoCl_2$. The medium was changed every other day over the course of the experiment. To avoid confluency throughout the 7 days culture period, a lower cell density compared to the MTT assay was chosen. After 1, 4 and 7 days respectively, the medium was removed and cells were gently washed once with PBS prior to addition of CyQUANT® Direct Cell Proliferation Assay kit in phenol-free high glucose DMEM (Gibco®, UK). As background reference, empty wells filled with CyQUANT® Direct Cell Proliferation Assay kit were used. After 1 h fluorescence was excited at 480 nm and emission was quantified at 535 nm using a microplate reader (SpectraMax M5, Molecular Devices, UK). Three independent repeats of the experiment were performed each time using a different donor. Each condition was run in quadruplicates.

5.2.9 Filamentous actin staining

To visualise hMSC morphology in presence of CoBG-conditioned medium, hMSCs were stained for filamentous actin (F-actin) after 1, 4 and 7 days of culture. Passage 5 hMSCs were seeded at a density of 4,000 cells/cm^2 on µ-Slide 8 Well Glass Bottom slides (ibidi®, UK). Cells were allowed to adhere for 24 h before medium was replaced by CoBG-conditioned or growth medium containing 10% (v/v) FBS (Seraplus, Pan-Biotech, Germany). Growth medium supplemented with 100 µM $CoCl_2$ served as positive control. At the indicated time points, F-actin staining was performed using standard procedures. In brief, cells were fixed with 4% (v/v) PFA (Sigma, UK) in PBS (Gibco®, UK) for 15 min at RT and washed three times afterwards. To permeabilise the cells, 0.2% (v/v) Triton X (Sigma Aldrich, UK) in PBS was added for 2 min. After three washes, cells were incubated in 3% (v/v) goat serum (Dako, UK) in 0.1% (v/v) Triton X/PBS for 30 min at RT. To stain the F-actin, Alexa Fluor 488® phalloidin (1:80) (Life Technologies, UK) in 1.5% (v/v) goat serum/0.1% (v/v) Triton X/PBS was added for 20 min to the cells and incubated protected from flight. To highlight the hMSC nuclei, 4′, 6-Diamidino-2-phenylindole dihydrochloride (Dapi) (1:5000) (Sigma, UK) was additionally added. Dapi is a cell permeable highly sensitive fluorescent probe for DNA. After three washes, the cells were imaged using an epifluorescent microscope (EVOS® FL Cell Imaging System; Life Technologies, UK). Phalloidin is a bicyclic heptapeptide which belongs to a family of toxins isolated from the death cap mushroom (*Amanita phalloides*). As phalliodin binds selectively to F-actin with very high affinity, it is commonly used for visualising the cytoskeleton of cells.

5.2.10 Colony forming units –fibroblast (CFU-F) assay

Classically, the CFU-F assay is used to measure the clonogenic potential of a population of MSCs and thus to identify the fraction of MSCs with early-progenitor like phenotype. A subset of MSCs is deemed as clonogenic if it is able to generate colonies from single cells when plated in culture. In order to perform a CFU-F assay, a single cell suspension is prepared and the cells are seeded at a very low density to be able to analyse cell proliferation independent from the presence of other cells. Here, 5 cells/cm^2 were seeded in 6-well plates in growth medium. After 24 h, the medium was exchanged to CoBG-conditioned or growth medium containing 20 mM HEPES (Gibco®, UK), 10% (v/v) FBS (Seraplus, Pan-Biotech, Germany) and 5 ng/µL bFGF (Fitzgerald, USA). Medium was replaced every 4 days. After 14 days, cells were washed once in PBS prior to addition of ice cold 70% (v/v) methanol in PBS for 10 min. After fixation, the cells were washed three times in PBS, followed by the addition of a solution of 0.5% (w/v) crystal violet (Sigma-Aldrich, UK) in 25% (v/v) methanol in PBS for 10 min at RT. Then, cells were repeatedly washed with PBS, air-dried and colonies of >35 cells were counted with the aid of an inverted light microscope (IX51 inverted microscopy system, Olympus, UK). Three independent repeats of the experiment were performed each time using a different donor. Each condition was run in quadruplicates.

5.2.11 Migration or scratch assay

To study the migration of hMSCs in the presence of CoBG-conditioned medium, a scratch assay was performed. In brief, passage 4 hMSCs were seeded at a density of 20,000 cells/cm^2 in a 48-well plate and grown until confluence. Cells were starved in serum free CoBG-conditioned or CoBG extract free α-MEM medium in the presence or absence of 100 μM $CoCl_2$ for 18 h. To mimic an injury-induced environment, a p1000 pipette tip was used to introduce a "scratch" in the confluent cell layer. Afterwards, cells were gently rinsed in serum-free α-MEM medium prior to addition of CoBG-conditioned or CoBG extract free α-MEM medium (with or without 100 μM $CoCl_2$) containing 2% (v/v) FBS (Seraplus, Plan-Biotech, Germany). Three independent repeats of the experiment were performed each time using a different donor. Each condition was run in quadruplicates. Cell migration was captured using an inverted light microscope (IX51 inverted microscopy system, Olympus, UK) after 0 h, 6 h, 24 h and 48 h. Using ImageJ, the distance between the edges of the scratch was quantified to measure cell migration. For each well, two images were taken and the width of the scratch was measured at 5 equally distributed points per image (in total 10 per scratch). Wound closure was calculated using the following formula: Wound closure rate = (the distance before healing - the distance after healing)/the distance before healing * 100%.

5.2.12 Statistical analysis

To determine statistical significance, a one-way ANOVA combined with Tukey *post-hoc* test was used for experiments with one time point. For experiments with multiple time points, a two-way ANOVA followed by Bonferroni *post-hoc* test was used. Results with *p*-values lower than 0.05 were deemed significant. All data are expressed as mean ± standard deviation (SD).

5.3 Results

Following on from the results presented in Chapter 4, the influence of CoBG dissolution products was further studied with respect to general hMSC behaviour and stem cell properties. For this purpose, the same glass compositions and protocols outlined previously to obtain CoBG-conditioned medium were used. Again, there was a special interest in addressing the question whether tuning of the cobalt ion concentration within the CoBG-conditioned medium had a dose-dependent effect.

5.3.1 Ionic composition of CoBG-conditioned α-MEM medium

To recapitulate, increasing amounts of cobalt ions were incorporated into the bioactive glass composition 49.46 mol% SiO_2, (23.08 – X mol%) CaO, X mol% CoO, 26.38 mol% Na_2O, 1.07 mol% P_2O_5 by substitution with calcium on a molar basis (where X equals 0, 1, 1.5 or 2 mol% cobalt substitution) to evaluate the influence of cobalt-doped bioactive glasses on hMSC behaviour and to identify cobalt dose-dependent effects. To prepare CoBG-conditioned medium, CoBG particles were incubated for 4 h in α-MEM. The cobalt ion release into α-MEM increased according to its molar content in the glasses (Table 5.2). Co^{2+} concentrations of 102 µM, 187 µM and 272 µM were measured in α-MEM medium conditioned with 1%CoBG, 1.5%CoBG and 2%CoBG particles, respectively. The measured cobalt ion content in the 100 µM $CoCl_2$ supplemented control was slightly lower than anticipated (85 µM). For all cobalt-containing compositions, the cobalt ion content in the conditioned medium fell within the range of concentrations routinely used to mimic hypoxia *in vitro* (100 - 300 µM) and was comparable to the results obtained with high glucose DMEM medium (Table 4.4). The elemental concentrations of silicon, calcium and phosphorous in the bioactive glass-conditioned media were comparable between all glass compositions. Similar to the observation made for DMEM, there was a lower amount of phosphorous present in the CoBG-conditioned medium compared to the control which was most likely due to a partial precipitation of calcium phosphate.

Table 5.2: Ion content of CoBG-conditioned α-MEM medium. Elemental concentrations of CoBG ionic dissolution products (Si, Ca, P and Co) in α-MEM medium. CoBG particles were incubated in α-MEM for 4 h at 37°C under constant agitation. Elemental concentrations of CoBG-conditioned and plain α-MEM medium (n = 7) as well as α-MEM medium supplemented with 100 μM $CoCl_2$ (n = 3) were measured by ICP-OES. Ion concentrations are presented as mean ± SD of 7 or 3 independent experiments, respectively (in ppm unless otherwise indicated). The ICP-OES was operated with the assistance of Miss Anu Solanki. ND = non-detectable.

	Si	Ca	P	Co	Co (μM)
α-MEM	ND	65 ± 4	29 ± 5	ND	ND
0%CoBG	66 ± 4	159 ± 10	15 ± 3	ND	ND
1%CoBG	62 ± 5	148 ± 10	18 ± 3	6 ± 1	102
1.5%CoBG	64 ± 5	158 ± 9	21 ± 4	11 ± 1	187
2%CoBG	62 ± 3	156 ± 14	17 ± 3	16 ± 2	272
100 μM $CoCl_2$	ND	59 ± 2	29 ± 2	5 ± 1	85

As mentioned in Chapters 3 and 4, partial dissolution of bioactive glasses causes an increase in pH in the BG-conditioned medium. To ensure that cell behaviour was not influenced by great discrepancies in pH between the CoBG-conditioned and bioactive glass free media, the pH was measured before and after equilibration (Table 5.3). Prior to cell culture, CoBG-conditioned medium was incubated for at least 4 h or over-night in a standard cell culture incubator (37°C, 5% (v/v) CO_2). Prior to equilibration, the pH differed notably when CoBG extract-free α-MEM was compared to CoBG-conditioned α-MEM. After equilibration, the differences in pH between α-MEM only and α-MEM containing CoBG extracts were markedly reduced. The pH of all media containing CoBG extracts were comparable.

Table 5.3: pH values of α-MEM and CoBG-conditioned α-MEM medium before and after equilibration. CoBG-conditioned and CoBG extract-free α-MEM media were equilibrated under standard cell culture conditions (37°C, 5% (v/v) CO_2) for at least 4 h or over-night. As an additional control 100 μM $CoCl_2$ was added to α-MEM medium and its pH measured along with the other conditions. pH values are expressed as a mean ± SD of 3 independent experiments.

	pH before	pH after
α-MEM	7.27 ± 0.15	7.29 ± 0.04
0%CoBG	8.25 ± 0.09	7.55 ± 0.08
1%CoBG	8.18 ±0.05	7.56 ± 0.05
1.5%CoBG	8.12 ± 0.10	7.56 ± 0.04
2%CoBG	8.21 ± 0.04	7.58 ± 0.09
100 μM $CoCl_2$	7.30 ± 0.20	7.30 ± 0.15

5.3.2 Stabilisation of HIF-1α by CoBG dissolution products

It is generally accepted that oxygen availability influences the behaviour of cells[209]. The HIF-1 pathway has been identified as major oxygen sensing mechanism in the cell and shown to mediate the cells' response to changes in oxygen tension. HIF-1α is the master regulatory protein of the HIF-1 pathway and is responsible for the transcriptional activation of hypoxia-responsive genes. Cobalt exerts its hypoxia-mimicking properties through the artificial, oxygen tension-independent stabilisation of HIF-1α. The ion's hypoxia-mimicking properties have been demonstrated in various cell types[206, 210, 391, 465].

To assess whether the CoBG dissolution products mimicked hypoxia in hMSCs, HIF-1α protein abundance was measured after 4 h and 48 h of culture in CoBG-conditioned medium (Fig. 5.2). Quantification of HIF-1α protein abundance is widely used to assess whether the HIF-1 pathway is activated. In the literature, 4 h is a commonly chosen time point to study the stabilisation of HIF-1α upon exposure to either low oxygen tension or hypoxia-mimicking agents. After 4 h, exposure to 1.5%CoBG, 2%CoBG as well as the 100 μM and 200 μM $CoCl_2$ controls significantly increased the amount of HIF-1α protein compared to 0%CoBG and CoBG extract-free α-MEM (growth medium) (Fig. 5.2A). 0%CoBG had no effect on HIF-1α stabilisation. After 48 h of culture in CoBG-conditioned or growth medium, the HIF-1α protein level remained significantly up-regulated in presence of 2%CoBG dissolution products, 100 μM $CoCl_2$ and 200 μM $CoCl_2$ compared to 0%CoBG or growth medium (Fig. 5.2B). 1.5%CoBG dissolution products increased HIF-1α abundance compared to 0%CoBG. The amount of HIF-1α was elevated in presence of 1%CoBG dissolution products after 4 h and 48 h; however, this was not statistically significant. Comparing the two time points, the degree of HIF-1α up-regulation appeared more pronounced after 4 h. When HIF-1α protein expression after 48 h was assessed by Western blot analysis, a prolonged enhancement of HIF-1α in presence of cobalt ions was further corroborated (Fig. 5.2C). Interestingly, HIF-1α protein appeared to be particularly up-regulated in presence of cobalt-containing CoBG release products, beyond the 100 μM $CoCl_2$ reference.

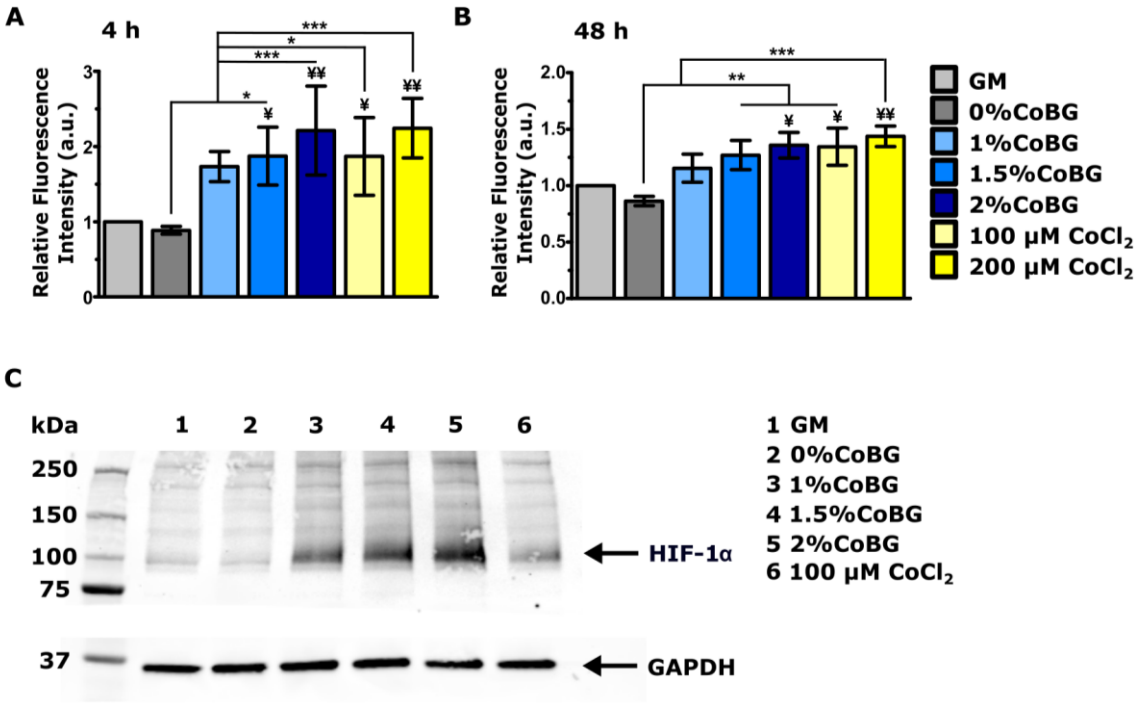


Figure 5.2: Effect of CoBG dissolution products on HIF-1α protein abundance. hMSCs were cultured for A) 4 h or B), C) 48 h in CoBG-conditioned or CoBG-free growth (GM) medium in presence or absence of 100 µM or 200 µM $CoCl_2$. A, B) The protein abundance of HIF-1α was quantified by In-Cell Western and normalised to DNA. Data are expressed as mean ± SD of A) 4 and B) 3 independent experiments using different donors. *p<0.05, **p<0.01, **p<0.001, as calculated by a one-way ANOVA with Tukey *post-hoc* test. For visual display, significant differences between GM and CoBG-conditioned medium are indicated separately. ¥p<0.05 (vs. GM), ¥¥p<0.01. C) HIF-1α protein expression in hMSC whole cell lysates was visualised by Western blot analysis.

5.3.3 hMSC metabolic activity and proliferation in CoBG conditioned medium

To investigate whether CoBG dissolution products had an influence on cell growth and proliferation, hMSCs were treated with the various CoBG-conditioned media as well as 100 µM $CoCl_2$ for up to 7 days (Fig. 5.3). A time and dose-dependent influence of $CoCl_2$ treatment on cell metabolic activity and proliferation has been observed in several studies[400, 466-469]. While at early time points (up to 24 h) $CoCl_2$ seemed to have either no or a positive influence on cell growth, prolonged exposure reduced metabolic activity and cell number compared to growth medium.

5.3.3.1 hMSC metabolic activity in presence of CoBG dissolution products

hMSC metabolic activity was measured by the MTT assay on days 1, 4 and 7 of culture (Fig. 5.2A). After 24 h of treatment, the metabolic activity was comparable between conditions. Similarly, there were no significant differences between conditions after 4 days of culture. After 7 days of culture, metabolic activity of hMSCs cultured in 1.5%CoBG-conditioned and 100 µM $CoCl_2$-supplemented

medium was significantly lower compared to 0%CoBG ($p<0.05$ and $p<0.01$ respectively). Furthermore, metabolic activity of hMSCs cultured in 2%CoBG-conditioned medium was significantly lower than in 0%CoBG ($p<0.001$) and 1%CoBG ($p<0.05$) as well as growth medium ($p<0.05$) on day 7, indicating a cobalt dose-dependent effect. Over time, metabolic activity was significantly increased in the 0%CoBG condition but not in the growth medium condition when days 1 and 7 were compared ($p<0.05$).

5.3.3.2 hMSC proliferation in presence of CoBG dissolution products

To investigate whether the differences in metabolic activity were due to lower cell numbers, cell proliferation was monitored using the CyQUANT® Direct Cell Proliferation Assay on days 1, 4 and 7 of culture (Fig. 5.3B). There were no differences in cell number on day 1 between conditions. After 4 and 7 days of culture cell number was significantly lower in presence of 2%CoBG dissolution products than in the 0%CoBG condition ($p<0.05$). Overall, the cell number seemed to increase over time for all conditions, yet the increase in signal intensity was only significant for 0%CoBG when days 1 and 4 and days 1 and 7 were compared ($p<0.05$). Corresponding to metabolic activity, there was no significant difference in cell number between growth medium and 1%CoBG as well as between 100 µM $CoCl_2$ and 1.5%CoBG. Overall, the results for hMSC metabolic activity correlate nicely with those obtained for cell proliferation. Thus, the bioactive glass induced differences in cell number may, at least partly, be responsible for the trends observed for metabolic activity.

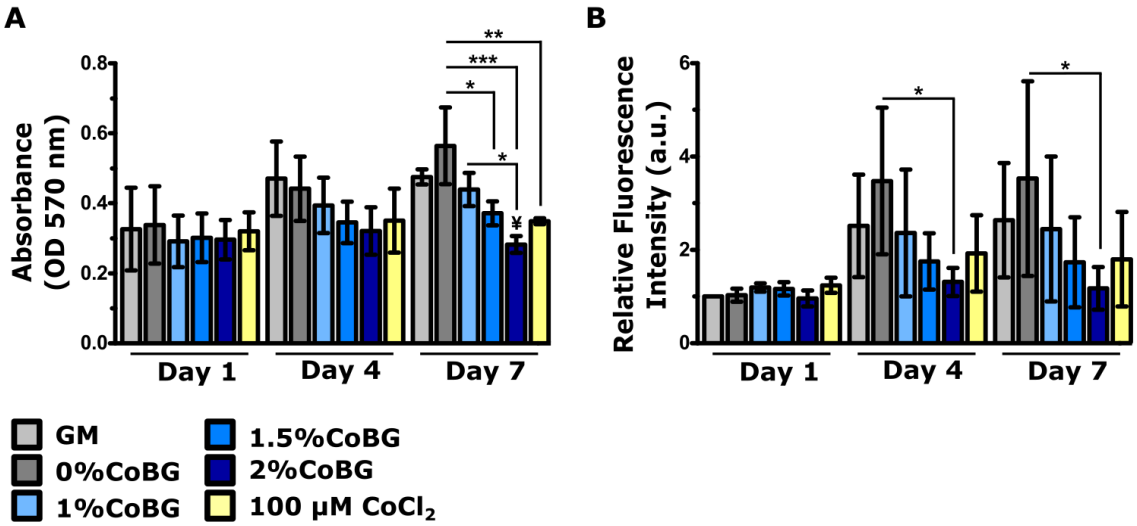


Figure 5.3: Effect of CoBG extracts on hMSC metabolic activity and cell abundance. hMSC were cultured in CoBG extract-free growth medium (GM) or CoBG-conditioned medium for up to 7 days. After 1, 4 and 7 days of treatment, A) metabolic activity was measured by the MTT assay and B) cell proliferation over time was assessed using the CyQUANT® Direct Cell Proliferation Assay. A, B) Data are expressed as mean ± SD of 3 independent experiments using different donors. B) Data were normalised to growth medium on day 1. Statistical significance was assessed by two-way ANOVA followed by Bonferroni *post-hoc* test. *p<0.05, **p<0.01, ***p<0.001. A) For visual display, significant differences between GM and CoBG-conditioned medium are indicated separately. ¥p<0.05 (vs. GM). A, B) Statistically significant changes over time are not indicated in the figure. A) Metabolic activity was significantly higher in presence of 0%CoBG extracts when days 1 and 7 were compared (p<0.01). B) Comparing days 1 and 4 as well as days 1 and 7, cell number increased significantly for 0%CoBG (p<0.05).

5.3.3.3 hMSC morphology in presence of CoBG dissolution products

To assess if cell morphology was altered in presence of CoBG dissolution products, the actin cytoskeleton of hMSCs was stained on days 1, 4 and 7 of culture (Fig. 5.4). Overall, there were no differences in cell morphology observed over time between conditions; however, cell density appeared to be lower in the 2%CoBG condition after 7 days of culture. The fact that there were no visible signs of an increased cell death in presence of cobalt-containing dissolution products or supplemented cobalt ions further indicated that the reduced cell number and metabolic activity were likely not due to an immediate cobalt-dependent cell death but rather a change in cell cycle or the induction of senescence.

After 24 h of exposure, hMSCs showed an elongated, fibroblast-like phenotype which progressively changed to a more flattened out morphology as cells became more confluent independent of the culture conditions. With increasing cell density, hMSCs appeared to aggregate in small bundles while retracting from other, neighbouring cells. A similar observation has been made by Grayson *et al.*, however, the bundle formation was only apparent in normoxic conditions and abrogated by hypoxia[431].

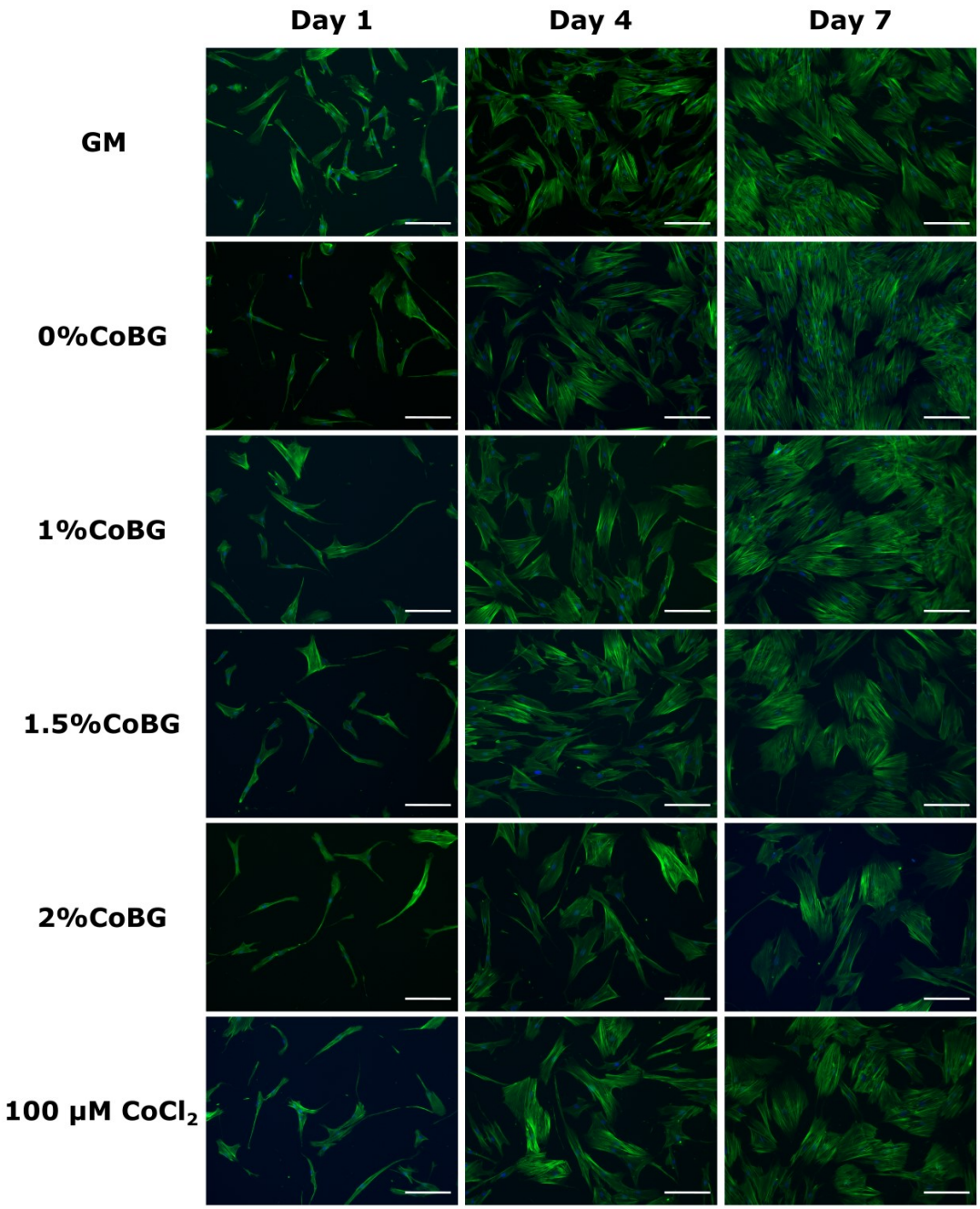


Figure 5.4: Effect of CoBG dissolution products on hMSC morphology. hMSC were cultured in growth (GM), $CoCl_2$-supplemented or CoBG-conditioned medium for up to 7 days. After, 1, 4 and 7 days hMSCs were stained for filamentous actin using phalloidin. Visual assessment of hMSC morphology suggested a progressive flattening of hMSCs over time irrespective of the culture medium. Scale bars = 200 µm.

5.3.4 Effect of CoBG extracts on CFU-F forming ability and hMSC migration

The therapeutic potential of MSCs for cell therapy and tissue engineering relies on the preservation of stem cell/progenitor cell-like properties. Previous *in vitro* and *in vivo* studies have demonstrated an increase in *OCT4* expression *in vitro* and an enhanced regenerative potential *in vivo* after (pre-)treatment with the hypoxia-mimicking agent $CoCl_2$. To evaluate the influence of CoBG dissolution products on hMSC stem-cell like properties and migration, CFU-F formation was assessed and a wound healing assay was performed.

5.3.4.1 CFU-F formation by hMSCs in presence of CoBG dissolution products

To investigate the influence of CoBG dissolution products on colony forming ability of hMSCs, cells were plated at 5 cells/cm^2 and cultured for 14 days in growth or CoBG-conditioned medium (Fig. 5.5). The number of colonies was significantly lower for all cobalt-containing CoBG conditions compared to growth medium (p<0.05). The presence of cobalt ions almost completely abolished colony formation with no colonies observed in the 1.5%CoBG and 2%CoBG conditions in three independent experiments using different donors. The number of colonies formed differed depending on the donor but showed a similar trend. The hMSCs commercially obtained from Lonza, UK formed the highest number of colonies likely owing to the younger age of the donor[416]. While the difference was not significant, the amount of colonies in presence of 0%CoBG dissolution products was consistently lower compared to growth medium in all independent experiments.

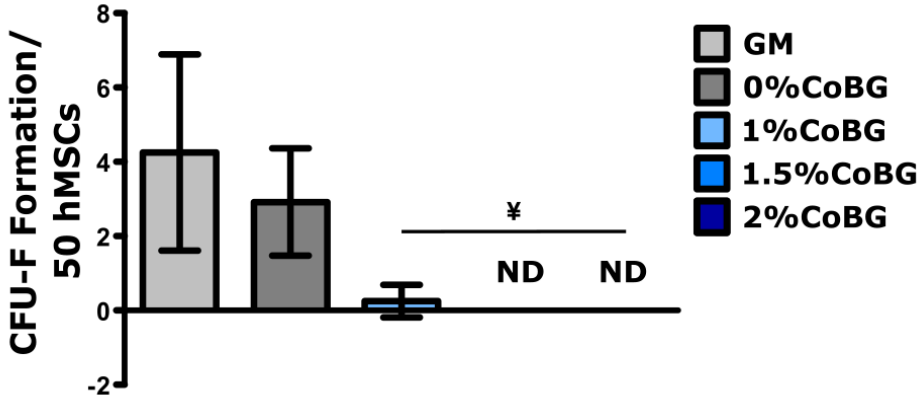


Figure 5.5: Effect of CoBG extracts on CFU-F formation by hMSCs. hMSC colony formation–fibroblast (CFU-F) efficiency was assessed after 14 days of culture in growth (GM) or CoBG-conditioned medium. In presence of bioactive glass dissolution products, the number of colonies was reduced with a particular influence of cobalt within the bioactive glass extracts. Data are expressed as mean ± SD of 3 independent experiments using different donors. ¥p<0.05 as calculated by a one-way ANOVA with Tukey *post-hoc* test. ND = non-detectable.

5.3.4.2 Migration of hMSCs in presence of CoBG dissolution products

To assess the effect of CoBG dissolution products on migration of hMSCs, a scratch assay was performed (Fig. 5.6A). In brief, hMSCs were grown until confluency and starved in CoBG-conditioned or growth medium with or without 100 µM $CoCl_2$ supplementation for 18 h prior to the introduction of a vertical "scratch" using a p1000 pipette tip. The width of the scratch was used as measure for hMSC migration and was determined after 0 h, 6 h, 24 h and 48 h. There were no significant differences between groups at all time points. Cells treated with growth medium, 0%CoBG and 1%CoBG had a comparable migratory activity. When wound closure over time was analysed, the width of the scratch was reduced significantly in all conditions save 2%CoBG after 24 h (compared to 6 h) (p<0.01 for growth medium, 0%CoBG, 1%CoBG and 100 µM $CoCl_2$, p<0.05 for 1.5%CoBG). This result implies a cobalt-concentration dependent effect within the CoBG dissolution products further underscoring the previously obtained results. When 6 h and 48 h were compared, wound closure was significantly higher for all conditions (all p<0.001).

As wound closure efficiency was not enhanced in presence of CoBG dissolution products or $CoCl_2$, it was investigated whether the protein level of CXCR4 was affected by CoBG-conditioned medium. CoBG-conditioned or growth medium was used to culture hMSCs for 24 h before CXCR4 protein expression was quantified by In-Cell Western analysis (Fig. 5.6B). There were no significant differences in CXCR4 expression in response to CoBG-dissolution products. However, this result needs to be considered with caution as only two independent experiments using different donors were performed. As CXCR4 has been identified as HIF-1α target gene, it was surprising that despite HIF-1α up-regulation CXCR4 levels remained comparable to growth medium. Since cells were permeabilised for In-Cell Western analysis, the fraction of CXCR4 protein within the plasma membrane may have been lost. CXCR4 is a 7-transmembrane G-protein coupled receptor with a predicted molecular weight for glycosylated monomers of 45 - 47 kDa. Therefore, whole cell lysates were subjected to Western blot analysis (Fig. 5.6C). Here, hMSCs were treated for 16 h in CoBG-conditioned medium with growth medium and medium supplemented with 100 µM $CoCl_2$ serving as references. Immunoblotting with the CXCR4 antibody resulted in several bands spanning molecular weights from approximately 50 kDa to 150 kDa. The lowest band corresponded to the band detected by the anti-CXCR4 antibody used for In-Cell Western analysis (Fig. 5.1B). Densiometric quantification of the 50 kDa band from two independent repeats using different donors showed a trend towards higher CXCR4 protein levels in presence of 1%CoBG and 1.5%CoBG dissolution products as well as 100 µM $CoCl_2$. However, the results obtained by Western blot analysis are very preliminary and need to be carefully evaluated. When the other bands were quantified, there was no common trend between donors. Previous studies using whole cell extracts of primary cells have reported heterogeneity in molecular weight for CXCR4[470]. Lapham *et al.* contributed the variations in molecular weight to glycosylation and ubiquitination[470]. Similarly, Wynn *et al.* observed bands corresponding to 66 kDa and 130 kDa in hMSC whole cell

extracts[441]. After deglycosylation with N-glycosidase F, a single band with a molecular weight of approximately 48 kDa was detected.

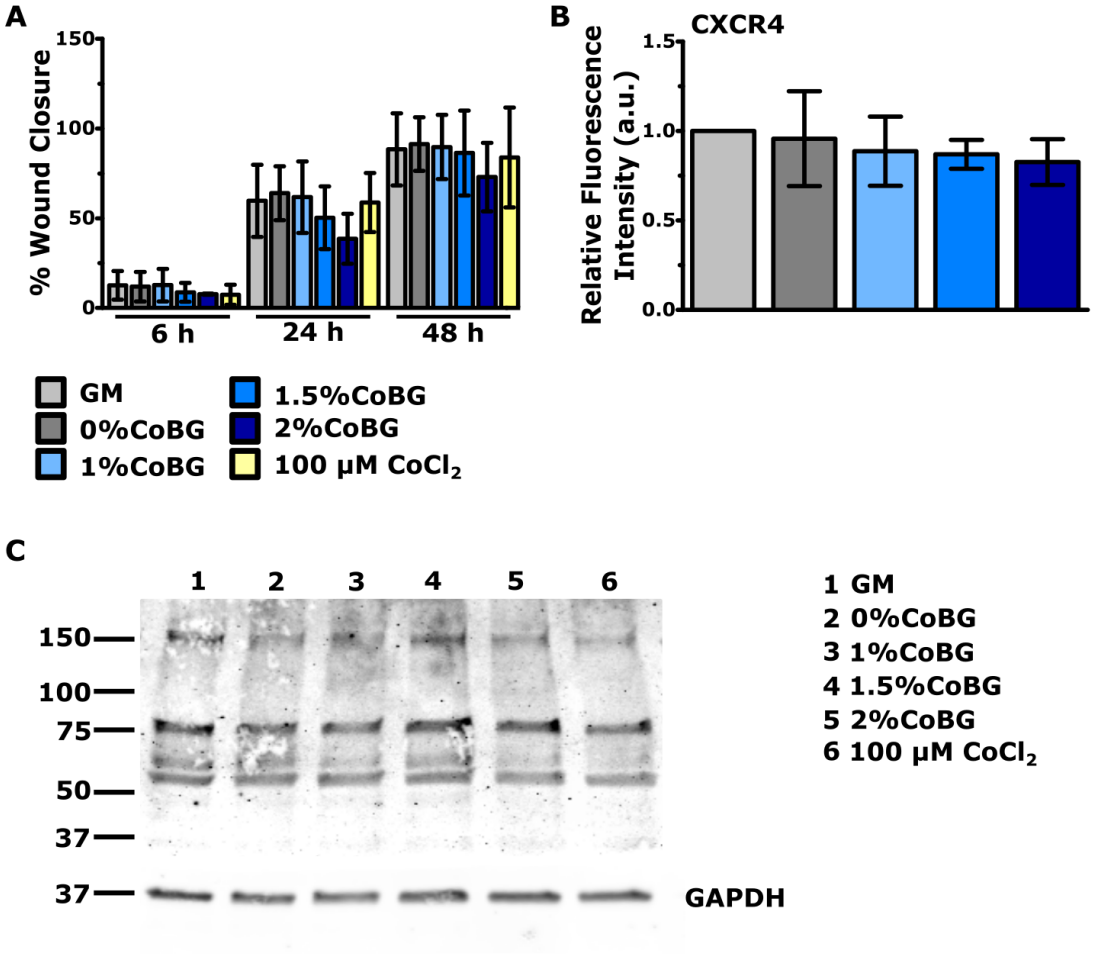


Figure 5.6: Effect of CoBG extracts on hMSC migration and CXCR4 expression. A) The scratch assay was used to determine the effect of CoBG-dissolution products on hMSC migration. Migration distance was captured at 6 h, 24 h and 48 h after a "scratch" was created in the cell monolayer. Percentages of wound closure at the indicated time points for all conditions are shown. Values are expressed relative to the width of the scratch at t = 0. Data are represented as mean ± SD of 3 independent experiments using different donors. Statistical significance was assessed by two-way ANOVA followed by Bonferroni *post-hoc* test. There were no statistical significant differences between groups. Statistically significant changes over time are not indicated in the figure. The width of the scratch was significantly smaller after 24 h (compared to 6 h) for all conditions save 2%CoBG (p<0.01 for growth medium (GM), 0%CoBG, 1%CoBG and 100 µM $CoCl_2$, p<0.05 for 1.5%CoBG). When 6 h and 48 h were compared, the width of the scratch was significantly reduced for all conditions (all p<0.001). B) CXCR4 protein expression in hMSCs cultured in growth (GM) or CoBG-conditioned medium for 24 h. Protein expression was measured by In-Cell Western analysis and is expressed relative to GM. Data are represented as mean ± SD of two independent experiments using different donors. C) Evaluation of CXCR4 protein expression in hMSCs after culture in CoBG-conditioned or GM medium for 16 h. Additionally, hMSCs were cultured in GM medium supplemented with 100 µM $CoCl_2$. Several bands were detected by the anti-CXCR4 antibody that likely owed to post-translational modification of CXCR4. The Western blot is representative of three independent experiments using different donors.

5.3.5 Downstream effect of CoBG dissolution products on hMSC cell cycle

Considering the cobalt dose-dependent reduction in cell proliferation and abolishment of CFU-F formation, the question was pursued whether the CoBG dissolution products had an influence on cell cycle regulation. Since cobalt has previously been shown to affect p21 expression, the p21 content in hMSCs was assessed after exposure to CoBG dissolution products. Previous studies observed changes in p21 protein expression after 12 h[471], 16 h[472] or 24 h[400] of hypoxic or $CoCl_2$ treatment. Therefore, it was chosen to investigate if CoBG dissolution products had an influence on p21 protein expression in hMSCs after 16 h of culture in growth medium, 100 µM $CoCl_2$ supplemented or CoBG-conditioned medium. Whole cell lysates from three different hMSC donors were subjected to Western blot analysis for p21 quantification (Fig. 5.7A). Comparison of p21 expression in three different donors showed that there was no common trend in p21 regulation that was dependent on the culture condition. This result may be explained by one or a combination of factors apart from donor variability: 1) regulation of p21 expression might have taken place at an earlier or later time point, 2) CoBG dissolution products may only induce subtle changes in p21 expression that were not detected as cells had not been synchronised in their cell cycle prior to the experiment or 3) as studies have shown that p21 expression is cell-density dependent[472], differences in hMSC confluence may have masked a possible influence of CoBG dissolution products.

As previously mentioned, the regulation of p21 is highly complex; however, p53 is a known inducer of p21 gene expression[454]. P53 is probably one of the most well-known transcription factors and famous for its role as tumour suppressor. One of its most prominent roles is to induce cell cycle arrest and, if appropriate, apoptosis in response to a variety of environmental stresses including DNA damage and hypoxia[473, 474]. While hypoxia is known to induce p53, the interplay between HIF-1α and p53 remains yet to be fully characterised. An *et al.* reported that induction of HIF-1α either by hypoxia or $CoCl_2$ resulted in an accumulation of p53 in MCF7 cells[475]. The authors claimed that the increase of p53 was mediated through HIF-1α dependent stabilisation of the protein but not by transcriptional transactivation. As p53 is known to activate p21[476] and the p53-p21 pathway is associated with growth arrest, p53 protein expression was quantified alongside of p21 (Fig. 5.7B). P53 protein abundance appeared to be differentially regulated by the different conditions and followed a similar trend in the three tested hMSC donors. After 16 h of culture in control or CoBG-conditioned medium, the p53 protein content was higher in growth medium than in all other conditions. The lack of p53 up-regulation might indicate that CoBG dissolution products did not activate the p53-dependent apoptosis pathway after 16 h of treatment. Interestingly, the level of p53 was lower in cells cultured in 100 µM $CoCl_2$ supplemented growth medium than $CoCl_2$-free growth medium. While this result warrants further confirmation, this may point towards a cobalt-dependent effect. Yet, cells treated with 0%CoBG dissolution products similarly had a lower p53 level.

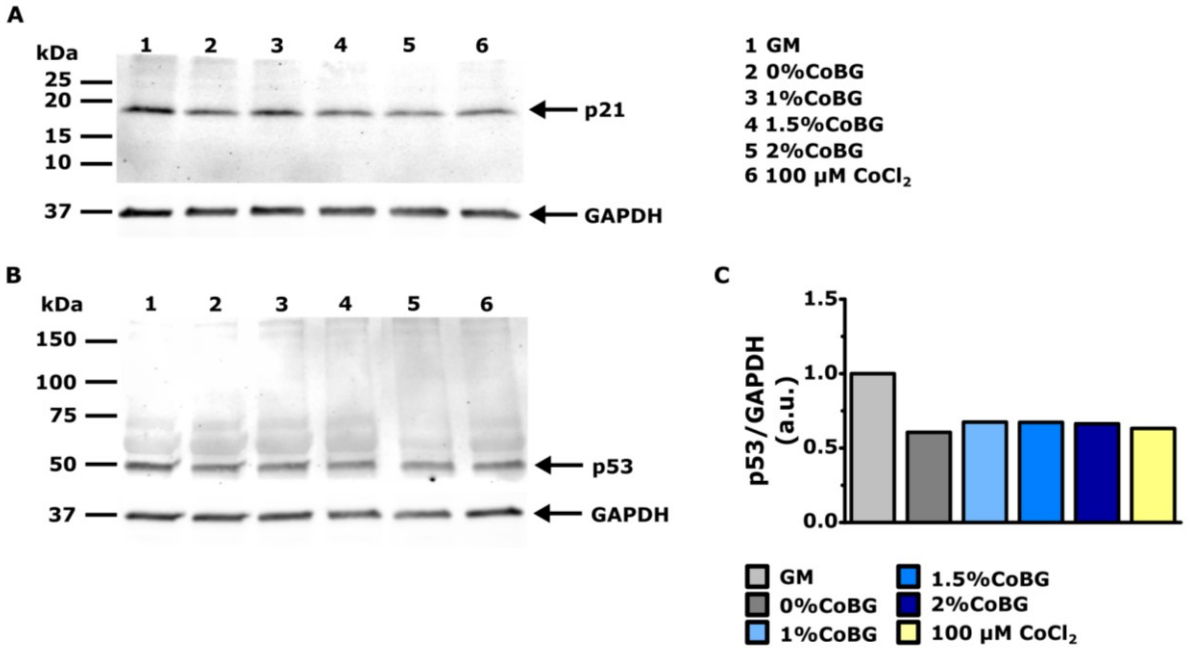


Figure 5.7: Effect of CoBG dissolution products on protein expression of the cell cycle regulators p21 and p53. A, B) hMSCs were cultured in growth (GM), 100 µM $CoCl_2$ supplemented or CoBG-conditioned medium for 16 h. Whole cell lysates of three different hMSC donors were subjected to Western blot analysis. A) There was no common trend in p21 protein expression when the independent repeats were compared. Exemplary Western blots of p21 and the loading control GAPDH are shown. B) P53 protein abundance seemed to be increased in growth medium compared to all other conditions. A representative Western blot of p53 with the loading control GAPDH is shown. C) Densitometry quantification of the cellular p53 content (normalised to GAPDH) for the representative Western blot shown in B).

5.3.6 Summary

Taken together, data presented in this chapter support the notion that CoBG-dissolution products influence hMSC behaviour in a cobalt-dose and exposure time-dependent manner. While 0%CoBG-conditioned medium performed at least as good as CoBG extract-free medium, the incorporation of cobalt appeared to induce a senescent-like state in hMSCs. Yet, culture in 1%CoBG-conditioned medium resulted in a similar outcome as CoBG extract-free medium outperforming 100 µM $CoCl_2$ despite similar cobalt ion levels. This observation may support the use of bioactive glasses as carriers for key ions to influence cell behaviour.

5.4 Discussion

In this chapter, the influence of a series of CoBGs with increasing cobalt content on hMSC behaviour was studied. In particular, the effect of the ions released from such glasses was evaluated. The cobalt ion content in the CoBG-conditioned α-MEM medium increased corresponding to the molar cobalt content in the glasses and fell within the range of concentrations routinely used to mimic hypoxia *in vitro*. The cobalt-containing CoBG dissolution products successfully enhanced HIF-1α stabilisation in hMSCs after 4 h. Continuous culture in CoBG dissolution products maintained this increase in HIF-1α stabilisation for at least 48 h. Azevedo *et al.* had previously shown an increase in HIF-1α activity in hMSCs after 8 h of exposure to CoBG-conditioned medium using the same CoBG compositions, corroborating the findings presented in this chapter[240]. Furthermore, Azevedo *et al.* demonstrated hypoxia target gene up-regulation in hMSCs in response to dissolution products derived from cobalt-doped bioactive glasses of the same compositions as used in this thesis. Therefore, an increase in HIF-1α abundance was assumed to promote the expression of HIF-1 downstream target genes. To prove this, the gene or protein level of HIF-1 targets such as VEGF should have been measured. Whether ion dissolution products from cobalt-free bioactive glasses have an effect on the HIF-1 pathway as well merits further research. Azevedo *et al.* have shown a differentially regulated gene expression of target genes of the HIF-1 pathway after exposure to 0%CoBG-conditioned medium[240]. In this context, a previous study has shown that calcium ions might affect HIF-1α synthesis and degradation[477]. Therefore, increased intracellular calcium levels through 0%CoBG dissolution products may cause a reduction in HIF-1α content[155].

Metabolic activity of hMSCs in presence of 0%CoBG dissolution products was comparable to the CoBG extract-free growth medium. In contrast, incorporation of cobalt into the glass composition or supplementation with 100 μM $CoCl_2$ significantly reduced metabolic activity compared to growth medium and 0%CoBG on day 7. Interestingly, 1%CoBG performed similarly to the growth medium condition underscoring the importance of carefully tailoring the cobalt release from biomaterials. Since no significant differences between conditions were observed after 24 h or 4 days, the length of exposure to CoBG dissolution products appeared to be critical. Supporting the observations described in this chapter, a cobalt dose-dependent reduction of hMSC metabolic activity has been reported in other studies for $CoCl_2$ concentrations of as low as 10 μM[466, 478]. The alamarBlue® assay described in Chapter 4 indicated an increase in metabolic activity in presence of cobalt-containing bioactive glass extracts after 48 h. The differences in outcome may be due to several factors. Firstly, the metabolic activity of hMSCs was evaluated at early time points using alamarBlue®. A significant increase in metabolic activity was observed with alamarBlue® for 1.5%CoBG after 48 h, a time point which was not studied using MTT assay. Secondly, alamarBlue® assay was performed on hMSCs cultured in DMEM CoBG-conditioned medium while hMSCs were cultured in α-MEM medium containing CoBG extracts for the MTT assay. While the ionic composition of both CoBG-conditioned media was similar, other medium

constituents, such as glucose, might differ and affect the response to cobalt. Apart from differences in experimental set-up, alamarBlue® and MTT assays work differently even though they are both colorimetric assays and rely on the reduction of the respective dyes. A number of enzymes can reduce both alamarBlue® and MTT, but only alamarBlue® is reduced by mitochondrial cytochromes. In addition to mitochondrial reductases, also cytoplasmic enzymes are known to reduce alamarBlue®. Interestingly, a difference in outcome between alamarBlue® and MTT assays was also observed by Dr. Maria Azevedo (PhD Thesis "Hypoxia-mimicking bioactive materials for skeletal tissue engineering", Imperial College London, Department of Materials, 2012) supporting the notion that cobalt ions may differentially affect the cellular cytoplasmic reduction potential and/ or mitochondrial enzyme activities, respectively.

Corresponding to the results observed for metabolic activity, cobalt-containing CoBG dissolution products had a dose and time-dependent effect on cell number. Medium conditioned with 0%CoBG did not significantly differ from bioactive glass-free growth medium, while previous studies have reported an enhanced cell proliferation in presence of bioactive glass dissolution products[147]. Corresponding to the results obtained with the MTT assay, cell proliferation was comparable between 1%CoBG and growth medium. In line with the findings presented herein, previous studies have observed lower cell numbers and a reduced metabolic activity in presence of cobalt ions compared to the respective control[224, 466]. Since there was no reduction in cell abundance or metabolic activity on days 4 and 7 of culture compared to day 1, cobalt appeared to influence cell proliferation rather than initiating cell death. Corroborating this hypothesis, in the study by Pacary *et al.*, cells accumulated in the G0/ G1 phase of the cell cycle in presence of cobalt ions and regulatory cell cycle proteins were found to be increased[400, 466]. Interestingly, low oxygen tension is usually associated with higher cell numbers and an enhanced rate of proliferation. In a study by Ren *et al.* the number of hMSCs treated with 100 µM $CoCl_2$ were compared with culture in a reduced oxygen environment (8%)[479]. After 3 days, the number of hMSCs was reduced in presence of $CoCl_2$ while low oxygen tension increased cell numbers compared to the normoxic control. This finding suggests a different mode of action of physiological hypoxia and hypoxia mimetic agents. Yet, there is also conflicting data as hMSC cell viability was only reduced by 500 µM $CoCl_2$ but unchanged in presence of 100 µM $CoCl_2$ after 4 days of exposure in a study by Ciavarella *et al.* possibly indicating donor-dependent effects[480]. To better characterise the influence of CoBG dissolution products on cell death, an apoptosis assay could have been performed.

Alterations in MSC morphology can be related to loss in progenitor-cell phenotype, differentiation and apoptosis to name a few mechanisms. To investigate if CoBG-dissolution products or the supplementation of $CoCl_2$ to growth medium had an influence on morphology, hMSCs were stained for F-actin. While there was no difference between conditions, hMSC morphology was found to flatten over time. Yet, cell density was lower after 7 days of culture in presence of 2%CoBG ion dissolution products underscoring the previously obtained results. In this context, culture time- and cell

density-dependent changes in MSC cell morphology have been previously described and correlated with proliferative and multilineage differentiation potential[481]. Small MSCs with a thin and spindle-like shape exhibited a good proliferative and multilineage differentiation capacity. In contrast, large, flat cell shape was associated with proliferative arrest and senescence and such cells have been termed "mature MSCs" by Colter *et al.* [482]. A previous study evaluated hMSC morphology in presence of hypoxia-mimicking agents $CoCl_2$ and deferoxamine by atomic force microscopy (AFM) and transmission electron microscopy (TEM)[466]. In contrast to the results presented in this chapter, Zeng *et al.* observed $CoCl_2$-dependent differences in cell morphology[466]. hMSCs were found to be elongated after 4 days of exposure to $CoCl_2$ and there were fewer cell-cell contacts accompanied with more gaps between adjacent cells. The discrepancies between the findings may be accounted for by the different source of hMSCs (umbilical cord vs. bone marrow), the age of the donors (infants vs. adults) or the passage numbers (3 vs. 5 - 6). Furthermore, cell morphology was evaluated by F-actin staining combined with a fluorescence microscope which is a rather crude approach compared to the use of AFM and TEM by Zeng *et al.*.

Previous studies have shown that hypoxia enhanced the stem cell-like properties of MSCs[384, 426] and exposure to 100 µM $CoCl_2$ for 7 days increased *OCT4* expression in periodontal ligament cells[450]. Data presented in this chapter demonstrated that the ability to form CFU-Fs was drastically reduced in the presence of cobalt-containing bioactive glass dissolution products. This finding may indicate a loss of replicative potential and/or stem cell properties which corroborates the data obtained by MTT/CyQUANT® Direct Cell Proliferation assays and the pronounced reduction of chondrogenic lineage commitment described in Chapter 4. Surprisingly, hMSCs cultured in 0%CoBG-conditioned medium formed fewer CFU-Fs than in growth medium; however, this was not statistically significant. Since cell proliferation was found to be at least comparable, a similar performance to growth medium could have been expected. With an average of 8% colony forming ability in the growth medium condition, the hMSCs did not show an exceptionally good replicative potential but performed better than other donors in the literature[404]. Ideally, CFU-F assays are performed with early-passage hMSCs that have preferably not undergone any freeze-thaw cycles. The hMSCs used in this chapter were frozen twice in the case of the commercially obtained hMSCs and once with respect to the hMSCs isolated at AO Foundation Davos. Cells from all donors had been initially expanded. Banfi *et al.* observed that a three week expansion of freshly isolated hMSCs reduced the fraction of clonogenic cells to 14%[483]. Interestingly, a study by Tamama *et al.* suggested that low oxygen tension enhanced CFU-F formation of immortalised MSCs despite gene knock down of HIF-1α, HIF-2α or HIF-1β by shRNAs[428]. The authors concluded that hypoxia promoted the CFU-F formation ability in a HIF-1 pathway independent manner. Yet, gene expression of the HIFs was not completely abrogated by the shRNAs and low amounts of the HIF proteins were still detected by Western blot analysis. Therefore, an influence of the HIF-1 pathway cannot be fully excluded. In contrast, transfection with constitutively stabilised HIF-1α in hMSCs increased the CFU-F efficiency in ambient conditions to levels observed with hypoxic culture

in a study by Park *et al.*[404]. As the constitutively stabilised HIF-1α did not enhance overall hMSC proliferation, the authors hypothesised that it selectively affected the proliferative potential of colony-forming mesenchymal progenitor cells. To further characterise the stem-cell like properties of hMSCs cultured in CoBG dissolution products, flow cytometry could have been used to monitor the expression of hMSC cell surface markers over time in culture.

Considering the results presented so far, the effect of CoBG dissolution products on hMSC behaviour had a dose- and time-dependent component. A treatment period longer than 4 days negatively affected cell metabolic activity and proliferation eventually abrogating the clonogenic potential of hMSCs as observed by the CFU-F assay. Therefore, it was decided to further assess the influence of CoBG dissolution products on hMSC behaviour at early time points and to investigate their influence on hMSC migration. CoBG-conditioned medium or 100 μM $CoCl_2$ supplementation had no significant effect on hMSC migration as assessed by a scratch wound healing assay. Similarly, no obvious change in CXCR4 protein expression was observed. Using reduced oxygen tension, Rosova *et al.* showed an increase in migration in a scratch wound healing assay in hypoxic conditions[449]. Schioppa *et al*. have shown in a transwell assay that hypoxic pre-conditioning enhanced the chemotactic response of HUVECs towards SDF-1 but not in absence of any stimuli[484]. In this chapter, the introduction of a "wound" served as stimuli for migration but the use of a transwell system with a SDF-1 gradient may have been a more suitable assay. Previous studies have demonstrated that CXCR4 expression was up-regulated in response to hypoxia on both, mRNA and protein levels in various cell types, including hMSCs[425, 445, 446, 484] and a similar effect was demonstrated by $CoCl_2$ treatment[448, 463]. $CoCl_2$ has been shown to up-regulate CXCR4 transcript and protein expression in microglia cells after 16 h[464]. In line with Wang *et al.* pre-conditioning of bone marrow-derived rat MSCs with 200 μM $CoCl_2$ for 24 h, enhanced the expression of CXCR4 on mRNA and protein level[448]. Yu *et al.* further observed enhanced scratch wound healing after the initial pre-conditioning[448]. Similarly, Liu *et al*. showed an up-regulation of CXCR4 in response to 100 μM $CoCl_2$ in murine MSCs which was accompanied by enhanced migration towards a SDF-1 gradient using transwell system[463]. As CXCR4 is a cell surface receptor, future work could use flow cytometry to determine the proportion of CXCR4 positive hMSCs in presence of CoBG-dissolution products. Alternatively, the plasma membrane fraction could have been isolated from the whole cell lysate and used to quantify CXCR4 receptors localised to the cell membrane by Western blot analysis. Yet, commercial membrane extraction kits have been shown to incorporate substantial cytosolic contamination suggesting that flow cytometric analysis would present a more favourable option[485]. Previous studies have shown that CXCR4 surface expression appears to be donor-dependent. Wynn *et al.* reported that only a small subset of hMSCs expressed CXCR4 on their cell surface while Honczarenko *et al.* detected a considerable bigger CXCR4 positive population[440, 441]. Yet, studies agree that the subset of CXCR4 positive cells decreases with increasing passage numbers[439-441]. In this chapter, bands likely corresponding to CXCR4 were detected by Western Bot analysis for both donors. In-Cell Western analysis using a different anti-CXCR4 antibody further corroborated this

finding. Future work could address the question, if CoBG-dissolution products had an effect on CXCR4 cell surface localisation.

As previous studies have linked an arrest in cell growth to p21 up-regulation by $CoCl_2$ treatment, a similar mechanism might have been responsible for the observations made in this chapter[400]. Quantification of p21 protein by Western blot analysis showed no common trend across the three donors. As p21 expression is influenced by many factors such as passage number[460] and confluency[472], a CoBG-dependent influence may have been masked. Furthermore, whole cell lysates were used for the data presented in this chapter. To focus on the p21 protein fraction that is actively involved in transcriptional regulation, future studies could investigate p21 protein expression in the nuclear fraction of cell lysates. Assessment of p53 revealed a reduction in protein abundance in all conditions compared to growth medium only. As both 0%CoBG and 100 µM $CoCl_2$ supplementation caused a lower level of p53, this effect can neither be attributed to bioactive glass dissolution products in general nor to the presence of cobalt ions. In contrast, Wenger *et al.* found that the hypoxia mimetics $CoCl_2$ and deferoxamine enhanced p53 expression while hypoxia (0.2%) was not sufficient to up-regulate p53[486]. Interestingly, the hypoxia mimetic deferoxamine enhanced p53 levels independently of HIF-1α suggesting supplementary pathways. In the study by Pacary *et al.* p53 gene expression was down-regulated by exposure to 100 µM $CoCl_2$ for 24 h[400]. Unfortunately, p53 expression was not quantified on protein level. To better define the influence of the conditions used in this chapter, more replicates of the experiment would be necessary. In order to fulfil its function, p53 needs to be phosphorylated[474]. Therefore, future work could assess the amount of phosphorylated p53 in hMSCs treated with the various CoBG-conditioned media or controls.

Overall, there seems to be a discrepancy between the effect of hypoxia as reported in the literature and the influence of the hypoxia mimetic cobalt, either in form of cobalt-containing CoBG dissolution products or $CoCl_2$ supplementation on hMSC behaviour. While cobalt ions mimic hypoxia in that they stabilise HIF-1α, there is evidence that cobalt treatment does not fully recapitulate low oxygen tension environments or may indeed induce additional effects in cells[479]. Several studies have shown that $CoCl_2$ treatment did not result in the predicted outcome observed with low oxygen tension[224, 487, 488]. In a study by Peters *et al.* the impact of cobalt ion exposure and oxygen deficiency on human endothelial cells were examined allowing a comparison between cobalt's hypoxia-mimicking effect and "real" hypoxia[224]. Both approaches lead to an increase of HIF-1α on protein and mRNA level. Yet, hypoxia had no adverse effect on cell number and proliferation after 24 h, while cobalt ions dose-dependently decreased both. Similarly, hypoxia stimulated the angiogenic response of endothelial cells *in vitro* when exposure to cobalt impaired the capillary-like sprout formation even at low concentrations suggesting a divergent mode of action. Likewise other studies have pointed towards differences between reduced oxygen tension and cobalt ions. Hypoxia was found to stimulate the transcription level of *COL1A1* in human dermal fibroblasts, yet $CoCl_2$ exposure failed to induce a comparable effect[489]. In accordance with the findings presented in this chapter, 100 µM $CoCl_2$ were found to reduce murine

MSC proliferation after 8 days of culture compared to control while hypoxic conditions (8% O_2) enhanced cell number over time[488]. The same study demonstrated further differences in gene expression patterns between the $CoCl_2$ treated and low oxygen tension group.

Similarly, the regulation of HIF-1α protein appears to differ between low oxygen tension and $CoCl_2$. HIF-1α protein expression in lung epithelial cells decreased after prolonged exposure (12 h) to reduced oxygen tension to normal levels while $CoCl_2$ treatment maintained a significantly higher level at the same time point[490]. This may offer an explanation for why $CoCl_2$ treatment does not necessarily induce the same functional results as seen with low oxygen tensions. Yet, the observed differences in functional outcome may also be attributed to the chosen oxygen tension and $CoCl_2$ concentration or indeed due to the overall treatment protocol. Generally, it is very difficult to compare one given reduced oxygen tension with a certain amount of $CoCl_2$. A cDNA microarray study on mouse embryonic fibroblasts cultured either in 1% O_2 or in presence of 100 µM $CoCl_2$ for 24 h revealed that out of the 286 clones differentially regulated by low oxygen tension only 54 clones overlapped with the genes influenced by $CoCl_2$ treatment indicating a profound difference in activation of signalling pathways[487]. In combination with the study presented herein these results highlight that while cobalt is a hypoxia-mimicking agent it likely does not fully recapitulate reduced oxygen levels. Notably, previous studies suggested a difference in the cellular HIF-1α regulation in response to acute and chronic hypoxia. Exposure to hypoxic environments for more than 24 h is generally referred to as "chronic". A study by Ginouvés *et al.* demonstrated that HIF-1α protein abundance decreased after initial up-regulation (4 h) to lower levels when exposed to 1% O_2 for 3 - 7 days in several cell types[491]. This effect owed to an induction of PHDs in chronic hypoxia that was further enhanced by a greater availability of O_2 due to inhibition of mitochondrial activity. Interestingly, such "desensitisation" of HIF-1α proved to be essential for cellular survival in hypoxic conditions as shown by the authors. Such a desensitisation may not have occurred in the system used for the experiments in this chapter as cobalt ions inhibit PHDs irrespective of the oxygen level. Furthermore, In-Cell Western analysis after 48 h demonstrated a prolonged stabilisation of HIF-1α.

Collectively, the large body of research concerned with cobalt is testament to the ion's powerful influence on cell behaviour. Both positive and negative effects have been reported necessitating further research into how to harness the hypoxia-mimicking properties of cobalt whilst minimising the undesired effects. With respect to biomaterials, a number of studies have developed promising cobalt-containing biomaterials and scaffold systems[234, 240, 241]. For example, Quinlan *et al.* demonstrated that cobalt-doped bioactive glass/ collagen-glycosaminoglycan scaffolds enhanced both the osteogenic response of MC3T3-E1 cells and the angiogenic response of HUVECs. Furthermore, cell number of MC3T3-E1 cells cultured on the scaffolds increased over time indicating that the cobalt content in the scaffolds was well tolerated. Perez *et al.* and Wu *et al.* observed cobalt concentration-dependent effects on cell number and metabolic activity in their respective scaffold systems reinforcing that tuning the

extent of cobalt incorporation and release is crucial for the success of cobalt-containing biomaterials[228, 237]. A matter difficult to address is that a given cobalt concentration will likely differentially affect different cell types. *In vivo*, a cell-type specific response can greatly affect the overall outcome as shown in a study by Zhang *et al.* which suggests that induction of an immune response by cobalt-containing TCP overruled the positive effect of the material on hMSC osteogenesis as observed *in vitro*[233]. As mentioned in Chapter 4, taking into account that hypoxia-like cell responses to cobalt concentrations much lower than the routinely used 100 μM have been observed, the amount of cobalt incorporated into future biomaterials and scaffolds should be carefully evaluated.

5.4.1 Limitations

As mentioned in the discussion in Chapter 4, performing the experiments presented in this chapter in parallel under low oxygen tension would have allowed to directly compare the effect of low oxygen tension and CoBG-conditioned medium. This additional condition would have presented a valuable reference point. Comparing the response of hMSCs to low oxygen tension to the response to CoBG extracts would have allowed to study a possible discrepancy between cobalt treatment and "real" hypoxia.

Even though *VEGF* gene and protein expression in response to CoBG-conditioned media has been demonstrated by Azevedo *et al.*, it would have been good to show the up-regulation of at least one of the target genes of the HIF-1 pathway to prove its activation in the work presented in this thesis[240].

5.5 Conclusion

Overall, it was demonstrated that cobalt-containing bioactive glass extracts or cobalt ion supplementation increased the protein abundance of HIF-1α in hMSCs in a cobalt dose-dependent manner. Metabolic activity and cell proliferation were reduced after 7 days of culture in presence of 2%CoBG dissolution products compared to 0%CoBG. CFU-F forming ability was nearly abrogated in presence of cobalt-containing dissolution products whilst there were no significant differences for cell migration. Taken together, the key to exploit the beneficial effects of cobalt within biomaterials seems to lie in carefully tuning its concentration both in the material and its release products. Possibly even more important is to tailor the time window of exposure to cobalt ions. Higher cobalt ion concentrations (up to 200 µM) seem to be tolerated by MSCs when applied for up to 24 h. For longer treatment periods lower concentrations are advised based on the data presented in this chapter. An interesting study has shown that cobalt ions accumulate in V79 Chinese hamster cells during continuous culture until a saturation point was reached after 12 h[199]. Yet, the end time point of the study was 24 h so that no long term data is available. In a study using HaCat cells, 40 µM was defined as non-cytotoxic while 400 µM was classified as mildly toxic[492]. The concentrations used in the present study, whilst being higher than the non-cytotoxic values, were well below 400 µM. The inhibitory effects observed in this study may have been due to a progressive built-up of cobalt within the cells or owed to differences between cell types[199]. Considering that the 1%CoBG condition performed similar to 0%CoBG and growth medium for experiments conducted up to 7 days is promising. Future studies should include a composition with an even lower cobalt substitution and/or release profile and investigate if the positive features associated with cobalt treatment can be captured. A question not addressed in this chapter is how CoBG dissolution products affect the cellular metabolism. Low oxygen tension induces a so-called metabolic switch from oxidative phosphorylation to glycolysis and it would be interesting to test how cobalt ions within bioactive glass extracts affect this system.

CHAPTER 6

Conclusions & Future directions

Motivation behind the thesis

Despite impressive advancements in the field of tissue engineering, clinical translation of tissue-engineered constructs is still limited. Currently, the most widely used approach in tissue engineering involves a triad of cells, scaffolds and growth factors or bioactive cues. The scaffold serves as template for the cells to attach, proliferate, differentiate and synthesise new extracellular matrix which ideally eventually replaces the scaffold. To improve the biological response to the scaffold, bioactive moieties tend to be incorporated. Such bioactive cues ideally guide and support cell differentiation and extracellular matrix synthesis. It is well established that cell behaviour can be influenced by physical and chemical cues. Indeed, *in vivo* cells interact with and are influenced by their surrounding extracellular matrix. Mesenchymal stem cells are considered a promising cell type for (osteochondral) tissue engineering applications due to their tri-lineage differentiation potential, the possibility to apply autologous cells as well as a considerable expansion potential *in vitro*.

Despite the superior characteristics of hMSCs, differentiation *in vitro*, in particular to the chondrogenic lineage, has not been fully optimised. *In vitro*-formed cartilaginous tissue tends to be inferior regarding the mechanical properties compared to healthy, native articular cartilage. Therefore, extensive research has been dedicated to improving *in vitro* culture conditions. To date, knowledge of the underlying mechanisms that determine the cell response to biomaterials and scaffolds remains limited. A better understanding of how bioactive moieties influence cell behaviour will enable the rational design of novel, better performing scaffolds.

Bioactive glasses are, as the name indicates, bioactive materials that are able to influence cell behaviour by direct cell-material interactions but also via their bioactive ionic dissolution products. It has been shown that such ionic dissolution products released from implants affected tissue formation *in vitro* and *in vivo*. The incorporation of therapeutic ions in scaffolds is a relatively simple and cost efficient way to promote the biological activity of biomaterials. Tailoring the composition of bioactive glasses allows a controlled release of such key therapeutic ions. Bioactive glasses have been extensively evaluated for the repair of bone defects but also more recently for soft tissue repair applications.

The aim of this thesis was to a) investigate how hMSCs respond to bioactive glass dissolution products in general and to b) explore if key therapeutic ion species can be used to direct hMSC behaviour. A better understanding of the impact of bioactive ions on hMSCs might guide future scaffold design thereby enhancing the biological response and ultimately improving the quality of tissue formed. With tissue-engineered constructs that enable the formation of native-like tissues *in vivo*, a better translation into clinical practice could be achieved.

Cell response to bioactive ions

To fully harness the potential of bioactive cues, a thorough understanding of the cellular response they elicit is essential. **Chapter 2** was building on a whole genome microarray analysis that focussed on hMSC response to strontium-containing bioactive glasses[250]. Most studies addressing the question how cells respond to biomaterials and/or particular cues are concerned with the desired outcome i.e. lineage commitment of stem cells or appropriate extracellular matrix production. This approach is reasonable and logical as it is important to know whether a material will fulfil its function. Yet, a lot of information may be lost by solely analysing the expression of selected groups of genes or proteins. Therefore, a whole genome microarray, a non-selective method, was applied to bioactive glass-conditioned medium treated cells. It was revealed that, in bioactive glass dissolution products, strontium dose-dependently strongly up-regulated the transcript levels of enzymes linked to the isoprenoid biosynthesis pathway. This finding spurred further research into how this differential regulation on a gene level translated into systemic changes in hMSCs. After confirming the results of the microarray by qPCR analysis for a selected group of genes, In-Cell Western analysis revealed a bioactive glass-dependent up-regulation of proteins associated to the isoprenoid biosynthesis pathway. Interestingly, changes in expression at the protein level were observed for FDFT1 and GGPS1 but not for HMCS1. These findings reinforce how modification of the ionic environment of cells can have a profound impact on gene expression and underline the potential of such therapeutic ion species for directing cell behaviour. The observed changes in gene and protein expression of isoprenoid biosynthesis pathway-associated enzymes were shown to cause an increase in the cholesterol content of the cellular plasma membrane in a strontium-dependent manner. Furthermore, the abundance of lipid rafts was increased in presence of strontium ions within the bioactive glass-conditioned medium. Both cholesterol and lipid rafts are crucial entities for regulating signal transduction across the plasma membrane. These findings expand the knowledge of how bioactive cues can influence cell behaviour and may contribute to the understanding of how cell-biomaterial interactions are regulated.

Future work on the impact of strontium-containing bioactive glasses would aim to examine how changes of signalling clusters in the cell membrane translate into changes in cell behaviour. In particular, the interaction of lipid rafts with the cytoskeleton is highly relevant for tissue engineering. Lipid rafts have been shown to regulate cellular polarity and adherence to the extracellular matrix as well as signalling events that influence cell migration. Building on the finding that strontium-containing bioactive glass dissolution products enhance pMLC expression, it would be highly interesting to investigate whether cell migration and cytoskeletal tension are affected. In particular, the effect on hMSCs in a 3D environment, e.g. for simplicity in a hydrogel, could offer exciting insights. Further to the preliminary results regarding hMSC pre-commitment, a more thorough study on the influence of strontium-containing bioactive glass dissolution products on hMSC differentiation could be performed.

Considering that subtle changes in the composition of the ionic environment can have a profound impact on gene expression and likely cell signalling events, in **Chapter 3**, hMSC chondrogenesis in presence of bioactive glass extracts was studied. Osteochondral defects continue to pose a challenge to the tissue engineering community as scaffolds have to fulfil the requirements of two tissues with very different mechanical and biological properties. Especially the regeneration of cartilage has proven difficult due to the tissue's inherently low capacity for self-repair. Current strategies to address this problem involve stratified constructs that offer zonal biomimetic cues optimised for the gradient structure of osteochondral tissue. The use of bioactive glass as (or the incorporation in) the bone-facing layer of such scaffolds has been evaluated with some success. In light of the strong influence of bioactive ions on cell behaviour, it is important to know how such bioactive glass dissolution products affect chondrogenic differentiation and if cell behaviour can be directed by tailoring their composition. To address this question, pelleted hMSCs were cultured in various bioactive glass-conditioned media in presence of chondrogenic supplements. Initial assessment showed that conditioned medium prepared from three out of four different bioactive glass compositions significantly increased metabolic activity. Proliferation of hMSCs in presence of BG extracts compared to BG-free medium was increased for each individual donor; however, due to donor variability cell number was not significantly different when all three donors were combined. There were no significant differences between the bioactive glass compositions. The DNA content of pellets after 21 days in culture was similar across all bioactive glass conditions and BG extract-free chondrogenic medium reinforcing the biocompatibility of the bioactive glass release products. Accumulation of sGAG normalised to DNA was significantly higher than on day 0 indicating successful chondrogenic differentiation in all conditions save Comp2-Sr. Notably, bioactive glass dissolution products appeared to have a composition-dependent effect on extracellular matrix formation as demonstrated by histology and immunohistochemistry. While Comp1-Ca and particularly Comp2-Ca performed at least as well as chondrogenic differentiation medium only, the incorporation of strontium reduced cartilage-like matrix production. Gene expression analysis of chondrogenic markers similarly indicated a composition-dependent influence, particularly for donor #6. There are two interesting outcomes from this work. Firstly, bioactive glass dissolution products were shown to allow chondrogenic differentiation of hMSCs despite their well-documented osteogenic properties. As a cautionary note it should be mentioned that the hMSCs were cultured in presence of chondrogenic supplements to guide commitment to the chondrogenic lineage. To know how bioactive glass extracts influence hMSC lineage commitment in another context, e.g. in presence of a mix of osteogenic and chondrogenic factors, would require further investigation. Secondly, it was demonstrated that the composition of the ion release products had a differential effect on *in vitro* cartilaginous tissue formation as shown by histological assessment further highlighting the impact of bioactive ions on cell behaviour.

Future work would aim at investigating whether the presence of bioactive ions has an influence on pellet formation. This is particularly interesting as integrins serve an important function in hMSC differentiation and have been shown to be affected by ions such as magnesium[493]. Bioactive glass extracts could either be exclusively added during the initial pellet formation period to examine whether the ions prime the hMSCs or throughout the whole experiment. In this work, the bioactive glass-conditioned medium was added only after pellet formation which may have prevented a stronger impact of the therapeutic ions. Additionally, it would be highly interesting to go one step further and compare the performance of different bioactive glass compositions as bone substrates of multi-layered scaffolds for osteochondral repair. To pursue this line of research, many questions regarding the scaffold design would need to be addressed. For example, it would have to be decided whether to incorporate bioactive glass particles in a composite or to fabricate a bioactive glass scaffold as bone substrate. The latter option may be hampered by materials properties as the formation of scaffolds may be, in fact, difficult for some of the compositions. Also the connection of a bioactive glass scaffold to polymer-or hydrogel-based layers may pose a challenge. Furthermore, the scaffold material for the cartilage layers and potentially the nature of the osteochondral interface would need to be defined.

Further exploring the notion that ion species can influence hMSC chondrogenesis, cobalt-containing bioactive glass extracts were evaluated in **Chapter 4**. Hypoxia fulfils not only an important function during embryonic development but hypoxic gradients are also crucial for the maintenance and repair of tissue in the adult. Hypoxic conditions can mediate angiogenesis, recruitment of progenitor cells and cell differentiation, for example after tissue damage. While hypoxia can be a transient stimulus, cartilage tissue is inherently hypoxic with oxygen tensions predicted to be below 8%. Cells adapt to changes in oxygen availability by activating oxygen dependent signalling pathways. The main oxygen sensing mechanism is the HIF-1 pathway which mediates the activation of a number of target genes such as *VEGF*, *EPO* or *SOX9*. Hypoxia has been shown to influence (stem) cell behaviour *in vitro* and is unquestionably a highly interesting concept for tissue engineering applications. Oxygen chambers have been used in a number of cell studies to artificially create a hypoxic environment. For tissue engineering purposes it is desirable, however, to design materials that are able to influence the HIF-1 pathway at the defect site. Cobalt is a well-known hypoxia-mimicking agent owing to its ability to stabilise HIF-1α. Continuing on from the previous findings that single ion species can have a pronounced impact on hMSC behaviour in general and chondrogenic differentiation in particular, it was sought to examine the influence of cobalt-containing bioactive glass dissolution products on hMSC chondrogenesis. As hypoxic conditions and $CoCl_2$ treatment were previously shown to enhance hMSC chondrogenesis, the question arose whether there was an optimum cobalt ion concentration. It was demonstrated that the incorporation of cobalt into bioactive glass dose-dependently reduced chondrogenesis of pelleted hMSCs. A similar effect was seen for donor #1 when seeded on PCL membranes. In line with the results of the previous chapter, medium containing release products of cobalt-free bioactive glass performed

at least as good as the chondrogenic medium only condition indicating a cobalt-dependent effect. The notion of a cobalt-dependent effect was further strengthened by preliminary results obtained by Raman spectroscopy as pellets cultured in cobalt-containing bioactive glass dissolution products shared characteristics with pellets cultured in $CoCl_2$ supplemented chondrogenic medium.

Future work would aim at investigating the influence of cobalt-containing bioactive glasses on pellet formation during the initial 3 day incubation period. Exposing hMSCs during that period to the release products might prime the hMSCs for subsequent chondrogenic differentiation in conventional chondrogenic medium. Furthermore, this approach would limit the overall exposure time to cobalt ions. Alternatively, a cobalt-containing bioactive glass with much lower cobalt content could be used to validate if there is a cobalt ion concentration that enhances hMSC chondrogenesis over a long term culture period.

Building on the knowledge obtained in Chapter 4, it was sought to explore in **Chapter 5** how CoBG dissolution products influenced the progenitor cell properties of hMSCs. There is exciting work being done on the impact of oxygen tension on MSC behaviour. In the bone marrow, MSCs reside in stem cell niches which are thought to be characterised by low oxygen tensions. There is evidence that hypoxia has a pronounced role in maintaining quiescence in multiple stem cell types. Appreciating the powerful influence of hypoxia, the use of hypoxia-mimicking agents has emerged as versatile tool to artificially activate the HIF-1 pathway, thereby modifying (stem) cell behaviour. Exposure to CoBG dissolution products or $CoCl_2$ significantly increased HIF-1α protein abundance in hMSCs after 4 h and 48 h suggesting a prolonged activation of the HIF-1 pathway. Culture of hMSCs in CoBG-conditioned or $CoCl_2$-supplemented medium reduced cell metabolic activity and proliferation over time in a cobalt dose-dependent manner. hMSCs cultured in 1%CoBG-conditioned medium performed comparable to 0%CoBG and growth medium suggesting that the cobalt ion release from bioactive glasses requires careful tailoring. Importantly, exposure time to Co^{2+} appeared to be a crucial factor as there were no differences in metabolic activity or proliferation after 24 h as measured by CyQUANT® Direct Cell Proliferation Assay and MTT assay. It was further demonstrated that CFU-F formation by hMSCs cultured in CoBG-conditioned medium was impaired in a cobalt-dependent manner. Migration of hMSCs in presence of cobalt-containing bioactive glass dissolution products was comparable to 0%CoBG and growth medium. Ultimately, the results of this chapter indicate that cobalt ions are strong modifiers of hMSC behaviour. The bioactive glasses used in this study are good carrier systems to deliver this hypoxia-mimicking agent. It was demonstrated, however, that the extent of cobalt release needs to be carefully tailored, especially for extended treatment periods. Importantly, longer exposure to Co^{2+} appeared to evoke undesirable outcomes, i.e. reduced metabolic activity and proliferation and reduced CFU-F formation as shown in Chapter 5.

In the literature, Co^{2+} has been used to pre-condition cells with promising results suggesting that the key to exploiting cobalt's hypoxia-mimicking effects lies in defined treatment windows of up to 24 h. Future work would therefore focus on evaluating the application of CoBG-dissolution products to prime hMSCs. It would be highly interesting to analyse how hMSCs respond to CoBG pre-conditioning on a gene level especially with respect to so-called stemness markers such as *OCT4*.

To summarise, the work contained within this thesis has expanded the knowledge on the response of hMSCs to bioactive ion species with implications for future (osteochondral) scaffold design. The biological activity of bioactive glasses stems in part from their ionic dissolution products. Therapeutic ions, either released from bioactive glasses or other materials, have shown great promise *in vitro* and *in vivo* to modify the biological response to implants. Understanding the underlying mechanisms and signalling pathways directing cell-biomaterial interactions will enable the development of rationally designed scaffolds.

For the experiments in Chapters 3 to 5, hMSCs derived from multiple donors were used to mimic a mixed patient population and to take donor variability into account. However, by using multiple donors it is more difficult to obtain statistically significant differences. The patient-derived hMSCs isolated at AO Foundation Davos were all derived from individuals undergoing total hip replacement surgery. This points towards a certain degree of morbidity of the joint which can negatively influence the "fitness" of the hMSCs or, indeed, point towards a reduced performance of the regenerative potential of hMSCs as underlying cause for the degeneration of the joint. Either way, the performance of such patient-derived hMSCs is likely restricted and inferior to hMSCs obtained from young, healthy individuals. In the work presented in this thesis, donor #6 which was commercially obtained from Lonza, UK, responded much stronger to the bioactive glass extracts presented in Chapter 3 than the patient-derived hMSCs from AO Foundation Davos. In line with this finding, the metabolic activity and the proliferative potential of donor #6 were superior to all other donors. While using different donors is valuable in the long term to obtain an overview of the donor specific responses to bioactive glass compositions, at this stage of the work, the variability intrinsic to the donors made the interpretation of the results difficult. Considering these donors independently and focusing on one donor at the time may have provided a more efficient way to better understand how bioactive glasses affect hMSC chondrogenesis.

While the focus of this thesis was solely on the dissolution products of bioactive glasses, for their therapeutic application, bioactive glasses would either be used as particulates, fabricated into scaffolds or incorporated as particles into composite scaffolds. When cells are seeded directly on bioactive glass (containing) scaffolds, many factors influence the cellular response. Apart from general scaffold parameters such as pore size, macro- and microstructure as well as (nano-)topography, there are some parameters specific to bioactive glasses. As outlined in Chapter 1, upon immersion in aqueous buffers, bioactive glasses partially dissolve, releasing ions into their surroundings. Following a

multistep process, a calcium-deficient carbonated hydroxyapatite (HCA) layer forms on the surface of bioactive glass scaffolds. *In vivo*, proteins and collagens are thought to absorb to this HCA layer facilitating the attachment of cells to the scaffold. In an *in vitro* setting, bioactive glass scaffolds are routinely pre-incubated in culture medium so that the proteins present in the medium can adhere to the scaffold. As a cautionary note it needs to be added that the interactions of cells with the HCA layer are incompletely understood as pointed out in the review by Jones[119]. In a next step, cells are thought to adhere to this HCA layer and to differentiate along the osteogenic lineage, eventually depositing new bone matrix. Osteogenesis has been attributed to the influence of bioactive glass dissolution products on progenitor cells while the HCA layer as such is thought to provide a suitable surface for osteogenic cells to attach and proliferate. It has previously been shown that the degradation rate of scaffolds *in vivo*, which depends among other factors on their fabrication but also on the bioactive glass composition itself, can influence the formation of new bone tissue. Similarly, the rise in pH associated to bioactive glass degradation influences the overall outcome. Zhang *et al.* showed that incorporation of strontium within mesoporous 3D bioactive glass scaffolds increased cell proliferation and ALP activity of MC3T3-E1 cells[494]. Similarly, incorporation of cobalt within 3D mesoporous bioactive glass scaffolds increased VEGF gene expression and protein release from hMSCs[237]. Taken together, both studies demonstrate that by incorporating key ion species into 3D bioactive glass scaffolds, cell behaviour can be modified. Whether this change in cell response was due to direct cell-scaffold interactions, ionic dissolution products or a mix thereof remains to be elucidated.

Unquestionably, there is a growing clinical need for tissue engineered constructs to replace damaged tissues. Great headway has been made in recent years and current tissue engineering approaches involve a triad of cells, bioactive cues and scaffolds with complex architectures. The most promising cell type for osteochondral tissue engineering applications is thought to be MSCs due to their tri-lineage differentiation potential and relative ease of expansion *in vitro*. Yet, differentiation protocols as well culture conditions warrant further optimisation. Tissue engineers have to address the daunting task of inducing native-like tissue growth, a process that has been optimised during evolution and that requires a considerable amount of time during embryonic and postnatal development. Unquestionably, the key to this endeavour lies in 1) understanding the cell response to biomaterials, 2) identifying the necessary cues for proper cell differentiation and 3) incorporating such moieties into scaffolds. Non-targeted methods such as the whole genome array introduced in Chapter 2 along with other high throughput methods may uncover (unexpected) pathways or molecules that govern such mechanisms and which may revolutionise the current approach to scaffold design.

References

1. Langer, R. & Vacanti, J.P. Tissue engineering. *Science* **260**, 920-926 (1993).
2. O'Brien, F.J. Biomaterials & scaffolds for tissue engineering. *Materials Today* **14**, 88-95 (2011).
3. Griffith, L.G. & Naughton, G. Tissue engineering - current challenges and expanding opportunities. *Science* **295**, 1009-1014 (2002).
4. Place, E.S., Evans, N.D. & Stevens, M.M. Complexity in biomaterials for tissue engineering. *Nature Materials* **8**, 457-470 (2009).
5. Hench, L.L. & Polak, J.M. Third-generation biomedical materials. *Science* **295**, 1014-1017 (2002).
6. Hench, L.L., Splinter, R.J., Allen, W.C. & Greenlee, T.K. Bonding mechanism at the interface of ceramic prosthetic materials. *Journal of Biomedical Materials Research Biomedical Materials Symposium* **2**, 117-141 (1972).
7. McCullen, S.D., Chow, A.G. & Stevens, M.M. In vivo tissue engineering of musculoskeletal tissues. *Current Opinion in Biotechnology* **22**, 715-720 (2011).
8. Loi, F., Córdova, L.A., Pajarinen, J., Lin, T.-h., Yao, Z. & Goodman, S.B. Inflammation, fracture and bone repair. *Bone* **86**, 119-130 (2016).
9. O'Keefe, R.J. & Mao, J. Bone tissue engineering and regeneration: from discovery to the clinic - an overview. *Tissue Engineering Part B: Reviews* **17**, 389-392 (2011).
10. Amini, A.R., Laurencin, C.T. & Nukavarapu, S.P. Bone tissue engineering: recent advances and challenges. *Critical Reviews in Biomedical Engineering* **40**, 363-408 (2012).
11. Adv Drug Deliv RevAdv Drug Deliv RevNat MaterCritical reviews in biomedical engineeringSaidak, Z. & Marie, P.J. Strontium signaling: Molecular mechanisms and therapeutic implications in osteoporosis. *Pharmacology & Therapeutics* **136**, 216-226 (2012).
12. De Long, W.G., Jr., Einhorn, T.A., Koval, K., McKee, M., Smith, W., Sanders, R. & Watson, T. Bone grafts and bone graft substitutes in orthopaedic trauma surgery. A critical analysis. *The Journal of Bone and Joint Surgery. American Volume* **89**, 649-658 (2007).
13. Fu, Q., Saiz, E., Rahaman, M.N. & Tomsia, A.P. Bioactive glass scaffolds for bone tissue engineering: state of the art and future perspectives. *Materials Science & Engineering. C, Materials for Biological Applications* **31**, 1245-1256 (2011).
14. Johnstone, B., Alini, M., Cucchiarini, M., Dodge, G.R., Eglin, D., Guilak, F., Madry, H., Mata, A., Mauck, R.L., Semino, C.E. & Stoddart, M.J. Tissue engineering for articular cartilage repair - the state of the art. *European Cells & Materials* **25**, 248-267 (2013).

15. Panseri, S., Russo, A., Cunha, C., Bondi, A., Di Martino, A., Patella, S. & Kon, E. Osteochondral tissue engineering approaches for articular cartilage and subchondral bone regeneration. *Knee Surgery, Sports Traumatology, Arthroscopy* **20**, 1182-1191 (2011).
16. Musumeci, G., Castrogiovanni, P., Leonardi, R., Trovato, F.M., Szychlinska, M.A., Di Giunta, A., Loreto, C. & Castorina, S. New perspectives for articular cartilage repair treatment through tissue engineering: A contemporary review. *World Journal of Orthopedics* **5**, 80-88 (2014).
17. Wieland, H.A., Michaelis, M., Kirschbaum, B.J. & Rudolphi, K.A. Osteoarthritis - an untreatable disease? *Nature Reviews Drug Discovery* **4**, 331-344 (2005).
18. Chen, A., Gupte, C., Akhtar, K., Smith, P. & Cobb, J. The global economic cost of osteoarthritis: how the UK compares. *Arthritis* **2012**, 6 (2012).
19. Weatherholt, A.M., Fuchs, R.K. & Warden, S.J. Specialized connective tissue: bone, the structural framework of the upper extremity. *Journal of Hand Therapy* **25**, 123-131; quiz 132 (2012).
20. Kruger, T.E., Miller, A.H. & Wang, J. Collagen scaffolds in bone sialoprotein - mediated bone regeneration. *The Scientific World Journal* **2013**, 812718 (2013).
21. Song, J., Malathong, V. & Bertozzi, C.R. Mineralization of synthetic polymer scaffolds: a bottom-up approach for the development of artificial bone. *Journal of the American Chemical Society* **127**, 3366-3372 (2005).
22. Sommerfeldt, D.W. & Rubin, C.T. Biology of bone and how it orchestrates the form and function of the skeleton. *European Spine Journal* **10 Suppl 2**, S86-95 (2001).
23. Landis, W.J., Hodgens, K.J., Arena, J., Song, M.J. & McEwen, B.F. Structural relations between collagen and mineral in bone as determined by high voltage electron microscopic tomography. *Microscopy Research and Technique* **33**, 192-202 (1996).
24. Chai, Y.C., Carlier, A., Bolander, J., Roberts, S.J., Geris, L., Schrooten, J., Van Oosterwyck, H. & Luyten, F.P. Current views on calcium phosphate osteogenicity and the translation into effective bone regeneration strategies. *Acta Biomaterialia* **8**, 3876-3887 (2012).
25. Sodek, K.L., Tupy, J.H., Sodek, J. & Grynpas, M.D. Relationships between bone protein and mineral in developing porcine long bone and calvaria. *Bone* **26**, 189-198 (2000).
26. Sapir-Koren, R. & Livshits, G. Bone mineralization and regulation of phosphate homeostasis. *IBMS BoneKEy* **8**, 286-300 (2011).
27. Nudelman, F., Lausch, A.J., Sommerdijk, N.A. & Sone, E.D. In vitro models of collagen biomineralization. *Journal of Structural Biology* (2013).
28. Bhosale, A.M. & Richardson, J.B. Articular cartilage: structure, injuries and review of management. *British Medical Bulletin* **87**, 77-95 (2008).
29. Darling, E.M. & Athanasiou, K.A. Growth factor impact on articular cartilage subpopulations. *Cell and Tissue Research* **322**, 463-473 (2005).

30. Eyre, D. Articular cartilage and changes in arthritis: collagen of articular cartilage. *Arthritis Research* **4**, 1-6 (2001).
31. Goldring, M.B. Chondrogenesis, chondrocyte differentiation, and articular cartilage metabolism in health and osteoarthritis. *Therapeutic Advances in Musculoskeletal Disease* **4**, 269-285 (2012).
32. Shen, G. The role of type X collagen in facilitating and regulating endochondral ossification of articular cartilage. *Orthodontics & Craniofacial Research* **8**, 11-17 (2005).
33. Newman, A.P. Articular cartilage repair. *The American Journal of Sports Medicine* **26**, 309-324 (1998).
34. Heng, B.C., Cao, T., Stanton, L.W., Robson, P. & Olsen, B. Strategies for directing the differentiation of stem cells into the osteogenic lineage in vitro. *Journal of Bone and Mineral Research* **19**, 1379-1394 (2004).
35. Long, M.W. Osteogenesis and bone-marrow-derived cells. *Blood Cells, Molecules &Diseases* **27**, 677-690 (2001).
36. Bianco, P., Fisher, L.W., Young, M.F., Termine, J.D. & Robey, P.G. Expression of bone sialoprotein (BSP) in developing human tissues. *Calcified Tissue International* **49**, 421-426 (1991).
37. Helder, M.N., Bronckers, A.L. & Woltgens, J.H. Dissimilar expression patterns for the extracellular matrix proteins osteopontin (OPN) and collagen type I in dental tissues and alveolar bone of the neonatal rat. *Matrix* **13**, 415-425 (1993).
38. Bronckers, A.L., Gay, S., Finkelman, R.D. & Butler, W.T. Developmental appearance of Gla proteins (osteocalcin) and alkaline phosphatase in tooth germs and bones of the rat. *Bone and Mineral* **2**, 361-373 (1987).
39. Sims, N.A. & Gooi, J.H. Bone remodeling: Multiple cellular interactions required for coupling of bone formation and resorption. *Seminars in Cell & Developmental Biology* **19**, 444-451 (2008).
40. Lin, G.L. & Hankenson, K.D. Integration of BMP, Wnt, and notch signaling pathways in osteoblast differentiation. *Journal of Cellular Biochemistry* **112**, 3491-3501 (2011).
41. Zheng, Y.H., Su, K., Jian, Y.T., Kuang, S.J. & Zhang, Z.G. Basic fibroblast growth factor enhances osteogenic and chondrogenic differentiation of human bone marrow mesenchymal stem cells in coral scaffold constructs. *Journal of Tissue Engineering and Regenerative Medicine* **5**, 540-550 (2011).
42. Javed, A., Chen, H. & Ghori, F.Y. Genetic and transcriptional control of bone formation. *Oral and Maxillofacial Surgery Clinics of North America* **22**, 283-293 (2010).
43. Robey, P.G. Cell sources for bone regeneration: the good, the bad, and the ugly (but promising). *Tissue Engineering Part B: Reviews* **17**, 423-430 (2011).

44. Salgado, A.J., Coutinho, O.P. & Reis, R.L. Bone tissue engineering: state of the art and future trends. *Macromolecular Bioscience* **4**, 743-765 (2004).
45. Kronenberg, H.M. Developmental regulation of the growth plate. *Nature* **423**, 332-336 (2003).
46. Alsalameh, S., Amin, R., Gemba, T. & Lotz, M. Identification of mesenchymal progenitor cells in normal and osteoarthritic human articular cartilage. *Arthritis & Rheumatology* **50**, 1522-1532 (2004).
47. Dowthwaite, G.P., Bishop, J.C., Redman, S.N., Khan, I.M., Rooney, P., Evans, D.J., Haughton, L., Bayram, Z., Boyer, S., Thomson, B., Wolfe, M.S. & Archer, C.W. The surface of articular cartilage contains a progenitor cell population. *Journal of Cell Science* **117**, 889-897 (2004).
48. Bertrand, J., Cromme, C., Umlauf, D., Frank, S. & Pap, T. Molecular mechanisms of cartilage remodelling in osteoarthritis. *The International Journal of Biochemistry & Cell Biology* **42**, 1594-1601 (2010).
49. Hollander, A.P., Dickinson, S.C. & Kafienah, W. Stem cells and cartilage development: complexities of a simple tissue. *Stem Cells* **28**, 1992-1996 (2010).
50. Mueller, M.B. & Tuan, R.S. Functional characterization of hypertrophy in chondrogenesis of human mesenchymal stem cells. *Arthritis & Rheumatology* **58**, 1377-1388 (2008).
51. Bush, P.G., Hall, A.C. & Macnicol, M.F. New insights into function of the growth plate: clinical observations, chondrocyte enlargement and a possible role for membrane transporters. *The Journal of Bone and Joint Surgery. British Volume* **90**, 1541-1547 (2008).
52. Stanton, L.A., Sabari, S., Sampaio, A.V., Underhill, T.M. & Beier, F. p38 MAP kinase signalling is required for hypertrophic chondrocyte differentiation. *Biochemical Journal* **378**, 53-62 (2004).
53. Wei, F., Zhou, J., Wei, X., Zhang, J., Fleming, B.C., Terek, R., Pei, M., Chen, Q., Liu, T. & Wei, L. Activation of Indian hedgehog promotes chondrocyte hypertrophy and upregulation of MMP-13 in human osteoarthritic cartilage. *Osteoarthritis Cartilage* **20**, 755-763 (2012).
54. Yoshida, C.A., Yamamoto, H., Fujita, T., Furuichi, T., Ito, K., Inoue, K., Yamana, K., Zanma, A., Takada, K., Ito, Y. & Komori, T. Runx2 and Runx3 are essential for chondrocyte maturation, and Runx2 regulates limb growth through induction of Indian hedgehog. *Genes & Development* **18**, 952-963 (2004).
55. Kwon, T.G., Zhao, X., Yang, Q., Li, Y., Ge, C., Zhao, G. & Franceschi, R.T. Physical and functional interactions between Runx2 and HIF-1alpha induce vascular endothelial growth factor gene expression. *Journal of Cellular Biochemistry* **112**, 3582-3593 (2011).
56. Wuthier, R.E. & Lipscomb, G.F. Matrix vesicles: structure, composition, formation and function in calcification. *Frontiers in Bioscience* **16**, 2812-2902 (2011).
57. Golub, E.E. Role of matrix vesicles in biomineralization. *Biochimica et Biophysica Acta* **1790**, 1592-1598 (2009).

58. Darling, E.M. & Athanasiou, K.A. Rapid phenotypic changes in passaged articular chondrocyte subpopulations. *Journal of Orthopaedic Research* **23**, 425-432 (2005).
59. Friedenstein, A.J., Chailakhjan, R.K. & Lalykina, K.S. Development of fibroblast colonies in monolayer cultures of guinea-pig bone marow and spleen cells. *Cell Proliferation* **3**, 393-403 (1970).
60. Owen, M. & Friedenstein, A.J. Stromal stem cells - marrow-derived osteogenic precursors. *Ciba Foundation Symposia* **136**, 42-60 (1988).
61. Bianco, P., Robey, P.G. & Simmons, P.J. Mesenchymal stem cells: revisiting history, concepts, and assays. *Cell Stem Cell* **2**, 313-319 (2008).
62. Caplan, A.I. Mesenchymal stem-cells. *Journal of Orthopaedic Research* **9**, 641-650 (1991).
63. Pittenger, M.F., Mackay, A.M., Beck, S.C., Jaiswal, R.K., Douglas, R., Mosca, J.D., Moorman, M.A., Simonetti, D.W., Craig, S. & Marshak, D.R. Multilineage potential of adult human mesenchymal stem cells. *Science* **284**, 143-147 (1999).
64. Dominici, M., Le Blanc, K., Mueller, I., Slaper-Cortenbach, I., Marini, F.C., Krause, D.S., Deans, R.J., Keating, A., Prockop, D.J. & Horwitz, E.M. Minimal criteria for defining multipotent mesenchymal stromal cells. The International Society for Cellular Therapy position statement. *Cytotherapy* **8**, 315-317 (2006).
65. Abdallah, B.M. & Kassem, M. Human mesenchymal stem cells: from basic biology to clinical applications. *Gene Therapy* **15**, 109-116 (2008).
66. Caplan, A.I. Adult mesenchymal stem cells for tissue engineering versus regenerative medicine. *Journal of Cellular Physiology* **213**, 341-347 (2007).
67. Dezawa, M., Kanno, H., Hoshino, M., Cho, H., Matsumoto, N., Itokazu, Y., Tajima, N., Yamada, H., Sawada, H., Ishikawa, H., Mimura, T., Kitada, M., Suzuki, Y. & Ide, C. Specific induction of neuronal cells from bone marrow stromal cells and application for autologous transplantation. *The Journal of Clinical Investigation* **113**, 1701-1710 (2004).
68. Luk, J.M., Wang, P.P., Lee, C.K., Wang, J.H. & Fan, S.T. Hepatic potential of bone marrow stromal cells: development of in vitro co-culture and intra-portal transplantation models. *Journal of Immunological Methods* **305**, 39-47 (2005).
69. Arvidson, K., Abdallah, B.M., Applegate, L.A., Baldini, N., Cenni, E., Gomez-Barrena, E., Granchi, D., Kassem, M., Konttinen, Y.T., Mustafa, K., Pioletti, D.P., Sillat, T. & Finne-Wistrand, A. Bone regeneration and stem cells. *Journal of Cellular and Molecular Medicine* **15**, 718-746 (2011).
70. Abdallah, B.M. & Kassem, M. The use of mesenchymal (skeletal) stem cells for treatment of degenerative diseases: current status and future perspectives. *Journal of Cellular Physiology* **218**, 9-12 (2009).
71. Jones, C.P. & Rankin, S.M. Bone marrow-derived stem cells and respiratory disease. *Chest* **140**, 205-211 (2011).

72. Najar, M., Raicevic, G., Fayyad-Kazan, H., Bron, D., Toungouz, M. & Lagneaux, L. Mesenchymal stromal cells and immunomodulation: a gathering of regulatory immune cells. *Cytotherapy* **18**, 160-171 (2016).
73. Caplan, A.I. & Sorrell, J.M. The MSC curtain that stops the immune system. *Immunology Letters* **168**, 136-139 (2015).
74. Colnot, C. Cell sources for bone tissue engineering: insights from basic science. *Tissue Engineering Part B: Reviews* **17**, 449-457 (2011).
75. Komori, T. Runx2, a multifunctional transcription factor in skeletal development. *Journal of Cellular Biochemistry* **87**, 1-8 (2002).
76. Komori, T., Yagi, H., Nomura, S., Yamaguchi, A., Sasaki, K., Deguchi, K., Shimizu, Y., Bronson, R.T., Gao, Y.H., Inada, M., Sato, M., Okamoto, R., Kitamura, Y., Yoshiki, S. & Kishimoto, T. Targeted disruption of Cbfa1 results in a complete lack of bone formation owing to maturational arrest of osteoblasts. *Cell* **89**, 755-764 (1997).
77. Ducy, P., Zhang, R., Geoffroy, V., Ridall, A.L. & Karsenty, G. Osf2/Cbfa1: a transcriptional activator of osteoblast differentiation. *Cell* **89**, 747-754 (1997).
78. Banerjee, C., Javed, A., Choi, J.Y., Green, J., Rosen, V., van Wijnen, A.J., Stein, J.L., Lian, J.B. & Stein, G.S. Differential regulation of the two principal Runx2/Cbfa1 n-terminal isoforms in response to bone morphogenetic protein-2 during development of the osteoblast phenotype. *Endocrinology* **142**, 4026-4039 (2001).
79. Fujita, T., Azuma, Y., Fukuyama, R., Hattori, Y., Yoshida, C., Koida, M., Ogita, K. & Komori, T. Runx2 induces osteoblast and chondrocyte differentiation and enhances their migration by coupling with PI3K-Akt signaling. *The Journal of Cell Biology* **166**, 85-95 (2004).
80. Akiyama, H. Control of chondrogenesis by the transcription factor Sox9. *Modern Rheumatology* **18**, 213-219 (2008).
81. Bi, W., Deng, J.M., Zhang, Z., Behringer, R.R. & de Crombrugghe, B. Sox9 is required for cartilage formation. *Nature Genetics* **22**, 85-89 (1999).
82. Akiyama, H., Chaboissier, M.-C., Martin, J.F., Schedl, A. & de Crombrugghe, B. The transcription factor Sox9 has essential roles in successive steps of the chondrocyte differentiation pathway and is required for expression of Sox5 and Sox6. *Genes & Development* **16**, 2813-2828 (2002).
83. Johnstone, B., Hering, T.M., Caplan, A.I., Goldberg, V.M. & Yoo, J.U. In vitro chondrogenesis of bone marrow-derived mesenchymal progenitor cells. *Experimental Cell Research* **238**, 265-272 (1998).
84. Pelttari, K., Winter, A., Steck, E., Goetzke, K., Hennig, T., Ochs, B.G., Aigner, T. & Richter, W. Premature induction of hypertrophy during in vitro chondrogenesis of human mesenchymal stem cells correlates with calcification and vascular invasion after ectopic transplantation in SCID mice. *Arthritis & Rheumatism* **54**, 3254-3266 (2006).

85. Mathews, S., Bhonde, R., Gupta, P.K. & Totey, S. Extracellular matrix protein mediated regulation of the osteoblast differentiation of bone marrow derived human mesenchymal stem cells. *Differentiation* **84**, 185-192 (2012).
86. Takarada, T., Nakazato, R., Tsuchikane, A., Fujikawa, K., Iezaki, T., Yoneda, Y. & Hinoi, E. Genetic analysis of Runx2 function during intramembranous ossification. *Development* (2015).
87. Fröhlich, M., Grayson, W.L., Wan, L.Q., Marolt, D., Drobnic, M. & Vunjak-Novakovic, G. Tissue engineered bone grafts: biological requirements, tissue culture and clinical relevance. *Current Stem Cell Research & Therapy* **3**, 254-264 (2008).
88. Mackie, E.J., Ahmed, Y.A., Tatarczuch, L., Chen, K.S. & Mirams, M. Endochondral ossification: how cartilage is converted into bone in the developing skeleton. *The International Journal of Biochemistry & Cell Biology* **40**, 46-62 (2008).
89. Lee, K., Lanske, B., Karaplis, A.C., Deeds, J.D., Kohno, H., Nissenson, R.A., Kronenberg, H.M. & Segre, G.V. Parathyroid hormone-related peptide delays terminal differentiation of chondrocytes during endochondral bone development. *Endocrinology* **137**, 5109-5118 (1996).
90. Matsuo, K. & Irie, N. Osteoclast-osteoblast communication. *Archives of Biochemistry and Biophysics* **473**, 201-209 (2008).
91. Thompson, E.M., Matsiko, A., Farrell, E., Kelly, D.J. & O'Brien, F.J. Recapitulating endochondral ossification: a promising route to in vivo bone regeneration. *Journal of Tissue Engineering and Regenerative Medicine* **9**, 889-902 (2015).
92. Karageorgiou, V. & Kaplan, D. Porosity of 3D biomaterial scaffolds and osteogenesis. *Biomaterials* **26**, 5474-5491 (2005).
93. Murphy, C.M., Haugh, M.G. & O'Brien, F.J. The effect of mean pore size on cell attachment, proliferation and migration in collagen–glycosaminoglycan scaffolds for bone tissue engineering. *Biomaterials* **31**, 461-466 (2010).
94. Deville, S., Saiz, E. & Tomsia, A.P. Freeze casting of hydroxyapatite scaffolds for bone tissue engineering. *Biomaterials* **27**, 5480-5489 (2006).
95. Habibovic, P. & de Groot, K. Osteoinductive biomaterials - properties and relevance in bone repair. *Journal of Tissue Engineering and Regenerative Medicine* **1**, 25-32 (2007).
96. Habibovic, P., Yuan, H., van der Valk, C.M., Meijer, G., van Blitterswijk, C.A. & de Groot, K. 3D microenvironment as essential element for osteoinduction by biomaterials. *Biomaterials* **26**, 3565-3575 (2005).
97. Chan, O., Coathup, M.J., Nesbitt, A., Ho, C.Y., Hing, K.A., Buckland, T., Campion, C. & Blunn, G.W. The effects of microporosity on osteoinduction of calcium phosphate bone graft substitute biomaterials. *Acta Biomaterialia* **8**, 2788-2794 (2012).
98. Saiz, E., Zimmermann, E.A., Lee, J.S., Wegst, U.G. & Tomsia, A.P. Perspectives on the role of nanotechnology in bone tissue engineering. *Dent Mater* **29**, 103-115 (2013).

99. Dalby, M.J., Gadegaard, N., Curtis, A.S. & Oreffo, R.O. Nanotopographical control of human osteoprogenitor differentiation. *Current Stem Cell Research & Therapy* **2**, 129-138 (2007).
100. Hutmacher, D.W., Teoh, S.H., Zein, I., Ranawake, M. & Lau, S. Tissue engineering research: the engineer's role. *Medical Device Technology* **11**, 33-39 (2000).
101. Epstein, N.E. Complications due to the use of BMP/INFUSE in spine surgery: the evidence continues to mount. *Surgical Neurology International* **4**, S343-S352 (2013).
102. Blokhuis, T.J. & Arts, J.J. Bioactive and osteoinductive bone graft substitutes: definitions, facts and myths. *Injury* **42 Suppl 2**, S26-29 (2011).
103. Urist, M.R. Bone: formation by autoinduction. *Science* **150**, 893-899 (1965).
104. Albrektsson, T. & Johansson, C. Osteoinduction, osteoconduction and osseointegration. *European Spine Journal* **10 Suppl 2**, S96-101 (2001).
105. Wilson, J. & Low, S.B. Bioactive ceramics for periodontal treatment: comparative studies in the Patus monkey. *Journal of Applied Biomaterials* **3**, 123-129 (1992).
106. Barradas, A.M., Yuan, H., van Blitterswijk, C.A. & Habibovic, P. Osteoinductive biomaterials: current knowledge of properties, experimental models and biological mechanisms. *European Cells & Materials* **21**, 407-429; discussion 429 (2011).
107. Brauer, D.S. Bioactive glasses - structure and properties. *Angewandte Chemie International Edition* **54**, 4160-4181 (2015).
108. LeGeros, R.Z. Calcium phosphate-based osteoinductive materials. *Chemical Reviews* **108**, 4742-4753 (2008).
109. El-Ghannam, A. Bone reconstruction: from bioceramics to tissue engineering. *Expert Review of Medical Devices* **2**, 87-101 (2005).
110. Chistolini, P., Ruspantini, I., Bianco, P., Corsi, A., Cancedda, R. & Quarto, R. Biomechanical evaluation of cell-loaded and cell-free hydroxyapatite implants for the reconstruction of segmental bone defects. *Journal of Materials Science. Materials in Medicine* **10**, 739-742 (1999).
111. Balas, F., Pérez-Pariente, J. & Vallet-Regí, M. In vitro bioactivity of silicon-substituted hydroxyapatites. *Journal of Biomedical Materials Research Part A* **66A**, 364-375 (2003).
112. Houmard, M., Fu, Q., Genet, M., Saiz, E. & Tomsia, A.P. On the structural, mechanical, and biodegradation properties of HA/beta-TCP robocast scaffolds. *Journal of Biomedical Materials Research. Part B, Applied Biomaterials* (2013).
113. Hutmacher, D.W., Schantz, J.T., Lam, C.X., Tan, K.C. & Lim, T.C. State of the art and future directions of scaffold-based bone engineering from a biomaterials perspective. *Journal of Tissue Engineering and Regenerative Medicine* **1**, 245-260 (2007).
114. Krüger, R. & Groll, J. Fiber reinforced calcium phosphate cements - on the way to degradable load bearing bone substitutes? *Biomaterials* **33**, 5887-5900 (2012).

115. Habibovic, P., van der Valk, C.M., van Blitterswijk, C.A., De Groot, K. & Meijer, G. Influence of octacalcium phosphate coating on osteoinductive properties of biomaterials. *Journal of Materials Science. Materials in Medicine* **15**, 373-380 (2004).
116. Rezwan, K., Chen, Q.Z., Blaker, J.J. & Boccaccini, A.R. Biodegradable and bioactive porous polymer/inorganic composite scaffolds for bone tissue engineering. *Biomaterials* **27**, 3413-3431 (2006).
117. Hench, L.L. The story of Bioglass. *Journal of Materials Science. Materials in Medicine* **17**, 967-978 (2006).
118. Hench, L.L., Splinter, R.J., Allen, W.C. & Greenlee, T.K. Bonding mechanisms at the interface of ceramic prosthetic materials. *Journal of Biomedical Materials Research* **5**, 117-141 (1971).
119. Jones, J.R. Review of bioactive glass: from Hench to hybrids. *Acta Biomaterialia* **9**, 4457-4486 (2013).
120. Lindfors, N.C. & Aho, A.J. Granule size and composition of bioactive glasses affect osteoconduction in rabbit. *Journal of Materials Science. Materials in Medicine* **14**, 365-372 (2003).
121. Shelby, J.E. Introduction to glass science and technology., Edn. 2nd. (The Royal Society of Chemistry., Cambridge; 2005).
122. Hench, L.L. & West, J.K. The sol-gel process. *Chemical Reviews* **90**, 33-72 (1990).
123. Zachariasen, W.H. The atomic arrangement in glass. *Journal of the American Chemical Society* **54**, 3841-3851 (1932).
124. Hench, L.L. Bioceramics: from concept to clinic. *Journal of the American Ceramic Society* **74**, 24 (1991).
125. Hench, L.L. Biomaterials: a forecast for the future. *Biomaterials* **19**, 1419-1423 (1998).
126. Rahaman, M.N., Day, D.E., Bal, B.S., Fu, Q., Jung, S.B., Bonewald, L.F. & Tomsia, A.P. Bioactive glass in tissue engineering. *Acta Biomaterialia* **7**, 2355-2373 (2011).
127. Wallace, K.E., Hill, R.G., Pembroke, J.T., Brown, C.J. & Hatton, P.V. Influence of sodium oxide content on bioactive glass properties. *Journal of Materials Science: Materials in Medicine* **10**, 697-701.
128. Fredholm, Y.C., Karpukhina, N., Brauer, D.S., Jones, J.R., Law, R.V. & Hill, R.G. Influence of strontium for calcium substitution in bioactive glasses on degradation, ion release and apatite formation. *Journal of the Royal Society, Interface* **9**, 880-889 (2012).
129. Ducheyne, P. & Qiu, Q. Bioactive ceramics: the effect of surface reactivity on bone formation and bone cell function. *Biomaterials* **20**, 2287-2303 (1999).
130. Filho, O.P., La Torre, G.P. & Hench, L.L. Effect of crystallization on apatite-layer formation of bioactive glass 45S5. *Journal of Biomedical Materials Research* **30**, 509-514 (1996).
131. Chen, Q.Z., Thompson, I.D. & Boccaccini, A.R. 45S5 Bioglass-derived glass-ceramic scaffolds for bone tissue engineering. *Biomaterials* **27**, 2414-2425 (2006).

132. Schepers, E., Declercq, M., Ducheyne, P. & Kempeneers, R. Bioactive glass particulate material as a filler for bone-lesions. *Journal of Oral Rehabilitation* **18**, 439-452 (1991).

133. Yun, H.-S., Park, J.-W., Kim, S.-H., Kim, Y.-J. & Jang, J.-H. Effect of the pore structure of bioactive glass balls on biocompatibility in vitro and in vivo. *Acta Biomaterialia* **7**, 2651-2660 (2011).

134. Foppiano, S., Marshall, S.J., Marshall, G.W., Saiz, E. & Tomsia, A.P. The influence of novel bioactive glasses on in vitro osteoblast behavior. *Journal of Biomedical Materials Research Part A* **71A**, 242-249 (2004).

135. Gough, J.E., Jones, J.R. & Hench, L.L. Nodule formation and mineralisation of human primary osteoblasts cultured on a porous bioactive glass scaffold. *Biomaterials* **25**, 2039-2046 (2004).

136. Jones, J.R., Tsigkou, O., Coates, E.E., Stevens, M.M., Polak, J.M. & Hench, L.L. Extracellular matrix formation and mineralization on a phosphate-free porous bioactive glass scaffold using primary human osteoblast (HOB) cells. *Biomaterials* **28**, 1653-1663 (2007).

137. Xynos, I.D., Hukkanen, M.V.J., Batten, J.J., Buttery, L.D., Hench, L.L. & Polak, J.M. Bioglass 45S5 stimulates osteoblast turnover and enhances bone formation in vitro: Implications and applications for bone tissue engineering. *Calcified Tissue International* **67**, 321-329 (2000).

138. Loty, C., Sautier, J.M., Tan, M.T., Oboeuf, M., Jallot, E., Boulekbache, H., Greenspan, D. & Forest, N. Bioactive glass stimulates in vitro osteoblast differentiation and creates a favorable template for bone tissue formation. *Journal of Bone and Mineral Research* **16**, 231-239 (2001).

139. Radin, S., Reilly, G., Bhargave, G., Leboy, P.S. & Ducheyne, P. Osteogenic effects of bioactive glass on bone marrow stromal cells. *Journal of Biomedical Materials Research Part A* **73A**, 21-29 (2005).

140. Hattar, S., Asselin, A., Greenspan, D., Oboeuf, M., Berdal, A. & Sautier, J.M. Potential of biomimetic surfaces to promote in vitro osteoblast-like cell differentiation. *Biomaterials* **26**, 839-848 (2005).

141. Bosetti, M., Zanardi, L., Hench, L. & Cannas, M. Type I collagen production by osteoblast-like cells cultured in contact with different bioactive glasses. *Journal of Biomedical Materials Research Part A* **64A**, 189-195 (2003).

142. Bosetti, M. & Cannas, M. The effect of bioactive glasses on bone marrow stromal cells differentiation. *Biomaterials* **26**, 3873-3879 (2005).

143. Khojasteh, A., Behnia, H., Naghdi, N., Esmaeelinejad, M., Alikhassy, Z. & Stevens, M. Effects of different growth factors and carriers on bone regeneration: a systematic review. *Oral Surgery, Oral Medicine, Oral Pathology and Oral Radiology* (2012).

144. Shin, H., Jo, S. & Mikos, A.G. Biomimetic materials for tissue engineering. *Biomaterials* **24**, 4353-4364 (2003).

145. Webster, T.J., Massa-Schlueter, E.A., Smith, J.L. & Slamovich, E.B. Osteoblast response to hydroxyapatite doped with divalent and trivalent cations. *Biomaterials* **25**, 2111-2121 (2004).

146. Hoppe, A., Guldal, N.S. & Boccaccini, A.R. A review of the biological response to ionic dissolution products from bioactive glasses and glass-ceramics. *Biomaterials* **32**, 2757-2774 (2011).

147. Xynos, I.D., Edgar, A.J., Buttery, L.D.K., Hench, L.L. & Polak, J.M. Ionic products of bioactive glass dissolution increase proliferation of human osteoblasts and induce Insulin-like growth factor II mRNA expression and protein synthesis. *Biochemical and Biophysical Research Communications* **276**, 461-465 (2000).

148. Xynos, I.D., Edgar, A.J., Buttery, L.D.K., Hench, L.L. & Polak, J.M. Gene-expression profiling of human osteoblasts following treatment with the ionic products of Bioglass 45S5 dissolution. *Journal of Biomedical Materials Research* **55**, 151-157 (2001).

149. Jell, G., Notingher, I., Tsigkou, O., Notingher, P., Polak, J.M., Hench, L.L. & Stevens, M.M. Bioactive glass-induced osteoblast differentiation: A noninvasive spectroscopic study. *Journal of Biomedical Materials Research Part A* **86A**, 31-40 (2008).

150. Tsigkou, O., Jones, J.R., Polak, J.M. & Stevens, M.M. Differentiation of fetal osteoblasts and formation of mineralized bone nodules by 45S5 Bioglass® conditioned medium in the absence of osteogenic supplements. *Biomaterials* **30**, 3542-3550 (2009).

151. Christodoulou, I., Buttery, L.D.K., Tai, G., Hench, L.L. & Polak, J.M. Characterization of human fetal osteoblasts by microarray analysis following stimulation with 58S bioactive gel-glass ionic dissolution products. *Journal of Biomedical Materials Research Part B: Applied Biomaterials* **77B**, 431-446 (2006).

152. Gorustovich, A.A., Roether, J.A. & Boccaccini, A.R. Effect of bioactive glasses on angiogenesis: a review of in vitro and in vivo evidences. *Tissue Engineering Part B: Reviews* **16**, 199-207 (2009).

153. Ojansivu, M., Vanhatupa, S., Björkvik, L., Häkkänen, H., Kellomäki, M., Autio, R., Ihalainen, J.A., Hupa, L. & Miettinen, S. Bioactive glass ions as strong enhancers of osteogenic differentiation in human adipose stem cells. *Acta Biomaterialia* **21**, 190-203 (2015).

154. Reilly, G.C., Radin, S., Chen, A.T. & Ducheyne, P. Differential alkaline phosphatase responses of rat and human bone marrow derived mesenchymal stem cells to 45S5 bioactive glass. *Biomaterials* **28**, 4091-4097 (2007).

155. Silver, I.A., Deas, J. & Erecińska, M. Interactions of bioactive glasses with osteoblasts in vitro: effects of 45S5 Bioglass®, and 58S and 77S bioactive glasses on metabolism, intracellular ion concentrations and cell viability. *Biomaterials* **22**, 175-185 (2001).

156. Laquerriere, P., Jallot, E., Kilian, L., Benhayoune, H. & Balossier, G. Effects of bioactive glass particles and their ionic products on intracellular concentrations. *Journal of Biomedical Materials Research Part A* **65A**, 441-446 (2003).

157. Jell, G. & Stevens, M.M. Gene activation by bioactive glasses. *Journal of Materials Science: Materials in Medicine* **17**, 997-1002 (2006).

158. Cabrera, W.E., Schrooten, I., De Broe, M.E. & D'Haese, P.C. Strontium and bone. *Journal of Bone and Mineral Research* **14**, 661-668 (1999).

159. Boivin, G., Deloffre, P., Perrat, B., Panczer, G., Boudeulle, M., Mauras, Y., Allain, P., Tsouderos, Y. & Meunier, P.J. Strontium distribution and interactions with bone mineral in monkey iliac bone after strontium salt (S 12911) administration. *Journal of Bone and Mineral Research* **11**, 1302-1311 (1996).

160. Schrooten, I., Cabrera, W., Goodman, W.G., Dauwe, S., Lamberts, L.V., Marynissen, R., Dorrine, W., De Broe, M.E. & D'Haese, P.C. Strontium causes osteomalacia in chronic renal failure rats. *Kidney International* **54**, 448-456 (1998).

161. Grynpas, M.D. & Marie, P.J. Effects of low doses of strontium on bone quality and quantity in rats. *Bone* **11**, 313-319 (1990).

162. Cattani-Lorente, M., Rizzoli, R. & Ammann, P. In vitro bone exposure to strontium improves bone material level properties. *Acta Biomaterialia* **9**, 7005-7013 (2013).

163. Peng, S., Zhou, G., Luk, K.D., Cheung, K.M., Li, Z., Lam, W.M., Zhou, Z. & Lu, W.W. Strontium promotes osteogenic differentiation of mesenchymal stem cells through the Ras/MAPK signaling pathway. *Cellular Physiology and Biochemistry* **23**, 165-174 (2009).

164. Peng, S., Liu, X.S., Wang, T., Li, Z., Zhou, G., Luk, K.D., Guo, X.E. & Lu, W.W. In vivo anabolic effect of strontium on trabecular bone was associated with increased osteoblastogenesis of bone marrow stromal cells. *Journal of Orthopaedic Research* **28**, 1208-1214 (2010).

165. Yang, F., Yang, D., Tu, J., Zheng, Q., Cai, L. & Wang, L. Strontium enhances osteogenic differentiation of mesenchymal stem cells and in vivo bone formation by activating Wnt/catenin signaling. *Stem Cells* **29**, 981-991 (2011).

166. N. I. H. Consensus Development Panel on Osteoporosis Prevention Diagnosis, a.T. Osteoporosis prevention, diagnosis, and therapy. *Journal of the Medical Association* **285**, 785-795 (2001).

167. Meunier, P.J., Roux, C., Ortolani, S., Diaz-Curiel, M., Compston, J., Marquis, P., Cormier, C., Isaia, G., Badurski, J., Wark, J.D., Collette, J. & Reginster, J.Y. Effects of long-term strontium ranelate treatment on vertebral fracture risk in postmenopausal women with osteoporosis. *Osteoporosis International* **20**, 1663-1673 (2009).

168. Reginster, J.Y., Seeman, E., De Vernejoul, M.C., Adami, S., Compston, J., Phenekos, C., Devogelaer, J.P., Curiel, M.D., Sawicki, A., Goemaere, S., Sorensen, O.H., Felsenberg, D. & Meunier, P.J. Strontium ranelate reduces the risk of nonvertebral fractures in postmenopausal women with osteoporosis: treatment of peripheral osteoporosis (TROPOS) study. *The Journal of Clinical Endocrinology and Metabolism* **90**, 2816-2822 (2005).

169. Bain, S.D., Jerome, C., Shen, V., Dupin-Roger, I. & Ammann, P. Strontium ranelate improves bone strength in ovariectomized rat by positively influencing bone resistance determinants. *Osteoporosis International* **20**, 1417-1428 (2009).

170. Canalis, E., Hott, M., Deloffre, P., Tsouderos, Y. & Marie, P.J. The divalent strontium salt S12911 enhances bone cell replication and bone formation in vitro. *Bone* **18**, 517-523 (1996).

171. Barbara, A., Delannoy, P., Denis, B.G. & Marie, P.J. Normal matrix mineralization induced by strontium ranelate in MC3T3-E1 osteogenic cells. *Metabolism* **53**, 532-537 (2004).

172. Baron, R. & Tsouderos, Y. In vitro effects of S12911-2 on osteoclast function and bone marrow macrophage differentiation. *European Journal of Pharmacology* **450**, 11-17 (2002).

173. Bonnelye, E., Chabadel, A., Saltel, F. & Jurdic, P. Dual effect of strontium ranelate: stimulation of osteoblast differentiation and inhibition of osteoclast formation and resorption in vitro. *Bone* **42**, 129-138 (2008).

174. Chavassieux, P., Meunier, P.J., Roux, J.P., Portero-Muzy, N., Pierre, M. & Chapurlat, R. Bone histomorphometry of transiliac paired bone biopsies after 6 or 12 months of treatment with oral strontium ranelate in 387 osteoporotic women: randomized comparison to alendronate. *Journal of Bone and Mineral Research* **29**, 618-628 (2014).

175. Yamaguchi, M. & Weitzmann, M.N. The intact strontium ranelate complex stimulates osteoblastogenesis and suppresses osteoclastogenesis by antagonizing NF-kappaB activation. *Molecular and Cellular Biochemistry* **359**, 399-407 (2012).

176. Fromigue, O., Hay, E., Barbara, A. & Marie, P.J. Essential role of nuclear factor of activated T cells (NFAT)-mediated Wnt signaling in osteoblast differentiation induced by strontium ranelate. *The Journal of Biological Chemistry* **285**, 25251-25258 (2010).

177. Brennan, T.C., Rybchyn, M.S., Green, W., Atwa, S., Conigrave, A.D. & Mason, R.S. Osteoblasts play key roles in the mechanisms of action of strontium ranelate. *British Journal of Pharmacology* **157**, 1291-1300 (2009).

178. Caudrillier, A., Hurtel-Lemaire, A.S., Wattel, A., Cournarie, F., Godin, C., Petit, L., Petit, J.P., Terwilliger, E., Kamel, S., Brown, E.M., Mentaverri, R. & Brazier, M. Strontium ranelate decreases receptor activator of nuclear factor-KappaB ligand-induced osteoclastic differentiation in vitro: involvement of the calcium-sensing receptor. *Molecular Pharmacology* **78**, 569-576 (2010).

179. Fromigue, O., Hay, E., Barbara, A., Petrel, C., Traiffort, E., Ruat, M. & Marie, P.J. Calcium sensing receptor-dependent and receptor-independent activation of osteoblast replication and survival by strontium ranelate. *Journal of Cellular and Molecular Medicine* **13**, 2189-2199 (2009).

180. Li, Y., Li, J., Zhu, S., Luo, E., Feng, G., Chen, Q. & Hu, J. Effects of strontium on proliferation and differentiation of rat bone marrow mesenchymal stem cells. *Biochemical and Biophysical Research Communications* **418**, 725-730 (2012).

181. Sila-Asna, M., Bunyaratvej, A., Maeda, S., Kitaguchi, H. & Bunyaratavej, N. Osteoblast differentiation and bone formation gene expression in strontium-inducing bone marrow mesenchymal stem cell. *The Kobe Journal of Medical Sciences* **53**, 25-35 (2007).
182. Goel, A., Rajagopal, R.R. & Ferreira, J.M. Influence of strontium on structure, sintering and biodegradation behaviour of CaO-MgO-SrO-SiO(2)-P(2)O(5)-CaF(2) glasses. *Acta Biomaterialia* **7**, 4071-4080 (2011).
183. O'Donnell, M.D. & Hill, R.G. Influence of strontium and the importance of glass chemistry and structure when designing bioactive glasses for bone regeneration. *Acta Biomaterialia* **6**, 2382-2385 (2010).
184. Gentleman, E., Fredholm, Y.C., Jell, G., Lotfibakhshaiesh, N., O'Donnell, M.D., Hill, R.G. & Stevens, M.M. The effects of strontium-substituted bioactive glasses on osteoblasts and osteoclasts in vitro. *Biomaterials* **31**, 3949-3956 (2010).
185. Hokin, B., Adams, M., Ashton, J. & Louie, H. Comparison of the dietary cobalt intake in three different Australian diets. *Asia Pacific Journal of Clinical Nutrition* **13**, 289-291 (2004).
186. Dabeka, R.W. & McKenzie, A.D. Survey of lead, cadmium, fluoride, nickel, and cobalt in food composites and estimation of dietary intakes of these elements by Canadians in 1986-1988. *Journal of AOAC International* **78**, 897-909 (1995).
187. EFSA Panel on Additives Products or Substances used in Animal Feed. Scientific opinion on the use of cobalt compounds as additives in animal nutrition. *EFSA Journal* **7**, 45 pp (2009).
188. EVM Expert Group on Vitamins and Minerals. Safe upper limits for vitamins and minerals. *The Committee on Toxicity of Chemicals in Food, Consumer Products and the Environment (COT)*, 1-360 (2003).
189. Finley, B.L., Unice, K.M., Kerger, B.D., Otani, J.M., Paustenbach, D.J., Galbraith, D.A. & Tvermoes, B.E. 31-day study of cobalt(II) chloride ingestion in humans: pharmacokinetics and clinical effects. *Journal of Toxicology and Environmental Health, Part A* **76**, 1210-1224 (2013).
190. Simonsen, L.O., Harbak, H. & Bennekou, P. Cobalt metabolism and toxicology - a brief update. *Science of The Total Environment* **432**, 210-215 (2012).
191. Patel, B., Favaro, G., Inam, F., Reece, M.J., Angadji, A., Bonfield, W., Huang, J. & Edirisinghe, M. Cobalt-based orthopaedic alloys: relationship between forming route, microstructure and tribological performance. *Materials Science and Engineering: C* **32**, 1222-1229 (2012).
192. Haynes, D.R., Rogers, S.D., Hay, S., Pearcy, M.J. & Howie, D.W. The differences in toxicity and release of bone-resorbing mediators induced by titanium and cobalt-chromium-alloy wear particles. *The Journal of Bone & Joint Surgery* **75**, 825-834 (1993).
193. Maxwell, P. & Salnikow, K. HIF-1, an oxygen and metal responsive transcription factor. *Cancer Biology & Therapy* **3**, 29-35 (2004).

194. Wright, J.V. Bio-identical steroid hormone replacement: selected observations from 23 years of clinical and laboratory practice. *Annals of the New York Academy of Sciences* **1057**, 506-524 (2005).

195. Endoh, H., Kaneko, T., Nakamura, H., Doi, K. & Takahashi, E. Improved cardiac contractile functions in hypoxia-reoxygenation in rats treated with low concentration Co2+. *American Journal of Physiology - Heart and Circulatory Physiology* **279**, H2713-H2719 (2000).

196. Singh, M., Shukla, D., Thomas, P., Saxena, S. & Bansal, A. Hypoxic preconditioning facilitates acclimatization to hypobaric hypoxia in rat heart. *Journal of Pharmacy and Pharmacology* **62**, 1729-1739 (2010).

197. Matsumoto, M., Makino, Y., Tanaka, T., Tanaka, H., Ishizaka, N., Noiri, E., Fujita, T. & Nangaku, M. Induction of renoprotective gene expression by cobalt ameliorates ischemic injury of the kidney in rats. *Journal of the American Society of Nephrology* **14**, 1825-1832 (2003).

198. Shrivastava, K., Shukla, D., Bansal, A., Sairam, M., Banerjee, P.K. & Ilavazhagan, G. Neuroprotective effect of cobalt chloride on hypobaric hypoxia-induced oxidative stress. *Neurochemistry International* **52**, 368-375 (2008).

199. Kasten, U., Hartwig, A. & Beyersmann, D. Mechanisms of cobalt(II) uptake into V79 Chinese hamster cells. *Archives of Toxicology* **66**, 592-597.

200. Wouters, B.G. & Koritzinsky, M. Hypoxia signalling through mTOR and the unfolded protein response in cancer. *Nature Reviews Cancer* **8**, 851-864 (2008).

201. Semenza, G.L. & Wang, G.L. A nuclear factor induced by hypoxia via de novo protein synthesis binds to the human erythropoietin gene enhancer at a site required for transcriptional activation. *Molecular and Cellular Biology* **12**, 5447-5454 (1992).

202. Wiener, C.M., Booth, G. & Semenza, G.L. In vivo expression of mRNAs encoding hypoxia-inducible factor 1. *Biochemical and Biophysical Research Communications* **225**, 485-488 (1996).

203. Tian, H., McKnight, S.L. & Russell, D.W. Endothelial PAS domain protein 1 (EPAS1), a transcription factor selectively expressed in endothelial cells. *Genes & Development* **11**, 72-82 (1997).

204. Gu, Y.Z., Moran, S.M., Hogenesch, J.B., Wartman, L. & Bradfield, C.A. Molecular characterization and chromosomal localization of a third alpha-class hypoxia inducible factor subunit, HIF3alpha. *Gene Expression* **7**, 205-213 (1998).

205. Kewley, R.J., Whitelaw, M.L. & Chapman-Smith, A. The mammalian basic helix–loop–helix/PAS family of transcriptional regulators. *The International Journal of Biochemistry & Cell Biology* **36**, 189-204 (2004).

206. Wang, G.L., Jiang, B.H., Rue, E.A. & Semenza, G.L. Hypoxia-inducible factor 1 is a basic-helix-loop-helix-PAS heterodimer regulated by cellular O2 tension. *Proceedings of the National Academy of Sciences* **92**, 5510-5514 (1995).

207. Ema, M., Hirota, K., Mimura, J., Abe, H., Yodoi, J., Sogawa, K., Poellinger, L. & Fujii-Kuriyama, Y. Molecular mechanisms of transcription activation by HLF and HIF1alpha in response to hypoxia: their stabilization and redox signal-induced interaction with CBP/p300. *The EMBO Journal* **18**, 1905-1914 (1999).

208. Semenza, G.L. HIF-1 and mechanisms of hypoxia sensing. *Current Opinion in Cell Biology* **13**, 167-171 (2001).

209. Simon, M. & Keith, B. The role of oxygen availability in embryonic development and stem cell function. *Nature Reviews Molecular Cell Biology* **9**, 285 - 296 (2008).

210. Epstein, A.C.R., Gleadle, J.M., McNeill, L.A., Hewitson, K.S., O'Rourke, J., Mole, D.R., Mukherji, M., Metzen, E., Wilson, M.I., Dhanda, A., Tian, Y.-M., Masson, N., Hamilton, D.L., Jaakkola, P., Barstead, R., Hodgkin, J., Maxwell, P.H., Pugh, C.W., Schofield, C.J. & Ratcliffe, P.J. C. elegans EGL-9 and mammalian homologs define a family of dioxygenases that regulate HIF by prolyl hydroxylation. *Cell* **107**, 43-54 (2001).

211. Berra, E., Benizri, E., Ginouvès, A., Volmat, V., Roux, D. & Pouysségur, J. HIF prolyl-hydroxylase 2 is the key oxygen sensor setting low steady-state levels of HIF-1α in normoxia. *The EMBO Journal* **22**, 4082-4090 (2003).

212. Lando, D., Peet, D.J., Gorman, J.J., Whelan, D.A., Whitelaw, M.L. & Bruick, R.K. FIH-1 is an asparaginyl hydroxylase enzyme that regulates the transcriptional activity of hypoxia-inducible factor. *Genes & Development* **16**, 1466-1471 (2002).

213. Ke, Q. & Costa, M. Hypoxia-Inducible Factor-1 (HIF-1). *Molecular Pharmacology* **70**, 1469-1480 (2006).

214. Chachami, G., Simos, G., Hatziefthimiou, A., Bonanou, S., Molyvdas, P.-A. & Paraskeva, E. Cobalt induces hypoxia-inducible factor-1α expression in airway smooth muscle cells by a reactive oxygen species– and PI3K-dependent mechanism. *American Journal of Respiratory Cell and Molecular Biology* **31**, 544-551 (2004).

215. Jiang, B.H., Semenza, G.L., Bauer, C. & Marti, H.H. Hypoxia-inducible factor 1 levels vary exponentially over a physiologically relevant range of O2 tension. *American Journal of Physiology - Cell Physiology* **271**, C1172-C1180 (1996).

216. Stroka, D.M., Burkhardt, T., Desbaillets, I., Wenger, R.H., Neil, D.A.H., Bauer, C., Gassmann, M. & Candinas, D. HIF-1 is expressed in normoxic tissue and displays an organ-specific regulation under systemic hypoxia. *The FASEB Journal* **15**, 2445-2453 (2001).

217. Manalo, D.J., Rowan, A., Lavoie, T., Natarajan, L., Kelly, B.D., Ye, S.Q., Garcia, J.G.N. & Semenza, G.L. Transcriptional regulation of vascular endothelial cell responses to hypoxia by HIF-1. *Blood* **105**, 659-669 (2005).

218. Yuan, Y., Hilliard, G., Ferguson, T. & Millhorn, D.E. Cobalt inhibits the interaction between hypoxia-inducible factor-α and von Hippel-Lindau protein by direct binding to hypoxia-inducible factor-α. *Journal of Biological Chemistry* **278**, 15911-15916 (2003).

219. Chandel, N.S., McClintock, D.S., Feliciano, C.E., Wood, T.M., Melendez, J.A., Rodriguez, A.M. & Schumacker, P.T. Reactive oxygen species generated at mitochondrial complex III stabilize hypoxia-inducible factor-1α during hypoxia: a mechanism of O2 sensing. *Journal of Biological Chemistry* **275**, 25130-25138 (2000).

220. Leonard, S., M. Gannett, P., Rojanasakul, Y., Schwegler-Berry, D., Castranova, V., Vallyathan, V. & Shi, X. Cobalt-mediated generation of reactive oxygen species and its possible mechanism. *Journal of Inorganic Biochemistry* **70**, 239-244 (1998).

221. Fandrey, J., Frede, S., Ehleben, W., Porwol, T., Acker, H. & Jelkmann, W. Cobalt chloride and desferrioxamine antagonize the inhibition of erythropoietin production by reactive oxygen species. *Kidney International* **51**, 492-496 (1997).

222. Ciafrè, S.A., Niola, F., Giorda, E., Farace, M.G. & Caporossi, D. CoCl2-simulated hypoxia in skeletal muscle cell lines: role of free radicals in gene up-regulation and induction of apoptosis. *Free Radical Research* **41**, 391-401 (2007).

223. Salnikow, K., Donald, S.P., Bruick, R.K., Zhitkovich, A., Phang, J.M. & Kasprzak, K.S. Depletion of intracellular ascorbate by the carcinogenic metals nickel and vobalt results in the induction of hypoxic stress. *Journal of Biological Chemistry* **279**, 40337-40344 (2004).

224. Peters, K., Schmidt, H., Unger, R., Kamp, G., Pröls, F., Berger, B. & Kirkpatrick, C.J. Paradoxical effects of hypoxia-mimicking divalent cobalt ions in human endothelial cells in vitro. *Molecular and Cellular Biochemistry* **270**, 157-166 (2005).

225. Liu, Q., Xu, Z., Mao, S., Chen, W., Zeng, R., Zhou, S. & Liu, J. Effect of hypoxia on hypoxia inducible factor-1α, insulin-like growth factor I and vascular endothelial growth factor expression in hepatocellular carcinoma HepG2 cells. *Oncology Letters* **9**, 1142-1148 (2015).

226. Han, Y.-H., Xia, L., Song, L.-P., Zheng, Y., Chen, W.-L., Zhang, L., Huang, Y., Chen, G.-Q. & Wang, L.-S. Comparative proteomic analysis of hypoxia-treated and untreated human leukemic U937 cells. *PROTEOMICS* **6**, 3262-3274 (2006).

227. Maes, C., Carmeliet, G. & Schipani, E. Hypoxia-driven pathways in bone development, regeneration and disease. *Nature Reviews Rheumatology* **8**, 358-366 (2012).

228. Perez, R.A., Kim, J.-H., Buitrago, J.O., Wall, I.B. & Kim, H.-W. Novel therapeutic core–shell hydrogel scaffolds with sequential delivery of cobalt and bone morphogenetic protein-2 for synergistic bone regeneration. *Acta Biomaterialia* **23**, 295-308 (2015).

229. Zhang, M., Wu, C., Li, H., Yuen, J., Chang, J. & Xiao, Y. Preparation, characterization and in vitro angiogenic capacity of cobalt substituted β-tricalcium phosphate ceramics. *Journal of Materials Chemistry* **22**, 21686-21694 (2012).

230. Liu, F., Zhang, X., Yu, X., Xu, Y., Feng, T. & Ren, D. In vitro study in stimulating the secretion of angiogenic growth factors of strontium-doped calcium polyphosphate for bone tissue engineering. *Journal of Materials Science: Materials in Medicine* **22**, 683-692 (2011).

231. Fan, W., Crawford, R. & Xiao, Y. Enhancing in vivo vascularized bone formation by cobalt chloride-treated bone marrow stromal cells in a tissue engineered periosteum model. *Biomaterials* **31**, 3580-3589 (2010).
232. Kulanthaivel, S., Roy, B., Agarwal, T., Giri, S., Pramanik, K., Pal, K., Ray, S.S., Maiti, T.K. & Banerjee, I. Cobalt doped proangiogenic hydroxyapatite for bone tissue engineering application. *Materials Science and Engineering: C* **58**, 648-658 (2016).
233. Chen, Z., Yuen, J., Crawford, R., Chang, J., Wu, C. & Xiao, Y. The effect of osteoimmunomodulation on the osteogenic effects of cobalt incorporated β-tricalcium phosphate. *Biomaterials* **61**, 126-138 (2015).
234. Tahmasebi Birgani, Z., Fennema, E., Gijbels, M.J., de Boer, J., van Blitterswijk, C.A. & Habibovic, P. Stimulatory effect of cobalt ions incorporated into calcium phosphate coatings on neovascularization in an in vivo intramuscular model in goats. *Acta Biomaterialia* **36**, 267-276 (2016).
235. Focaroli, S., Teti, G., Salvatore, V., Orienti, I. & Falconi, M. Calcium/cobalt alginate beads as functional scaffolds for cartilage tissue engineering. *Stem Cells International* **2016**, 12 (2016).
236. Lee, I.-H., Yu, H.-s., Lakhkar, N.J., Kim, H.-W., Gong, M.-S., Knowles, J.C. & Wall, I.B. Development, characterisation and biocompatibility testing of a cobalt-containing titanium phosphate-based glass for engineering of vascularized hard tissues. *Materials Science and Engineering: C* **33**, 2104-2112 (2013).
237. Wu, C., Zhou, Y., Fan, W., Han, P., Chang, J., Yuen, J., Zhang, M. & Xiao, Y. Hypoxia-mimicking mesoporous bioactive glass scaffolds with controllable cobalt ion release for bone tissue engineering. *Biomaterials* **33**, 2076-2085 (2012).
238. Hoppe, A., Brandl, A., Bleiziffer, O., Arkudas, A., Horch, R.E., Jokic, B., Janackovic, D. & Boccaccini, A.R. In vitro cell response to Co-containing 1393 bioactive glass. *Materials Science and Engineering: C* **57**, 157-163 (2015).
239. Azevedo, M.M., Jell, G., O'Donnell, M.D., Law, R.V., Hill, R.G. & Stevens, M.M. Synthesis and characterization of hypoxia-mimicking bioactive glasses for skeletal regeneration. *Journal of Materials Chemistry* **20**, 8854-8864 (2010).
240. Azevedo, M.M., Tsigkou, O., Nair, R., Jones, J.R., Jell, G. & Stevens, M.M. Hypoxia inducible factor-stabilizing bioactive glasses for directing mesenchymal stem cell behavior. *Tissue Engineering Part A* **21**, 382-389 (2014).
241. Quinlan, E., Partap, S., Azevedo, M.M., Jell, G., Stevens, M.M. & O'Brien, F.J. Hypoxia-mimicking bioactive glass/collagen glycosaminoglycan composite scaffolds to enhance angiogenesis and bone repair. *Biomaterials* **52**, 358-366 (2015).
242. Diba, M., Tapia, F., Boccaccini, A.R. & Strobel, L.A. Magnesium-containing bioactive glasses for biomedical applications. *International Journal of Applied Glass Science* **3**, 221-253 (2012).

243. Varanasi, V.G., Saiz, E., Loomer, P.M., Ancheta, B., Uritani, N., Ho, S.P., Tomsia, A.P., Marshall, S.J. & Marshall, G.W. Enhanced osteocalcin expression by osteoblast-like cells (MC3T3-E1) exposed to bioactive coating glass (SiO2–CaO–P2O5–MgO–K2O–Na2O system) ions. *Acta Biomaterialia* **5**, 3536-3547 (2009).

244. Wang, X., Li, X., Ito, A. & Sogo, Y. Synthesis and characterization of hierarchically macroporous and mesoporous CaO–MO–SiO2–P2O5 (M = Mg, Zn, Sr) bioactive glass scaffolds. *Acta Biomaterialia* **7**, 3638-3644 (2011).

245. Keeting, P.E., Oursler, M.J., Wiegand, K.E., Bonde, S.K., Spelsberg, T.C. & Riggs, B.L. Zeolite A increases proliferation, differentiation, and transforming growth factor beta production in normal adult human osteoblast-like cells in vitro. *Journal of Bone and Mineral Research* **7**, 1281-1289 (1992).

246. Reffitt, D.M., Ogston, N., Jugdaohsingh, R., Cheung, H.F.J., Evans, B.A.J., Thompson, R.P.H., Powell, J.J. & Hampson, G.N. Orthosilicic acid stimulates collagen type 1 synthesis and osteoblastic differentiation in human osteoblast-like cells in vitro. *Bone* **32**, 127-135 (2003).

247. Maeno, S., Niki, Y., Matsumoto, H., Morioka, H., Yatabe, T., Funayama, A., Toyama, Y., Taguchi, T. & Tanaka, J. The effect of calcium ion concentration on osteoblast viability, proliferation and differentiation in monolayer and 3D culture. *Biomaterials* **26**, 4847-4855 (2005).

248. Beck, G.R., Jr. & Knecht, N. Osteopontin regulation by inorganic phosphate is ERK1/2-, protein kinase C-, and proteasome-dependent. *The Journal of Biological Chemistry* **278**, 41921-41929 (2003).

249. Julien, M., Khoshniat, S., Lacreusette, A., Gatius, M., Bozec, A., Wagner, E.F., Wittrant, Y., Masson, M., Weiss, P., Beck, L., Magne, D. & Guicheux, J. Phosphate-dependent regulation of MGP in osteoblasts: role of ERK1/2 and Fra-1. *Journal of Bone and Mineral Research* **24**, 1856-1868 (2009).

250. Autefage, H., Gentleman, E., Littmann, E., Hedegaard, M.A.B., Von Erlach, T., O'Donnell, M., Burden, F.R., Winkler, D.A. & Stevens, M.M. Sparse feature selection methods identify unexpected global cellular response to strontium-containing materials. *Proceedings of the National Academy of Sciences* **112**, 4280-4285 (2015).

251. Meunier, P.J., Roux, C., Seeman, E., Ortolani, S., Badurski, J.E., Spector, T.D., Cannata, J., Balogh, A., Lemmel, E.M., Pors-Nielsen, S., Rizzoli, R., Genant, H.K. & Reginster, J.Y. The effects of strontium ranelate on the risk of vertebral fracture in women with postmenopausal osteoporosis. *N Engl J Med* **350**, 459-468 (2004).

252. Newman, S.D., Lotfibakhshaiesh, N., O'Donnell, M., Walboomers, X.F., Horwood, N., Jansen, J.A., Amis, A.A., Cobb, J.P. & Stevens, M.M. Enhanced osseous implant fixation with strontium-substituted bioactive glass coating. *Tissue Engineering Part A* **20**, 1850-1857 (2014).

253. O'Donnell, M.D., Candarlioglu, P.L., Miller, C.A., Gentleman, E. & Stevens, M.M. Materials characterisation and cytotoxic assessment of strontium-substituted bioactive glasses for bone regeneration. *Journal of Materials Chemistry* **20**, 8934-8941 (2010).
254. Nurenberg, G. & Volmer, D.A. The analytical determination of isoprenoid intermediates from the mevalonate pathway. *Analytical and Bioanalytical Chemistry* **402**, 671-685 (2012).
255. McTaggart, S.J. Isoprenylated proteins. *Cellular and Molecular Life Sciences* **63**, 255-267 (2006).
256. Buhaescu, I. & Izzedine, H. Mevalonate pathway: a review of clinical and therapeutical implications. *Clinical Biochemistry* **40**, 575-584 (2007).
257. Konstantinopoulos, P.A., Karamouzis, M.V. & Papavassiliou, A.G. Post-translational modifications and regulation of the RAS superfamily of GTPases as anticancer targets. *Nature Reviews Drug Discovery* **6**, 541-555 (2007).
258. Zhang, F.L. & Casey, P.J. Protein prenylation: molecular mechanisms and functional consequences. *Annual Review of Biochemistry* **65**, 241-269 (1996).
259. Goldstein, J.L. & Brown, M.S. Regulation of the mevalonate pathway. *Nature* **343**, 425-430 (1990).
260. Simons, K. & Ikonen, E. How cells handle cholesterol. *Science* **290**, 1721-1726 (2000).
261. Spector, A.A. & Yorek, M.A. Membrane lipid composition and cellular function. *Journal of Lipid Research* **26**, 1015-1035 (1985).
262. Singer, S.J. & Nicolson, G.L. The fluid mosaic model of the structure of cell membranes. *Science* **175**, 720-731 (1972).
263. Brown, D.A. & London, E. Functions of lipid rafts in biological membranes. *Annual Review of Cell and Developmental Biology* **14**, 111-136 (1998).
264. Simons, K. & Toomre, D. Lipid rafts and signal transduction. *Nature Reviews Molecular Cell Biology* **1**, 31-39 (2000).
265. Lemaire-Ewing, S., Lagrost, L. & Neel, D. Lipid rafts: a signalling platform linking lipoprotein metabolism to atherogenesis. *Atherosclerosis* **221**, 303-310 (2012).
266. Korade, Z. & Kenworthy, A.K. Lipid rafts, cholesterol, and the brain. *Neuropharmacology* **55**, 1265-1273 (2008).
267. Silva, L.C., Futerman, A.H. & Prieto, M. Lipid raft composition modulates sphingomyelinase activity and ceramide-induced membrane physical alterations. *Biophysical Journal* **96**, 3210-3222 (2009).
268. Sanchez-Wandelmer, J., Davalos, A., Herrera, E., Giera, M., Cano, S., de la Pena, G., Lasuncion, M.A. & Busto, R. Inhibition of cholesterol biosynthesis disrupts lipid raft/caveolae and affects insulin receptor activation in 3T3-L1 preadipocytes. *Biochimica et Biophysica Acta* **1788**, 1731-1739 (2009).

269. Rodan, G.A. & Fleisch, H.A. Bisphosphonates: mechanisms of action. *Journal of Clinical Investigation* **97**, 2692-2696 (1996).

270. Luckman, S.P., Hughes, D.E., Coxon, F.P., Russell, R.G.G. & Rogers, M.J. Nitrogen-Containing Bisphosphonates Inhibit the Mevalonate Pathway and Prevent Post-Translational Prenylation of GTP-Binding Proteins, Including Ras. *Journal of Bone and Mineral Research* **13**, 581-589 (1998).

271. van Beek, E., Pieterman, E., Cohen, L., Löwik, C. & Papapoulos, S. Farnesyl pyrophosphate synthase os the molecular target of nitrogen-containing bisphosphonates. *Biochemical and Biophysical Research Communications* **264**, 108-111 (1999).

272. Freed-Pastor, William A., Mizuno, H., Zhao, X., Langerød, A., Moon, S.-H., Rodriguez-Barrueco, R., Barsotti, A., Chicas, A., Li, W., Polotskaia, A., Bissell, Mina J., Osborne, Timothy F., Tian, B., Lowe, Scott W., Silva, Jose M., Børresen-Dale, A.-L., Levine, Arnold J., Bargonetti, J. & Prives, C. Mutant p53 disrupts mammary tissue architecture via the mevalonate pathway. *Cell* **148**, 244-258 (2012).

273. Ahn, K., Huh, J.W., Park, S.J., Kim, D.S., Ha, H.S., Kim, Y.J., Lee, J.R., Chang, K.T. & Kim, H.S. Selection of internal reference genes for SYBR green qRT-PCR studies of rhesus monkey (Macaca mulatta) tissues. *BMC Molecular Biology* **9**, 78 (2008).

274. Schmittgen, T.D. & Livak, K.J. Analyzing real-time PCR data by the comparative C(T) method. *Nature Protocols* **3**, 1101-1108 (2008).

275. Kavanagh, K.L., Dunford, J.E., Bunkoczi, G., Russell, R.G. & Oppermann, U. The crystal structure of human geranylgeranyl pyrophosphate synthase reveals a novel hexameric arrangement and inhibitory product binding. *The Journal of Biological Chemistry* **281**, 22004-22012 (2006).

276. Lencer, W.I. & Tsai, B. The intracellular voyage of cholera toxin: going retro. *Trends in Biochemical Sciences* **28**, 639-645 (2003).

277. Finkelstein, R.A. & Dorner, F. Cholera enterotoxin (choleragen). *Pharmacology & Therapeutics* **27**, 37-47 (1985).

278. Heyningen, S.V. Cholera toxin: interaction of subunits with ganglioside GM1. *Science* **183**, 656-657 (1974).

279. Blank, N., Schiller, M., Krienke, S., Wabnitz, G., Ho, A.D. & Lorenz, H.M. Cholera toxin binds to lipid rafts but has a limited specificity for ganglioside GM1. *Immunology and Cell Biology* **85**, 378-382 (2007).

280. Mattheyses, A.L., Simon, S.M. & Rappoport, J.Z. Imaging with total internal reflection fluorescence microscopy for the cell biologist. *Journal of Cell Science* **123**, 3621-3628 (2010).

281. Sepulveda, P., Jones, J.R. & Hench, L.L. In vitro dissolution of melt-derived 45S5 and sol-gel derived 58S bioactive glasses. *Journal of Biomedical Materials Research* **61**, 301-311 (2002).

282. Rodal, S.K., Skretting, G., Garred, O., Vilhardt, F., van Deurs, B. & Sandvig, K. Extraction of cholesterol with methyl-beta-cyclodextrin perturbs formation of clathrin-coated endocytic vesicles. *Molecular Biology of the Cell* **10**, 961-974 (1999).

283. Eberle, D., Hegarty, B., Bossard, P., Ferre, P. & Foufelle, F. SREBP transcription factors: master regulators of lipid homeostasis. *Biochimie* **86**, 839-848 (2004).

284. Portilho, D.M., Soares, C.P., Morrot, A., Thiago, L.S., Butler-Browne, G., Savino, W., Costa, M.L. & Mermelstein, C. Cholesterol depletion by methyl-beta-cyclodextrin enhances cell proliferation and increases the number of desmin-positive cells in myoblast cultures. *European Journal of Pharmacology* **694**, 1-12 (2012).

285. Do, R., Kiss, R.S., Gaudet, D. & Engert, J.C. Squalene synthase: a critical enzyme in the cholesterol biosynthesis pathway. *Clinical Genetics* **75**, 19-29 (2009).

286. Brusselmans, K., Timmermans, L., Van de Sande, T., Van Veldhoven, P.P., Guan, G., Shechter, I., Claessens, F., Verhoeven, G. & Swinnen, J.V. Squalene synthase, a determinant of raft-associated cholesterol and modulator of cancer cell proliferation. *Journal of Biological Chemistry* **282**, 18777-18785 (2007).

287. Santos, N.C., Ter-Ovanesyan, E., Zasadzinski, J.A., Prieto, M. & Castanho, M.A. Filipin-induced lesions in planar phospholipid bilayers imaged by atomic force microscopy. *Biophysical Journal* **75**, 1869-1873 (1998).

288. Santocildes-Romero, M.E., Crawford, A., Hatton, P.V., Goodchild, R.L., Reaney, I.M. & Miller, C.A. The osteogenic response of mesenchymal stromal cells to strontium-substituted bioactive glasses. *Journal of Tissue Engineering and Regenerative Medicine* **9**, 619-631 (2015).

289. Strobel, L.A., Hild, N., Mohn, D., Stark, W.J., Hoppe, A., Gbureck, U., Horch, R.E., Kneser, U. & Boccaccini, A.R. Novel strontium-doped bioactive glass nanoparticles enhance proliferation and osteogenic differentiation of human bone marrow stromal cells. *Journal of Nanoparticle Research* **15**, 1-9 (2013).

290. Zhang, Y., Cui, X., Zhao, S., Wang, H., Rahaman, M.N., Liu, Z., Huang, W. & Zhang, C. Evaluation of injectable strontium-containing borate bioactive glass cement with enhanced osteogenic capacity in a critical-sized rabbit femoral condyle defect model. *ACS Applied Materials & Interfaces* **7**, 2393-2403 (2015).

291. Schumacher, M., Lode, A., Helth, A. & Gelinsky, M. A novel strontium(II)-modified calcium phosphate bone cement stimulates human-bone-marrow-derived mesenchymal stem cell proliferation and osteogenic differentiation in vitro. *Acta Biomaterialia* **9**, 9547-9557 (2013).

292. Kilian, K.A., Bugarija, B., Lahn, B.T. & Mrksich, M. Geometric cues for directing the differentiation of mesenchymal stem cells. *Proceedings of the National Academy of Sciences* **107**, 4872-4877 (2010).

293. McBeath, R., Pirone, D.M., Nelson, C.M., Bhadriraju, K. & Chen, C.S. Cell shape, cytoskeletal tension, and RhoA regulate stem cell lineage commitment. *Developmental Cell* **6**, 483-495 (2004).

294. Head, B.P., Patel, H.H. & Insel, P.A. Interaction of membrane/lipid rafts with the cytoskeleton: impact on signaling and function: membrane/lipid rafts, mediators of cytoskeletal arrangement and cell signaling. *Biochimica et Biophysica Acta (BBA) - Biomembranes* **1838**, 532-545 (2014).

295. Kameda, T., Mano, H., Yamada, Y., Takai, H., Amizuka, N., Kobori, M., Izumi, N., Kawashima, H., Ozawa, H., Ikeda, K., Kameda, A., Hakeda, Y. & Kumegawa, M. Calcium-sensing receptor in mature osteoclasts, which are bone resorbing cells. *Biochemical and Biophysical Research Communications* **245**, 419-422 (1998).

296. Yamaguchi, T., Chattopadhyay, N., Kifor, O., Butters, R.R., Jr., Sugimoto, T. & Brown, E.M. Mouse osteoblastic cell line (MC3T3-E1) expresses extracellular calcium (Ca2+o)-sensing receptor and its agonists stimulate chemotaxis and proliferation of MC3T3-E1 cells. *Journal of Bone and Mineral Research* **13**, 1530-1538 (1998).

297. Dvorak-Ewell, M.M., Chen, T.H., Liang, N., Garvey, C., Liu, B., Tu, C., Chang, W., Bikle, D.D. & Shoback, D.M. Osteoblast extracellular Ca2+ -sensing receptor regulates bone development, mineralization, and turnover. *Journal of Bone and Mineral Research* **26**, 2935-2947 (2011).

298. Martino, N.A., Lange-Consiglio, A., Cremonesi, F., Valentini, L., Caira, M., Guaricci, A.C., Ambruosi, B., Sciorsci, R.L., Lacalandra, G.M., Reshkin, S.J. & Dell'Aquila, M.E. Functional expression of the extracellular calcium sensing receptor (CaSR) in equine umbilical cord matrix size-sieved stem cells. *PLoS One* **6**, e17714 (2011).

299. Ben Azouna, N., Jenhani, F., Regaya, Z., Berraeis, L., Ben Othman, T., Ducrocq, E. & Domenech, J. Phenotypical and functional characteristics of mesenchymal stem cells from bone marrow: comparison of culture using different media supplemented with human platelet lysate or fetal bovine serum. *Stem Cell Research & Therapy* **3**, 6 (2012).

300. Parhami, F., Mody, N., Gharavi, N., Ballard, A.J., Tintut, Y. & Demer, L.L. Role of the cholesterol biosynthetic pathway in osteoblastic differentiation of marrow stromal cells. *Journal of Bone and Mineral Research* **17**, 1997-2003 (2002).

301. Kha, H.T., Basseri, B., Shouhed, D., Richardson, J., Tetradis, S., Hahn, T.J. & Parhami, F. Oxysterols regulate differentiation of mesenchymal stem cells: pro-bone and anti-fat. *Journal of Bone and Mineral Research* **19**, 830-840 (2004).

302. Richardson, J.A., Amantea, C.M., Kianmahd, B., Tetradis, S., Lieberman, J.R., Hahn, T.J. & Parhami, F. Oxysterol-induced osteoblastic differentiation of pluripotent mesenchymal cells is mediated through a PKC- and PKA-dependent pathway. *Journal of Cellular Biochemistry* **100**, 1131-1145 (2007).

303. Li, H., Guo, H. & Li, H. Cholesterol loading affects osteoblastic differentiation in mouse mesenchymal stem cells. *Steroids* **78**, 426-433 (2013).

304. Baker, N., Sohn, J. & Tuan, R.S. Promotion of human mesenchymal stem cell osteogenesis by PI3-kinase/Akt signaling, and the influence of caveolin-1/cholesterol homeostasis. *Stem Cell Research & Therapy* **6**, 238 (2015).

305. Miguez-Pacheco, V., Hench, L.L. & Boccaccini, A.R. Bioactive glasses beyond bone and teeth: emerging applications in contact with soft tissues. *Acta Biomaterialia* **13**, 1-15 (2015).

306. Baino, F., Novajra, G., Miguez-Pacheco, V., Boccaccini, A.R. & Vitale-Brovarone, C. Bioactive glasses: special applications outside the skeletal system. *Journal of Non-Crystalline Solids* **432, Part A**, 15-30 (2016).

307. Pelletier, J.-P., Roubille, C., Raynauld, J.-P., Abram, F., Dorais, M., Delorme, P. & Martel-Pelletier, J. Disease-modifying effect of strontium ranelate in a subset of patients from the Phase III knee osteoarthritis study SEKOIA using quantitative MRI: reduction in bone marrow lesions protects against cartilage loss. *Annals of the Rheumatic Diseases* (2013).

308. Reginster, J.-Y., Badurski, J., Bellamy, N., Bensen, W., Chapurlat, R., Chevalier, X., Christiansen, C., Genant, H., Navarro, F., Nasonov, E., Sambrook, P.N., Spector, T.D. & Cooper, C. Efficacy and safety of strontium ranelate in the treatment of knee osteoarthritis: results of a double-blind, randomised placebo-controlled trial. *Annals of the Rheumatic Diseases* **72**, 179-186 (2013).

309. Loty, C., Forest, N., Boulekbache, H., Kokubo, T. & Sautier, J.M. Behavior of fetal rat chondrocytes cultured on a bioactive glass-ceramic. *Journal of Biomedical Materials Research* **37**, 137-149 (1997).

310. Suominen, E., Aho, A.J., Vedel, E., Kangasniemi, I., Uusipaikka, E. & Yli-Urpo, A. Subchondral bone and cartilage repair with bioactive glasses, hydroxyapatite, and hydroxyapatite-glass composite. *Journal of Biomedical Materials Research* **32**, 543-551 (1996).

311. Aho, A.J., Tirri, T., Kukkonen, J., Strandberg, N., Rich, J., Seppala, J. & Yli-Urpo, A. Injectable bioactive glass/biodegradable polymer composite for bone and cartilage reconstruction: Concept and experimental outcome with thermoplastic composites of poly(epsilon-caprolactone-CO-D,L-lactide) and bioactive glass S53P4. *Journal of Materials Science-Materials in Medicine* **15**, 1165-1173 (2004).

312. Tellisi, N. & Ashammakhi, N. Comparison of meshes, gels and ceramic for cartilage tissue engineering in vitro. *European Journal of Plastic Surgery* **35**, 159-170 (2008).

313. Lindfors, N. Clinical experience on bioactive glass S53P4 in reconstructive surgery in the upper extremity showing bone remodelling, vascularization, cartilage repair and antibacterial properties of S53P4. *Journal of Biotechnology & Biomaterials* **01** (2011).

314. Bal, B.S., Rahaman, M.N., Jayabalan, P., Kuroki, K., Cockrell, M.K., Yao, J.Q. & Cook, J.L. In vivo outcomes of tissue-engineered osteochondral grafts. *Journal of Biomedical Materials Research Part B: Applied Biomaterials* **93B**, 164-174 (2010).

315. Jayabalan, P., Tan, A.R., Rahaman, M.N., Bal, B.S., Hung, C.T. & Cook, J.L. Bioactive glass 13-93 as a subchondral substrate for tissue-engineered osteochondral constructs: a pilot study. *Clinical Orthopaedics and Related Research®* **469**, 2754-2763 (2011).

316. Jiang, J., Tang, A., Ateshian, G.A., Guo, X.E., Hung, C.T. & Lu, H.H. Bioactive stratified polymer ceramic-hydrogel scaffold for integrative osteochondral repair. *Annals of Biomedical Engineering* **38**, 2183-2196 (2010).

317. Ahtiainen, K., Sippola, L., Nurminen, M., Mannerström, B., Haimi, S., Suuronen, R., Hyttinen, J., Ylikomi, T., Kellomäki, M. & Miettinen, S. Effects of chitosan and bioactive glass modifications of knitted and rolled polylactide-based 96/4 L/D scaffolds on chondrogenic differentiation of adipose stem cells. *Journal of Tissue Engineering and Regenerative Medicine* **9**, 55-65 (2015).

318. Asselin, A., Hattar, S., Oboeuf, M., Greenspan, D., Berdal, A. & Sautier, J.-M. The modulation of tissue-specific gene expression in rat nasal chondrocyte cultures by bioactive glasses. *Biomaterials* **25**, 5621-5630 (2004).

319. Henrotin, Y., Labasse, A., Zheng, S.X., Galais, P., Tsouderos, Y., Crielaard, J.M. & Reginster, J.Y. Strontium ranelate increases cartilage matrix formation. *Journal of Bone and Mineral Research* **16**, 299-308 (2001).

320. Wang, J., Zhu, X., Liu, L., Shi, X., Yin, L., Zhang, Y., Li, X., Wang, Z. & Liu, G. Effects of strontium on collagen content and expression of related genes in rat chondrocytes cultured in vitro. *Biological Trace Element Research* **153**, 212-219 (2013).

321. Okita, N., Honda, Y., Kishimoto, N., Liao, W., Azumi, E., Hashimoto, Y. & Matsumoto, N. Supplementation of strontium to a chondrogenic medium promotes chondrogenic differentiation of human dedifferentiated fat cells. *Tissue Engineering Part A* **21**, 1695-1704 (2015).

322. Alexandersen, P., Karsdal, M.A., Qvist, P., Reginster, J.Y. & Christiansen, C. Strontium ranelate reduces the urinary level of cartilage degradation biomarker CTX-II in postmenopausal women. *Bone* **40**, 218-222 (2007).

323. Bruyere, O., Delferriere, D., Roux, C., Wark, J.D., Spector, T., Devogelaer, J.-P., Brixen, K., Adami, S., Fechtenbaum, J., Kolta, S. & Reginster, J.-Y. Effects of strontium ranelate on spinal osteoarthritis progression. *Annals of the Rheumatic Diseases* **67**, 335-339 (2008).

324. Pelletier, J.-P., Kapoor, M., Fahmi, H., Lajeunesse, D., Blesius, A., Maillet, J. & Martel-Pelletier, J. Strontium ranelate reduces the progression of experimental dog osteoarthritis by inhibiting the expression of key proteases in cartilage and of IL-1β in the synovium. *Annals of the Rheumatic Diseases* **72**, 250-257 (2013).

325. Yu, D.-g., Ding, H.-f., Mao, Y.-q., Liu, M., Yu, B., Zhao, X., Wang, X.-q., Li, Y., Liu, G.-w., Nie, S.-b., Liu, S. & Zhu, Z.-a. Strontium ranelate reduces cartilage degeneration and subchondral bone remodeling in rat osteoarthritis model. *Acta Pharmacologica Sinica* **34**, 393-402 (2013).

326. Jahnen-Dechent, W. & Ketteler, M. Magnesium basics. *Clinical Kidney Journal* **5**, i3-i14 (2012).

327. Vormann, J., Forster, C., Zippel, U., Lozo, E., Gunther, T., Merker, H.J. & Stahlmann, R. Effects of magnesium deficiency on magnesium and calcium content in bone and cartilage in developing rats in correlation to chondrotoxicity. *Calcified Tissue International* **61**, 230-238 (1997).

328. Gruber, H.E., Ingram, J., Norton, H.J., Wei, L.Y., Frausto, A., Mills, B.G. & Rude, R.K. Alterations in growth plate and articular cartilage morphology are associated with reduced SOX9 localization in the magnesium-deficient rat. *Biotechnic & Histochemistry* **79**, 45-52 (2004).

329. Lee, C.H., Wen, Z.H., Chang, Y.C., Huang, S.Y., Tang, C.C., Chen, W.F., Hsieh, S.P., Hsieh, C.S. & Jean, Y.H. Intra-articular magnesium sulfate (MgSO4) reduces experimental osteoarthritis and nociception: association with attenuation of N-methyl-d-aspartate (NMDA) receptor subunit 1 phosphorylation and apoptosis in rat chondrocytes. *Osteoarthritis and Cartilage* **17**, 1485-1493 (2009).

330. Feyerabend, F., Witte, F., Kammal, M. & Willumeit, R. Unphysiologically high magnesium concentrations support chondrocyte proliferation and redifferentiation. *Tissue Engineering* **12**, 3545-3556 (2006).

331. Dou, Y., Li, N., Zheng, Y. & Ge, Z. Effects of fluctuant magnesium concentration on phenotype of the primary chondrocytes. *Journal of Biomedical Materials Research Part A* **102**, 4455-4463 (2014).

332. Nakatani, S., Mano, H., Ryanghyok, I.M., Shimizu, J. & Wada, M. Excess magnesium inhibits excess calcium-induced matrix-mineralization and production of matrix gla protein (MGP) by ATDC5 cells. *Biochemical and Biophysical Research Communications* **348**, 1157-1162 (2006).

333. García, A.J. Get a grip: integrins in cell–biomaterial interactions. *Biomaterials* **26**, 7525-7529 (2005).

334. Leem, Y.-H., Lee, K.-S., Kim, J.-H., Seok, H.-K., Chang, J.-S. & Lee, D.-H. Magnesium ions facilitate integrin alpha 2- and alpha 3-mediated proliferation and enhance alkaline phosphatase expression and activity in hBMSCs. *Journal of Tissue Engineering and Regenerative Medicine*, n/a-n/a (2014).

335. Shimaya, M., Muneta, T., Ichinose, S., Tsuji, K. & Sekiya, I. Magnesium enhances adherence and cartilage formation of synovial mesenchymal stem cells through integrins. *Osteoarthritis and Cartilage* **18**, 1300-1309 (2010).

336. Li, R.W., Kirkland, N.T., Truong, J., Wang, J., Smith, P.N., Birbilis, N. & Nisbet, D.R. The influence of biodegradable magnesium alloys on the osteogenic differentiation of human mesenchymal stem cells. *Journal of Biomedical Materials Research Part A* **102**, 4346-4357 (2014).

337. Valerio, P., Pereira, M.M., Goes, A.M. & Leite, M.F. The effect of ionic products from bioactive glass dissolution on osteoblast proliferation and collagen production. *Biomaterials* **25**, 2941-2948 (2004).

338. Lee, H.-S., Huang, G.-T., Chiang, H., Chiou, L.-L., Chen, M.-H., Hsieh, C.-H. & Jiang, C.-C. Multipotential mesenchymal stem cells from femoral bone marrow near the site of osteonecrosis. *Stem Cells* **21**, 190-199 (2003).

339. Li, Z., Kupcsik, L., Yao, S.-J., Alini, M. & Stoddart, M.J. Chondrogenesis of human bone marrow mesenchymal stem cells in fibrin–polyurethane composites. *Tissue Engineering Part A* **15**, 1729-1737 (2008).

340. Labarca, C. & Paigen, K. Simple, rapid, and sensitive DNA assay procedure. *Analytical Biochemistry* **102**, 344-352 (1980).

341. Farndale, R.W., Buttle, D.J. & Barrett, A.J. Improved quantitation and discrimination of sulfated glycosaminoglycans by use of dimethylene blue. *Biochimica et Biophysica Acta* **883**, 173-177 (1986).

342. Sridharan, G. & Shankar, A.A. Toluidine blue: a review of its chemistry and clinical utility. *Journal of Oral and Maxillofacial Pathology : JOMFP* **16**, 251-255 (2012).

343. Kaufman, J.M., Audran, M., Bianchi, G., Braga, V., Diaz-Curiel, M., Francis, R.M., Goemaere, S., Josse, R., Palacios, S., Ringe, J.D., Felsenberg, D. & Boonen, S. Efficacy and safety of strontium ranelate in the treatment of osteoporosis in men. *The Journal of Clinical Endocrinology & Metabolism* **98**, 592-601 (2013).

344. Carvalho, S.M., Oliveira, A.A.R., Jardim, C.A., Melo, C.B.S., Gomes, D.A., de Fátima Leite, M. & Pereira, M.M. Characterization and induction of cementoblast cell proliferation by bioactive glass nanoparticles. *Journal of Tissue Engineering and Regenerative Medicine* **6**, 813-821 (2012).

345. Jadali, A. & Kwan, K.Y. Activation of PI3K signaling prevents aminoglycoside-induced hair cell death in the murine cochlea. *Biology Open* **5**, 698-708 (2016).

346. Camplejohn, K.L. & Allard, S.A. Limitations of safranin 'O' staining in proteoglycan-depleted cartilage demonstrated with monoclonal antibodies. *Histochemistry* **89**, 185-188 (1988).

347. Mackay, A.M., Beck, S.C., Murphy, J.M., Barry, F.P., Chichester, C.O. & Pittenger, M.F. Chondrogenic differentiation of cultured human mesenchymal stem cells from marrow. *Tissue Engineering* **4**, 415-428 (1998).

348. Bahney, C.S., Hu, D.P., Taylor, A.J., Ferro, F., Britz, H.M., Hallgrimsson, B., Johnstone, B., Miclau, T. & Marcucio, R.S. Stem cell–derived endochondral cartilage stimulates bone healing by tissue transformation. *Journal of Bone and Mineral Research* **29**, 1269-1282 (2014).

349. DeLise, A.M., Fischer, L. & Tuan, R.S. Cellular interactions and signaling in cartilage development. *Osteoarthritis and Cartilage* **8**, 309-334 (2000).

350. Boskey, A. & Camacho, N.P. FT-IR imaging of native and tissue-engineered bone and cartilage. *Biomaterials* **28**, 2465-2478 (2007).

351. Dorling, K.M. & Baker, M.J. Rapid FTIR chemical imaging: highlighting FPA detectors. *Trends in Biotechnology* **31**, 437-438 (2013).

352. Chonanant, C., Jearanaikoon, N., Leelayuwat, C., Limpaiboon, T., Tobin, M.J., Jearanaikoon, P. & Heraud, P. Characterisation of chondrogenic differentiation of human mesenchymal stem cells using synchrotron FTIR microspectroscopy. *Analyst* **136**, 2542-2551 (2011).

353. Potter, K., Kidder, L.H., Levin, I.W., Lewis, E.N. & Spencer, R.G.S. Imaging of collagen and proteoglycan in cartilage sections using Fourier transform infrared spectral imaging. *Arthritis & Rheumatism* **44**, 846-855 (2001).

354. Camacho, N.P., West, P., Torzilli, P.A. & Mendelsohn, R. FTIR microscopic imaging of collagen and proteoglycan in bovine cartilage. *Biopolymers* **62**, 1-8 (2001).

355. Cerruti, M.G., Greenspan, D. & Powers, K. An analytical model for the dissolution of different particle size samples of Bioglass® in TRIS-buffered solution. *Biomaterials* **26**, 4903-4911 (2005).

356. Sun, J.-Y., Yang, Y.-S., Zhong, J. & Greenspan, D.C. The effect of the ionic products of Bioglass® dissolution on human osteoblasts growth cycle in vitro. *Journal of Tissue Engineering and Regenerative Medicine* **1**, 281-286 (2007).

357. Yoo, J.U., Barthel, T.S., Nishimura, K., Solchaga, L., Caplan, A.I., Goldberg, V.M. & Johnstone, B. The chondrogenic potential of human bone-marrow-derived mesenchymal progenitor cells. *The Journal of Bone & Joint Surgery* **80**, 1745-1757 (1998).

358. Adesida, A., Mulet-Sierra, A. & Jomha, N. Hypoxia mediated isolation and expansion enhances the chondrogenic capacity of bone marrow mesenchymal stromal cells. *Stem Cell Research & Therapy* **3**, 9 (2012).

359. Zscharnack, M., Poesel, C., Galle, J. & Bader, A. Low oxygen expansion improves subsequent chondrogenesis of ovine bone-marrow-derived mesenchymal stem cells in collagen type I hydrogel. *Cells Tissues Organs* **190**, 81-93 (2009).

360. Murdoch, A.D., Grady, L.M., Ablett, M.P., Katopodi, T., Meadows, R.S. & Hardingham, T.E. Chondrogenic differentiation of human bone marrow stem cells in transwell cultures: generation of scaffold-free cartilage. *Stem Cells* **25**, 2786-2796 (2007).

361. Zhang, L., Su, P., Xu, C., Yang, J., Yu, W. & Huang, D. Chondrogenic differentiation of human mesenchymal stem cells: a comparison between micromass and pellet culture systems. *Biotechnology Letters* **32**, 1339-1346 (2010).

362. Kretlow, J.D., Jin, Y.-Q., Liu, W., Zhang, W., Hong, T.-H., Zhou, G., Baggett, L.S., Mikos, A.G. & Cao, Y. Donor age and cell passage affects differentiation potential of murine bone marrow-derived stem cells. *BMC Cell Biology* **9**, 1-13 (2008).

363. Choudhery, M.S., Badowski, M., Muise, A., Pierce, J. & Harris, D.T. Donor age negatively impacts adipose tissue-derived mesenchymal stem cell expansion and differentiation. *Journal of Translational Medicine* **12**, 8-8 (2014).

364. Scharstuhl, A., Schewe, B., Benz, K., Gaissmaier, C., Bühring, H.-J. & Stoop, R. Chondrogenic potential of human adult mesenchymal stem cells is independent of age or osteoarthritis etiology. *Stem Cells* **25**, 3244-3251 (2007).

365. Scotti, C., Tonnarelli, B., Papadimitropoulos, A., Scherberich, A., Schaeren, S., Schauerte, A., Lopez-Rios, J., Zeller, R., Barbero, A. & Martin, I. Recapitulation of endochondral bone formation using human adult mesenchymal stem cells as a paradigm for developmental engineering. *Proceedings of the National Academy of Sciences* **107**, 7251-7256 (2010).

366. Priestley, J. & Hey, W. Observations on different kinds of air. By Joseph Priestley, L L. D. F. R. S. *Philosophical Transactions* **62**, 147-264 (1772).

367. Grimshaw, M.J. & Mason, R.M. Bovine articular chondrocyte function in vitro depends upon oxygen tension. *Osteoarthritis and Cartilage* **8**, 386-392 (2000).

368. Silver, I.A. & Maroudas, A. Measurement of PH and ionic composition of pericellular sites [and discussion]. *Philosophical Transactions of the Royal Society of London B: Biological Sciences* **271**, 261-272 (1975).

369. Zhou, S., Cui, Z. & Urban, J.P.G. Factors influencing the oxygen concentration gradient from the synovial surface of articular cartilage to the cartilage–bone interface: a modeling study. *Arthritis & Rheumatism* **50**, 3915-3924 (2004).

370. Duval, E., Leclercq, S., Elissalde, J.-M., Demoor, M., Galéra, P. & Boumédiene, K. Hypoxia-inducible factor 1α inhibits the fibroblast-like markers type I and type III collagen during hypoxia-induced chondrocyte redifferentiation: hypoxia not only induces type II collagen and aggrecan, but it also inhibits type I and type III collagen in the hypoxia-inducible factor 1α–dependent redifferentiation of chondrocytes. *Arthritis & Rheumatism* **60**, 3038-3048 (2009).

371. Domm, C., Schünke, M., Christesen, K. & Kurz, B. Redifferentiation of dedifferentiated bovine articular chondrocytes in alginate culture under low oxygen tension. *Osteoarthritis and Cartilage* **10**, 13-22 (2002).

372. Malda, J., van Blitterswijk, C.A., van Geffen, M., Martens, D.E., Tramper, J. & Riesle, J. Low oxygen tension stimulates the redifferentiation of dedifferentiated adult human nasal chondrocytes. *Osteoarthritis and Cartilage* **12**, 306-313 (2004).

373. Murphy, C.L. & Polak, J.M. Control of human articular chondrocyte differentiation by reduced oxygen tension. *Journal of Cellular Physiology* **199**, 451-459 (2004).
374. Li, S., Oreffo, R.O.C., Sengers, B.G. & Tare, R.S. The effect of oxygen tension on human articular chondrocyte matrix synthesis: Integration of experimental and computational approaches. *Biotechnology and Bioengineering* **111**, 1876-1885 (2014).
375. Filardo, G., Madry, H., Jelic, M., Roffi, A., Cucchiarini, M. & Kon, E. Mesenchymal stem cells for the treatment of cartilage lesions: from preclinical findings to clinical application in orthopaedics. *Knee Surgery, Sports Traumatology, Arthroscopy* **21**, 1717-1729 (2013).
376. Sekiya, I., Larson, B.L., Smith, J.R., Pochampally, R., Cui, J. & Prockop, D.J. Expansion of human adult stem cells from bone marrow stroma: conditions that maximize the yields of early progenitors and evaluate their quality. *Stem Cells* **20** (2002).
377. Markway, B.D., Tan, G.-K., Brooke, G., Hudson, J.E., Cooper-White, J.J. & Doran, M.R. Enhanced chondrogenic differentiation of human bone marrow-derived mesenchymal stem cells in low oxygen environment micropellet cultures. *Cell Transplantation* **19**, 29-42 (2010).
378. Kanichai, M., Ferguson, D., Prendergast, P.J. & Campbell, V.A. Hypoxia promotes chondrogenesis in rat mesenchymal stem cells: A role for AKT and hypoxia-inducible factor (HIF)-1α. *Journal of Cellular Physiology* **216**, 708-715 (2008).
379. Meyer, E.G., Buckley, C.T., Thorpe, S.D. & Kelly, D.J. Low oxygen tension is a more potent promoter of chondrogenic differentiation than dynamic compression. *Journal of Biomechanics* **43**, 2516-2523 (2010).
380. Sheehy, E.J., Buckley, C.T. & Kelly, D.J. Oxygen tension regulates the osteogenic, chondrogenic and endochondral phenotype of bone marrow derived mesenchymal stem cells. *Biochemical and Biophysical Research Communications* **417**, 305-310 (2012).
381. Wang, D.W., Fermor, B., Gimble, J.M., Awad, H.A. & Guilak, F. Influence of oxygen on the proliferation and metabolism of adipose derived adult stem cells. *Journal of Cellular Physiology* **204**, 184-191 (2005).
382. Khan, W., Adesida, A. & Hardingham, T. Hypoxic conditions increase hypoxia-inducible transcription factor 2alpha and enhance chondrogenesis in stem cells from the infrapatellar fat pad of osteoarthritis patients. *Arthritis Research & Therapy* **9**, R55 (2007).
383. Lee, H.-H., Chang, C.-C., Shieh, M.-J., Wang, J.-P., Chen, Y.-T., Young, T.-H. & Hung, S.-C. Hypoxia enhances chondrogenesis and prevents terminal differentiation through PI3K/Akt/FoxO dependent anti-apoptotic effect. *Scientific Reports* **3**, 2683 (2013).
384. Boyette, L.B., Creasey, O.A., Guzik, L., Lozito, T. & Tuan, R.S. Human bone marrow-derived mesenchymal stem cells display enhanced clonogenicity but impaired differentiation with hypoxic preconditioning. *Stem Cells Translational Medicine* **3**, 241-254 (2014).

385. Malladi, P., Xu, Y., Chiou, M., Giaccia, A.J. & Longaker, M.T. Effect of reduced oxygen tension on chondrogenesis and osteogenesis in adipose-derived mesenchymal cells. *American Journal of Physiology - Cell Physiology* **290**, C1139-C1146 (2006).

386. Cicione, C., Muiños-López, E., Hermida-Gómez, T., Fuentes-Boquete, I., Díaz-Prado, S. & Blanco, F.J. Effects of severe hypoxia on bone Marrow mesenchymal stem cells differentiation potential. *Stem Cells International* **2013**, 232896 (2013).

387. Amarilio, R., Viukov, S.V., Sharir, A., Eshkar-Oren, I., Johnson, R.S. & Zelzer, E. HIF1α regulation of Sox9 is necessary to maintain differentiation of hypoxic prechondrogenic cells during early skeletogenesis. *Development* **134**, 3917-3928 (2007).

388. Zhang, C., Yang, F., Cornelia, R., Tang, W., Swisher, S. & Kim, H. Hypoxia-inducible factor-1 is a positive regulator of Sox9 activity in femoral head osteonecrosis. *Bone* **48**, 507-513 (2011).

389. Robins, J.C., Akeno, N., Mukherjee, A., Dalal, R.R., Aronow, B.J., Koopman, P. & Clemens, T.L. Hypoxia induces chondrocyte-specific gene expression in mesenchymal cells in association with transcriptional activation of Sox9. *Bone* **37**, 313-322 (2005).

390. Thoms, B.L., Dudek, K.A., Lafont, J.E. & Murphy, C.L. Hypoxia promotes the production and inhibits the destruction of human articular cartilage. *Arthritis & Rheumatism* **65**, 1302-1312 (2013).

391. Tsuchida, S., Arai, Y., Takahashi, K.A., Kishida, T., Terauchi, R., Honjo, K., Nakagawa, S., Inoue, H., Ikoma, K., Ueshima, K., Matsuki, T., Mazda, O. & Kubo, T. HIF-1α-induced HSP70 regulates anabolic responses in articular chondrocytes under hypoxic conditions. *Journal of Orthopaedic Research* **32**, 975-980 (2014).

392. Mobasheri, A.L.I., Platt, N., Thorpe, C. & Shakibaei, M. Regulation of 2-deoxy-d-glucose transport, lactate metabolism, and MMP-2 secretion by the hypoxia mimetic cobalt chloride in articular chondrocytes. *Annals of the New York Academy of Sciences* **1091**, 83-93 (2006).

393. Duval, E., Baugé, C., Andriamanalijaona, R., Bénateau, H., Leclercq, S., Dutoit, S., Poulain, L., Galéra, P. & Boumédiene, K. Molecular mechanism of hypoxia-induced chondrogenesis and its application in in vivo cartilage tissue engineering. *Biomaterials* **33**, 6042-6051 (2012).

394. Seo, A.R., Lim, M.H., Kim, K.H., Chang, O.H., Song, S.U., Park, S.R., Min, B.-H. & Choi, B.H. Hypoxia mimicking compounds induce chondrogenic differentiation of human clonal mesenchymal stem cells (hcMSCs) via hypoxia-inducing factor 1 alpha (HIF-1 alpha). *Tissue Engineering and Regenerative Medicine* **8**, 133-140 (2011).

395. Jeon, E.S., Shin, J.H., Hwang, S.J., Moon, G.J., Bang, O.Y. & Kim, H.H. Cobalt chloride induces neuronal differentiation of human mesenchymal stem cells through upregulation of microRNA-124a. *Biochemical and Biophysical Research Communications* **444**, 581-587 (2014).

396. Attia, M., Santerre, J.P. & Kandel, R.A. The response of annulus fibrosus cell to fibronectin-coated nanofibrous polyurethane-anionic dihydroxyoligomer scaffolds. *Biomaterials* **32**, 450-460 (2011).

397. Iu, J., Santerre, J.P. & Kandel, R.A. Inner and outer annulus fibrosus cells exhibit differentiated phenotypes and yield changes in extracellular matrix protein composition in vitro on a polycarbonate urethane scaffold. *Tissue Engineering Part A* **20**, 3261-3269 (2014).

398. McCullen, S.D., Autefage, H., Callanan, A., Gentleman, E. & Stevens, M.M. Anisotropic Fibrous Scaffolds for Articular Cartilage Regeneration. *Tissue Engineering Part A* **18**, 2073-2083 (2012).

399. Steele, J.A.M., McCullen, S.D., Callanan, A., Autefage, H., Accardi, M.A., Dini, D. & Stevens, M.M. Combinatorial scaffold morphologies for zonal articular cartilage engineering. *Acta Biomaterialia* **10**, 2065-2075 (2014).

400. Pacary, E., Legros, H., Valable, S., Duchatelle, P., Lecocq, M., Petit, E., Nicole, O. & Bernaudin, M. Synergistic effects of CoCl2 and ROCK inhibition on mesenchymal stem cell differentiation into neuron-like cells. *Journal of Cell Science* **119**, 2667-2678 (2006).

401. Pacary, E., Tixier, E., Coulet, F., Roussel, S., Petit, E. & Bernaudin, M. Crosstalk between HIF-1 and ROCK pathways in neuronal differentiation of mesenchymal stem cells, neurospheres and in PC12 neurite outgrowth. *Molecular and Cellular Neuroscience* **35**, 409-423 (2007).

402. Agrawal, A., Guttapalli, A., Narayan, S., Albert, T.J., Shapiro, I.M. & Risbud, M.V. Normoxic stabilization of HIF-1α drives glycolytic metabolism and regulates aggrecan gene expression in nucleus pulposus cells of the rat intervertebral disk. *American Journal of Physiology - Cell Physiology* **293**, C621-C631 (2007).

403. Graven, K.K., Bellur, D., Klahn, B.D., Lowrey, S.L. & Amberger, E. HIF-2α regulates glyceraldehyde-3-phosphate dehydrogenase expression in endothelial cells. *Biochimica et Biophysica Acta (BBA) - Gene Structure and Expression* **1626**, 10-18 (2003).

404. Park, I.-H., Kim, K.-H., Choi, H.-K., Shim, J.-S., Whang, S.-Y., June Hahn, S., Kwon, O.-J. & Oh, I.-H. Constitutive stabilization of hypoxia-inducible factor alpha selectively promotes the self-renewal of mesenchymal progenitors and maintains mesenchymal stromal cells in an undifferentiated state. *Exp Mol Med* **45**, e44 (2013).

405. Tsai, C.-C., Chen, Y.-J., Yew, T.-L., Chen, L.-L., Wang, J.-Y., Chiu, C.-H. & Hung, S.-C. Hypoxia inhibits senescence and maintains mesenchymal stem cell properties through down-regulation of E2A-p21 by HIF-TWIST. *Blood* **117**, 459-469 (2011).

406. Gentleman, E., Swain, R.J., Evans, N.D., Boonrungsiman, S., Jell, G., Ball, M.D., Shean, T.A.V., Oyen, M.L., Porter, A. & Stevens, M.M. Comparative materials differences revealed in engineered bone as a function of cell-specific differentiation. *Nature Materials* **8**, 763-770 (2009).

407. Swain, R.J., Jell, G. & Stevens, M.A. Non-invasive analysis of cell cycle dynamics in single living cells with Raman micro-spectroscopy. *Journal of Cellular Biochemistry* **104**, 1427-1438 (2008).

408. Babur, B.K., Ghanavi, P., Levett, P., Lott, W.B., Klein, T., Cooper-White, J.J., Crawford, R. & Doran, M.R. The interplay between chondrocyte redifferentiation pellet size and oxygen concentration. *PLoS One* **8**, e58865 (2013).

409. Estes, B.T. & Guilak, F. in Adipose-Derived Stem Cells: Methods and Protocols. (eds. M.J. Gimble & A.B. Bunnell) 201-217 (Humana Press, Totowa, NJ; 2011).

410. Bianchessi, M., Chen, Y., Durgam, S., Pondenis, H. & Stewart, M. Effect of fibroblast growth factor 2 on equine synovial fluid chondroprogenitor expansion and chondrogenesis. *Stem Cells International*.

411. Caplan, A.I. & Bruder, S.P. Mesenchymal stem cells: building blocks for molecular medicine in the 21st century. *Trends in Molecular Medicine* **7**, 259-264 (2001).

412. Murphy, M.B., Moncivais, K. & Caplan, A.I. Mesenchymal stem cells: environmentally responsive therapeutics for regenerative medicine. *Exp Mol Med* **45**, e54 (2013).

413. Alvarez-Viejo, M., Menendez-Menendez, Y., Blanco-Gelaz, M.A., Ferrero-Gutierrez, A., Fernandez-Rodriguez, M.A., Gala, J. & Otero-Hernandez, J. Quantifying mesenchymal stem cells in the mononuclear cell fraction of bone marrow samples obtained for cell therapy. *Transplantation Proceedings* **45**, 434-439 (2013).

414. DiGirolamo, C.M., Stokes, D., Colter, D., Phinney, D.G., Class, R. & Prockop, D.J. Propagation and senescence of human marrow stromal cells in culture: a simple colony-forming assay identifies samples with the greatest potential to propagate and differentiate. *British Journal of Haematology* **107**, 275-281 (1999).

415. Crisostomo, P.R., Wang, M., Wairiuko, G.M., Morrell, E.D., Terrell, A.M., Seshadri, P., Nam, U.H. & Meldrum, D.R. High passage number of stem cells adversely affects stem cell activation and myocardial protection. *Shock* **26**, 575-580 (2006).

416. Hoch, A.I. & Leach, J.K. Concise review: optimizing expansion of bone marrow mesenchymal stem/stromal cells for clinical applications. *Stem Cells Translational Medicine* **3**, 643-652 (2014).

417. Spencer, J.A., Ferraro, F., Roussakis, E., Klein, A., Wu, J., Runnels, J.M., Zaher, W., Mortensen, L.J., Alt, C., Turcotte, R., Yusuf, R., Cote, D., Vinogradov, S.A., Scadden, D.T. & Lin, C.P. Direct measurement of local oxygen concentration in the bone marrow of live animals. *Nature* **508**, 269-273 (2014).

418. Das, R., Jahr, H., van Osch, G.J.V.M. & Farrell, E. The role of hypoxia in bone marrow–derived mesenchymal stem cells: considerations for regenerative medicine approaches. *Tissue Engineering Part B: Reviews* **16**, 159-168 (2009).

419. Yamamoto, Y., Fujita, M., Tanaka, Y., Kojima, I., Kanatani, Y., Ishihara, M. & Tachibana, S. Low oxygen tension enhances proliferation and maintains stemness of adipose tissue–derived stromal cells. *BioResearch Open Access* **2**, 199-205 (2013).
420. Berniakovich, I. & Giorgio, M. Low oxygen tension maintains multipotency, whereas normoxia increases differentiation of mouse bone marrow stromal cells. *International Journal of Molecular Sciences* **14**, 2119 (2013).
421. Saller, M.M., Prall, W.C., Docheva, D., Schönitzer, V., Popov, T., Anz, D., Clausen-Schaumann, H., Mutschler, W., Volkmer, E., Schieker, M. & Polzer, H. Increased stemness and migration of human mesenchymal stem cells in hypoxia is associated with altered integrin expression. *Biochemical and Biophysical Research Communications* **423**, 379-385 (2012).
422. Basciano, L., Nemos, C., Foliguet, B., de Isla, N., de Carvalho, M., Tran, N. & Dalloul, A. Long term culture of mesenchymal stem cells in hypoxia promotes a genetic program maintaining their undifferentiated and multipotent status. *BMC Cell Biology* **12**, 1-12 (2011).
423. Fehrer, C., Brunauer, R., Laschober, G., Unterluggauer, H., Reitinger, S., Kloss, F., Gully, C., Gassner, R. & Lepperdinger, G. Reduced oxygen tension attenuates differentiation capacity of human mesenchymal stem cells and prolongs their lifespan. *Aging Cell* **6**, 745 - 757 (2007).
424. Holzwarth, C., Vaegler, M., Gieseke, F., Pfister, S., Handgretinger, R., Kerst, G. & Muller, I. Low physiologic oxygen tensions reduce proliferation and differentiation of human multipotent mesenchymal stromal cells. *BMC Cell Biology* **11**, 11 (2010).
425. Hung, S.-C., Pochampally, R.R., Hsu, S.-C., Sanchez, C., Chen, S.-C., Spees, J. & Prockop, D.J. Short-term exposure of multipotent stromal cells to low oxygen increases their expression of CX3CR1 and CXCR4 and their engraftment in vivo. *PLoS One* **2**, e416 (2007).
426. Grayson, W.L., Zhao, F., Izadpanah, R., Bunnell, B. & Ma, T. Effects of hypoxia on human mesenchymal stem cell expansion and plasticity in 3 D constructs. *Journal of Cellular Physiology* **207** (2006).
427. Vertelov, G., Kharazi, L., Muralidhar, M., Sanati, G., Tankovich, T. & Kharazi, A. High targeted migration of human mesenchymal stem cells grown in hypoxia is associated with enhanced activation of RhoA. *Stem Cell Research & Therapy* **4**, 5 (2013).
428. Tamama, K., Kawasaki, H., Kerpedjieva, S.S., Guan, J., Ganju, R.K. & Sen, C.K. Differential roles of hypoxia inducible factor subunits in multipotential stromal cells under hypoxic condition. *Journal of Cellular Biochemistry* **112**, 804-817 (2011).
429. Potier, E., Ferreira, E., Andriamanalijaona, R., Pujol, J., Oudina, K., Logeart-Avramoglou, D. & Petite, H. Hypoxia affects mesenchymal stromal cell osteogenic differentiation and angiogenic factor expression. *Bone* **40**, 1078 - 1087 (2007).
430. Wagegg, M., Gaber, T., Lohanatha, F.L., Hahne, M., Strehl, C., Fangradt, M., Tran, C.L., Schönbeck, K., Hoff, P., Ode, A., Perka, C., Duda, G.N. & Buttgereit, F. Hypoxia promotes

osteogenesis but suppresses adipogenesis of human mesenchymal stromal cells in a hypoxia-inducible factor-1 dependent manner. *PLoS One* **7**, e46483 (2012).

431. Grayson, W., Zhao, F., Bunnell, B. & Ma, T. Hypoxia enhances proliferation and tissue formation of human mesenchymal stem cells. *Biochemical and Biophysical Research Communications* **358**, 948 - 953 (2007).

432. D'Ippolito, G., Diabira, S., Howard, G., Roos, B. & Schiller, P. Low oxygen tension inhibits osteogenic differentiation and enhances stemness of human MIAMI cells. *Bone* **39**, 513 - 522 (2006).

433. Martin-Rendon, E., Hale, S.J.M., Ryan, D., Baban, D., Forde, S.P., Roubelakis, M., Sweeney, D., Moukayed, M., Harris, A.L., Davies, K. & Watt, S.M. Transcriptional profiling of human cord blood CD133+ and cultured bone marrow mesenchymal stem cells in response to hypoxia. *Stem Cells* **25** (2007).

434. Ohnishi, S., Yasuda, T., Kitamura, S. & Nagaya, N. Effect of hypoxia on gene expression of bone marrow-derived mesenchymal stem cells and mononuclear cells. *Stem Cells* **25** (2007).

435. Muscari, C., Giordano, E., Bonafè, F., Govoni, M., Pasini, A. & Guarnieri, C. Priming adult stem cells by hypoxic pretreatments for applications in regenerative medicine. *Journal of Biomedical Science* **20**, 63-63 (2013).

436. Esfahani, M., Karimi, F., Afshar, S., niknazar, S., Sohrabi, S. & Najafi, R. Prolyl hydroxylase inhibitors act as agents to enhance the efficiency of cell therapy. *Expert Opinion on Biological Therapy* **15**, 1739-1755 (2015).

437. Liu, L., Yu, Q., Lin, J., Lai, X., Cao, W., Du, K., Wang, Y., Wu, K., Hu, Y., Zhang, L., Xiao, H., Duan, Y. & Huang, H. Hypoxia-inducible factor-1α is essential for hypoxia-induced mesenchymal stem cell mobilization into the peripheral blood. *Stem Cells and Development* **20**, 1961-1971 (2011).

438. Rankin, S.M. Chemokines and adult bone marrow stem cells. *Immunology Letters* **145**, 47-54 (2012).

439. Ahmadbeigi, N., Seyedjafari, E., Gheisari, Y., Atashi, A., Omidkhoda, A. & Soleimani, M. Surface expression of CXCR4 in unrestricted somatic stem cells and its regulation by growth factors. *Cell Biology International* **34**, 687-692 (2010).

440. Honczarenko, M., Le, Y., Swierkowski, M., Ghiran, I., Glodek, A.M. & Silberstein, L.E. Human bone marrow stromal cells express a distinct set of biologically functional chemokine receptors. *Stem Cells* **24**, 1030-1041 (2006).

441. Wynn, R.F., Hart, C.A., Corradi-Perini, C., O'Neill, L., Evans, C.A., Wraith, J.E., Fairbairn, L.J. & Bellantuono, I. A small proportion of mesenchymal stem cells strongly expresses functionally active CXCR4 receptor capable of promoting migration to bone marrow. *Blood* **104**, 2643-2645 (2004).

442. Ceradini, D.J., Kulkarni, A.R., Callaghan, M.J., Tepper, O.M., Bastidas, N., Kleinman, M.E., Capla, J.M., Galiano, R.D., Levine, J.P. & Gurtner, G.C. Progenitor cell trafficking is regulated by hypoxic gradients through HIF-1 induction of SDF-1. *Nature Medicine* **10**, 858-864 (2004).
443. Sun, X., Wei, L., Chen, Q. & Terek, R.M. CXCR4/SDF1 mediate hypoxia induced chondrosarcoma cell invasion through ERK signaling and increased MMP1 expression. *Molecular Cancer* **9**, 17-17 (2010).
444. Ishikawa, T., Nakashiro, K., Klosek, S.K., Goda, H., Hara, S., Uchida, D. & Hamakawa, H. Hypoxia enhances CXCR4 expression by activating HIF-1 in oral squamous cell carcinoma. *Oncology Reports* **21**, 707-712 (2009).
445. Staller, P., Sulitkova, J., Lisztwan, J., Moch, H., Oakeley, E.J. & Krek, W. Chemokine receptor CXCR4 downregulated by von Hippel-Lindau tumour suppressor pVHL. *Nature* **425**, 307-311 (2003).
446. Liu, H., Liu, S., Li, Y., Wang, X., Xue, W., Ge, G. & Luo, X. The role of SDF-1-CXCR4/CXCR7 axis in the therapeutic effects of hypoxia-preconditioned mesenchymal stem cells for renal ischemia/reperfusion injury. *PLoS One* **7**, e34608 (2012).
447. Yu, X., Chen, D., Zhang, Y., Wu, X., Huang, Z., Zhou, H., Zhang, Y. & Zhang, Z. Overexpression of CXCR4 in mesenchymal stem cells promotes migration, neuroprotection and angiogenesis in a rat model of stroke. *Journal of the Neurological Sciences* **316**, 141-149 (2012).
448. Yu, X., Lu, C., Liu, H., Rao, S., Cai, J., Liu, S., Kriegel, A.J., Greene, A.S., Liang, M. & Ding, X. Hypoxic preconditioning with cobalt of bone marrow mesenchymal stem cells improves cell migration and enhances therapy for treatment of ischemic acute kidney injury. *PLoS One* **8**, e62703 (2013).
449. Rosová, I., Dao, M., Capoccia, B., Link, D. & Nolta, J.A. Hypoxic preconditioning results in increased motility and improved therapeutic potential of human mesenchymal stem cells. *Stem Cells* **26**, 2173-2182 (2008).
450. Osathanon, T., Vivatbutsiri, P., Sukarawan, W., Sriarj, W., Pavasant, P. & Sooampon, S. Cobalt chloride supplementation induces stem-cell marker expression and inhibits osteoblastic differentiation in human periodontal ligament cells. *Archives of Oral Biology* **60**, 29-36 (2015).
451. Müller, H.-D., Cvikl, B., Gruber, R., Watzek, G. & Agis, H. Prolyl hydroxylase Inhibitors increase the production of vascular endothelial growth factor in dental pulp–derived cells. *Journal of Endodontics* **38**, 1498-1503 (2012).
452. Zan, T., Du, Z., Li, H., Li, Q. & Gu, B. Cobalt chloride improves angiogenic potential of CD133+ cells. *Frontiers in bioscience (Landmark edition)* **17**, 2247-2258 (2012).
453. Milosevic, J., Adler, I., Manaenko, A., Schwarz, S., Walkinshaw, G., Arend, M., Flippin, L., Storch, A. & Schwarz, J. Non-hypoxic stabilization of hypoxia-inducible factor alpha (HIF-α): relevance in neural progenitor/stem cells. *Neurotoxicity Research* **15**, 367-380 (2009).

454. Abbas, T. & Dutta, A. p21 in cancer: intricate networks and multiple activities. *Nature Reviews Cancer* **9**, 400-414 (2009).

455. Coqueret, O. New roles for p21 and p27 cell-cycle inhibitors: a function for each cell compartment? *Trends in Cell Biology* **13**, 65-70 (2003).

456. Bach, A., Bender–Sigel, J., Schrenk, D., Flügel, D. & Kietzmann, T. The antioxidant quercetin inhibits cellular proliferation via HIF-1-dependent induction of p21WAF. *Antioxidants & Redox Signaling* **13**, 437-448 (2009).

457. Carmeliet, P. Abnormal blood vessel development and lethality in embryos lacking a single VEGF allele. *Nature* **380**, 435-439 (1996).

458. Koshiji, M., Kageyama, Y., Pete, E.A., Horikawa, I., Barrett, J.C. & Huang, L.E. HIF-1α induces cell cycle arrest by functionally counteracting Myc. *The EMBO Journal* **23**, 1949-1956 (2004).

459. He, M., Wang, Q.Y., Yin, Q.Q., Tang, J., Lu, Y., Zhou, C.X., Duan, C.W., Hong, D.L., Tanaka, T., Chen, G.Q. & Zhao, Q. HIF-1α downregulates miR-17/20a directly targeting p21 and STAT3: a role in myeloid leukemic cell differentiation. *Cell Death and Differentiation* **20**, 408-418 (2013).

460. Yew, T.-L., Chiu, F.-Y., Tsai, C.-C., Chen, H.-L., Lee, W.-P., Chen, Y.-J., Chang, M.-C. & Hung, S.-C. Knockdown of p21Cip1/Waf1 enhances proliferation, the expression of stemness markers, and osteogenic potential in human mesenchymal stem cells. *Aging Cell* **10**, 349-361 (2011).

461. Zaman, K., Ryu, H., Hall, D., O'Donovan, K., Lin, K.-I., Miller, M.P., Marquis, J.C., Baraban, J.M., Semenza, G.L. & Ratan, R.R. Protection from oxidative stress–induced apoptosis in cortical neuronal cultures by iron chelators is associated with enhanced DNA binding of hypoxia-inducible factor-1 and ATF-1/CREB and increased expression of glycolytic enzymes, p21waf1/cip1, and erythropoietin. *The Journal of Neuroscience* **19**, 9821-9830 (1999).

462. Leontieva, O.V., Natarajan, V., Demidenko, Z.N., Burdelya, L.G., Gudkov, A.V. & Blagosklonny, M.V. Hypoxia suppresses conversion from proliferative arrest to cellular senescence. *Proceedings of the National Academy of Sciences* **109**, 13314-13318 (2012).

463. Liu, H., Xue, W., Ge, G., Luo, X., Li, Y., Xiang, H., Ding, X., Tian, P. & Tian, X. Hypoxic preconditioning advances CXCR4 and CXCR7 expression by activating HIF-1α in MSCs. *Biochemical and Biophysical Research Communications* **401**, 509-515 (2010).

464. Wang, X., Li, C., Chen, Y., Hao, Y., Zhou, W., Chen, C. & Yu, Z. Hypoxia enhances CXCR4 expression favoring microglia migration via HIF-1α activation. *Biochemical and Biophysical Research Communications* **371**, 283-288 (2008).

465. Triantafyllou, A., Liakos, P., Tsakalof, A., Georgatsou, E., Simos, G. & Bonanou, S. Cobalt induces hypoxia-inducible factor-1α (HIF-1α) in HeLa cells by an iron-independent, but ROS-, PI-3K- and MAPK-dependent mechanism. *Free Radical Research* **40**, 847-856 (2006).

466. Zeng, H.-L., Zhong, Q., Qin, Y.-L., Bu, Q.-Q., Han, X.-A., Jia, H.-T. & Liu, H.-W. Hypoxia-mimetic agents inhibit proliferation and alter the morphology of human umbilical cord-derived mesenchymal stem cells. *BMC Cell Biology* **12**, 32 (2011).

467. Bedessem, B., Marie-Paule, M., Hamel, M., Giroud, F. & Stéphanou, A. Effects of the hypoxia-mimetic agents DFO and CoCl2 on HeLa-Fucci cells. *Journal of Cell Biology & Cell Metabolism* **2** (2015).

468. Ardyanto, T.D., Osaki, M., Tokuyasu, N., Nagahama, Y. & Ito, H. CoCl2-induced HIF-1alpha expression correlates with proliferation and apoptosis in MKN-1 cells: a possible role for the PI3K/Akt pathway. *International Journal of Oncology* **29** (2006).

469. Dai, Z.-J., Gao, J., Ma, X.-B., Yan, K., Liu, X.-X., Kang, H.-F., Ji, Z.-Z., Guan, H.-T. & Wang, X.-J. Up-regulation of hypoxia inducible factor-1α by cobalt chloride correlates with proliferation and apoptosis in PC-2 cells. *Journal of Experimental & Clinical Cancer Research* **31**, 1-7 (2012).

470. Lapham, C.K., Romantseva, T., Petricoin, E., King, L.R., Manischewitz, J., Zaitseva, M.B. & Golding, H. CXCR4 heterogeneity in primary cells: possible role of ubiquitination. *Journal of Leukocyte Biology* **72**, 1206-1214 (2002).

471. Wang, G., Hazra, T.K., Mitra, S., Lee, H.-M. & Englander, E.W. Mitochondrial DNA damage and a hypoxic response are induced by CoCl(2) in rat neuronal PC12 cells. *Nucleic Acids Research* **28**, 2135-2140 (2000).

472. Cho, Y.-S., Bae, J.-M., Chun, Y.-S., Chung, J.-H., Jeon, Y.-K., Kim, I.-S., Kim, M.-S. & Park, J.-W. HIF-1α controls keratinocyte proliferation by up-regulating p21(WAF1/Cip1). *Biochimica et Biophysica Acta (BBA) - Molecular Cell Research* **1783**, 323-333 (2008).

473. Silins, I., Finnberg, N., Ståhl, A., Högberg, J. & Stenius, U. Reduced ATM kinase activity and an attenuated p53 response to DNA damage in carcinogen-induced preneoplastic hepatic lesions in the rat. *Carcinogenesis* **22**, 2023-2031 (2001).

474. Levine, A.J. p53, the cellular gatekeeper for growth and division. *Cell* **88**, 323-331 (1997).

475. An, W.G., Kanekal, M., Simon, M.C., Maltepe, E., Blagosklonny, M.V. & Neckers, L.M. Stabilization of wild-type p53 by hypoxia-inducible factor 1α. *Nature* **392**, 405-408 (1998).

476. Schmid, T., Zhou, J. & Brüne, B. HIF-1 and p53: communication of transcription factors under hypoxia. *Journal of Cellular and Molecular Medicine* **8**, 423-431 (2004).

477. Koh, M.Y., Spivak-Kroizman, T.R. & Powis, G. HIF-1 regulation: not so easy come, easy go. *Trends in Biochemical Sciences* **33**, 526-534 (2008).

478. Schröck, K., Lutz, J., Mändl, S., Hacker, M.C., Kamprad, M. & Schulz-Siegmund, M. Co(II)-mediated effects of plain and plasma immersion ion implanted cobalt-chromium alloys on the osteogenic differentiation of human mesenchymal stem cells. *Journal of Orthopaedic Research* **33**, 325-333 (2015).

479. Ren, H., Cao, Y., Zhao, Q., Li, J., Zhou, C., Liao, L., Jia, M., Zhao, Q., Cai, H., Han, Z.C., Yang, R., Chen, G. & Zhao, R.C. Proliferation and differentiation of bone marrow stromal cells under hypoxic conditions. *Biochemical and Biophysical Research Communications* **347**, 12-21 (2006).

480. Ciavarella, C., Fittipaldi, S., Pedrini, S., Vasuri, F., Gallitto, E., Freyrie, A., Stella, A., Gostjeva, E. & Pasquinelli, G. In vitro alteration of physiological parameters do not hamper the growth of human multipotent vascular wall-mesenchymal stem cells. *Frontiers in Cell and Developmental Biology* **3**, 36 (2015).

481. Sekiya, I., Larson, B.L., Smith, J.R., Pochampally, R., Cui, J.-G. & Prockop, D.J. Expansion of human adult stem cells from bone marrow stroma: conditions that maximize the yields of early progenitors and evaluate their quality. *Stem Cells* **20**, 530-541 (2002).

482. Colter, D.C., Class, R., DiGirolamo, C.M. & Prockop, D.J. Rapid expansion of recycling stem cells in cultures of plastic-adherent cells from human bone marrow. *Proceedings of the National Academy of Sciences* **97**, 3213-3218 (2000).

483. Banfi, A., Muraglia, A., Dozin, B., Mastrogiacomo, M., Cancedda, R. & Quarto, R. Proliferation kinetics and differentiation potential of ex vivo expanded human bone marrow stromal cells: implications for their use in cell therapy. *Experimental Hematology* **28**, 707-715 (2000).

484. Schioppa, T., Uranchimeg, B., Saccani, A., Biswas, S.K., Doni, A., Rapisarda, A., Bernasconi, S., Saccani, S., Nebuloni, M., Vago, L., Mantovani, A., Melillo, G. & Sica, A. Regulation of the chemokine receptor CXCR4 by hypoxia. *The Journal of Experimental Medicine* **198**, 1391-1402 (2003).

485. Bünger, S., Roblick, U.J. & Habermann, J.K. Comparison of five commercial extraction kits for subsequent membrane protein profiling. *Cytotechnology* **61**, 153-159 (2009).

486. Wenger, R.H., Camenisch, G., Desbaillets, I., Chilov, D. & Gassmann, M. Up-regulation of hypoxia-inducible factor-1α is not sufficient for hypoxic/anoxic p53 induction. *Cancer Research* **58**, 5678-5680 (1998).

487. Vengellur, A., Woods, B.G., Ryan, H.E., Johnson, R.S. & Lapres, J.J. Gene expression profiling of the hypoxia signaling pathway in hypoxia-inducible factor 1α null mouse embryonic fibroblasts. *Gene Expression* **11**, 181-197 (2003).

488. Ren, H., Cao, Y., Zhao, Q., Li, J., Zhou, C., Liao, L., Jia, M., Zhao, Q., Cai, H., Han, Z., Yang, R., Chen, G. & Zhao, R. Proliferation and differentiation of bone marrow stromal cells under hypoxic conditions. *Biochemical and Biophysical Research Communications* **347**, 12 - 21 (2006).

489. Falanga, V., Zhou, L. & Yufit, T. Low oxygen tension stimulates collagen synthesis and COL1A1 transcription through the action of TGF-β1. *Journal of Cellular Physiology* **191**, 42-50 (2002).

490. Uchida, T., Rossignol, F., Matthay, M.A., Mounier, R., Couette, S., Clottes, E. & Clerici, C. Prolonged hypoxia differentially regulates hypoxia-inducible factor (HIF)-1α and HIF-2α expression in lung epithelial cells: implications of natural antisense HIF-1α. *Journal of Biological Chemistry* **279**, 14871-14878 (2004).

491. Ginouvès, A., Ilc, K., Macías, N., Pouysségur, J. & Berra, E. PHDs overactivation during chronic hypoxia "desensitizes" HIFα and protects cells from necrosis. *Proceedings of the National Academy of Sciences* **105**, 4745-4750 (2008).

492. Ortega, R., Bresson, C., Fraysse, A., Sandre, C., Devès, G., Gombert, C., Tabarant, M., Bleuet, P., Seznec, H., Simionovici, A., Moretto, P. & Moulin, C. Cobalt distribution in keratinocyte cells indicates nuclear and perinuclear accumulation and interaction with magnesium and zinc homeostasis. *Toxicology Letters* **188**, 26-32 (2009).

493. LaPointe, V.L.S., Verpoorte, A. & Stevens, M.M. The changing integrin expression and a role for integrin β8 in the chondrogenic differentiation of mesenchymal stem cells. *PLoS One* **8**, e82035 (2013).

494. Zhang, J., Zhao, S., Zhu, Y., Huang, Y., Zhu, M., Tao, C. & Zhang, C. Three-dimensional printing of strontium-containing mesoporous bioactive glass scaffolds for bone regeneration. *Acta Biomaterialia* **10**, 2269-2281 (2014).

Appendices

A Positive and Negative Controls for Antibodies used for Immunohistochemical Analysis

B Proliferation of hMSCs in Presence of BG Dissolution Products (Donor #1 and hMSCs Purchased from PromoCell)

C DNA and sGAG Profiles Presented Separately for all Donors

D Histological and Immunohistochemical Characterisation of Extracellular Matrix Production by pelleted hMSCs (Donor#5)

E DNA and sGAG Profiles Presented Separately for all Donors

F Histological Characterisation of Extracellular Matrix Production by Pelleted hMSCs (Donors #1, #2, #3 and #4)

G Histological Characterisation of Extracellular Matrix Production by hMSCs seeded on PCL mats (Donors #2 and #3)

H Pure Raman spectra of GAG, collagen and lipids

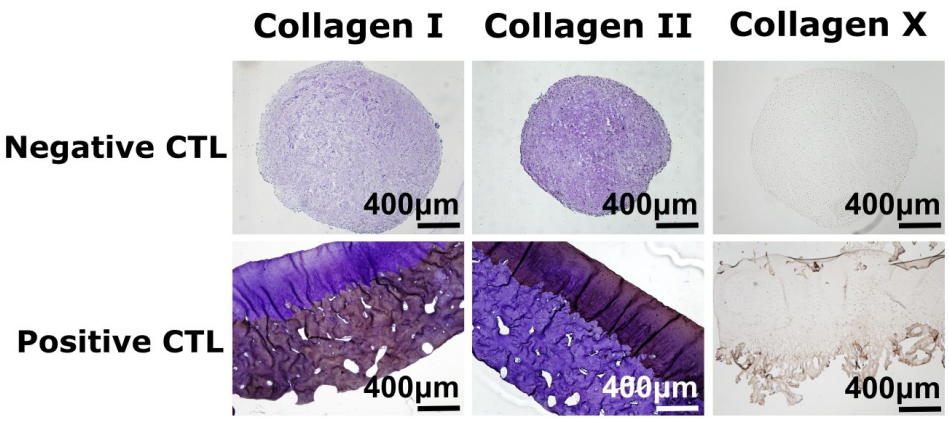
Appendix A

Chapter 3

Positive and Negative Controls for Antibodies used for Immunohistochemical Analysis

Sections of the bovine osteochondral region were used as positive controls. The 10 µm sections were embedded in paraffin, so that the sections had to be separately processed from the OCT embedded pellet sections up until the Avidin D/Biotin blocking step. In brief, sections were de-waxed (2 x 15 min in Histo-Clear (Fisher Scientific, UK), 2 min each in 100% EtOH and 90% EtOH) before blocking endogenous peroxidase by incubation in 1% (v/v) 30% H_2O_2 (Sigma, UK) in methanol (Sigma, UK) for 10 min. Sections were washed in running tap water for 10 min prior to heat mediated antigen retrieval in 10 mM citrate buffer at pH 6. From here onwards, all sections were processed according to the protocol outlined in 3.2.10.

Positive and negative controls of antibodies used for IHC of type I, II and X collagens. Sections of the bovine osteochondral region were used as positive controls. As negative controls served hMSC pellets incubated with the respective secondary antibodies only. Representative images (donor #4) are shown.

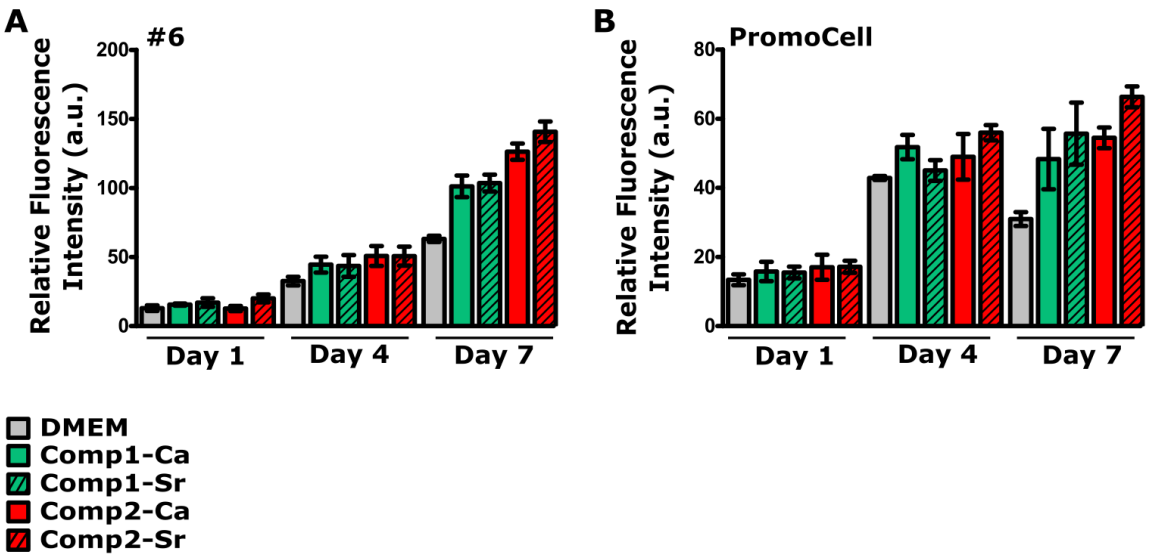


Appendix B

Chapter 3

Proliferation of hMSCs in Presence of BG Dissolution Products (Donor #1 and hMSCs Purchased from PromoCell)

Effect of various BG extracts on hMSC cell number. BG-conditioned or plain DMEM medium was used to culture hMSCs for up to 7 days. At the indicated time points cell proliferation over time was assessed using the CyQUANT® Direct Cell Proliferation Assay. Data are expressed as mean ± SD of 4 biological replicates for A) donor #6 (Lonza, UK) and B) hMSCs purchased from PromoCell. As the donors are displayed separately, no statistical analysis was performed.

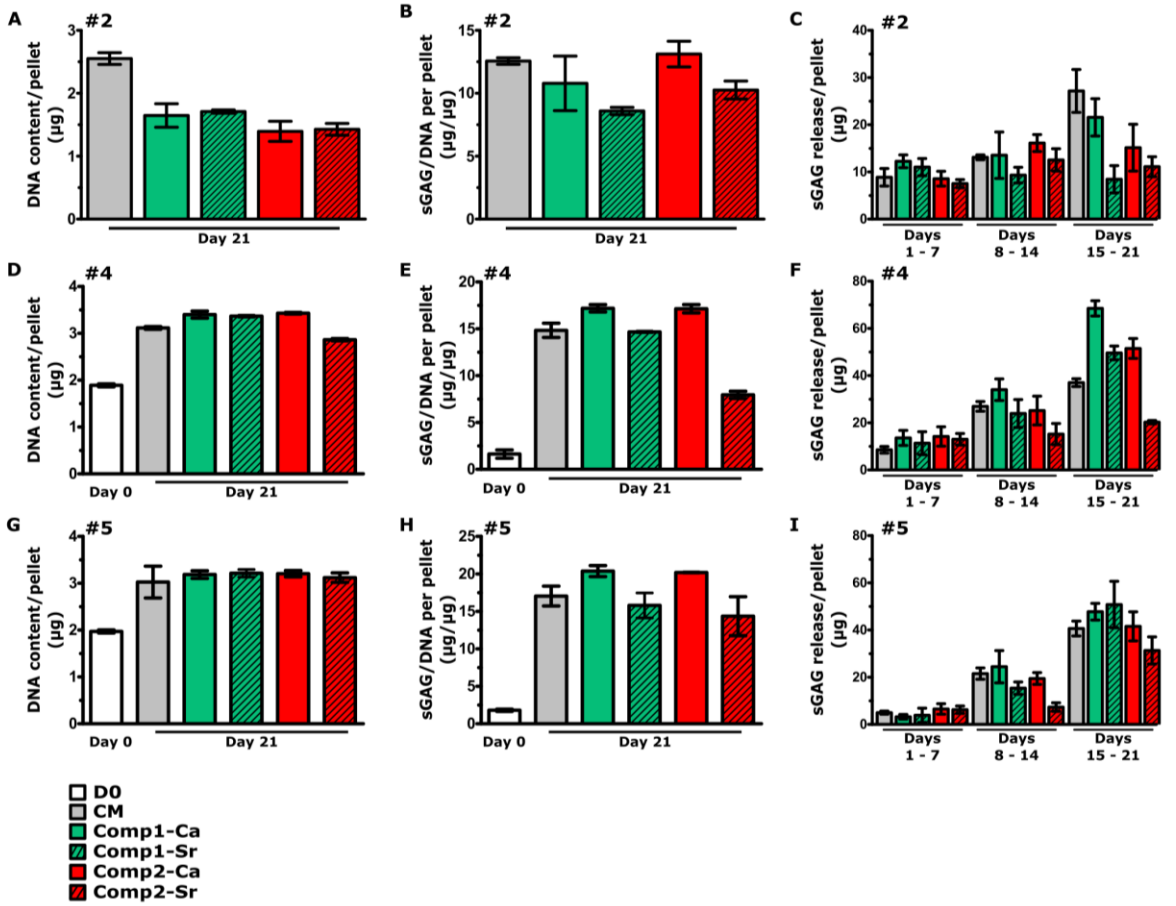


Appendix C

Chapter 3

DNA and sGAG Profiles Presented Separately for all Donors

Chondrogenic differentiation in presence of bioactive glass dissolution products. A - I) hMSC pellets were cultured in BG-conditioned medium in presence of chondrogenic supplements or chondrogenic (CM) medium for up to 21 days. A, D, G) The amount of DNA and B, E, H) sulphated glycosaminoglycans (sGAG) was measured on day 21. The sGAG content of pellets was normalised to the respective DNA content. C, E, I) Media was retained to assess sGAG released to media during the 21 day culture. Data are expressed as mean ± SD of 3 biological replicates per donor (#2, #4, #5). Statistical analysis was not performed on single donors. D0 = day 0.

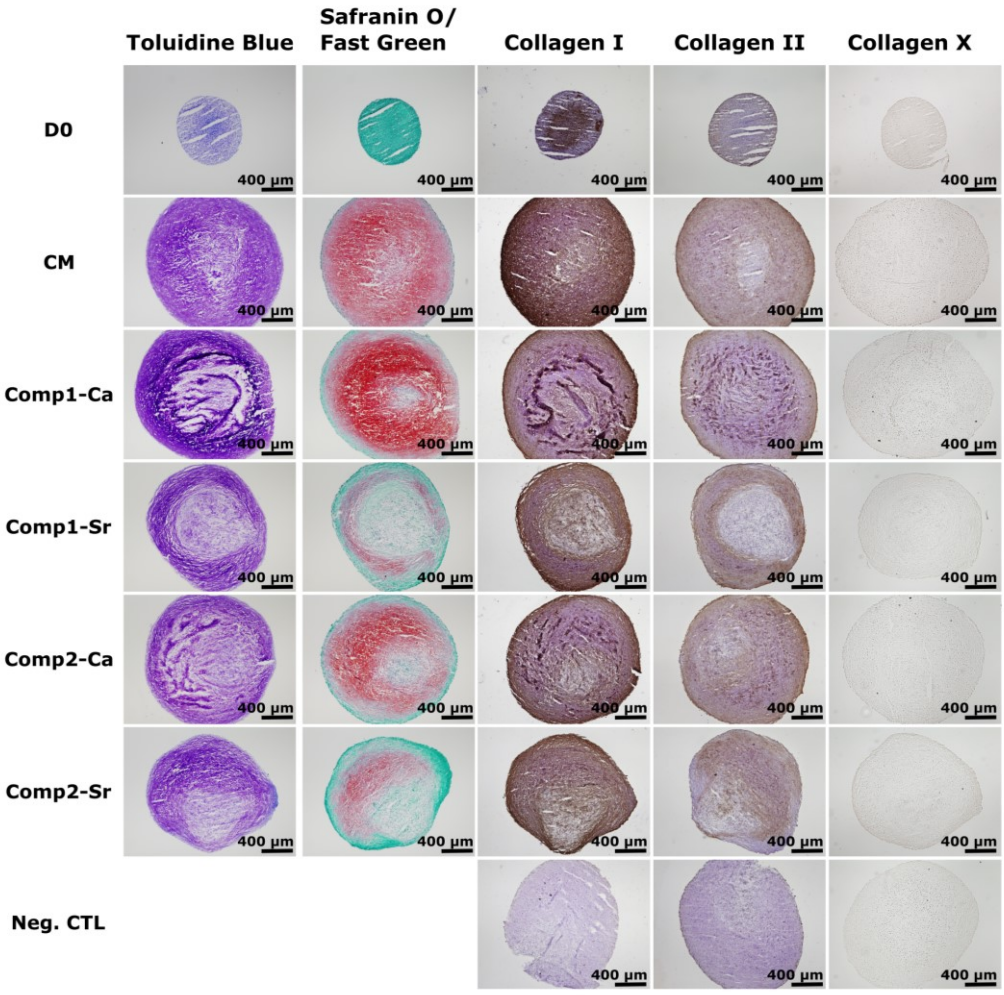


Appendix D

Chapter 3

Histological and Immunohistochemical Characterisation of Extracellular Matrix Production by pelleted hMSCs (Donor#5)

Characterization of *in vitro*-formed extracellular matrix in presence of BG extracts. The quality of the cartilage-like tissue formed by hMSCs was assessed by a) Toluidine Blue, and b) Safranin O/Fast Green staining as well as immunohistochemistry for type I, II and X collagens. Prior to histological/immunohistochemical assessment, hMSCs were grown as pellets in BG-conditioned medium containing chondrogenic supplements or chondrogenic medium (CM) for 21 days. Representative images (donor #5) are shown. Neg. CTL = negative control for immunohistochemistry.

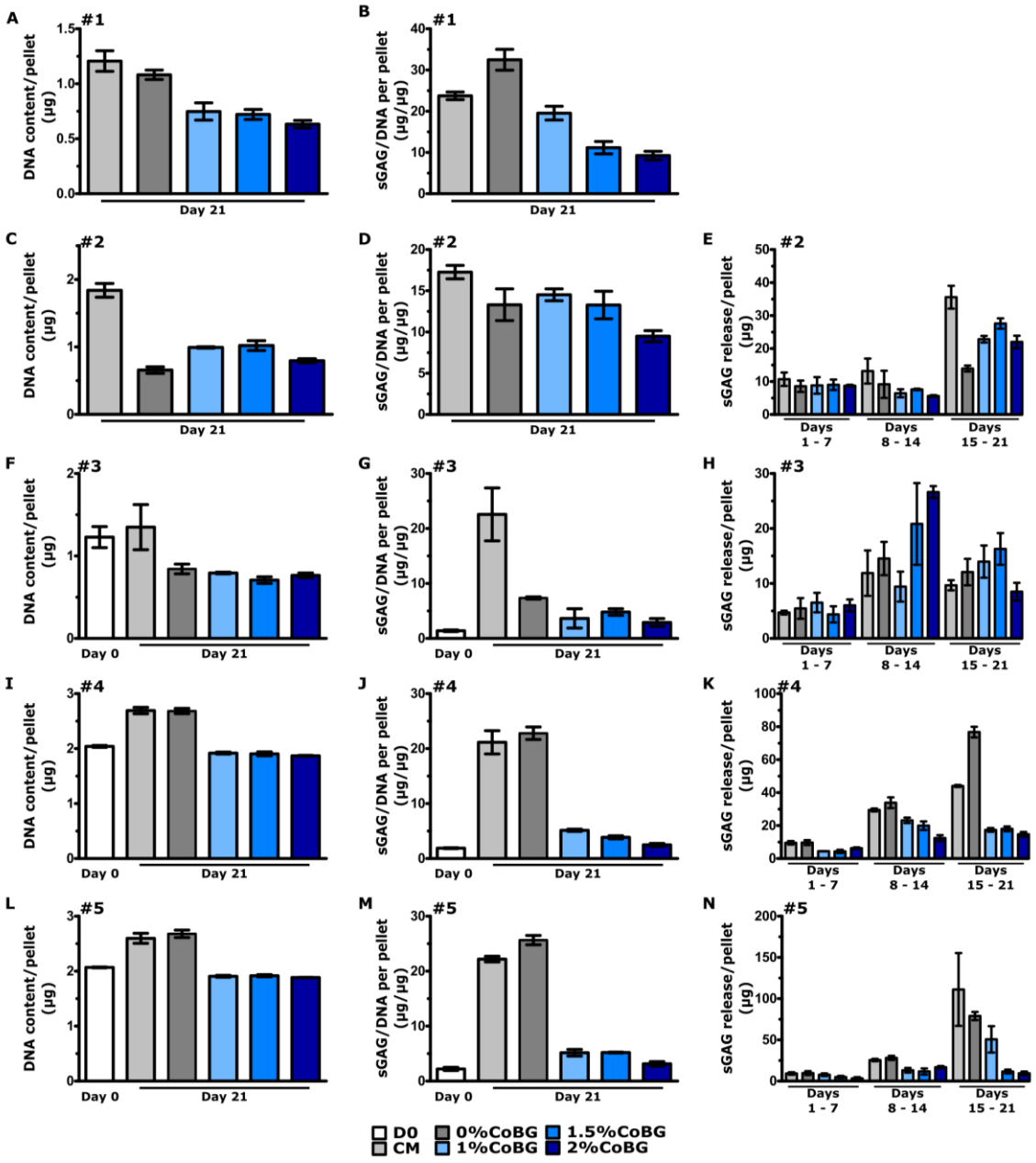


Appendix E

Chapter 4

DNA and sGAG Profiles Presented Separately for all Donors

Effect of CoBG dissolution products on sGAG production and release by hMSCs in pellet culture. hMSC pellets were cultured in CoBG-conditioned medium containing chondrogenic supplements or chondrogenic medium (CM) for 21 days prior to quantification of A, C, F, I, L) DNA by Hoechst and B, D, G, J, M) sulphated glycosaminoglycans (sGAG) by DMMB. The sGAG content of pellets was normalised to the respective DNA content. E, H, K, M) The sGAG release from pellets was measured over the entire culture period using DMMB. Donors #1 - #5 are presented separately. Data are expressed as mean ± SD of 3 biological replicates. Statistical analysis was not performed on single donors. D0 = day 0.

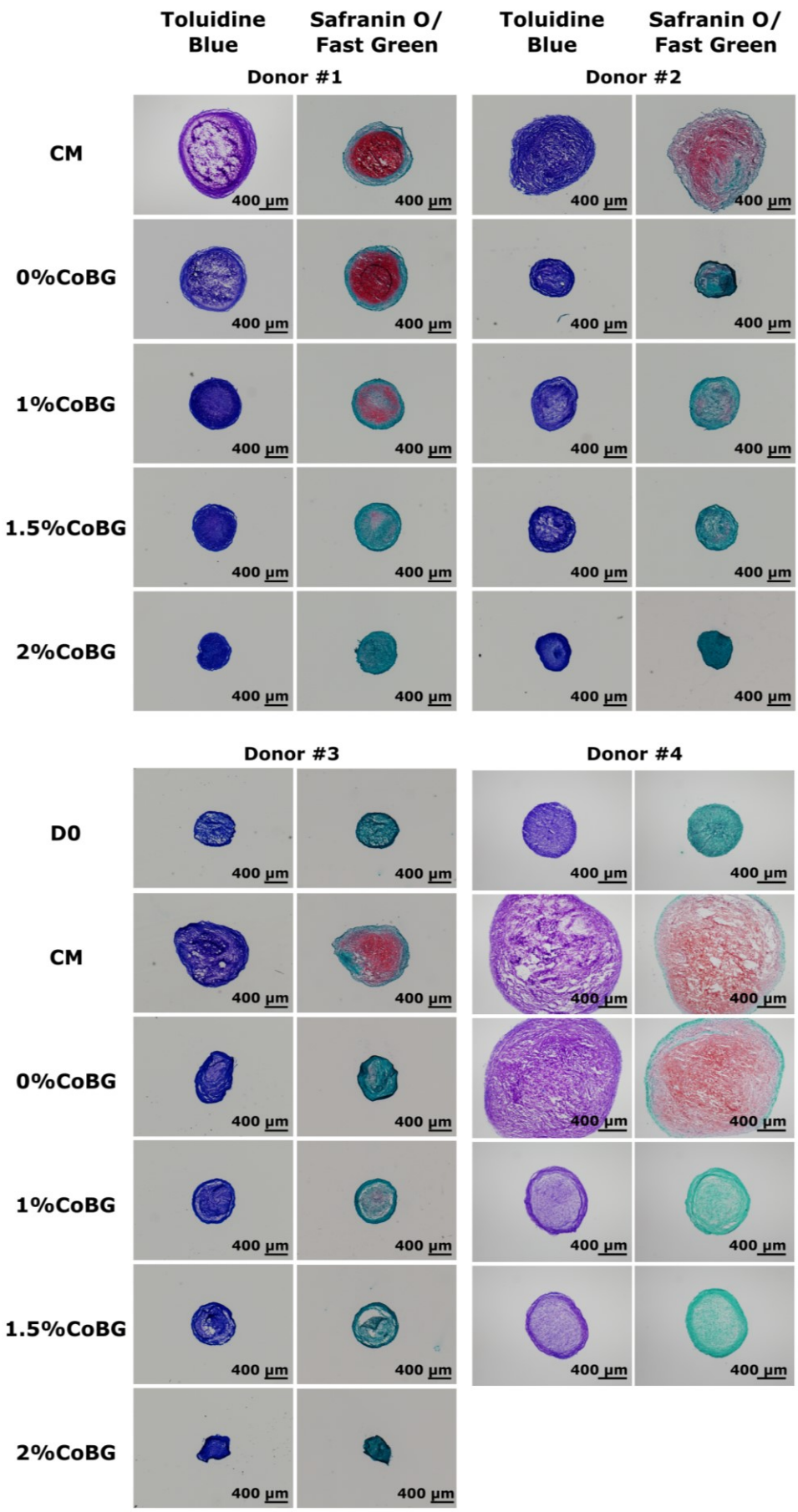

A
#1
DNA content/pellet (µg)
Day 21
B
#1
sGAG/DNA per pellet (µg/µg)
Day 21
C
#2
DNA content/pellet (µg)
Day 21
D
#2
sGAG/DNA per pellet (µg/µg)
Day 21
E
#2
sGAG release/pellet (µg)
Days 1 - 7
Days 8 - 14
Days 15 - 21
F
#3
DNA content/pellet (µg)
Day 0
Day 21
G
#3
sGAG/DNA per pellet (µg/µg)
Day 0
Day 21
H
#3
sGAG release/pellet (µg)
Days 1 - 7
Days 8 - 14
Days 15 - 21
I
#4
DNA content/pellet (µg)
Day 0
Day 21
J
#4
sGAG/DNA per pellet (µg/µg)
Day 0
Day 21
K
#4
sGAG release/pellet (µg)
Days 1 - 7
Days 8 - 14
Days 15 - 21
L
#5
DNA content/pellet (µg)
Day 0
Day 21
M
#5
sGAG/DNA per pellet (µg/µg)
Day 0
Day 21
N
#5
sGAG release/pellet (µg)
Days 1 - 7
Days 8 - 14
Days 15 - 21
D0
CM
0%CoBG
1%CoBG
1.5%CoBG
2%CoBG

Appendix F

Chapter 4

Histological Characterisation of Extracellular Matrix Production by Pelleted hMSCs (Donors #1, #2, #3 and #4)

Effect of CoBG dissolution products on *in vitro* cartilage-like tissue formation by hMSC pellets. Prior to histological assessment, hMSCs were grown as pellets in CoBG-conditioned medium containing chondrogenic supplements or chondrogenic medium (CM) for 21 days. The quality of the cartilage-like tissue formed by hMSC pellets was assessed by a) Toluidine Blue and b) Safranin O/ Fast Green staining. Representative images of donors #1, #2, #3 and #4) are shown. D0 = day 0.

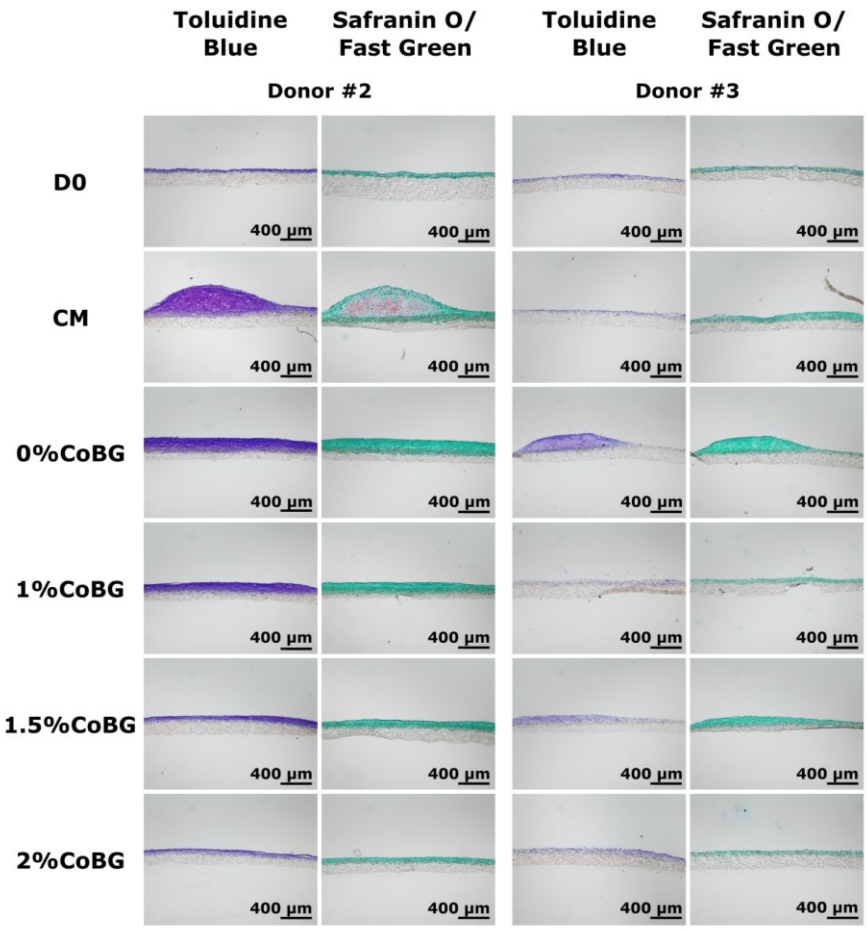

Toluidine Blue
Safranin O/ Fast Green
Toluidine Blue
Safranin O/ Fast Green
Donor #1
Donor #2
CM
0%CoBG
1%CoBG
1.5%CoBG
2%CoBG
Donor #3
Donor #4
D0
CM
0%CoBG
1%CoBG
1.5%CoBG
2%CoBG
400 µm

Appendix G

Chapter 4

Histological Characterisation of Extracellular Matrix Production by hMSCs seeded on PCL mats (Donors #2 and #3)

Effect of CoBG dissolution products on *in vitro* cartilage-like tissue formation by hMSCs seeded on PCL membranes. Prior to histological analysis, hMSCs seeded on PCL membranes were cultured in chondrogenic medium (CM) or CoBG-conditioned medium supplemented with chondrogenic factors for 21 days. The quality of the cartilage-like tissue formed by hMSC seeded on PCL membranes was examined by a) Toluidine Blue and b) Safranin O/Fast Green staining. Representative images for donors #2 and #3 are shown. D0 = day 0.



Appendix H

Chapter 4

Pure Raman spectra of GAG, collagen and lipids.

Pure Raman spectra of GAG (A), collagen (B) and lipids (C) were used for the semi-quantitative assessment of GAG, collagen and lipid components in hMSC pellets. The pure spectra were obtained from powders prepared from the respective pure components using the same conditions as the pellets. Representative for GAG, a spectrum of powdered aggrecan (aggrecan from bovine articular cartilage, A1960, Sigma-Aldrich) was obtained. Representative for collagen, powder prepared from type II collagen was used (collagen from chicken sternal cartilage (Type II), C9301, Sigma-Aldrich, UK). For lipids, a spectrum of phosphatidylcholine was obtained (L-α-Phosphatidylcholine from egg yolk, P3556, Sigma-Aldrich, UK).

